

Spatial models for cellular network planning

Thanh Tung Vu

▶ **To cite this version:**

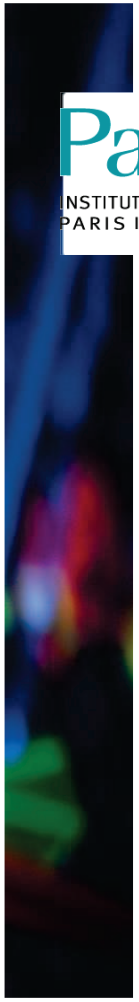
Thanh Tung Vu. Spatial models for cellular network planning. Other. Télécom ParisTech, 2012. English. NNT : 2012ENST0043 . tel-01081064

HAL Id: tel-01081064
https://pastel.hal.science/tel-01081064

Submitted on 6 Nov 2014

HAL is a multi-disciplinary open access archive for the deposit and dissemination of scientific research documents, whether they are published or not. The documents may come from teaching and research institutions in France or abroad, or from public or private research centers.

L'archive ouverte pluridisciplinaire **HAL**, est destinée au dépôt et à la diffusion de documents scientifiques de niveau recherche, publiés ou non, émanant des établissements d'enseignement et de recherche français ou étrangers, des laboratoires publics ou privés.



ParisTech
INSTITUT DES SCIENCES ET TECHNOLOGIES
PARIS INSTITUTE OF TECHNOLOGY

TELECOM ParisTech

2012-ENST-043

EDITE ED 130

Doctorat ParisTech

T H È S E

pour obtenir le grade de docteur délivré par

Télécom ParisTech

présentée et soutenue publiquement par

Thanh Tung VU

20/09/2012

Modèles spatiaux pour la planification cellulaire

Directeurs de thèse : **Laurent DECREUSEFOND**

Philippe MARTINS

Jury

M. James LEDOUX, Professeu, INSA Rennes	Président
M. Xavier LAGRANGE, Professeur, Télécom Bretagne	Rapporteur
M. Brian L.MARK, Professeur, Université de George Manson	Rapporteur
M. Bartlomiej BLASZCZYSZYN , Professeur, INRIA-ENS Paris	Examinateur
M. Jean-Mark KELIF, Ingénieur de recherche, Orange Labs	Examinateur
M. Laurent DECREUSEFOND, Professeur, Télécom Paristech	Directeur de thèse
M. Philippe MARTINS, Professeur, Télécom Paristech	Directeur de thèse

T H È S E

Télécom ParisTech
Ecole de l'Institut Télécom – membre de ParisTech
46, rue Barrault – 75634 Paris Cedex 13 – Tél. + 33 (0)1 45 81 77 77 – www.telecom-paristech.fr

Spatial models for cellular network planning

Thanh Tung Vu

Abstract

Nowadays, cellular technology is almost everywhere. It has had an explosive success over the last two decades and the volume of traffic will still increase in the near future. For this reason, it is also regarded as one cause of world-wide energy consumption, with high impact on carbon dioxide emission. On the other hand, new mathematical tools have enabled the conception of new models for cellular networks: one of these tools is stochastic geometry, or more particularly spatial Poisson point process. In the last decade, researchers have successfully used stochastic geometry to quantify outage probability, through-put or coverage of cellular networks by treating deployment of mobile stations or (and) base stations as Poisson point processes on a plane. These results also take into account to impact of mobility on the performance of such networks.

In this thesis, we apply the theory of Poisson point process to solve some problems of cellular networks, in particular we analyze the energy consumption of cellular networks. This thesis has two main parts. The first part deals with some dimensioning and coverage problems in cellular network. We uses stochastic analysis to provide bounds for the overload probability of OFDMA systems thanks to concentration inequalities and we apply it to solve a dimensioning problem. We also compute the outage probability and handover probability of a typical user. The second part is dedicated to introduce different models for energy consumption of cellular networks. In the first model, the initial location of users form a Poisson point process and each user is associated with an ON-OFF process of activity. In the second model, arrival of users forms a time-space Poisson point process. We also study the impact of mobility of users by assuming that users randomly move during its sojourn. We focus on the distribution of consumed energy by a base station. This consumed energy is divided into the additive part and the broadcast part. We obtain analytical expressions for the moments of the additive part as well as the mean and variance of the consumed energy. We are able to find an error bound for Gaussian approximation of the additive part. We prove that the mobility of users has a positive impact on the energy consumption. It does not increase or decrease the consumed energy in average but reduces its variance to zero in high mobility regime. We also characterize the convergent rate in function of user's speed.

Résumé des travaux de thèse

Résumé court

Aujourd'hui, la technologie cellulaire est à peu près partout. Elle a eu un succès explosif au cours des deux dernières décennies et le volume de trafic correspondant va encore augmenter dans un proche avenir. Pour cette raison, la consommation d'énergie que cette activité représente dans le monde entier devient non négligeable. C'est l'un des aspects que nous étudions dans cette thèse au travers de modèles basés sur la géométrie stochastique. D'autre part, de nouveaux outils mathématiques ont permis de construire de nouveaux modèles pour les réseaux cellulaires: un de ces outils est la géométrie aléatoire, ou plus particulièrement l'analyse des processus de Poisson spatiaux. Dans la dernière décennie, les chercheurs ont utilisé avec succès la géométrie aléatoire pour quantifier probabilité d'outage, le débit ou la couverture des réseaux cellulaires en traitant le déploiement de stations mobiles ou stations de base (et) en tant que processus ponctuels de Poisson sur un plan. Ces résultats prennent également en compte l'impact de la mobilité sur la performance de ces réseaux.

Dans cette thèse, nous enrichissons et appliquons la théorie des processus de Poisson spatiaux pour résoudre certains problèmes issus de la conception et du déploiement des réseaux cellulaire. Cette thèse comporte deux parties principales. La première partie est consacrée à la résolution de quelques problèmes de dimensionnement et de couverture des réseaux cellulaires. Nous calculons la probabilité de surcharge de systèmes OFDMA grâce aux inégalités de concentration et aux développements d'Edgeworth, pour lesquels nous prouvons des bornes d'erreur explicites, et nous l'appliquons à résoudre un problème de dimensionnement. Nous calculons également la probabilité d'outage et la taux de handover pour un utilisateur typique.

La seconde partie est consacrée à l'étude de différents modèles pour la consommation d'énergie dans les réseaux cellulaires. Dans le premier modèle, l'emplacement initial des utilisateurs forme un processus de Poisson ponctuel et à chaque utilisateur est associé un processus d'activité de type ON-OFF. Dans le second modèle, l'arrivée des utilisateurs constitue un processus de Poisson en espace et en temps, une dynamique connue sous le nom de dynamique de Glauber. Nous étudions également l'impact de la mobilité des utilisateurs en supposant que les utilisateurs se déplacent de manière aléatoire pendant leur séjour. Nous nous intéressons dans toutes ces situations, à la distribution de l'énergie consommée par une station de base. Cette énergie est divisé en deux parties: la partie additive et la partie diffusive. Nous obtenons des expressions analytiques pour les moments

de la partie additive ainsi que la moyenne et la variance de l'énergie totale consommée. Nous trouvons une borne d'erreur pour l'approximation gaussienne de la partie additive. Nous prouvons que la mobilité des utilisateurs a un impact positif sur la consommation d'énergie. Il n'augmente ni ne réduit l'énergie consommée en moyenne, mais réduit sa variance à 0 en régime de mobilité élevé. Nous caractérisons aussi le taux de convergence en fonction de la vitesse des utilisateurs.

Motivation

Communications cellulaires ont réalisé une évolution incroyable pendant ces vingt dernières années. Les technologiques avancées dans les systèmes cellulaires et la conception cellulaire ont rendu possibles les services que l'on ne pouvait pas imaginer il y a vingt ans. Téléphonie mobile, et plus particulièrement GSM, ont été le premier service dans le monde entier avec plus de 5 milliards les clients d'aujourd'hui.

Les systèmes de troisième génération comme l'UMTS ont essayé pour fournir une interface radio universel adapté à la fois du circuit et des services de transfert de données. Le succès des technologies 3G ont été très décevante au début. Toutefois, les développements récents tels que HSPA, HSPA + et systèmes de quatrième génération tendent à montrer que cellulaire les communications sont maintenant à la veille d'une nouvelle révolution majeure. ces nouveaux technologies va changer le mode de vie de beaucoup de gens en apportant eux de nouveaux services et des services pratiques. Smartphones modernes sont désormais construit sur les plates-formes informatiques mobiles, l'informatique plus avancée et capacités de connectivité que jamais et à des prix abordables. Les gens sont maintenant en mesure d'utiliser les services de données tels que l'accès Internet localisation„ le transfert de fichiers à partir de pratiquement n'importe où, même dans une grande mobilité.

Le trafic de données associés à ces services est de plus en plus importante. D'un point de vue des opérateurs, les ressources sont nécessaire pour satisfaire les demandes des utilisateurs et de remplir la besoin de la qualité de service. Une telle évolution nécessite de plus en plus des ressources du spectre mais, malheureusement, cette ressource est limitée. Par conséquent, les opérateurs ont besoin de concevoir des méthodes de plus en plus inovantes pour dimensioner déployer leur réseau de façon efficace. Planification cellulaire est le processus utilisé pour concevoir, dimensioner et de déployer un réseau mobile prenant en qualité de service contraintes. Il s'agit d'une procédure complexe qui nécessite de prendre en compte de nombreux critères:

- Un opérateur doit répondre à la demande de trafic et de QoS de son clients. Pour atteindre cet objectif, il est nécessaire de déployer ressources des stations de base, antennes, ces routeurs, commutateurs ou liens de transmission. Le dimensionnement est le processus qui détermine le nombre de ressources nécessaires pour satisfaire le trafic et les contraintes de QoS.

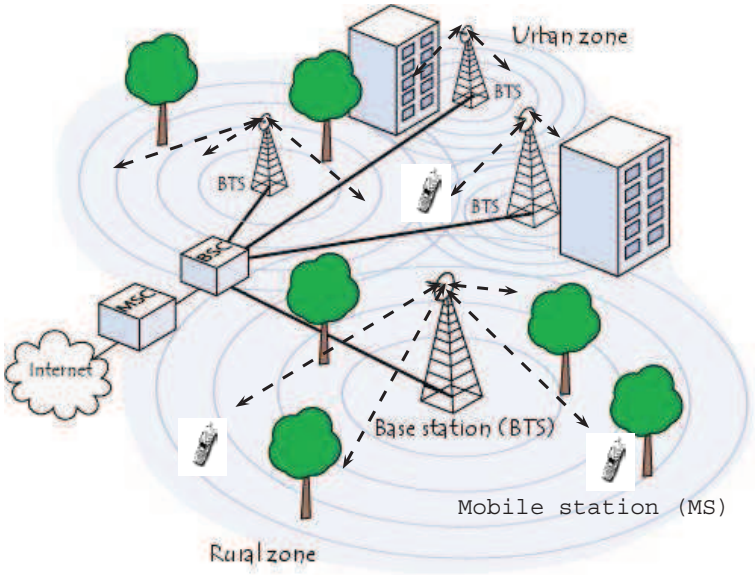


Figure 1: Une architecture typique des réseaux cellulaires (Source: Internet).

- La couverture est le processus qui confère qu'une cellule particulière fournit la qualité radio nécessaires pour se conformer les demandes de QoS des utilisateurs.
- La capacité détermine le nombre d'abonnés qui peuvent être pris en charge par un réseau en tenant compte de la QoS et la contraintes de radio.

De l'autre coté, selon plusieurs études, 0,5% de l'énergie électrique du monde est consommé par réseau cellulaire et 80% de cela est consommée par les sites de stations de base. Jusqu'à 90% de la consommation d'énergie des réseaux cellulaire est des dépenses opérationnelles de l'opérateur (OPEX). Un BS connecté au réseau électrique peut coûter environ 3000 $ par année pour faire fonctionner, tandis qu'un BS hors réseau peut coûter dix fois plus. Compte tenu de la croissance de la consommation énergétique des réseaux mobiles, il devient clair que le coût de l'énergie est essentiel pour l'OPEX des opérateurs. La dépense d'énergie pour faire fonctionner des réseaux cellulaires devrait tripler au cours des sept prochaines années.

D'autre part, la technologie de l'information et de la communication (TIC) est un facteur de plus en plus rapide des émissions de carbone dans le monde. Actuellement il a une superficie d'environ 2%. Dans les TIC, le secteur des communications cellulaires d'aujourd'hui a actuellement une petite part, mais on s'attend à une augmentation significative à l'avenir. La téléphonie mobile compte annuellement pour environ 125 millions de tonnes de carbone, ce qui représente environ 0,25% des émissions mondiales.

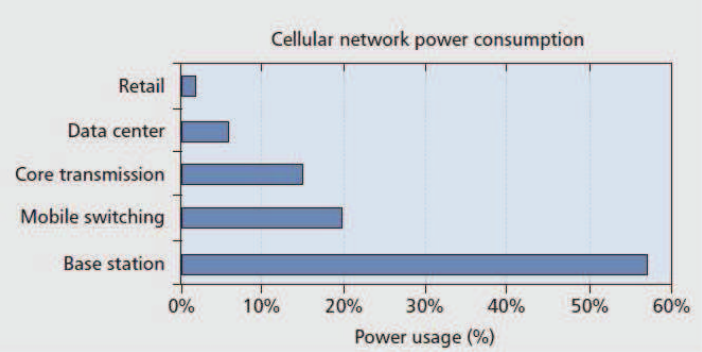


Figure 2: La consommation énergétique dans un réseau cellulaire.

Bien qu'il existe de nombreuses pistes de recherche pour l'optimisation de la consommation d'énergie dans les réseaux cellulaires, étonnamment il n'existe pas de modèle stochastique pour l'analyser. Pour modéliser les réseaux cellulaires, plusieurs approches peuvent être envisagées. Théorie de la file d'atente fournit de bons outils qui ont été adoptées dans de nombreuses études de modélisation cellulaire, principalement pour évaluer le blocage de l'utilisateur, le délai ou la capacité du réseau. Géométrie aléatoire et processus ponctuel de Poisson sont également bien connus comme des outils puissants pour modéliser les réseaux cellulaires. Cependant, jusqu'à cette thèse

"Comment modéliser analytiquement la consommation d'énergie dans le réseau cellulaire de façon stochastique"? est encore une question ouverte. Y at-il un modèle inspiré de la théorie de la queue, la géométrie stochastique et processus ponctuel de Poisson ou peut-être tous?

Etat de l'art

Dans cette section, nous expliquons pourquoi et comment la géométrie stochastique en général et des processus spatiaux ponctuels de Poisson en particulier peuvent modéliser des systèmes de communication sans fil. Nous donnons aussi un bref détail sur Calcul de Malliavin pour les processus de Poisson.

Le premier système de télégraphie sans fil a été inventé il y a un siècle. De nos jours, les systèmes de communication sans fil sont constitués des réseaux cellulaires (comme décrit dans la section précédente), les réseaux ad hoc, réseaux de capteurs, réseaux Wi-Fi et d'autres qui sont appliquées à tous les aspects de la vie. Dans contrairement aux systèmes filaires, des systèmes sans fil il ya une plus grande quantité d'incertitude et de hasard, par example sur les locations de noeud ou de conditions de canal. En général il y a des interférences, car de nombreux noeuds partagent le même canal. Une configuration

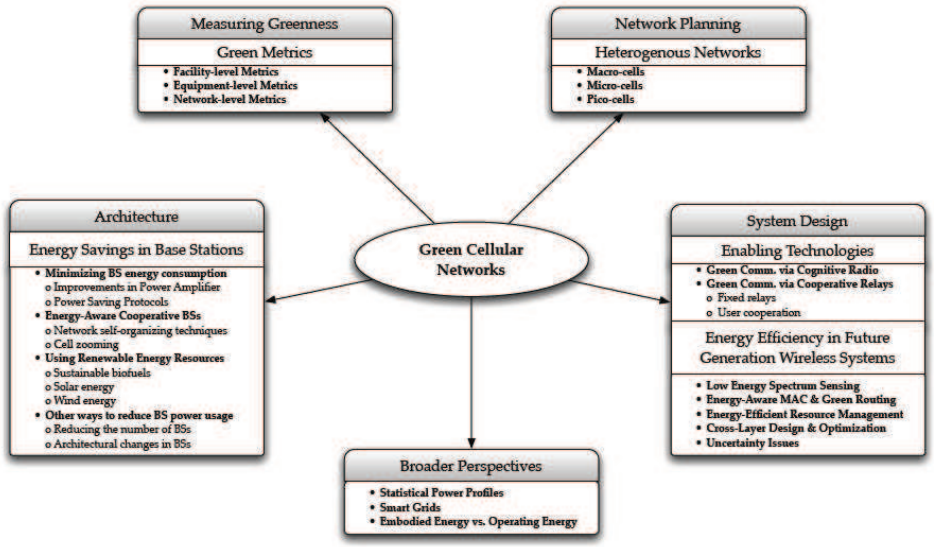


Figure 3: Les axes de recherche actuelles en Green Networking([1]).

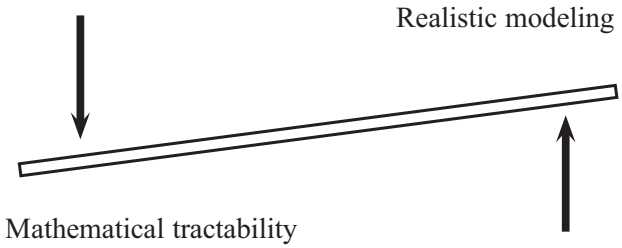


Figure 4: Trade-off between tractability et modélisation réaliste.

d'utilisateurs actifs n'est jamais figé dans le temps: les noeuds peuvent se déplacer ou tout simplement changer leur état. Le signal reçu dépend de la distance entre l'émetteur et le récepteur, et l'état du canal appelé évanouissement, peut varier de temps à autre. Modèles pour les systèmes de communication sans fil doit capturer toutes ces incertitudes et aléas. Cependant, il est difficile de modéliser un système parfaitement: la plus réaliste d'un modèle, moins docile qu'elle est. Il ya toujours un équilibre entre la modélisation réaliste et traçabilité (illustré sur la figure 4).

Processus de Poisson ponctuel est largement utilisée car elle possède le plus grand arsenal de résultats. Il est plus simple à faire des calculs que les autre modèles de processus pontuel et, par conséquent, il est plus tractable. Cette modélisation consiste à traiter l'architecture d'un réseau donnée par un réseau aléatoire et de l'analyser de façon statistique. Déterminer les performances du réseau avec la configuration déterministe de noeuds est beaucoup plus difficile. Processus ponctuel de Poisson, d'autre part, permet de caractériser le comportement moyen sur de nombreuses réalisations spatiales (snapshot) d'un

réseau. Il est également utilisé pour faire des modèles la configuration de noeuds varier en temps et de la mobilité, pour la première fois, dans cette thèse.

Depuis les travaux [2], [3], processus ponctuel de Poisson ont été beaucoup utilisé pour modéliser des systèmes de communication sans fil. Il est utilisé avec succès pour caractériser la distribution d'interférence, probabilité d'outage, la capacité, la connectivité ou retard dans les grands réseaux ad hoc [4],[5], [6], [7], [8], etc, voir aussi [9] ou [10] pour un panorama. Il est également utilisé pour étudier la performance et l'optimisation des réseaux de capteurs [11], [12], etc. Processus ponctuel de Poisson est appliqué sur les réseaux cellulaires comme dans [13], [2], [14], etc.

Processus ponctuel de Poisson, avec calcul de Malliavin et la méthode de Stein, a permis à la communauté de la recherche pour obtenir des résultats théoriques [15], [16], [17], [18].. Toutefois, l'application de ces mathématiques modernes sur les réseaux de communication sans fil est très limité. Ce n'est que récemment, il a été appliqué pour résoudre le problème de la couverture complète sur les réseaux de capteurs, voir [19]..

Les outils de base de calcul de Malliavin consistent en un gradient et un opérateur de divergence qui sont reliés par une formule d'intégration par parties. Pour un processus ponctuel de Poisson w dans un espace E et une fonctionnel F dépendant de w, l'opérateur gradient D_y peut être défini par $D_yF(w) = F(w \cup y) - F(w)$ avec $y \in E$. Une base de l'analyse stochastique des processus de Poisson est que, pour une large classe de la variable aléatoire F , la représentation du chaos de F est garantie:

$$F = \sum_{n=0}^{\infty} \frac{1}{n!} I_n(f_n)$$

où I_N est une intégrale multiple de Poisson et la fonction f_n est calculé grâce à l'opérateur gradient.

$$f_n(y_1, ..., y_n) = \mathbf{E}\left[D_{y_1} ... D_{y_n} F\right] \cdot$$

C'est intéressant de noter que c'est similaire à la manière dont le développement de Taylor en analyse classique est établie:

$$g(x) = \sum_{n=0}^{\infty} a_n \frac{x^n}{n!} \quad \text{where} \quad a_n = \frac{\partial^n g}{\partial x^n}(0).$$

Voici la correspondance:

Analyse	Analyse stochastique
$f(x)$	F
$f(0)$	$\mathbf{E}\left[F\right]$
$\frac{\partial^n g}{\partial x^n}$	D^n
$\frac{\partial^n g}{\partial x^n}(0)$	$\mathbf{E}\left[D^n F\right]$

Contributions

Ce travail vise à fournir de nouveaux modèles qui peuvent être appliqués dans le processus de planification cellulaire. Les modèles proposé prennent en compte de l'effet de la distribution spatiale des utilisateurs et des stations de base. Les enquêtes menées dans ce travail s'appuient de façon significative sur la géométrie stochastique, théorie des processus ponctuels et méthodes de distribution de probabilité d'approximation. Le plus important contributions de ces enquêtes peuvent être classés dans la les trois domaines suivants:

- Cette thèse propose de nouveaux modèles spatiaux pour l'évaluation de performance de plusieurs aspects des réseaux OFDMA. Le premier problème abordée est le dimensionnement d'une cellule OFDMA en termes de ressources des blocs ou des sous-canaux. Le but est de trouver des expressions analytiques de la probabilité de blocage. Deux approches différentes ont été considéré. Dans une première approche, la borne supérieure de la probabilité de blocage a été calculée. Cette borne est assez grossier, mais toujours surdimensionner les ressources nécessaires dans la cellule. L'excès de ressources a un avantage. Il offre une certaine robustesse contre la inexactitude de modélisation de la propagation radio. Une seconde approche repose sur les méthodes d'approximations (l'expansions d'Egdeworth). Ils donnent estimations précises de la probabilité de blocage pour la radio bien connu paramètres de propagation, mais au détriment d'un manque de robustesse. Une borne d'erreur de l'expansions d'Egdeworth a également été dévéloppée. Cette borne donne un surdimensionnement acceptable si on a la connaissance précise des paramètres du réseaux.

- Outage et handover sont deux issues cruciales dans les systèmes cellulaires. Outage est étroitement liée à la couverture. Probabilité d'outage fournit un indicateur de la qualité de couverture dans un réseau. Cette thèse développe des expressions plus général desprobabilités d'outage en faisant l'hypothèse que les stations de base répartissent suivant un processus de Poisson dans le plan. Les performances de handover est aussi une centrale question. Cette métrique est nécessaire pour avoir une estimation de la handover du trafic et donc de dimensionner proprement les cellules. Les expressions fermées pour la probabilité de handover sont également développées dans ce travail.

- Enfin la consommation d'énergie dans les réseaux cellulaires est également pris en compte dans ce travail. La thèse propose des modèles qui rendent possible d'estimer la consommation d'énergie dans une cellule en tenant le trafic et la distribution spatiale de compte d'utilisateurs. Ces modèles peuvent être utilisés à des sites dimensions qui n'ont pas accès à l'alimentation électrique ou d'optimiser le rayon des cellules.

Cette thèse se compose de trois parties. La première partie présente les éléments du processus de Poisson. La deuxième partie est une application pour dimensionner le système

OFDMA. La deuxième partie applique la théorie présentée dans la première partie d'étudier la consommation énergétique de réseaux cellulaires. Nous résumons le contenu de chaque chapitre de cette thèse en plus de détails dans la suite.

Chapitre 2 donne une introduction et des résultats sur le processus ponctuel de Poisson que nous utiliserons tout au long de la thèse. Nous définissons d'abord le processus de Poisson d'une manière compréhensible et présentons quelques propriétés importantes telles que la distribution du nombre de points et le théorème de Campbell ou de certaines opérations préservant de la loi de Poisson. Nous étudions ensuite la distribution des fonctionnelles linéaires dépendant d'un processus de Poisson car beaucoup de fontionnelles d'intérêt ont cette forme. Nous présentons une borne supérieure sur la distribution(appelée l'inégalité de concentration) et une borne d'erreur d'approximation gaussienne de telles fonctionnelles. Nous passons ensuite au calcul de Malliavin sur le processus de Poisson. Elle permet de décomposer un grand famille de fonctionnelles dépendantes du processus ponctuel de Poisson comme la somme orthogonale de chaos, où le n^{ime} chaos est la contribution de chaque ensemble de n points de la processus. Bornes sur la distribution et l'approximation Gaussienne d'une fonctionnelle générale est également présentée, qui généralisent les résultats dans le cas linéaire.

Voici les nouveaux résultats dans le chapitre 2. Considérons un processus de Poisson w d'intensité $\lambda\nu$ et une fonction f de E à $\mathbb{R}$. Définissons $\sigma = \|f\|_{L^2(\nu)}\sqrt{\lambda}$ et $f_\sigma = f/\sigma$. Considérons le fonctionel

$$N^\lambda = \int_E f_\sigma(x)(\,\mathrm{d}\,w(z) - \lambda\,\mathrm{d}\,\nu(z)) = \overline{F}_\lambda - \mathbf{E}\left[\overline{F}_\lambda\right].$$

Définissons également

$$m(p,\,\lambda) := \int_E |f_\sigma(z)|^p \lambda\,\mathrm{d}\,\nu(z) = \|f\|_{L^2(\nu)}^{-p}\|f\|_{L^p(\nu)}^p \lambda^{1-p/2}.$$

Les polynômes d'Hermite sont définis par

$$H_k(x)\Phi(x) = (-1)^k \frac{d^k}{dx^k}\exp(-x^2/2)/\sqrt{2\pi}.$$

Les polynômes de Bell $B_n(a_1, ..., a_n)$ sont définies comme suivant

$$\exp\left\{\sum_{n=1}^{\infty}\frac{a_n}{n!}\theta^n\right\} = \sum_{n=1}^{\infty}\frac{B_n(a_1, a_2, ..., a_n)}{n!}\theta^n$$

for all $a_1, ..., a_n$ and θ such that all above terms are correctly defined.

Les cinq premiers polynômes de Bell sont:

$$\begin{aligned} B_1(a_1) &= a_1 \\ B_2(a_1,a_2) &= a_1^2 + a_2 \\ B_3(a_1,a_2,a_3) &= a_1^3 + 3a_1a_2 + a_3 \\ B_4(a_1,a_2,a_3,a_4) &= a_1^4 + 4a_1^2a_2 + 4a_1a_3 + 3a_2^2 + a_4 \\ B_5(a_1,a_2,a_3,a_4,a_5) &= a_1^5 + 10a_1^3a_2 + 10a_1^2a_3 + 15a_1a_2^2 + 5a_1a_4 + 10a_2a_3 + a_5 \end{aligned}$$

On peut calculer les moments d'un fontionel linéaire dépendant d'un processus de Poisson par les polynômes de Bell:

Theorem 1 (Formule de Campbell généralisé)**.** *Les cumulants de* $F = \int_E f \, \mathrm{d}\, w$ *est* $\kappa_i^F = \int_E f^i(z) \, \mathrm{d}\, \nu(z)$ *(*$i = 1..n$*). Les moments and les moments centraux de* F *peuvent être calculés par*

$$\boxed{\mathbf{m}_i[F] = B_i\left(\int_E f(z) \, \mathrm{d}\, \nu(z), \int_E f^2(z) \, \mathrm{d}\, \nu(z), ..., \int_E f^i(z) \, \mathrm{d}\, \nu(z)\right)} \tag{1}$$

and

$$\boxed{\mathbf{c}_i[F] = B_i\left(0, \int_E f^2(z) \, \mathrm{d}\, \nu(z), ..., \int_E f^i(z) \, \mathrm{d}\, \nu(z)\right).} \tag{2}$$

La borne de l'approximation Gaussienne est donnée par le théorème suivant:

Theorem. *Pour n'importe quelle fonction de Lipschitz* G *de* $\mathbb{R}$ *à* $\mathbb{R}$*, on a*

$$\boxed{\left|\mathbf{E}_{\lambda\nu}\left[G(N^\lambda)\right] - \int_{\mathbb{R}} G \, \mathrm{d}\, \mu\right| \leq \frac{1}{2}\sqrt{\frac{\pi}{2}} \, m(3,\, \lambda) \, \|G\|_{Lip}.}$$

On peut aller un peu plus loin dans le dévéloppement, on obtient la borne d'érreur pour le dévéloppement d'Egdeworth dans les deux théorèmes suivants:

Theorem. *Pour* $G \in \mathcal{C}_b^3(\mathbb{R}, \mathbb{R})$*, on a*

$$\boxed{\begin{array}{l} \left|\mathbf{E}_{\lambda\nu}\left[G(N^\lambda)\right] - \int_{\mathbb{R}} G(y) \, \mathrm{d}\, \mu(y) - \frac{1}{6} \, m(3,\, \lambda) \, \int_{\mathbb{R}} G(y) H_3(y) \, \mathrm{d}\, \mu(y)\right| \\ \leq \left(\frac{m(3,1)^2}{6} + \frac{m(4,1)}{9}\sqrt{\frac{2}{\pi}}\right) \frac{\|G^{(3)}\|_\infty}{\lambda}. \end{array}}$$

Theorem. *Pour $G \in \mathcal{C}_b^5$, on a*

$$\boxed{\begin{array}{rcl}\mathbf{E}_{\lambda\nu}\left[G(N^\lambda)\right] & = & \int_{\mathbb{R}} G(y)\ \mathrm{d}\,\mu(y) + \frac{m(3,1)}{6\sqrt{\lambda}} \int_{\mathbb{R}} G^{(3)}(y)\ \mathrm{d}\,\mu(y) + \frac{m(3,1)^2}{72\lambda} \int_{\mathbb{R}} G^{(6)}(y)\ \mathrm{d}\,\mu(y) \\ & & + \frac{m(4,1)}{24\lambda} \int_{\mathbb{R}} G^{(4)}(y)\ \mathrm{d}\,\mu(y) + G_\lambda \|G^{(5)}\|_\infty.\end{array}}$$

où

$$\boxed{G_\lambda \leq \frac{m(3,1)}{\lambda^{3/2}} \left(\frac{2}{45}\, m(3,1)^2 + (\frac{4}{135} + \frac{\pi^2}{128})\sqrt{\frac{2}{\pi}}\ m(4,1) \right).}$$

Le chapitre 3 propose une modèle analytique pour le dimensionnement des réseaux OFDMA base comme les systèmes WiMAX et LTE. Dans tel système, chaque utilisateur demande certainnombre de sous-canaux qui dépend de leur SNR, par conséquent, de leur position et le shadowing qu'ils éprouvent. Le système est surchargé lorsque le nombre de sous-canaux requis est supérieur au nombre de sous-canaux disponibles. Nous donnons une expression exacte mais qui n'est pas fermée de la probabilité de surcharge et de donner ensuite une méthode algorithmique pour calculer le nombre de sous-canaux qui garantit une probabilité de surcharge de moins de'un seuil donné. Nous montrons que approximation gaussienne conduit aux valeurs optimistes et sont donc inutilisables. Nous ensuite introduisons des expansions d'Edgeworth avec des bornes d'erreur et de montrer que, en choisissant le bon ordre de l'expansion, on peut avoir une valeur approximative de dimensionnement facile à calculer et avec des performances garanties. Comme les valeurs obtenues sont fortement dépendante des paramètres du système, qui s'est avéré être plutôt indéterminé, nous fournissons une procédure basée sur l'inégalité de concentration pour des fonctionnelles de processus de Poisson, qui cède à un surdimensionnement. Ce chapitre s'appuie sur des résultats récents sur les inégalités de concentration et établir de nouveaux résultats sur l'expansion Edgeworth présentés dans le chapitre 2. Ce chapitre est basé sur le papier [20], qui a été publiée dans la conférence ValueTools 2012.

Dans le chapitre 4, nous considérons les réseaux cellulaires stochastiques où les emplacements des stations de base constituent un processus ponctuel de Poisson homogène et chaque mobile est connecté à la station de base qui fournit la meilleure puissance de signal en moyen. Le mobile est en outage si le SINR tombe en dessous d'un certain seuil. La décision de handover doit être effectué si le mobile est en outage pendant plusieurs slots de temps. La probabilité d'outage et la probabilité de handover sont évaluées en tenant compte de l'effet de pathloss, shadowing, Rayleigh fading, facteur de réutilisation de fréquence et la formation de conventionel faisceau. L'hypothèse principale est que les fading de Rayleigh changent chaque intervalle de temps mais tous les autres composants du réseau restent statiques pendant la période d'étude. Ce chapitre est basé sur le document de [21], ce qui a été publié dans la conférence WPMC 2012.

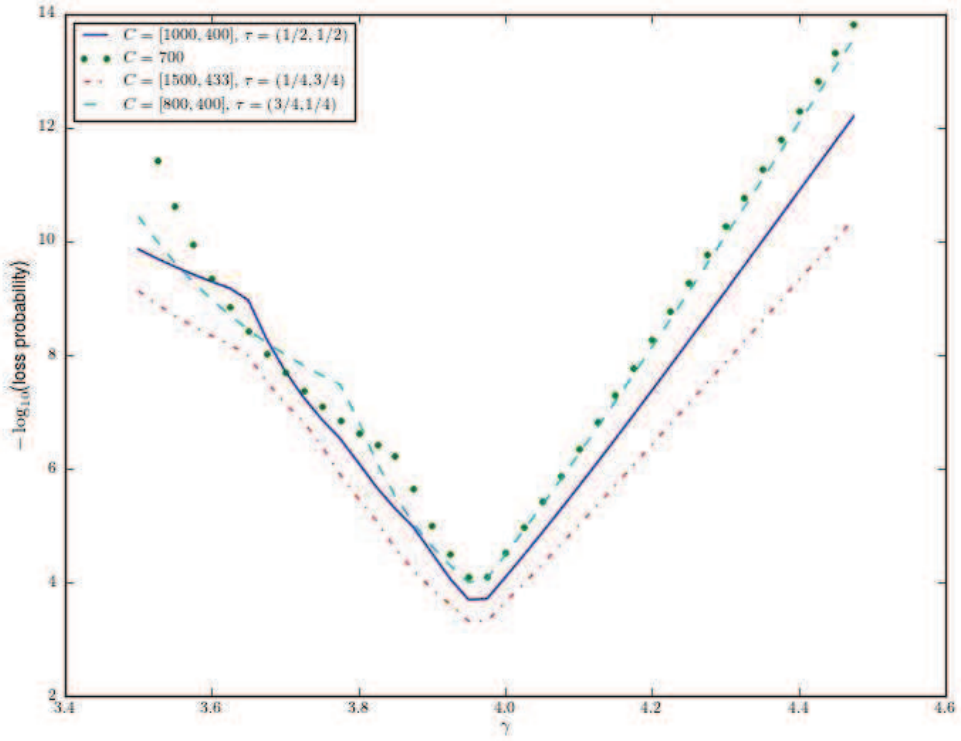


Figure 5: Impact de γ et τ en probabilité de surcharge (chapitre 3)

Chapitre 5 introduit un cadre théorique général pour analyser les réseaux limitées en bruit. Plus précisément, nous considérons deux processus ponctuels de Poisson homogènes de stations de base et des utilisateurs. Général modèle de propagation du signal radio et l'effet de fading sont également pris en compte. La principale différence de notre modèle par rapport à d'autres existant modèles est que l'utilisateur se connecte à ses meilleurs serveurs, mais pas nécessairement le plus proche. Nous fournissons formule générale pour la probabilité d'outage. On étudie fonctionnelles liées au SNR, ainsi que la somme de ceux-ci fonctionnelles entre tous les utilisateurs par cellule. Pour ces derniers, l'espérance et la des bornes sur la variance sont obtenues.

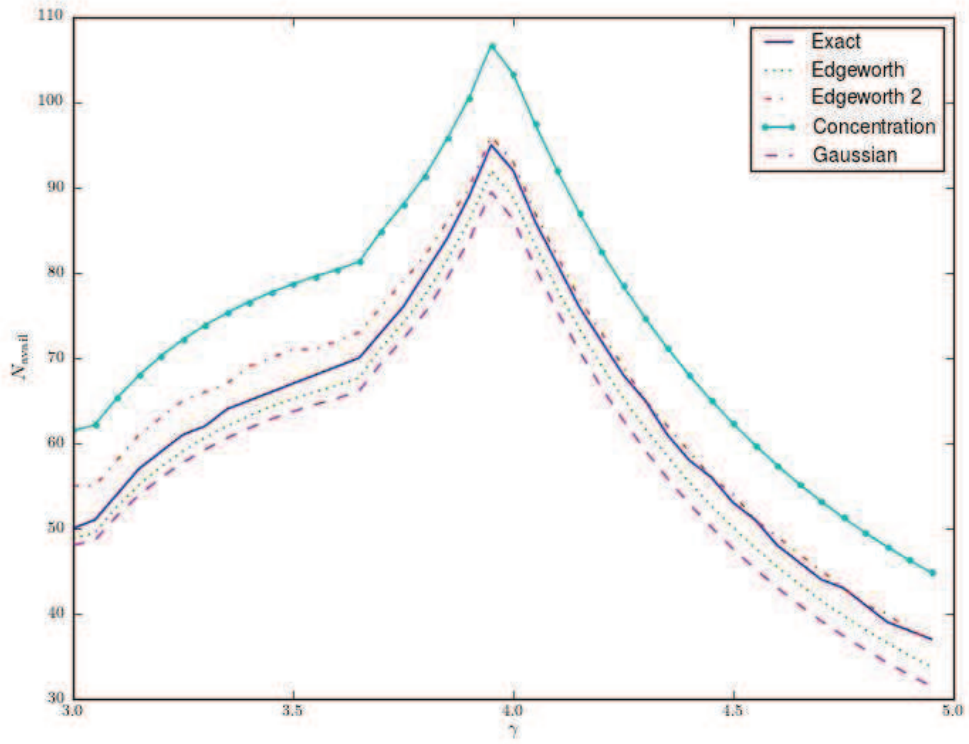


Figure 6: Estimation de N_{avail} en fonction de γ par des différents méthodes (chapitre 3)

Chapitre 6 présente un général modèle de consommation énergétique pour une station de base dans un réseau cellulaire. Nous présentons d'abord la consommation de puissance en tant que fonction de la configuration d'utilisateurs actifs à chaque temps. L'énergie consommée pendant une période de temps est alors définie comme l'intégrale de la puissance consommée au cours de cette durée. Nous divisons l'énergie consommée en deux parties: la une partie de diffusion servi à transmettre le même message à tous les utilisateurs dans la cellule, et la partie additif qui est la somme de tous quantités d'énergie utilisée par chaque utilisateur à la fois dans la voie descendante et la voie montante. Nous introduisons ensuite le modèle général pour la mobilité de l'utilisateur, où trajectoires des utilisateurs sont i.i.d. Enfin, nous étudions un mModèle de base pour chaque instance où la configuration des utilisateurs actifs est un processus ponctuel de Poisson. Nous montrons que la l'énergie consommée est une fonction croissante du rayon de cellule et qu'il y a toujours un rayon de cellule optimale dans le point de vue économique dont on considère le côut de deployement.

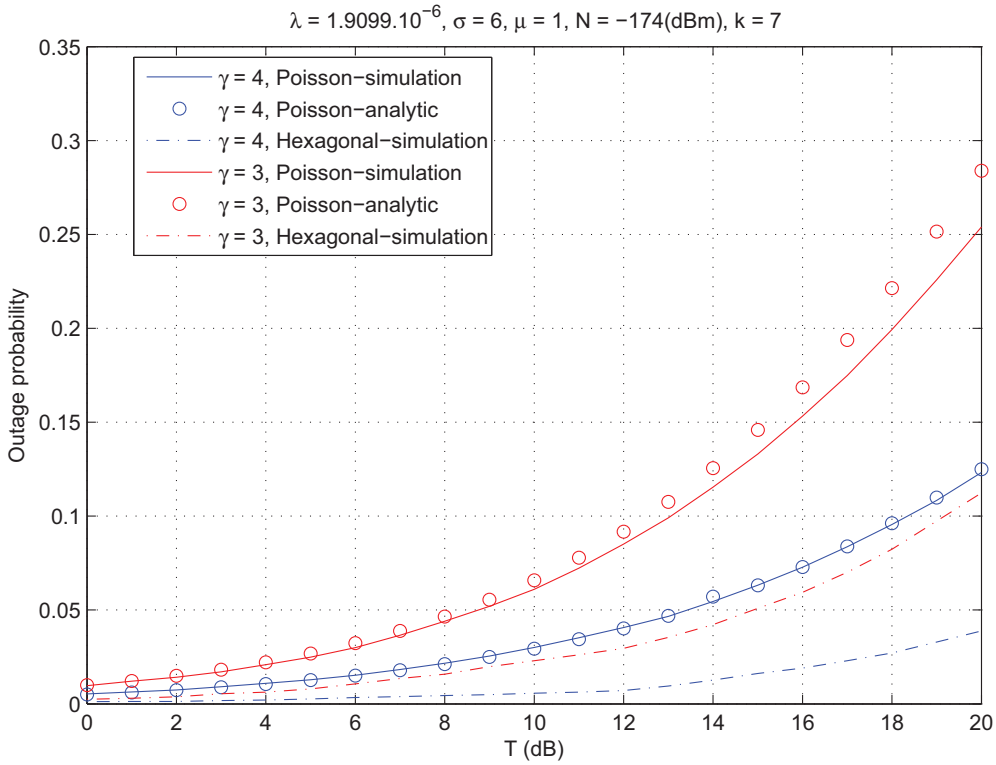


Figure 7: Probabilité d'outage vs le seuil de SINR(chapitre 4)

Nous étudions ensuite la consommation d'énergie de réseau cellulaire en deux modèles de dynamique des utilisateurs. Dans le chapitre 7, nous supposons que chaque utilisateur est associé à une activité ON-OFF processus dans le temps. Dans le chapitre 8 nous ne supposons pas utilisateur soit allumé ou éteint. Au contraire, nous supposons que les utilisateurs arrivent à la suite d'un Poisson point processdans l'espace et le temps et font des communications au cours du temps certains étant modélisée par une variable aléatoire. Nous sommes en mesure de fournir des expressions analytiques pour les statistiques de l'énergie consommée et les bornes de sa distribution. Nous considérons ensuite l'impact de la mobilité et nous montrons que lorsque les utilisateurs déplacent, l'énergie moyenne consommée ne change pas alors que sa variance diminue à zéro lorsque les utilisateurs déplacent rapidement. C'est un très surpris résultat car il est vrai pour n'importe quel modèle de mobilité. Dans le modèle ON-OFF, nous sommes en mesure de caractériser le taux de décroissance de la variance en fonction de la vitesse de l'utilisateur. Dans les deux modèles, nous fournissons des expressions asymptotiques lorsque le système fonctionne pendant un temps très long. Les deux chapitres sont basées sur [22] et [23] qui sont actuellement soumis pour publication.

Liste des publications

Voici la liste des publications réalisées pendant la thèse:

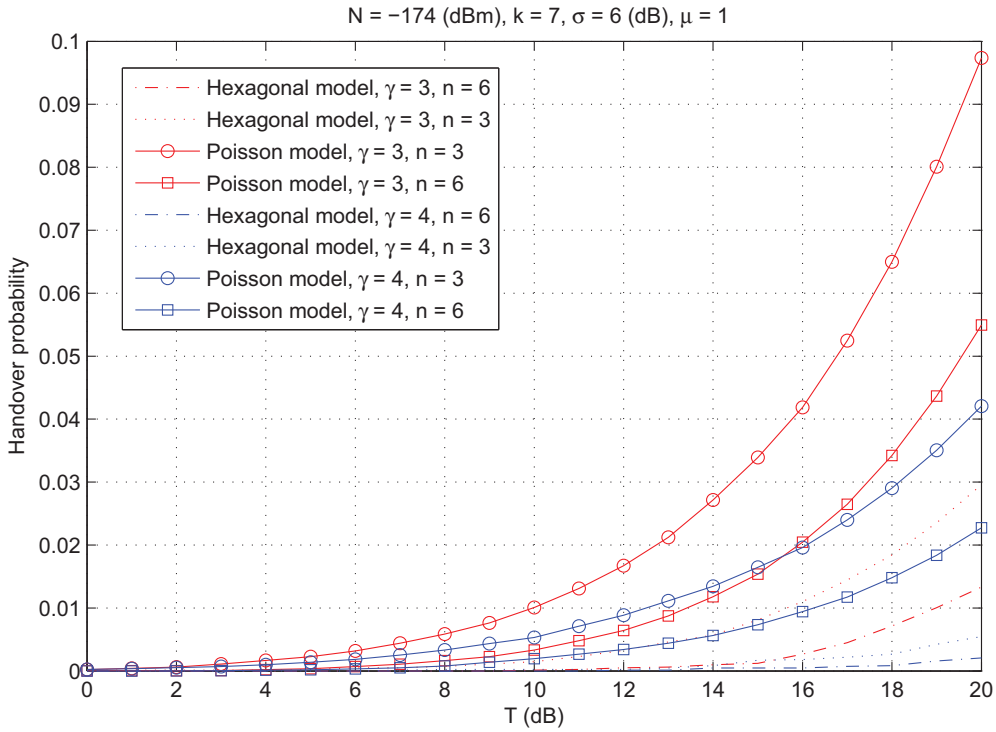


Figure 8: Probabilité de handover vs seuil de SINR (chapitre 4)

- *Robust methods for LTE and WiMAX dimensioning*, L. Decreusefond and E. Ferraz and Ph. Martins and T.-T. Vu , Valuetools 2012, Cargese, France
- *An Analytical Model for Evaluating Outage and Handover Probability of Cellular Networks*, L. Decreusefond and Ph. Martins and T.-T. Vu, WPMC'12, Taipei, Taiwan
- *Energy consumption in cellular network: ON-OFF model and impact of mobility*, L. Decreusefond and Ph. Martins and T.-T. Vu, submitted to IEEE INFOCOM 2013, Turin, Italy
- *Energy consumption in cellular network: Generalized Glauber model*, L. Decreusefond and Ph. Martins and T.-T. Vu, in preparation

Perspectives

Dans cette thèse, nous avons utilisé des modèles abstraits pour analyser la consommation d'énergie sur les réseaux cellulaires qui simplifie hypothèses sur la traffic, la mobilité, ... Notre modèle de consommation d'énergie est seulement à l'état initial et nous avons besoin de beaucoup d'amélioration pour modéliser avec plus de précision. Pourtant, nous avons tirées de ces modèles abstraits d'un grand nombre de résultats intéressants qui méritent d'être poursuivies.

Il y a quelques pistes de recherches futures comme ci-dessous:

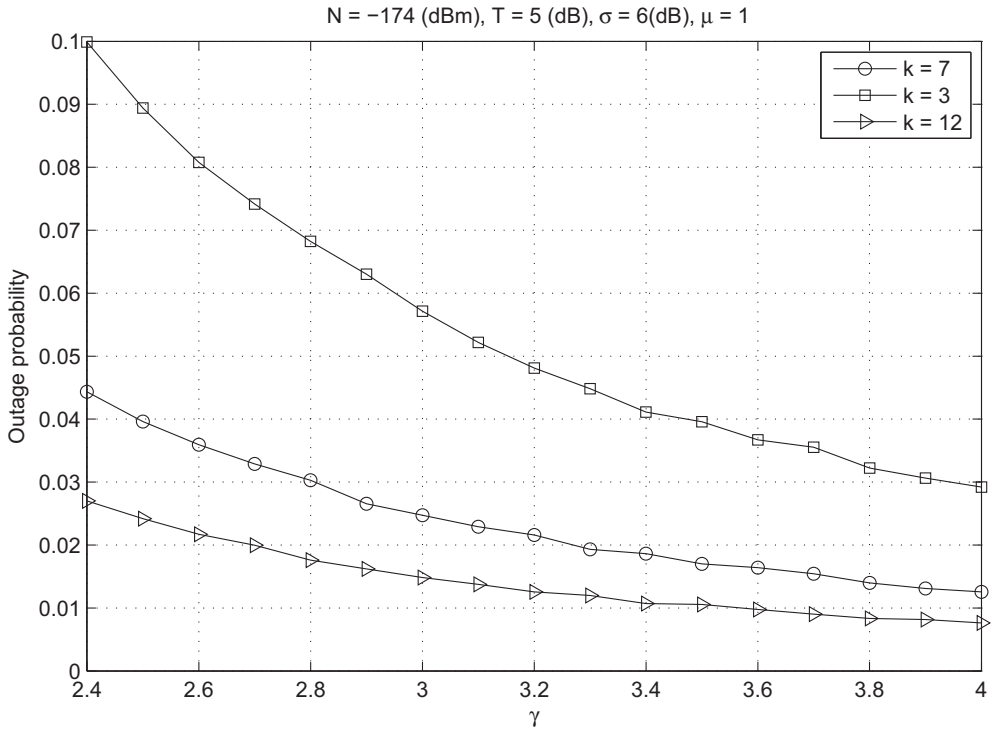


Figure 9: Probabilité d'outage vs path loss exponent γ, modèle de Poisson (chapitre 4)

1. **modèle avec perte:** Dans cette thèse, nous avons supposé que le système ne se limite pas à la puissance transmise ou des ressources de sorte qu'il n'ya pas de perte d'appel. Dans un système réel, comme OFDMA un, la ressource est toujours limité donc il ya toujours une petite fraction de l'appel à être perdu, retardé ou interrompu. Si le système est conçu de telle sorte que la probabilité de perdre une communication est très petite, sans perte sur-modèle peut être une bonne approximation. Cependant, nous aimerions construire un modèle pour désigner cette réalité et nous voulons savoir, par exemple, si la tendance prise par la mobilité est le même que chez les non-perte de modèle. Nous notons que la perte de réseau spatial est déjà considéré dans la littérature citeKarray2007Thesis,[57],[58], ... Il peut être utilisé dans l'analyse ultérieure.

2. **Considérant shadowing, fading, interference:** Pour la raison de traçabilité, nous avons supposé que les canaux entre les utilisateurs et les stations de base ne sont pas affectés par fading ou shadowing. Il est possible de tenir compte de ces éléments dans une recherche future que le système peut également décrit comme un Poisson point process. En outre, le réseau cellulaire est particulièrement limitée par interférence. Par conséquent, il serait intéressant de mesurer l'impact des interférences sur la consommation d'énergie des réseaux cellulaires.

3. **Comparaison avec la simulation / test / données réelles:** Nos modèles de consommation d'énergie sont purement théoriques. En raison de la limite de temps, nous n'avons pas encore construit un simulateur. A l'avenir, nous aimerions comparer les résultats obtenus dans cette thèse à une simulation numérique ou des données

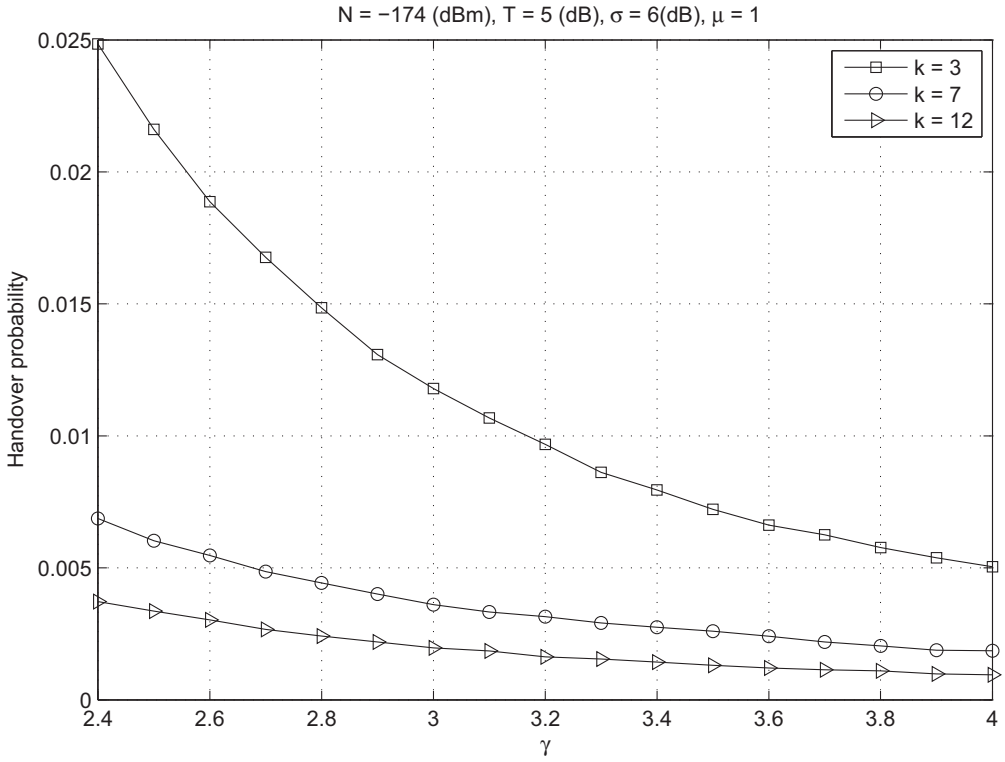


Figure 10: Probabilité de handover vs path loss exponent γ, modèle de Poisson, $n = 3$(chapitre 4)

réelles. Un de notre conclusions est que la mobilité n'a pas d'impact sur la moyenne de consommation d'énergie, mais une grande mobilité diminue sa variance à zéro. Il serait intéressant de voir si cette conclusion est précis dans le monde réel.

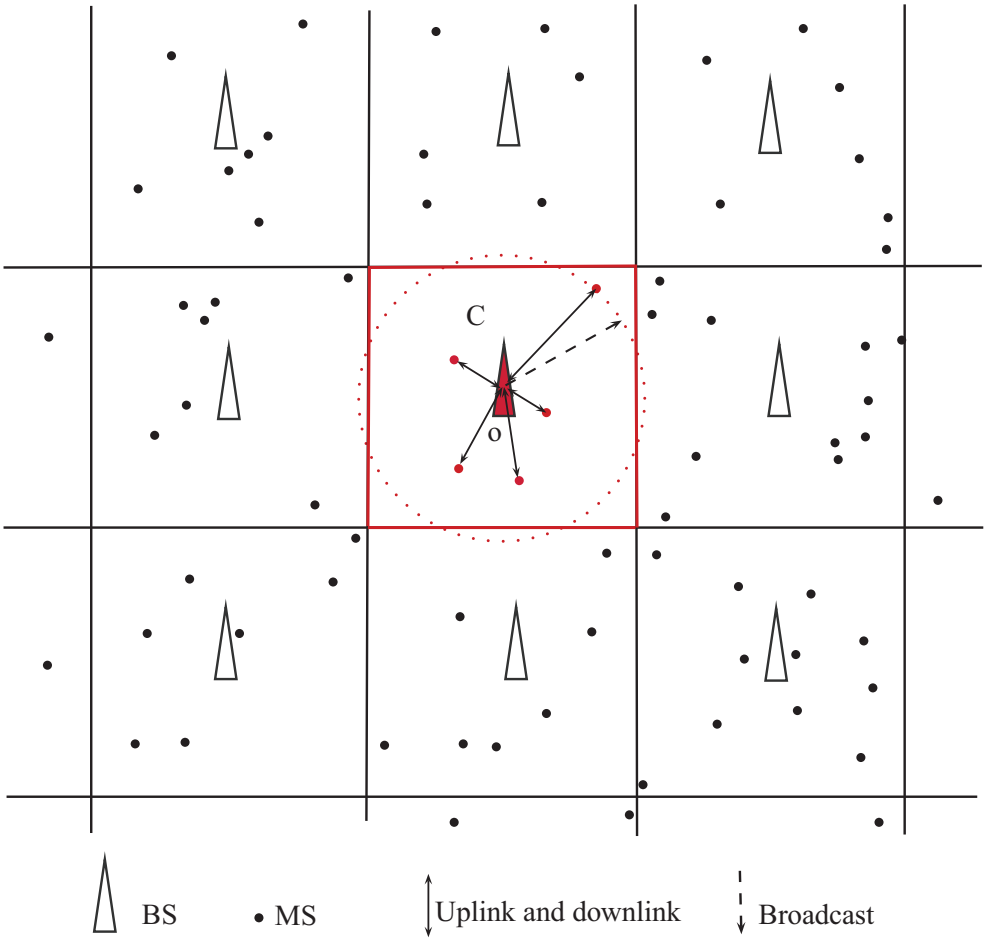


Figure 11: Modèle de consommation de puissance (chapitre 6).

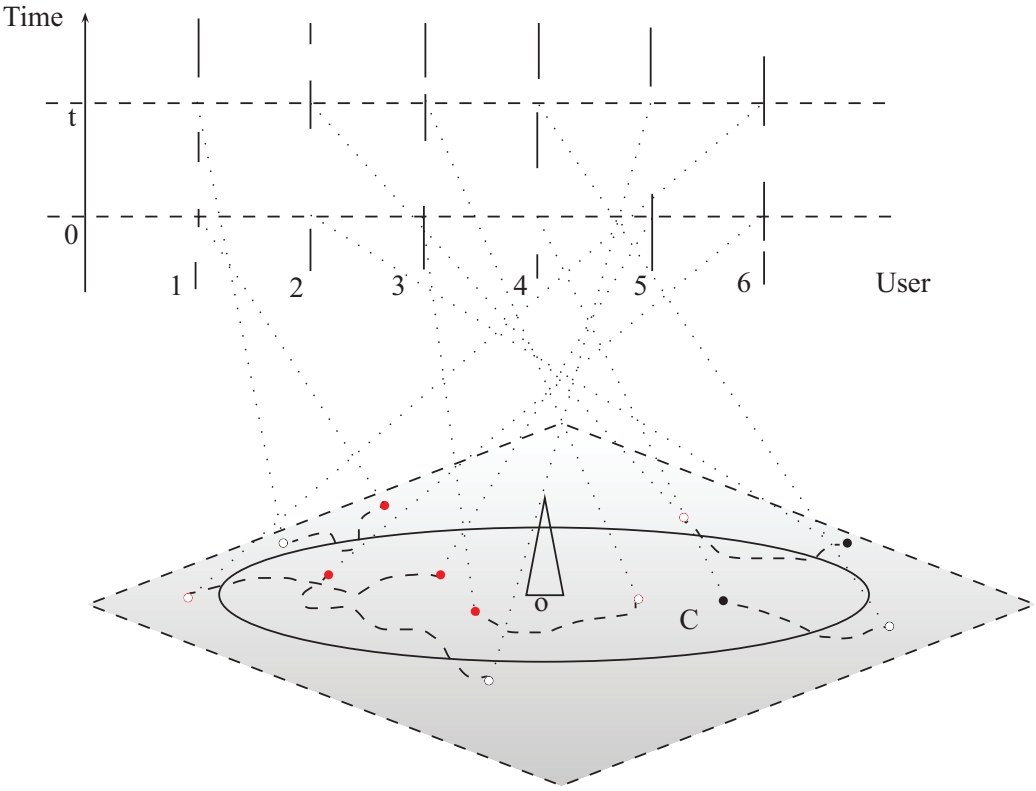


Figure 12: Modèle ON-OFF (chapitre 7).

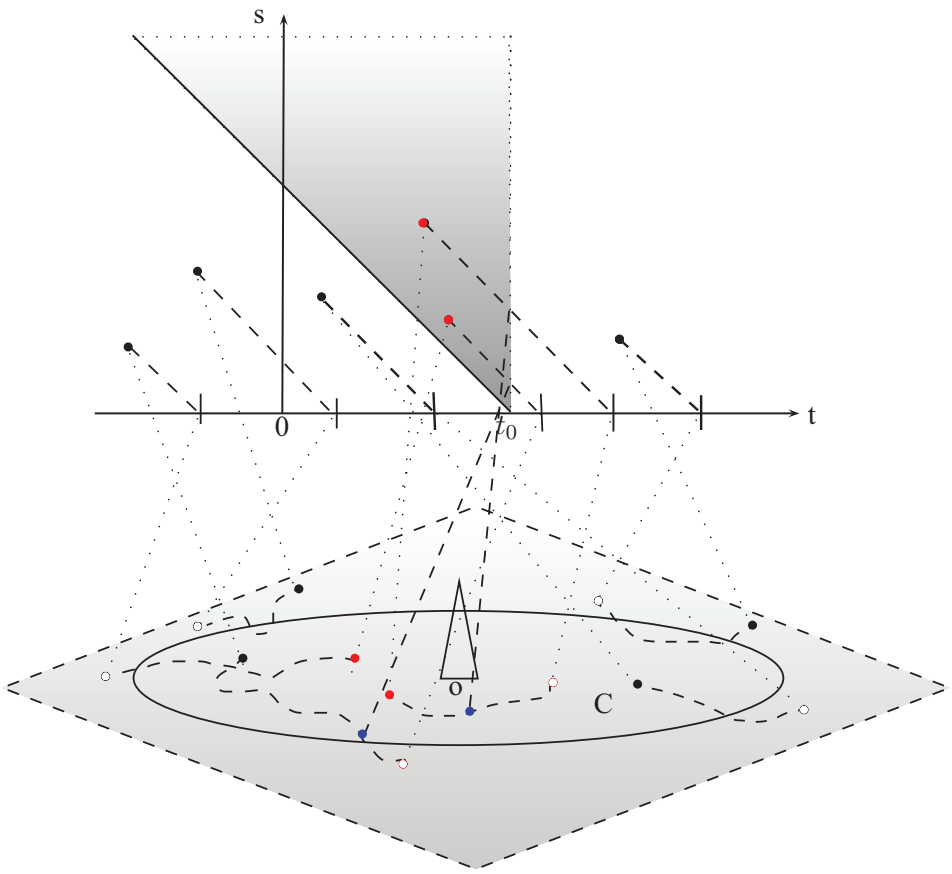


Figure 13: Modèle Glauber généralisé (chapitre 8)

Contents

Page

1 Introduction **5**
1.1 Motivation . . . 5
1.2 Thesis outline and contributions . . . 6
1.3 List of publications . . . 8
1.4 Notations . . . 8

I Mathematical background and contributions **11**

2 Poisson point process **13**
2.1 Introduction . . . 13
2.2 The use of Poisson point process on wireless modelling . . . 13
2.3 Poisson point process . . . 15
2.4 Malliavin calculus on Poisson point process . . . 17
2.5 Distribution of linear functional of Poisson point process . . . 20
2.5.1 Moments . . . 21
2.5.2 Existing results on Gaussian approximation, Edgeworth expansion and concentration inequality . . . 22
2.5.3 New results . . . 25
2.6 Conclusion . . . 27

II Dimensioning and coverage models **29**

3 Robust methods for LTE and WiMAX dimensioning **31**
3.1 Introduction . . . 31
3.2 System Model . . . 34
3.3 Loss probability . . . 36
3.3.1 Exact method . . . 36
3.3.2 Approximations . . . 37
3.3.3 Robust upper-bound . . . 38
3.4 Applications to OFDMA and LTE . . . 39

4 An analytic model for evaluating outage and handover probability of cellular wireless networks **43**
4.1 Introduction . . . 43
4.2 System model . . . 44

4.3 Outage analysis . . . 47
4.4 Handover analysis . . . 48
4.5 Numerical results and comparison to the hexagonal model . . . 50
4.6 Conclusion . . . 51

5 On noise-limited networks 53
5.1 Introduction . . . 53
5.2 Model . . . 54
5.3 Poisson point process of path loss fading . . . 56
5.4 Capacity . . . 59
5.5 Examples . . . 64
5.5.1 Number of users in a cell . . . 64
5.5.2 Number of users in outage in a cell . . . 65
5.5.3 Number of covered users in a cell . . . 65
5.5.4 Total bit rate of a cell . . . 66
5.5.5 Discussion on the distribution of $S_o(f)$ . . . 66
5.6 Conclusion . . . 68

III Energy consumption models 69

6 Presentation of energy consumption model and mobility model 71
6.1 Introduction . . . 71
6.2 Model for energy consumption . . . 71
6.3 Model for mobility of users . . . 74
6.4 Basic model . . . 75
6.5 Conclusion . . . 79

7 ON-OFF model 81
7.1 Introduction . . . 81
7.2 Model . . . 82
7.3 Motionless case . . . 84
7.4 Impact of mobility . . . 89
7.5 Special cases . . . 94
7.5.1 Completely aimless mobility model . . . 94
7.5.2 Always on users . . . 96
7.6 Summary and Conclusion . . . 98

8 Generalized Glauber model 99
8.1 Introduction . . . 99
8.2 Model description and main results . . . 100
8.2.1 Generalized Glauber dynamic . . . 100
8.2.2 Generalized Glauber dynamic with mobility . . . 103
8.3 Analysis in no mobility case . . . 105
8.3.1 Proof of Theorem 49 . . . 110
8.3.2 Proof of theorem 50 . . . 110
8.3.3 Proof of theorem 51 . . . 111
8.4 Impact of mobility . . . 111
8.4.1 Lemmas . . . 111

8.4.2 Proof of Theorem 54 . . . 113
8.4.3 Special case: Completely aimless mobility model . . . 114
8.5 Conclusion . . . 116

IV Conclusion **119**

9 Conclusion and future works **121**
9.1 Summary . . . 121
9.2 Future works . . . 122

10 Appendix **125**
10.1 ON-OFF exponential process: Basic properties . . . 125
10.2 Hermite polynomials . . . 127
10.3 Ornstein-Uhlenbeck semi-group . . . 127

Bibliography **137**

Chapter 1

Introduction

Contents

1.1 Motivation 5
1.2 Thesis outline and contributions 6
1.3 List of publications 8
1.4 Notations 8

1.1 Motivation

Cellular communications have realized an amazing evolution for the last twenty years. Technological advances in cellular systems and cellular phones design have made possible services that one could not imagine twenty years ago. Mobile telephony, and more particularly GSM, have been the first worldwide service with more than 5 billions customers today. The third generation systems such as UMTS have tried to provide a universal radio interface both adapted to circuit and data services transfer. Success of 3G technologies have been quite disappointing at the beginning. However, recent developments such as HSPA, HSPA+ and fourth generation systems tend to show that cellular communications are now at the eve of a new major revolution. These new technologies will change the way of life of many people by bringing them new convenient utilities and services. Modern smartphones are now built on mobile computing platforms, with more advanced computing and connectivity abilities than ever and at affordable prices. People are now able to use data services such as localization, Internet access, files transferring from almost anywhere even in high mobility.

Data traffic associated with these services is more and more important. From a network operator point of view resources are necessary to satisfy user demands and fulfill quality of service requirements. Such an evolution requires more and more spectrum resources but unfortunately this resource is scarce. As a result network operators need to design more and more efficient methods to design and deploy their network. Cellular planning is the process used to design, dimension and deploy a mobile network taking into quality of service constraints. This is a complex procedure that requires to take into account many criteria :

- An operator needs to satisfy traffic and QoS demands of its customers. To fulfill that objective, it is necessary to deploy resources such base stations, antennas, routers,

switches or transmission links. Dimensioning is the process that determines the number of resources necessary to satisfy traffic and QoS constraints.

- Coverage is the process that grants that a particular cell provides the necessary radio quality to comply with users' QoS constraints.
- Capacity determines the number of subscribers that can be supported by a network taking into account QoS and radio constraints.

This work intends to provide new models that can be applied in the cellular planning process. The proposed solutions model and take into account the effect of spatial distribution of users and bases stations. The investigations carried out in this work rely significantly on stochastic geometry, point process theory and probability distribution approximation methods. The most important contributions of these investigations can be classified into the following three areas:

- This thesis proposes new spatial models for the performance evaluation of several aspects of OFDMA networks. The first problem addressed is the dimensioning of an OFDMA cell in terms of resource blocks or subchannels. The purpose is to find analytical expressions of the blocking probability. Two different approaches have been considered. In a first approach, upper bounds of blocking probability have been computed. These bounds are quite coarse but always overdimension the resources need in the cell. That excess of resources has an advantage. It provides some robustness against the inaccuracy of radio propagation modeling. A second approach relies on approximations methods (Egdeworth expansions). They give accurate estimations of the blocking probability for well known radio propagation parameters but at the expense of a lack of robustness.
- Outage and handover are both critical issues in cellular systems. Outage is tightly related with the coverage issue. Outage probability provides an indicator of the coverage quality in a network. This thesis develops outage probabilities expressions more general than classical expressions obtained in hexagonal or Voronoi Tessellations models. The performance of handover is also a central issue. That metric is necessary to have an estimate of the handover traffic and hence to dimension cells properly. Closed forms for handover probability are also developed in this investigation work.
- Finally energy consumption in cellular networks is also considered in that work. The thesis proposes models that make it possible to estimate energy consumption in a cell taking into account traffic and spatial distribution of users. The proposed models can be used to dimension sites that do not have access to power supply facilities.

1.2 Thesis outline and contributions

This thesis consists of three parts. The first part introduces the elements of Poisson point process. The second part is an application to dimensioning the OFDMA systems. The second part applies the theory presented in the first part to study the energy consumption of cellular networks.

Let us highlight the content of each chapter of this thesis in more details. Chapter 2 gives an introduction and results on Poisson point process that we use throughout this thesis. We first define Poisson point process in an understandable way and present some of

its important properties such as the distribution of the number of points and the Campbell Theorem or some operations preserving the Poisson law. We then study the distribution of linear functionals depending on a Poisson point process as many functionals of interest have this form. We present an upper bound on tail distribution (called concentration inequality) and an error bound of Gaussian approximation of such functionals. We then turn to the Malliavin calculus on Poisson point process. It allows one to decompose a large family of functional depending on Poisson point process as the sum of orthogonal chaos, where the n^{th} chaos is the contribution of every set of n points of the process. Bounds on the tail distribution and Gaussian approximation of a general functional is also presented, that generalize bounds in the linear case.

The chapter 3 proposes an analytic model for dimensioning OFDMA based networks like WiMAX and LTE systems. In such a system, users require a number of subchannels which depends on their SNR, hence of their position and the shadowing they experience. The system is overloaded when the number of required subchannels is greater than the number of available subchannels. We give an exact though not closed expression of the loss probability and then give an algorithmic method to derive the number of subchannels which guarantees a loss probability less than a given threshold. We show that Gaussian approximation leads to optimistic values and are thus unusable. We then introduce Edgeworth expansions with error bounds and show that by choosing the right order of the expansion, one can have an approximate dimensioning value easy to compute and with guaranteed performance. As the values obtained are highly dependent from the parameters of the system, which turned to be rather undetermined, we provide a procedure based on concentration inequality for Poisson functionals, which yields to conservative dimensioning. This chapter relies on recent results on concentration inequalities and establish new results on Edgeworth expansions presented in the chapter 2. This chapter is based on the paper [20], which is accepted for publication.

In the chapter 4, we consider stochastic cellular networks where base stations locations form a homogeneous Poisson point process and each mobile is attached to the base station that provides the best mean signal power. The mobile is in outage if the SINR falls below some threshold. The handover decision has to be made if the mobile is in outage during several time slots. The outage probability and the handover probability are evaluated in taking into account the effect of path loss, shadowing, Rayleigh fast fading, frequency factor reuse and conventional beamforming. The main assumption is that the Rayleigh fast fading changes each time slot while other network components remain static during the period of study. This chapter is based on the paper [21], which is accepted for publication.

Chapter 5 introduces a general theoretical framework to analyze noise limited networks. More precisely, we consider two homogenous Poisson point processes of base stations and users. General model of radio signal propagation and effect of fading are also considered. The main difference of our model with respect to other existing models is that a user connects to his best servers but not necessarily the closest one. We provide general formula for the outage probability. We study functionals related to the SNR as well as the sum of these functionals over all users per cell. For the latter, the expectation and bounds on the variance are obtained.

Chapter 6 presents a general energy consumption model for a base station in a cellular network. We first introduce the power consumption as a function of the configuration of active users at each time. The energy consumed during a time period is then defined as the integral of the consumed power during this duration. We divide the consumed energy into two parts: the broadcast part served to transmit the same message to all users

in the cell, and the additive part which sums up all the energy used by each user both in downlink and uplink modes. We then introduce the general model for user's mobility, where trajectories of users are i.i.d. Finally we study a basic model where for each instance the configuration of active users is a Poisson point process. We show that the consumed energy is an increasing function of the cell radius and that there is always an optimal cell radius in the economical point of view.

We then study the energy consumption of cellular network in two models for dynamic of users. In the chapter 7, we assume that each user is associated with an activity ON-OFF process in time. In the chapter 8 we no longer assume that a user is on or off. Rather we assume that users arrive following a Poisson point process in space and time and make communications during certain time being modeled by a random variable. We are able to provide analytic expressions for statistics of consumed energy and bounds on its distribution. We then consider the impact of mobility and we show that when users move, the average consumed energy does not change while its variance decreases to zero when users move fast. This is a strong result as it holds true for any mobility model. In the ON-OFF model we are able to characterize the decay rate of variance in function of user's speed. In both models, we provide asymptotic expressions when the system works for a very long time. The two chapters are based on [22] and [23] which are currently submitted for publication.

1.3 List of publications

Here is the list of publications:

- *Robust methods for LTE and WiMAX dimensioning*, L. Decreusefond and E. Ferraz and Ph. Martins and T.-T. Vu , Valuetools 2012, Cargese, France
- *An Analytical Model for Evaluating Outage and Handover Probability of Cellular Networks*, L. Decreusefond and Ph. Martins and T.-T. Vu, WPMC'12, Taipei, Taiwan
- *Energy consumption in cellular network: ON-OFF model and impact of mobility*, L. Decreusefond and Ph. Martins and T.-T. Vu, submitted to IEEE INFOCOM 2013, Turin, Italy
- *Energy consumption in cellular network: Generalized Glauber model*, L. Decreusefond and Ph. Martins and T.-T. Vu, in preparation

1.4 Notations

Tables 1.2 and 1.1 present all mathematical notations and abbreviations used throughout this thesis.

Abbreviation	Explanation
LHS	Left hand side
RHS	Right hand side
PDF	Probability density function
CDF	Cumulative distribution function
CCDF	Complementary cumulative distribution function
BS	Base station
Càdlàg (function)	Right continuous with left limits (function)

Table 1.1: Abbreviations

Symbols	Definition
$\mathbb{R}^+$	$[0,\infty)$
D	differential operator
$\mathbf{P}(A)$	probability of event A
$\mathbf{E}[X]$	expectation of random variable X
$\mathbf{V}[X]$	variance of random variable X
$\mathbf{m}_n[X]$	n^{th} order moment of random variable X
$\mathbf{c}_n[X]$	n^{th} order central moment of random variable X
$p_X(t)$	PDF of the random variable X
$F_X(t)$	CDF of real random variable X
$\overline{F}_X(t)$	CCDF function (tail distribution) of real random variable X
λ_n^X	n^{th} order standardized cumulant of real random variable X
$\mathbf{B}(x,r)$, $\mathbf{B}_d(x,r)$	ball of radius r centered at x (in d dimension)
$\overline{\mathbf{B}}(x,r)$, $\overline{\mathbf{B}}_d(x,r)$	$\mathbb{R}^d/\mathbf{B}(x,r)$
$\mathbf{1}_{\{A\}}(x)$	indicator function
$\mathbf{C}[X,Y]$	covariance of two random variable X,Y
o	the origin (of $\mathbb{R}^d$)
C	usually designated to the cell administered by the BS located at o
$C(r)$	$C \cap \mathbf{B}(o,r)$
$\overline{C}(r)$	$C \cap \overline{\mathbf{B}}(o,r)$
$Q(u) = \frac{1}{\sqrt{2\pi}} \int_{-\infty}^{u} e^{-\frac{x^2}{2}} \,\mathrm{d}\, x$	CDF of a standard Gaussian random variable
$\overline{Q}(u) = \frac{1}{\sqrt{2\pi}} \int_{u}^{\infty} e^{-\frac{x^2}{2}} \,\mathrm{d}\, x$	CCDF of a standard Gaussian random variable
$u \wedge v$	$\min\{u,v\}$ for $u,v \in \mathbb{R}$
$u \vee v$	$\max\{u,v\}$ for $u,v \in \mathbb{R}$
$L^n(E,\nu)$ or $L^n(\nu)$	$\{f : E \to \mathbb{R}, \int_E \lvert f(x)\rvert^n \,\mathrm{d}\,\nu(x) < \infty\}$ where ν is a measure on E ($n > 0$ is not necessarily integer)
$\lVert f\rVert_{L^n(\nu)}$	$(\int_E \lvert f(x)\rvert^n \,\mathrm{d}\,\nu(x))^{\frac{1}{n}}$, L^n-norm
$f(x) \sim g(x)$ as $x \to a$	$\lim_{x\to a} \frac{f(x)}{g(x)} = 1$
$f(x) = \Theta(g(x))$ as $x \to a$	$0 < \liminf_{x\to a} \frac{f(x)}{g(x)} \leq \limsup_{x\to a} \frac{f(x)}{g(x)} < \infty$

Table 1.2: Mathematical notations.

Part I

Mathematical background and contributions

Chapter 2

Poisson point process

Contents

2.1 Introduction 13
2.2 The use of Poisson point process on wireless modelling 13
2.3 Poisson point process 15
2.4 Malliavin calculus on Poisson point process 17
2.5 Distribution of linear functional of Poisson point process . . . 20
2.5.1 Moments 21
2.5.2 Existing results on Gaussian approximation, Edgeworth expansion and concentration inequality 22
2.5.3 New results 25
2.6 Conclusion 27

2.1 Introduction

In this chapter, we review main mathematical results used in this thesis. We first present the application of stochastic geometry and Poisson point process in wireless networks. We then define Poisson measure on Polish space and Poisson point process. We study the distribution of linear functional of Poisson point process. We introduce some basics of Malliavin calculus on Poisson space then present results on a large class of functional of Poisson point process. We derive useful results concerning Poisson point process. Materials in this chapter are collected from literature, mainly from [24], [17], [25], [26], [27], [18], [15], [28], [16], and we also add new results from our recent work [20].

2.2 The use of Poisson point process on wireless modelling

In this section, we explain why and how stochastic geometry in general and spatial Poisson point processes in particular can help modeling the wireless communication systems. We also give a brief detail on Malliavin calculus for Poisson point process.

More than a century ago, the first wireless telegraph system was invented. Nowadays, wireless communication systems consist of cellular networks (as described in the previous chapter), ad hoc networks, sensor networks, wi-fi networks and others that are applied to all aspects of life. In contrary to wired systems, in wireless systems there is a much greater

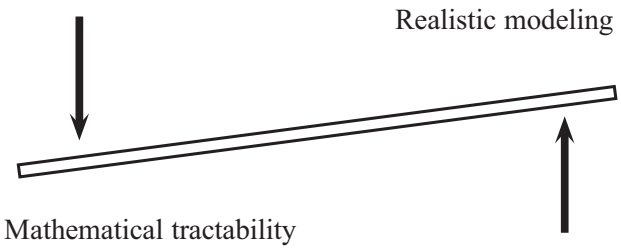


Figure 2.1: Trade-off between tractability and realistic modeling.

amount of uncertainty and randomness on node locations or channel conditions and usually there is interference because many nodes share the same medium. A configuration of active users is never fixed in time: nodes can move or simply change their state. The received signal depends on the distance between the transmitter and the receiver, and the channel's condition called fading, can vary from time to time. Models for wireless communication systems must capture all these uncertainty and randomness. However, it is difficult to model perfectly a system: the more realistic a model is, the less tractable it is. There is always a balance between realistic modeling and tractability (illustrated in figure 2.1).

Poisson point process is widely used because it has the largest arsenal of results. It is more simple to deal with than other point process model and more importantly, it is more tractable. This modeling consists of treating the given architecture of the network as random and analyzing it in a statistical way. Determining the network performance with deterministic configuration of nodes is much more difficult. Poisson point process, on the other hand, allows one to characterize the average behavior over many spatial realizations (snapshot) of a network. It also used to model time varying configuration of nodes and mobility, for the first time, in this thesis.

Since the works [2], [3], Poisson point processes have been the basis of stochastic geometry modeling of large wireless communication systems. It is successfully used to characterize the distribution of interference, outage probability, transport capacity, connectivity or delay in large ad hoc networks [4],[5], [6], [7], [8], etc, see also [9] or [10] for an overview. It is also used to study the performance and optimization of sensor networks [11], [12], etc . Poisson point process is applied on cellular networks as in [13], [2], [14], etc.

Poisson point process, together with Malliavin calculus and Stein method, has allowed the research community to obtain theoretical results [15], [16], [17], [18]. However the application of this modern mathematics on wireless communication networks is very limited. Only recently, it was applied to solve the problem of full coverage on sensor networks, see [19].

The basic tools of Malliavin calculus consist in a gradient and a divergence operator which are linked by an integration by parts formula. For a Poisson point process w in a space E and a functional F depending on w, the gradient operator D_y can be defined by $D_yF(w) = F(w \cup y) - F(w)$ with $y \in E$. A basic of the stochastic analysis of Poisson point process is that for a large class of random variable F, the chaos representation of F is guaranteed:

$$F = \sum_{n=0}^{\infty} \frac{1}{n!} I_n(f_n)$$

where I_n is the multiple Poisson integral and the function f_n is computed thanks to the

gradient operator.

$$f_n(y_1, ..., y_n) = \mathbf{E}\left[D_{y_1}...D_{y_n}F\right].$$

Interestingly, this is similar to the way as Taylor expansion in analysis is established:

$$g(x) = \sum_{n=0}^{\infty} a_n \frac{x^n}{n!} \quad \text{where} \quad a_n = \frac{\partial^n g}{\partial x^n}(0).$$

Here we have the correspondence:

Analysis	Stochastic analysis
$f(x)$	F
$f(0)$	$\mathbf{E}[F]$
$\frac{\partial^n g}{\partial x^n}$	D^n
$\frac{\partial^n g}{\partial x^n}(0)$	$\mathbf{E}[D^n F]$

Basics and results on Poisson point process are presented in details in the next section.

2.3 Poisson point process

Let E be a $\sigma-$compact metric space (i.e E can be partitioned into a countable union of compact metric spaces) with a diffuse Radon measure ν. The space of configurations of E is the set of locally finite simple point measures

$$\Omega^E := \left\{ w = \sum \epsilon_{z_i} (\text{at most countable}), z_i \in E \right\},$$

where ϵ_z denotes the Dirac measure at $z \in E$, i.e

$$\epsilon_z(A) = \mathbf{1}_{\{z \in A\}}, A \in \mathcal{B}(E).$$

Here, simple measure means that $w(\{z\}) \leq 1$ and locally finite measure means that $w(K) < \infty$ for all compact $K \subset E$. The configuration space Ω^E is endowed with the vague topology and its associated σ-algebra denoted by $\mathcal{F}^E$.

For convenience, it is quite often to identify an element $w = \sum \epsilon_{z_i}$ with its corresponding support, i.e the unordered set $\{z_1, ..., z_n\}, n \in N \cup \{+\infty\}$. Also, $w(A)$ counts the number of points in $A \in \mathcal{B}(E)$. The distribution of point process w is characterized by the family of finite dimensional distributions $(w(A_1), ..., w(A_n))$ where $A_1, ..., A_n$ are mutually disjoint compact subsets of E.

Definition 1. *w is a Poisson point process (PPP) of intensity ν if for all set $(A_1, ..., A_n)$ of mutually disjoint compact subsets of E:*

$$\mathbf{P}(w(A_1) = k_1, ..., w(A_n) = k_n) = \prod_{i=1}^{n} \left(e^{-\nu(A_i)} \frac{(\nu(A_i))^{k_i}}{k_i!} \right).$$

If $E = \mathbb{R}^d$; $\mathcal{B}$ is Borel algebra of $\mathbb{R}^d$ and $\nu(\mathrm{d}\, z) = \lambda\, \mathrm{d}\, z$, we will call w the homogenous Poisson point process with intensity parameter λ on $\mathbb{R}^d$.

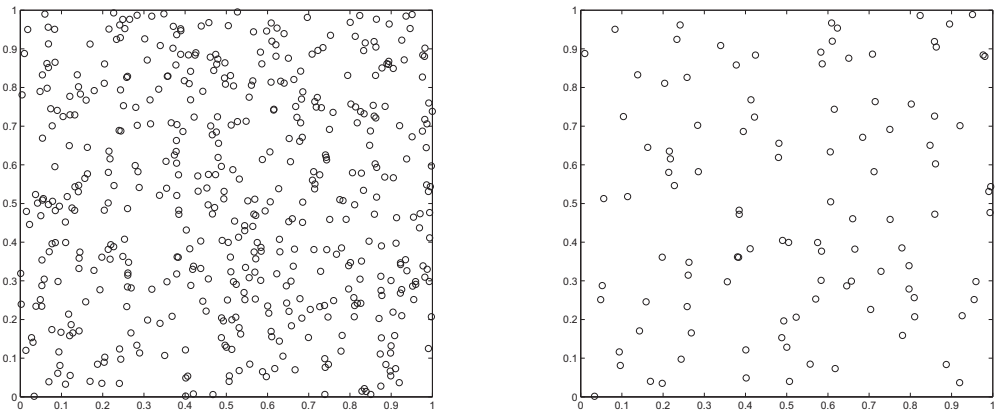


Figure 2.2: A realization of homogenous Poisson point process of intensity $\lambda = 2.10^{-3}$ and its thinning with $p(z) = 0.2$.

Roughly speaking, the number of points of w falling into a subset A follows Poisson distribution of parameter $\nu(A)$, and the number of points falling into 2 disjoint subsets are independent.

In what follows, we describe some operations on point process that preserves the Poisson law ([24]).

- (Superposition) For n Poisson point process $w_1, ..., w_n$ of intensities $\nu_1, ..., \nu_n$ ($n < \infty$), we call $w = \sum_{i=1}^{n} w_i$ their superposition. It is well known that w is a Poisson point process with intensity $\nu = \sum_{i=1}^{n} \nu_i$.
- (Thinning) Consider a Poisson point process w of intensity ν and a function $p : E \to [0, 1]$. The thinning of w with retention function p is given by $w^p = \sum \delta_i \epsilon_{z_i}$ where the random variables $\{\delta_i\}_i$ are independent given w and $\mathbf{P}(\delta_i = 1|w) = p(z_i) = 1 - \mathbf{P}(\delta_i = 0|w)$. If p is $\nu-$ measurable then w^p is a Poisson point process of intensity $p\nu$ with $p\nu(A) = \int_A p(z)\, \mathrm{d}\,\nu(z)$.
- (Transformation, displacement theorem) Consider another $\sigma-$compact metric space E' and a probability kernel $p(z, .)$, i.e for all $z \in E$, $p(z, .)$ is a probability measure in E'. The transformation of a Poisson point process w by p with intensity ν in E is defined as $w_p = \sum \epsilon_{z'_i}$ where $z'_1, z'_2, ...$ are independent given w and has the probability $\mathbf{P}(z'_i \in A'|w) = p(z_i, A')$. It is shown that w^p is a Poisson point process of intensity $\nu'(A') = \int_E p(z, A')\, \mathrm{d}\,\nu(z)$.

Consider a second $\sigma-$compact metric space E'. For each point z_i of w, we associate with a random mark $m_i \in E'$. The mark point process $\widetilde{w}$ can be presented as

$$\widetilde{w} = \sum_i \epsilon_{(z_i, m_i)},$$

where ϵ is the Dirac measure on $E \times E'$. $\widetilde{w}$ is said to be independent marked if the marks are mutually independent given a realization of w and the distribution of marks depends only on the location of its parent point $\mathbf{P}(m \in .|w) = \mathbf{P}(m \in .|z) = \mathrm{d}\, K_z(m)$ with a

probability kernel $K_.(.)$ from E to E'. By displacement theorem we can prove that if w is a Poisson point processwith intensity ν, then $\widetilde{w}$ is a Poisson point processin $E \times E'$ with intensity measure:

$$\widetilde{\nu}(A \times A') = \int_A \int_{A'} \mathrm{d}\, K_z(m)\, \mathrm{d}\, \nu(z), \qquad A \subset E, A' \subset E'.$$

If additionally the marks are independent of their parent point, i.e $\mathrm{d}\, M_z(m)$ is the same as $\mathrm{d}\, M(m)$ then $\widetilde{w}$ is a Poisson point processin $E \times E'$ with intensity $\mathrm{d}\, \nu(z) \times \mathrm{d}\, K(m)$.

2.4 Malliavin calculus on Poisson point process

In this section we introduce basics of Malliavin calculus on Poisson space and then present some results on general functional depending on a Poisson point process.

A real function $f : E^n \to \mathbb{R}$ is called symmetric if

$$f(z_{\sigma(1)}, \cdots, z_{\sigma(n)}) = f(z_1, \cdots, z_n)$$

for all permutations σ of $_n$.

The space of symmetric square integrable random variables with respect to ν is denoted by $L^2(\nu)^{\circ n}$. Let $\Delta_n = \{(z_1, \cdots, z_n) \in E^n \mid z_i \neq z_j, \forall i \neq j\}$. For $f \in L^2(\nu)^{\circ n}$, the multiple Poisson stochastic integral $I_n(f_n)$ is then defined as

$$I_n(f_n)(w) = \int_{\Delta_n} f_n(z_1, \cdots, z_n)(\mathrm{d}\, w(z_1) - \mathrm{d}\, \nu(z_1)) \cdots (\mathrm{d}\, w(z_n) - \mathrm{d}\, \nu(z_n)).$$

It is well known that,

$$\mathbf{E}\left[\sum_{\substack{z_i \neq z_j \in w \\ 1 \leq i < j \leq n}} f(z_1, \cdots, z_n)\right] = \int_{E^n} f(z_1, \cdots, z_n)\, \mathrm{d}\, \nu(z_1) \cdots \mathrm{d}\, \nu(z_n). \tag{2.1}$$

If $n = 1$, (2.1) is the same as Campbell's formula. From this, by introduction we can show that $\mathbf{E}[I_n(f_n)] = 0$.

If $f_n \in L^2(\nu)^{\circ n}$ and $g_m \in L^2(\nu)^{\circ m}$, $n \geq m$, the following isometry formula holds:

$$\mathbf{E}[I_n(f_n) I_m(g_m)] = n! \mathbf{1}_{\{m=n\}} \langle f_n, g_m \rangle_{L^2(\nu)^{\circ n}} \tag{2.2}$$

(see [17]). Here

$$\langle f_n, g_n \rangle_{L^2(\nu)^{\circ n}} = \int_{E^n} f_n(z_1, ..., z_n) g_n(z_1, ..., z_n)\, \mathrm{d}\, \nu(z_1) ... \mathrm{d}\, \nu(z_n)$$

For $f_n \in L^2(\nu)^{\circ n}$ and $g_m \in L^2(\nu)^{\circ m}$, we define $f_n \times_k^l g_m$, $0 \leq l \leq k$, to be the function:

$$(y_{l+1}, \cdots, y_n, x_{k+1}, \cdots, x_m) \longmapsto$$
$$\int_{Y^l} f_n(y_1, \cdots, y_n) g_m(y_1, \cdots, y_k, x_{k+1}, \cdots, x_m)\, \mathrm{d}\, \nu(y_1) \ldots \mathrm{d}\, \nu(y_l). \tag{2.3}$$

We denote by $f_n \circ_k^l g_m$ the symmetrization in $n+m-k-l$ variables of $f_n \times_k^l g_m$, $0 \leq l \leq k$. This leads us to the next proposition, shown in [17]:

Proposition 2. *For $f_n \in L^2(\nu)^{\circ n}$ and $g_m \in L^2(\nu)^{\circ m}$, we have*

$$I_n(f_n)I_m(g_m) = \sum_{s=0}^{2(n\wedge m)} I_{n+m-s}(h_{n,m,s}),$$

where

$$h_{n,m,s} = \sum_{s\leq 2i\leq 2(s\wedge n\wedge m)} i!\binom{n}{i}\binom{m}{i}\binom{i}{s-i} f_n \circ_i^{s-i} g_m$$

belongs to $L^2(\nu)^{\circ n+m-s}$, $0 \leq s \leq 2(m\wedge n)$.

In what follows, given $f \in L^2(\nu)^{\circ q}$ ($q \geq 2$) and $z \in E$, we denote by $f(*,z)$ the function on E^{q-1} given by $(x_1,\cdots,x_{q-1}) \longmapsto f(x_1,\cdots,x_{q-1},z)$.

Furthermore, we have:

Theorem 3. *Every random variable $F \in L^2(\Omega^E, \mathbf{P})$ admits a (unique) Wiener-Poisson decomposition of the type*

$$\boxed{F = \mathbf{E}[F] + \sum_{n=1}^{\infty} I_n(f_n),} \tag{2.4}$$

where the series converges in $L^2(\Omega^E,\mathbf{P})$ and, for each $n \geq 1$, f_n is an element of $L^2(\nu)^{\circ n}$. Moreover, we have the isometry equation:

$$\boxed{\mathbf{V}[F] = \sum_{n=1}^{\infty} n!\|f_n\|^2_{L^2(\nu)^{\circ n}}.} \tag{2.5}$$

Definition 2. *Let Dom D be the the set of random variables $F \in L^2(\Omega^E,\mathbf{P})$ admitting a chaotic decomposition such that*

$$\sum_{n=1}^{\infty} n.n!\|f_n\|^2_{L^2(\nu)^{\circ n}} < \infty.$$

Let D be defined by

$$D \ : \ Dom\ D \to L^2(\Omega^E \times E, \mathbf{P}\times\nu),$$

such that

$$F = \mathbf{E}[F] + \sum_{n\geq 1} I_n(f_n) \longmapsto D_z F(*) = \sum_{n\geq 1} nI_{n-1}(f_n(*,z)).$$

Theorem 4. *We have*

$$\boxed{D_z F(w) = F(w+\epsilon_z) - F(w),\ \ \mathrm{d}\mathbf{P}\times\mathrm{d}\nu\ a.e.\cdot}$$

The theorem 4 says that, the operator D is nothing else but simply the difference made on F by adding a point z on w. The integration by parts then says that, for any $F \in \text{Dom } D$, any $u \in L^2(\nu)$,

$$\mathbf{E}\left[F \int_E u(z)(\,\mathrm{d}\, w(z) - \,\mathrm{d}\,\nu(z))\right] = \mathbf{E}\left[\int_E D_z F\, u(z)\,\,\mathrm{d}\,\nu(z)\right]. \tag{2.6}$$

It is well known that F is a linear functional (see the next section) $F = \int_E f\,\,\mathrm{d}\, w$ if and only if the chaos representation of F is $F = \mathbf{E}[F] + I_1(f)$ and in this case $D_z F = f(z)$ and thus $\mathbf{V}[F] = \int_E |D_z F|^2\,\,\mathrm{d}\, z$. Generally, F has the form

$$F = \sum_{i=1}^{k} \sum_{(z_1,...,z_i)\in\Delta_i; z_j \in w} f_i(z_1, ..., z_i)$$

if and only if the chaos representation of F has the form

$$F = \mathbf{E}[F] + \sum_{i=1}^{k} I_i(g_i)$$

where $g_1, ..., g_k$ can be derived from $f_1, ..., f_k$.

Using the difference operator D, we can bound the variance of F as follows:

Theorem 5. *([17], [15]) $\forall F \in L^2(\Omega^E, \mathbf{P})$ we have:*

$$\boxed{\mathbf{V}[F] \leq \mathbf{E}\left[\int_E |D_z F|^2\,\,\mathrm{d}\, z\right]\cdot} \tag{2.7}$$

Equality occurs if and only if F is linear.

Corollary 1. *$\forall F \in L^2(\Omega^E, \mathbf{P})$ such that $|D_z F| \leq f(z)$ for some non negative measurable function $f : E \to \mathbb{R}$ for all z, w then:*

$$\boxed{\mathbf{V}[F] \leq \int_E f^2(z)\,\,\mathrm{d}\,\nu(z)\cdot} \tag{2.8}$$

Theorem 6. *([17],[29]) Consider two functionals $F, G \in L^2(\Omega^E, \mathbf{P})$. Assume that $D_z F, D_z G \geq 0$, $\mathbf{P} \times \nu$ a.s. then*

$$\boxed{\mathbf{C}[F, G] \geq 0.}$$

As a consequence, $\mathbf{V}[F + G] \geq \mathbf{V}[F] + \mathbf{V}[G]$.

Definition 3. *The Ornstein-Uhlenbeck operator L is given by*

$$LF = -\sum_{n=1}^{\infty} n I_n(f_n),$$

whenever $F \in$ Dom L, given by those $F \in L^2(\nu)^{\circ n}$ such that their chaotic expansion verifies

$$\sum_{n=1}^{\infty} n^2.n!\|f_n\|^2_{L^2(\nu)^{\circ n}} < \infty.$$

Note that $\mathbf{E}[LF] = 0$, by definition and (2.2).

Definition 4. *For $F \in L^2(\mathbf{P})$ such that $\mathbf{E}[F] = 0$, we may define L^{-1} by*

$$L^{-1}F = -\sum_{n=1}^{\infty} \frac{1}{n} I_n(f_n).$$

The three Malliavin-type operators defined above give us way derive upper bounds on the distribution of a functional F(theorem 8) and an estimate of error on Gaussian approximation (theorem 7), results which is more general than the ones introduced on the previous sections.

Theorem 7. *([18]) Let $F \in Dom\ D$ be such that $\mathbf{E}[F] = 0$ and $\mathbf{V}[F] = 1$. Then,*

$$\boxed{\begin{array}{rcl} d_W(F, \mathcal{N}(0,1)) & \leq & \mathbf{E}\left[\left|1 - \int_E [D_z F \times D_z L^{-1} F]\ \mathrm{d}\,\nu(z)\right|\right] \\ & & + \int_E \mathbf{E}\left[|D_z F|^2 \left|D_z L^{-1} F\right|\right]\ \mathrm{d}\,\nu(z). \end{array}}$$

Here d_W is the Wasserstein distance.

Theorem 8. *[15], Let $F \in Dom\ D$. Assume that $|DF| \leq M$, $\mathbf{P} \times \nu$ a.s., for some $M \geq 0$ and $\int_E |D_z F|^2\ \mathrm{d}\,\nu(z) \leq \alpha^2, \mathbf{P}-$a.s. Then for all $u > 0$ we have*

$$\boxed{\mathbf{P}(F - \mathbf{E}[F] \geq u) \leq \exp\left\{-\frac{\alpha^2}{M^2} g\left(\frac{u.M}{\alpha^2}\right)\right\}} \tag{2.9}$$

for $M > 0$ and

$$\mathbf{P}(F - \mathbf{E}[F] \geq a) \leq \exp\left\{-\frac{\alpha^2}{2u^2}\right\} \tag{2.10}$$

for $M = 0$ where $g(t) = (1+t)\ln(1+t) - t$.

Corollary 2. *Let $F \in Dom\ D$. Assume that $|DF| \leq M$, $\mathbf{P} \times \nu$ a.s., for some $M > 0$ and $|D_z F| \leq f(z), \mathbf{P}-$a.s. for some non negative function $f \in L^2(\nu)$. Then for all $u > 0$ we have*

$$\boxed{\mathbf{P}(F - \mathbf{E}[F] \geq u) \leq \exp\left\{-\frac{\int_E f^2(z)\ \mathrm{d}\,\nu(z)}{M^2} g\left(\frac{uM}{\int_E f^2(z)\ \mathrm{d}\,\nu(z)}\right)\right\}.} \tag{2.11}$$

2.5 Distribution of linear functional of Poisson point process

We call F a linear functional of w if there exists $f : E \to \mathbb{R}$ such that

$$F = \int_E f(z)\ \mathrm{d}\,w(z) = \sum_{z \in w} f(z).$$

We assume that $f \in L^1(\nu)$. In this section we are interested in the distribution of F.

Let $\mathcal{L}_w(.)$ be the Laplace functional of w, i.e:

$$\mathcal{L}_w(u) = \mathbf{E}\left[e^{-\int_E u(z)\ \mathrm{d}\,w(z)}\right] \tag{2.12}$$

Theorem 9. *([17]) The Laplace functional of w satisfies:*

$$\boxed{\mathcal{L}_w(u) = e^{-\int_E (1-e^{-u(z)})\,\mathrm{d}\,\nu(z)}, \qquad u \in L^1(\nu)\cdot} \tag{2.13}$$

From the above theorem the moment generating function (MGF) of F is expressed as follows:

$$\boxed{\mathbf{E}\left[e^{\int_E f\,\mathrm{d}\,w}\right] = e^{\int_E (e^{f(z)}-1)\,\mathrm{d}\,\nu(z)}.} \tag{2.14}$$

2.5.1 Moments

The complete Bell polynomials $B_n(a_1, ..., a_n)$ are defined as follows:

$$\exp\left\{\sum_{n=1}^{\infty} \frac{a_n}{n!}\theta^n\right\} = \sum_{n=1}^{\infty} \frac{B_n(a_1, a_2, ..., a_n)}{n!}\theta^n$$

for all $a_1, ..., a_n$ and θ such that all above terms are correctly defined.

The first five Bell complete polynomials are given as:

$$\begin{aligned}
B_1(a_1) &= a_1 \\
B_2(a_1, a_2) &= a_1^2 + a_2 \\
B_3(a_1, a_2, a_3) &= a_1^3 + 3a_1a_2 + a_3 \\
B_4(a_1, a_2, a_3, a_4) &= a_1^4 + 4a_1^2a_2 + 4a_1a_3 + 3a_2^2 + a_4 \\
B_5(a_1, a_2, a_3, a_4, a_5) &= a_1^5 + 10a_1^3a_2 + 10a_1^2a_3 + 15a_1a_2^2 + 5a_1a_4 + 10a_2a_3 + a_5
\end{aligned}$$

It is well known that the coefficients of Bell's polynomial are always non negative. If a random variable S has n first cumulants $\kappa_1^S, ..., \kappa_n^S$ then its moments and central moments of S can be expressed as:

$$\begin{aligned}
\mathbf{m}_n[S] &= \mathbf{E}[S^n] = B_n(\kappa_1^S, ..., \kappa_n^S) \\
\mathbf{c}_n[S] &= \mathbf{E}[(S - \mathbf{E}[S])^n] = B_n(0, \kappa_2^S ..., \kappa_n^S)
\end{aligned}$$

Now consider a linear functional F of w, i.e $F = \int_E f\,\mathrm{d}\,w$ for some non-negative ν-measurable function f. We can compute the cumulants, the moments and central moments of F by Bell complete polynomials as follows:

Theorem 10 (Generalization of Campbell's formulas)**.** *Assume that $f \in \cap_{i=1}^n L^i(E, \nu)$. The cumulants of $F = \int_E f\,\mathrm{d}\,w$ is $\kappa_i^F = \int_E f^i(z)\,\mathrm{d}\,\nu(z)$ $(i = 1..n)$. The moments and central moments of F are given as:*

$$\boxed{\mathbf{m}_i[F] = B_i\left(\int_E f(z)\,\mathrm{d}\,\nu(z), \int_E f^2(z)\,\mathrm{d}\,\nu(z), ..., \int_E f^i(z)\,\mathrm{d}\,\nu(z)\right)} \tag{2.15}$$

and

$$\boxed{\mathbf{c}_i[F] = B_i\left(0, \int_E f^2(z)\,\mathrm{d}\,\nu(z), ..., \int_E f^i(z)\,\mathrm{d}\,\nu(z)\right)} \tag{2.16}$$

for $i = 1, 2, ..., n$.

Proof. We apply the theorem 9 to get that:

$$\begin{aligned}\mathbf{E}\left[e^{\theta F}\right] &= e^{\int_E (e^{\theta f(z)}-1)\,\mathrm{d}\,\nu(z)} \\ &= e^{\int_E \sum_{n=1}^{\infty} \theta^n f^n(z)\,\mathrm{d}\,\nu(z)} \\ &= e^{\sum_{n=1}^{\infty} \theta^n \int_E f^n(z)\,\mathrm{d}\,\nu(z)}\end{aligned}$$

By definition of cumulant, we have $\kappa_i^F = \int_E f^i(z)\,\mathrm{d}\,\nu(z)$, and thus the expressions for moments and central moments of F are straightforward. □

As a direct consequence, one can easily obtain from the above theorem two useful formulas (Campbell's theorem):

Corollary 3 (Campbell's theorem). *Let $F = \int_E f\,\mathrm{d}\,w$ then*

$$\boxed{\begin{aligned}\mathbf{E}[F] &= \int_E f(z)\,\mathrm{d}\,\nu(z), \quad f \in L^1(\nu) \\ \mathbf{V}[F] = \mathbf{E}\left[(F-\mathbf{E}[F])^2\right] &= \int_E f^2(z)\,\mathrm{d}\,\nu(z), \quad f \in L^2(\nu)\cdot\end{aligned}} \tag{2.17}$$

Notice that if we consider a independent making Poisson point process $\widetilde{w} = \sum \epsilon_{(z_i,m_i)}$ with a probability kernel K from E to the space of marks E' and $F = \sum f(z_i, m_i)$ then

$$\int_E \int_{E'} f^i(z,m)\,\mathrm{d}\,K_z(m)\,\mathrm{d}\,\nu(z) = \int_E \mathbf{E}\left[f^i(z,m)\right]\,\mathrm{d}\,\nu(z)\cdot$$

Campbell's formula is written:

$$\begin{aligned}\mathbf{E}[F] &= \int_E \mathbf{E}[f(z,m)]\,\mathrm{d}\,\nu(z), \\ \mathbf{V}[F] &= \int_E \mathbf{E}\left[f^2(z,m)\right]\,\mathrm{d}\,\nu(z)\cdot\end{aligned}$$

2.5.2 Existing results on Gaussian approximation, Edgeworth expansion and concentration inequality

We have now expressions for moments and central moments of F. We note that the central moments of F is always non negative as f is supposed to be non negative. One can ask if there is mean to compute the tail distribution of F. Gaussian approximation seems to be a first answer one can think of due to the central limit theorem (CLT). An error bound of Gaussian approximation for sum of n i.i.d random variables is known as Berry-Esseen theorem. It is possible to find an alternative version of this error bound for linear functional of PPP. Let $Q(a) = \frac{1}{\sqrt{2\pi}} \int_{-\infty}^{a} e^{-u^2/2}\,\mathrm{d}\,u$ be the CDF of a standard Gaussian random variable and $\overline{Q}$ be its CCDF.

Theorem 11. *Consider $F = \int_E f\,\mathrm{d}\,w$ with $f \in L^2(\nu)$. Let $\overline{F} = \frac{F-\mathbf{E}[F]}{\mathbf{V}[F]}$, then:*

$$\boxed{\left|\mathbf{P}(\overline{F} \le a) - Q(a)\right| \le \frac{\int_E |f(z)|^3\,\mathrm{d}\,\nu(z)}{(\int_E f^2(z)\,\mathrm{d}\,\nu(z))^{3/2}}\cdot} \tag{2.18}$$

Proof. Unfortunately there is no elementary proof for this theorem, we must apply the theorem 7 for $\overline{F}$. First, note that the chaos presentation of $\overline{F}$ is $\overline{F} = I_1(\frac{f}{\mathbf{V}[F]})$. Then

$$D_z\overline{F} = D_z L^{-1}\overline{F} = \frac{f(z)}{\mathbf{V}[F]}.$$

Thus, $\mathbf{V}[F] = \int_E f(z)\,\mathrm{d}\,\nu(z)$ and $D_z L^{-1}\overline{F} = D_z\overline{F} = \frac{f}{\mathbf{V}[F]}$. We now apply theorem 7 to get (2.18).

□

Now instead of $\mathrm{d}\,\nu(z)$, we consider $\lambda\,\mathrm{d}\,\nu(z)$ in the above theorem, and let $F_\lambda, \overline{F}_\lambda$ the corresponding versions of $F, \overline{F}$, we get:

$$\left|\mathbf{P}(\overline{F}_\lambda \leq a) - Q(a)\right| \leq \frac{\int_E |f(z)|^3\,\mathrm{d}\,\nu(z)}{\sqrt{\lambda}(\int_E f^2(z)\,\mathrm{d}\,\nu(z))^{3/2}}. \tag{2.19}$$

The last inequality shows that the error of Gaussian approximation is around $O(\frac{1}{\sqrt{\lambda}})$. It is worth noted that the error bound for Gaussian approximation of the sum of n i.i.d variables is $O(\frac{1}{\sqrt{n}})$.

An improvement for Gaussian approximation is known as Edgeworth expansion. Let

$$\lambda_n^F = \frac{\kappa_n^F}{(\mathbf{V}[F])^{n/2}} = \frac{\int_E f^n(z)\,\mathrm{d}\,\nu(z)}{(\int_E f^2(z)\,\mathrm{d}\,\nu(z))^{n/2}}$$

be the n^{th} standardized cumulant of F. The Edgeworth expansion for the distribution of $\overline{F}$ is given as:

$$\mathbf{P}(\overline{F} \leq a) = Q(a) + \sum_{n=1}^{\infty} P_n(-D)Q(a) \tag{2.20}$$

where P_n is polynomial of degree $3n$ and D is the differential operator. The first five terms are:

$$\begin{aligned}
\mathbf{P}(\overline{F} > a) \;=\; & \overline{Q}(a) + \\
& + \frac{\lambda_3^F}{6}Q^{(3)}(a) - \\
& - \left(\frac{\lambda_4^F}{24}Q^{(4)}(a) + \frac{(\lambda_3^F)^2}{72}Q^{(6)}(a)\right) + \\
& + \left(\frac{\lambda_5^F}{120}Q(5)(a) + \frac{\lambda_3^F\lambda_4^F}{144}Q^{(7)}(a) + \frac{(\lambda_3^F)^3}{1296}Q^{(9)}(a)\right) - \\
& - \left(\frac{\lambda_6^F}{720}Q^{(3)}(a) + (\frac{(\lambda_4^F)^2}{1152} + \frac{\lambda_3^F\lambda_5^F}{720})Q^{(8)}(a) + \frac{(\lambda_3^F)^2\lambda_4^F}{1782}Q^{(10)}(a) + \frac{(\lambda_3^F)^4}{31104}Q^{(12)}(a)\right) + \\
& \ldots
\end{aligned}$$

For the best of our knowledge, no error bound for Edgeworth expansions exists in the literature. Even we cannot find any reference in Edgeworth expansions of linear functional of Poisson point process. However, if $f(z) \geq 0$ we can rewrite (2.19) as:

$$\left|\mathbf{P}(\overline{F} \leq a) - Q(a)\right| \leq \lambda_3^F. \tag{2.21}$$

This provides a hint that, error bounds may be expressed as function of cumulants of F under appreciate conditions of f.

We have presented the Gaussian approximation and Edgeworth expansions for linear functionals. We are now interested in upper bounds on the distribution of F, which can be called concentration inequality.

Theorem 12. *Let $M, a > 0$.*

Assume that $0 \leq f(z) \leq M$ $\nu-$a.s and $f \in L^2(E,\nu)$, then:

$$\boxed{\mathbf{P}(F > \mathbf{E}[F] + a) \leq \exp\left\{-\frac{\mathbf{E}[F]}{M} g\left(\frac{a}{\mathbf{E}[F]}\right)\right\}} \tag{2.22}$$

where $g(u) = (1+u)\ln(1+u) - u$.

Assume that $|f(z)| \leq M$ $\nu-$a.s and $f \in L^2(E,\nu)$, then

$$\mathbf{P}(F > \mathbf{E}[F] + a) \leq \exp\left\{-\frac{\mathbf{V}[F]}{M^2} g\left(\frac{a.M}{\mathbf{V}[F]}\right)\right\} \tag{2.23}$$

Assume that $f(z) \leq 0$ $\nu-$a.s and $f \in L^2(E,\nu)$, then

$$\mathbf{P}(F > \mathbf{E}[F] + a) \leq \exp\left\{-\frac{\mathbf{V}[F]}{2a^2}\right\} \tag{2.24}$$

The above theorem can be directly derived from 2, which will be introduced in the next section. However let us take this opportunity to prove this theorem in a very nice, simple and elementary fashion, exactly the same way as Bennett built his concentration inequality for the sum of n i.i.d random variables.

Proof. Using Chernoff's bound we have:

$$\begin{aligned}\mathbf{P}(F > \mathbf{E}[F] + a) &\leq \mathbf{E}\left[e^{\theta F}\right] / e^{\theta(\mathbf{E}[F]+a)} \\ &= e^{\int_E \left(e^{\theta f(z)} - 1 - \theta f(z)\right) \mathrm{d}\,\nu(z) - \theta a}\end{aligned}$$

Now assume that $0 \leq f(z) \leq M$ $\nu-$a.s . Observe that the function $\frac{e^x-1}{x}$ is increasing on $\mathbb{R}_+$, we have $\frac{e^{\theta f(z)}-1}{\theta f(z)} \leq \frac{e^{\theta M}-1}{\theta M}$ for $f(z) \neq 0$, thus

$$e^{\theta f(z)} - 1 \leq \frac{e^{\theta M} - 1}{M} f(z)$$

$\nu-$a.s . We deduce that:

$$\begin{aligned}\mathbf{P}(F > \mathbf{E}[F] + a) &\leq \exp\left\{\int_E \left(\frac{e^{\theta M} - 1}{M} f(z) - \theta f(z)\right) \mathrm{d}\,\nu(z) - \theta a\right\} \\ &= \exp\left\{\frac{e^{\theta M} - 1 - \theta M}{M} \mathbf{E}[F] - \theta a\right\}.\end{aligned}$$

We minimize the L.H.S in θ, by some elementary manipulations, we reach the optimal value $\theta = \frac{1}{M}\ln\left(1 + \frac{a}{\mathbf{E}[F]}\right)$ and we obtain (2.22).

Now assume that $|f(z)| \leq M$ $\nu-$a.s . Observe that the function $\frac{e^x-1-x}{x^2}$ is increasing on $\mathbb{R}$ (the value at 0 is $1/2$), we have that

$$e^{\theta f(z)} - \theta f(z) - 1 \leq \frac{e^{\theta M} - 1 - \theta M}{M^2} f^2(z)$$

$\nu-$a.s . Thus,

$$\begin{aligned}\mathbf{P}(F > \mathbf{E}[F] + a) &\leq \exp\left\{\int_E \left(\frac{e^{\theta M} - \theta M - 1}{M^2} f^2(z)\right) \mathrm{d}\,\nu(z) - \theta a\right\} \\ &= \exp\left\{\frac{e^{\theta M} - 1 - \theta M}{M^2}\mathbf{V}[F] - \theta a\right\}.\end{aligned}$$

We find that $\theta = \frac{1}{M}\ln\left(1 + \frac{aM}{\mathbf{V}[F]}\right)$ minimizes the L.H.S and apply this value we obtain (2.23).

Now assume that $f(z) \leq 0$ $\nu-$a.s . By the same argument as above

$$e^{\theta f(z)} - \theta f(z) - 1 \leq \frac{\theta^2}{2} f^2(z).$$

Thus,

$$\begin{aligned}\mathbf{P}(F > \mathbf{E}[F] + a) &\leq \exp\left\{\frac{\theta^2}{2}\int_E f^2(z)\ \mathrm{d}\,\nu(z) - \theta a\right\} \\ &= \exp\left\{\frac{\theta^2}{2}\mathbf{V}[F] - \theta a\right\}.\end{aligned}$$

Minimizing the LHS by $\theta = \frac{a}{\mathbf{V}[F]}$ we obtain (2.24). □

2.5.3 New results

In this subsection we present our new asymptotic results on the distribution of a functional F of a Poisson process as its intensity goes to infinity. We consider the measure $\lambda\,\mathrm{d}\,\nu(z)$ instead of $\mathrm{d}\,\nu(z)$ and we are interested in F_λ and $\overline{F}_\lambda$ and let $m(p,\,\lambda) = \lambda_n^{F_\lambda}$. We denote by $\sigma = \|f\|_{L^2(\nu)}\sqrt{\lambda}$ and $f_\sigma = f/\sigma$. Note that $\|f_\sigma\|_{L^2(\nu)} = 1/\lambda$ and that

$$m(p,\,\lambda) := \int_E |f_\sigma(z)|^p \lambda\,\mathrm{d}\,\nu(z) = \|f\|_{L^2(\nu)}^{-p}\|f\|_{L^p(\nu)}^p \lambda^{1-p/2}.$$

For $\lambda > 0$, let

$$N^\lambda = \int_E f_\sigma(x)(\mathrm{d}\,w(z) - \lambda\,\mathrm{d}\,\nu(z)) = \overline{F}_\lambda - \mathbf{E}\left[\overline{F}_\lambda\right].$$

In what follows, we consider $G(N^\lambda)$ where $G : \mathbb{R} \to \mathbb{R}$. A functional will be of particular interest in the sequel: If $G = \mathbf{1}_{\{t \geq T\}}$ then

$$\mathbf{P}(N^\lambda \geq T) = \mathbf{E}\left[G(N^\lambda)\right].$$

The proof of the following theorem may be found in [30] and deduced also from [17, 18]:

Theorem 13. *Let $f \in L^2(\nu)$. Then, for any Lipschitz function G from $\mathbb{R}$ to $\mathbb{R}$, we have*

$$\boxed{\left|\mathbf{E}_{\lambda\nu}\left[G(N^\lambda)\right] - \int_{\mathbb{R}} G\,\mathrm{d}\,\mu\right| \leq \frac{1}{2}\sqrt{\frac{\pi}{2}}\ m(3,\,\lambda)\,\|G\|_{Lip}.}$$

We can go further in the expansion by precising the next term. This result is new and appeared in [20].

Theorem 14. *For $G \in \mathcal{C}_b^3(\mathbb{R}, \mathbb{R})$,*

$$\boxed{\begin{array}{l}\left|\mathbf{E}_{\lambda\nu}\left[G(N^\lambda)\right] - \int_{\mathbb{R}} G(y)\,\mathrm{d}\,\mu(y) - \frac{1}{6}\, m(3,\,\lambda)\, \int_{\mathbb{R}} G(y)H_3(y)\,\mathrm{d}\,\mu(y)\right| \\ \leq \left(\frac{m(3,1)^2}{6} + \frac{m(4,1)}{9}\sqrt{\frac{2}{\pi}}\right) \frac{\|G^{(3)}\|_\infty}{\lambda}.\end{array}} \tag{2.25}$$

Proof. According to the Taylor formula,

$$\begin{aligned} &D_x G(N^\lambda) = G(N^\lambda + f_\sigma(x)) - G(N^\lambda) \\ &= G'(N^\lambda) f_\sigma(x) + \frac{1}{2} f_\sigma^2(x)\, G''(N^\lambda) + \frac{1}{2} f_\sigma(x)^3 \int_0^1 r^2 G^{(3)}(rN^\lambda + (1-r) f_\sigma(x))\,\mathrm{d}\,r. \end{aligned} \tag{2.26}$$

Hence, according to (2.6) and (2.26),

$$\begin{aligned} \mathbf{E}_{\lambda\nu}\left[N^\lambda (P_t G)'(N^\lambda)\right] &= \mathbf{E}_{\lambda\nu}\left[\int_E f_\sigma(x) D_x (P_t G)'(N^\lambda) \lambda\,\mathrm{d}\,\nu(x)\right] \\ &= \mathbf{E}_{\lambda\nu}\left[(P_t G)''(N^\lambda)\right] + \frac{1}{2}\int_E f_\sigma^3(x)\lambda\,\mathrm{d}\,\nu(x) \mathbf{E}_{\lambda\nu}\left[(P_t G)^{(3)}(N^\lambda)\right] \\ &\quad + \frac{1}{2}\int_E f_\sigma^4(x)\lambda\,\mathrm{d}\,\nu(x) \mathbf{E}_{\lambda\nu}\left[\int_0^1 (P_t G)^{(4)}(rN^\lambda + (1-r) f_\sigma(x)) r^2\,\mathrm{d}\,r\right] \\ &\quad = A_1 + A_2 + A_3. \end{aligned}$$

Hence,

$$|A_3| \leq \frac{e^{-4t}}{6\sqrt{1-e^{-2t}}} \sqrt{\frac{2}{\pi}} m(4,\,\lambda)\, \|G^{(3)}\|_\infty.$$

Moreover, according to Theorem 13,

$$\begin{aligned} \left|\mathbf{E}_{\lambda\nu}\left[(P_t G)^{(3)}(N^\lambda)\right] - \int_{\mathbb{R}} (P_t G)^{(3)}(x)\,\mathrm{d}\,\mu(x)\right| &\leq \frac{1}{2}\sqrt{\frac{\pi}{2}}\, m(3,\,\lambda) \|(P_t G)^{(4)}\|_\infty \\ &\leq \frac{1}{2}\, m(3,\,\lambda) \frac{e^{-4t}}{\sqrt{1-e^{-2t}}} \|G^{(3)}\|_\infty. \end{aligned}$$

Then, we have,

$$|A_2 - \frac{1}{2} m(3,\,\lambda) \int_{\mathbb{R}} (P_t G)^{(3)}(x)\,\mathrm{d}\,\mu(x)| \leq \frac{1}{4}\, m(3,\,\lambda)^2 \frac{e^{-4t}}{\sqrt{1-e^{-2t}}} \|G^{(3)}\|_\infty.$$

Hence,

$$\mathbf{E}_{\lambda\nu}\left[N^\lambda (P_t G)'(N^\lambda) - (P_t G)''(N^\lambda)\right] = \frac{1}{2} m(3,\,\lambda) \int_{\mathbb{R}} (P_t G)^{(3)}(x)\,\mathrm{d}\,\mu(x) + R(t),$$

where

$$R(t) \leq \left(\frac{m(3,\,\lambda)^2}{4} + \frac{m(4,\,\lambda)}{6}\sqrt{\frac{2}{\pi}}\right) \|G^{(3)}\|_\infty \frac{e^{-4t}}{\sqrt{1-e^{-2t}}}.$$

Now then,

$$\begin{aligned} \int_{\mathbb{R}} (P_t G)^{(3)}(x)\,\mathrm{d}\,\mu(x) &= e^{-3t} \int_R \int_{\mathbb{R}} G^{(3)}(e^{-t}x + \sqrt{1-e^{-2t}}y)\,\mathrm{d}\,\mu(y) \\ &= e^{-3t} \int_{\mathbb{R}} G^{(3)}(y)\,\mathrm{d}\,\mu(y) \\ &= e^{-3t} \int_R G(y) H_3(y)\,\mathrm{d}\,\mu(y), \end{aligned}$$

since the Gaussian measure on $\mathbb{R}^2$ is rotation invariant and according to (10.2). Remarking that

$$\int_0^\infty e^{-4t}(1-e^{-2t})^{-1/2}\,\mathrm{d}\,t = 2/3$$

and applying (10.4) to $x = N^\lambda$, the result follows. □

This development is not new in itself but to the best of our knowledge, it is the first time that there is an estimate of the error bound. Following the same lines, we can pursue the expansion up to any order provided that G be sufficiently differentiable. Namely, for $G \in \mathcal{C}_b^5$, we have

$$\begin{array}{rcl}\mathbf{E}_{\lambda\nu}\left[G(N^\lambda)\right] & = & \int_{\mathbb{R}} G(y)\,\mathrm{d}\,\mu(y) + \frac{m(3,1)}{6\sqrt{\lambda}}\int_{\mathbb{R}} G^{(3)}(y)\,\mathrm{d}\,\mu(y) + \frac{m(3,1)^2}{72\lambda}\int_{\mathbb{R}} G^{(6)}(y)\,\mathrm{d}\,\mu(y) \\ & & + \frac{m(4,1)}{24\lambda}\int_{\mathbb{R}} G^{(4)}(y)\,\mathrm{d}\,\mu(y) + G_\lambda \|G^{(5)}\|_\infty.\end{array}$$

where

$$G_\lambda \leq \frac{m(3,1)}{\lambda^{3/2}}\left(\frac{2}{45}\,m(3,1)^2 + (\frac{4}{135}+\frac{\pi^2}{128})\sqrt{\frac{2}{\pi}}\;m(4,1)\right). \tag{2.27}$$

2.6 Conclusion

In this chapter we introduce all the mathematical tools used throughout this thesis. First we have presented the notion of Poisson point process. After, we have introduced the notation of Malliavin calculus applied to Poisson point process and presented useful results, which are upper bounds on the distribution of random variables depending on a Poisson point process. Then we have studied the distribution of linear functional of Poisson point process, we have presented some new results on Edgeworth expansion.

Part II

Dimensioning and coverage models

Chapter 3

Robust methods for LTE and WiMAX dimensioning

Contents

3.1 Introduction 31
3.2 System Model 34
3.3 Loss probability 36
3.3.1 Exact method 36
3.3.2 Approximations 37
3.3.3 Robust upper-bound 38
3.4 Applications to OFDMA and LTE 39

3.1 Introduction

Future wireless systems will widely rely on OFDMA (Orthogonal Frequency Division Multiple Access) multiple access technique. OFDMA can satisfy end user's demands in terms of throughput. It also fulfills operator's requirements in terms of capacity for high data rate services. Systems such as 802.16e and 3G-LTE (Third Generation Long Term Evolution) already use OFDMA on the downlink. Dimensioning of OFDMA systems is then of the utmost importance for wireless telecommunications industry.

OFDM (Orthogonal Frequency Division Multiplex) is a multi carrier technique especially designed for high data rate services. It divides the spectrum in a large number of frequency bands called (orthogonal) subcarriers that overlap partially in order to reduce spectrum occupation. Each subcarrier has a small bandwidth compared to the coherence bandwidth of the channel in order to mitigate frequency selective fading. User data is then transmitted in parallel on each sub carrier. In OFDM systems, all available subcarriers are affected to one user at a given time for transmission. OFDMA extends OFDM by making it possible to share dynamically the available subcarriers between different users. In that sense, it can then be seen as multiple access technique that both combines FDMA and TDMA features. OFDMA can also be possibly combined with multiple antenna (MIMO) technology to improve either quality or capacity of systems.

In practical systems, such as WiMAX or 3G-LTE, subcarriers are not allocated individually for implementation reasons mainly inherent to the scheduler design and physical

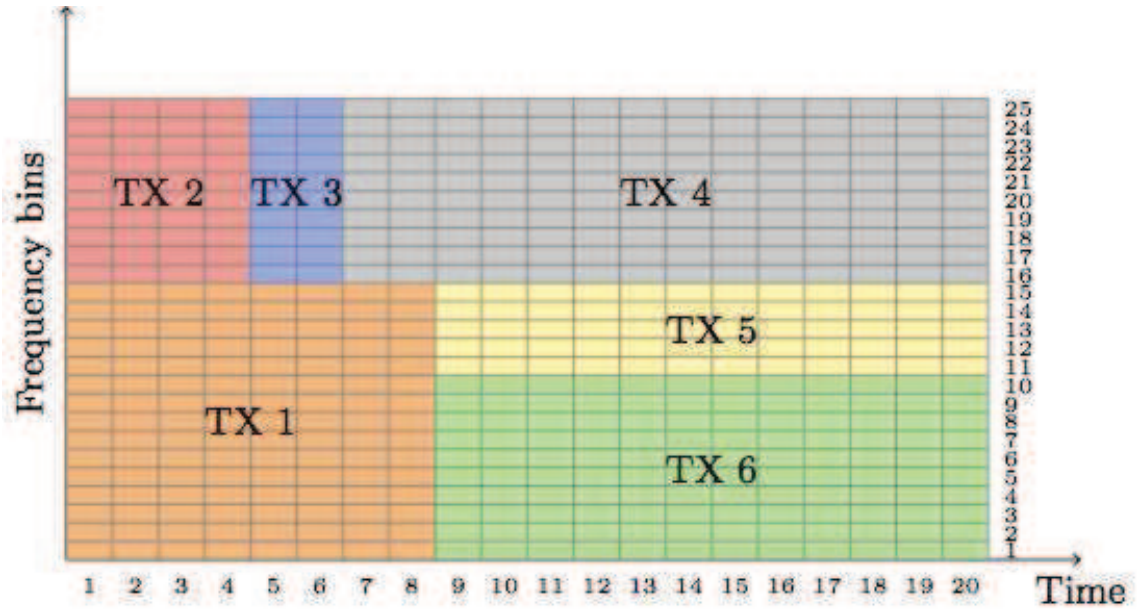


Figure 3.1: OFDMA principle : subcarriers are allocated according to the required transmission rate

layer signaling. Several subcarriers are then grouped in subchannels according to different strategies specific to each system. In OFDMA systems, the unit of resource allocation is mainly the subchannels. The number of subchannels required by a user depends on his channel's quality and the required bit rate. If the number of demanded subchannels by all users in the cell is greater than the available number of subchannel, the system is overloaded and suffer packet losses. The questions addressed here can then be stated as follows: how many subchannels must be assigned to a BS to ensure a small overloading probability ? Given the number of available subchannels, what is the maximum load, in terms of mean number of customers per unit of surface, that can be tolerated ? Both questions rely on accurate estimations of the loss probability.

The objectives of this chapter are twofold: First, construct and analyze a general performance model for an isolated cell equipped with an OFDMA system as described above. We allows several classes of customers distinguished by their transmission rate and we take into account path-loss with shadowing. We then show that for a Poissonian configuration of users in the cell, the required number subchannels follows a compound Poisson distribution. The second objective is to compare different numerical methods to solve the dimensioning problem. In fact, there exists an algorithmic approach which gives the exact result potentially with huge memory consumption. On the other hand, we use and even extend some recent results on functional inequalities for Poisson processes to derive some approximations formulas which turn to be rather effective at a very low cost. When it comes to evaluate the performance of a network, the quality of such a work may be judged according to several criteria. First and foremost, the exactness is the most used criterion: it means that given the exact values of the parameters, the real system, the performances of which may be estimated by simulation, behaves as close as possible to the computed behavior. The sources of errors are of three kinds: The mathematical model may be too rough to take into account important phenomena which alter the performances of the system, this is known as the epistemic risk. Another source may be in the mathematical

Symbols	Physical meaning
γ	Pathloss exponent
k	User's class
λ	Intensity of users
K	Number of classes
τ_k	Probability that a user is of the class k
C_k	Transmission rate of class k
N_{max}	Maximum number of subchannels (resource units) for a user
N_{avail}	Number of subchannels at the BS
N_{total}	Number of subchannels demanded by all users in the cell
β_{min}	Outage threshold
l_k	Maximum number of subchannels (resource units) for a user of class k
$\beta_{k,l}$	A user of class k uses exactly k subchannels if the SINR is in the interval $[\beta_{k,l}, \beta_{k,l-1})$ $(1 \leq l \leq l_k)$
$\zeta_{k,l}$	Mean number of users of class k using l subchannels

Table 3.1: Notations and parameters in this chapter.

resolution of the model where we may be forced to use approximate algorithms to find some numerical values. The third source lies in the lack of precision in the determination of the parameters characterizing the system: They may be hard, if not impossible, to measure with the desired accuracy. It is thus our point of view that exactness of performance analysis is not all the matter of the problem, we must also be able to provide confidence intervals and robust analysis. That is why, we insist on error bounds in our approximations.

Resources allocation on OFDMA systems have been extensively studied over the last decade, often with joint power and subcarriers allocation, see for instance [31, 32, 33, 34]. The problem of OFDMA planning and dimensioning have been more recently under investigation. In [35], the authors propose a dimensioning of OFDMA systems focusing on link outage but not on the other parameters of the systems. In [36], the authors give a general methodology for the dimensioning of OFDMA systems, which mixes a simulation based determination of the distribution of the signal-to-interference-plus-noise ratio (SINR) and a Markov chain analysis of the traffic. In [37, 38], the authors propose a dimensioning method for OFDMA systems using Erlang's loss model and Kaufman-Roberts recursion algorithm. In [39], the authors study the effect of Rayleigh fading on the performance of OFDMA networks.

The chapter is organized as follows. In Section 3.2, we describe the system model and set up the problem. In Section 3.3, we examine four methods to derive an exact, approximate or robust value of the number of subchannels necessary to ensure a given loss probability. In Section 3.4, we apply these formulas to the particular situation of OFDMA systems.

Important notations and parameters used in this chapter are summarized in the table 3.1.

3.2 System Model

In practical systems, such as WiMAX or 3G-LTE, resource allocation algorithms work at subchannel level. The subcarriers are grouped into subchannels that the system allocates to different users according to their throughput demand and mobility pattern. For example, in WiMAX, there are three modes available for building subchannels: FUSC (Fully Partial Usage of Subchannels), PUSC (Partial Usage of SubChannels) and AMC (Adaptive modulation and coding). In FUSC, subchannels are made of subcarriers spread over all the frequency band. This mode is generally more adapted to mobile users. In AMC, the subcarriers of a subchannel are adjacent instead of being uniformly distributed over the spectrum. AMC is more adapted to nomadic or stationary users and generally provides higher capacity.

The grouping of subcarriers into subchannels raises the problem of the estimation of the quality of a subchannel. Theoretically channel quality should be evaluated on each subcarrier of the corresponding subchannel to compute the associated capacity. This work assumes that it is possible to consider a single channel gain for all the subcarriers making part of a subchannel (for example via channel gains evaluated on pilot subcarriers).

We consider a circular cell C of radius R with a base station (BS for short) at its center. The transmission power dedicated to each subchannel by the base station is denoted by P. Each subchannel has a bandwidth W (in kHz). The received signal power for a mobile station at distance d from the BS can be expressed as

$$P(d) = \frac{PK_\gamma}{d^\gamma} GF := P_\gamma G d^{-\gamma}, \tag{3.1}$$

where K_γ is a constant equal to the attenuation at a reference distance, denoted by d_{ref}, that separates far field from near field propagation. Namely,

$$K_\gamma = \left(\frac{c}{4\pi f d_{\text{ref}}}\right)^2 d_{\text{ref}}^\gamma,$$

where f is the radio-wave frequency. The variable γ is the path-loss exponent which indicates the power at which the path loss increases with distance. Its depends on the specific propagation environment, in urban area, it is in the range from 3 to 5. It must be noted that this propagation model is an approximate model, difficult to calibrate for real life situations. In particular, it might be reasonable to envision models where γ depends on the distance so that the attenuation would be proportional to $d^{\gamma(d)}$. Because of the complexity of such a model, γ is often considered as constant but the path-loss is multiplied by two random variables G and F which represent respectively the shadowing, i.e. the attenuation due to obstacles, and the Rayleigh fading, i.e. the attenuation due to local movements of the mobile. Usually, G is taken as a log-normal distribution: $G = 10^{S/10}$, where $S \sim \mathcal{N}(\kappa, v^2)$. As to F, it is customary to choose an exponential distribution with parameter 1. Both, the shadowing and the fading experienced by each user are supposed to be independent from other users' shadowing and fading. For the sake of simplicity, we will here treat the situation where only shadowing is taken into account, the computations would be pretty much like the forthcoming ones and the results rather similar should we consider Rayleigh fading.

All active users in the cell compete to have access to some of the N_{avail} available subchannels. There are K classes of users distinguished by the transmission rate they require: C_k is the rate of class k customers and τ_k denotes the probability that a customer

belongs to class k. A user, at distance d from the BS, is able to receive the signal only if the signal-to-interference-plus-noise ratio SNR $= \frac{P(d)}{I}$ is above some constant β_{min} where I is the noise plus interference power and $P(d)$ is the received signal power at distance d, see (3.1). If the SNR is below the critical threshold, then the user is said to be in outage and cannot proceed with his communication. In this work we assume that $I = constant$, which can be seen as the system is noise limited (high reuse factor) or we take into account only the worse interference.

To avoid excess demands, the operator may impose a maximum number $N_{\max}$ of allocated subchannels to each user at each time slot. According to the Shannon formula, for a user demanding a service of bit rate C_k, located at distance d from the BS and experiencing a shadowing g, the number of requires subchannels is thus the minimum of $N_{\max}$ and of

$$N_{\text{user}} = \begin{cases} \left\lceil \dfrac{C_k}{W \log_2 (1 + P_\gamma g d^{-\gamma}/I)} \right\rceil & \text{if } P_\gamma g d^{-\gamma}/I \geq \beta_{min}, \\ 0 & \text{otherwise,} \end{cases}$$

where $\lceil x \rceil$ means the minimum integer number not smaller than x.

We make the simplifying assumption that the allocation is made at every time slot and that there is no buffering neither in the access point nor in each mobile station. All the users have independently from others a probability p to have a packet to transmit at each slot. This means, that each user has a traffic pattern which follows a geometric process of intensity p. We also assume that users are dispatched in the cell according to a Poisson process of intensity λ_0. According to the thinning theorem for Poisson processes, this induces that active users form a Poisson process of intensity $\lambda = \lambda_0 p$. This intensity is kept fixed over the time. That may result from two hypothesis: Either we consider that for a small time scale, users do not move significantly and thus the configuration does not evolve. Alternatively, we may consider that statistically, the whole configuration of active users has reached its equilibrium so that the distribution of active users does not vary through time though each user may move.

From the previous considerations, a user is characterized by three independent parameters: his position, his class and the intensity of the shadowing he is experiencing. We model this as a Poisson process on $E = B(0,\, R) \times \{1, \cdots, K\} \times \mathbb{R}^+$ of intensity measure

$$\lambda \, \mathrm{d}\nu(x) := \lambda(\, \mathrm{d}x \times \, \mathrm{d}\tau(k) \times \, \mathrm{d}\rho(g))$$

where $B(0,\, R) = \{x \in \mathbb{R}^2,\, \|x\| \leq R\}$, τ is the probability distribution of classes given by $\tau(\{k\}) = \tau_k$ and ρ is the distribution of the random variable G defined above. We set

$$f(x,\, k,\, g) = \min \left(N_{\max}, \mathbf{1}_{\{P_\gamma g \|x\|^{-\gamma} \geq I \beta_{min}\}} \left\lceil \frac{C_k}{W \log_2 (1 + P_\gamma g \|x\|^{-\gamma}/I)} \right\rceil \right).$$

The total number of demanding subchannels of all users in the cell is then:

$$N_{\text{tot}} = \int_{\text{cell}} f(x,\, k,\, g) \;\; \mathrm{d}\omega(x,\, k,\, g).$$

We are interested in the loss probability which is given by

$$\mathbf{P}(N_{\text{tot}} \geq N_{\text{avail}}).$$

We first need to compute the different moment of f with respect to ν in order to apply Theorem 13 and Theorem 14. For, we set

$$l_k = N_{\max} \wedge \left\lceil \frac{C_k}{W \log_2(1+\beta_{\min})} \right\rceil,$$

where $a \wedge b = \min(a, b)$. Furthermore, we introduce $\beta_{k,0} = \infty$,

$$\beta_{k,l} = \frac{I}{P_\gamma}\left(2^{C_k/Wl} - 1\right),\ 1 \le k \le K,\ 1 \le l \le l_k - 1,$$

and $\beta_{k,l_k} = I\beta_{\min}/P_\gamma$. Parameter $\beta_{k,l}$ gives the minimum SINR for which l resource units are necessary to provide the bit rate of class k (i.e. C_k). In other words to use exactly l resource units, the SINR should be in interval $[\beta_{k,l}, \beta_{k,l-1})$.

Theorem 15. *Let* $\zeta_{k,l} = \pi(\beta_{k,l}^{-2/\gamma} \wedge R^2 - \beta_{k,l-1}^{-2/\gamma} \wedge R^2)\ 10^{(\kappa + \frac{v^2}{10\gamma}\ln 10)/5\gamma}$. *For any* $p \ge 0$, *we have:*

$$\int f^p\ d\nu = \sum_{k=1}^{K} \tau_k \sum_{l=1}^{l_k} l^p\, \zeta_{k,l}. \tag{3.2}$$

Proof. By the very definition of the ceiling function, we have

$$\int_E f^p\ \mathrm{d}\nu = \sum_{k=1}^{K} \tau_k \sum_{l=1}^{l_k} l^p \int_{\text{cell}} \int_{\mathbb{R}} \mathbf{1}_{[\beta_{k,l};\beta_{k,l-1})}(g\|x\|^{-\gamma})\ \mathrm{d}\rho(g)\ \mathrm{d}x.$$

By some elementary manipulations, we have

$$\int_{\text{cell}} \mathbf{1}_{[\beta_{k,l};\beta_{k,l-1})}(g\|x\|^{-\gamma})\ \mathrm{d}x = \pi(\beta_{k,l}^{-2/\gamma} \wedge R^2 - \beta_{k,l-1}^{-2/\gamma} \wedge R^2) g^{2/\gamma}.$$

Thus, we have

$$\begin{aligned}\int_{\text{cell}} \int_{\mathbb{R}} \mathbf{1}_{[\beta_{k,l};\beta_{k,l-1})}(g\|x\|^{-\gamma})\ \mathrm{d}\rho(g)\ \mathrm{d}x & \\ &= \pi(\beta_{k,l}^{-2/\gamma} \wedge R^2 - \beta_{k,l-1}^{-2/\gamma} \wedge R^2)\mathbf{E}\left[10^{S/5\gamma}\right] \\ &= \pi(\beta_{k,l}^{-2/\gamma} \wedge R^2 - \beta_{k,l-1}^{-2/\gamma} \wedge R^2)\ 10^{(\kappa + \frac{v^2}{10\gamma}\ln 10)/5\gamma}.\end{aligned}$$

□

3.3 Loss probability

3.3.1 Exact method

Since f is deterministic, N_{tot} follows a compound Poisson distribution: it is distributed as

$$\sum_{k=1}^{K} \sum_{l=1}^{l_k} l\, N_{k,l}$$

where $(N_{k,l},\ 1 \le k \le K,\ 1 \le l \le l_k)$ are independent Poisson random variables, the parameter of $N_{k,l}$ is $\lambda\tau_k\zeta_{k,l}$. Using the properties of Poisson random variables, we can

reduce the complexity of this expression. Let $L = \max(l_k,\, 1 \le k \le K)$ and for $l \in \{1, \cdots, L\}$, let $K_l = \{k,\, l_k \ge l\}$. Then, $N_{\rm tot}$ is distributed as

$$\sum_{l=1}^{L} l\, M_l$$

where $(M_l,\, 1 \le l \le l_k)$ are independent Poisson random variables, the parameter of M_l being $m_l := \sum_{k \in K_l} \lambda \tau_k \zeta_{k,l}$. For each l, it is easy to construct an array which represents the distribution of lM_l by the following rule:

$$p_l(w) = \begin{cases} 0 & \text{if } w \mod l \neq 0, \\ \exp(-m_l) m_l^q / q! & \text{if } w = ql. \end{cases}$$

By discrete convolution, the distribution of $N_{\rm tot}$ and then its cumulative distribution function, are easily calculable. The value of $N_{\rm avail}$ which ensures a loss probability below the desired threshold is found by inspection. The only difficulty with this approach is to determine where to truncate the Poisson distribution functions for machine representation. According to large deviation theory [40],

$$\mathbf{P}(\text{Poisson}(\theta) \ge a\theta) \le \exp(-\theta(a \ln a + 1 - a)).$$

When θ is known, it is straightforward to choose $a(\theta)$ so that the right-hand-side of the previous equation is smaller than the desired threshold. The total memory size is thus proportional to $\max(m_l a(m_l) l,\, 1 \le l \le l_k)$. This may be memory (and time) consuming if the parameters of some Poisson random variables or the threshold are small. This method is well suited to estimate loss probability since it gives exact results within a reasonable amount of time but it is less useful for dimensioning purpose. Given $N_{\rm avail}$, if we seek for the value of λ which guarantees a loss probability less than the desired threshold, there is no better way than trial and error. At least, the subsequent methods even imprecise may help to evaluate the order of magnitude of λ for the first trial.

3.3.2 Approximations

We use the same notations as in the subsection 2.5.3, i.e , $\sigma = \|f\|_{L^2(\nu)} \sqrt{\lambda}$, $f_\sigma = f/\sigma$ and

$$m(p,\, \lambda) = \lambda_n^{F_\lambda} = \int_E |f_\sigma(z)|^p \lambda \, \mathrm{d}\nu(z) = \|f\|_{L^2(\nu)}^{-p} \|f\|_{L^p(\nu)}^p \lambda^{1-p/2}.$$

We begin by the classical Gaussian approximation. It is clear that

$$\begin{aligned} \mathbf{P}\Big(\int_E f \, \mathrm{d}\omega \ge N_{\rm avail}\Big) = & \quad \mathbf{P}\Big(\textstyle\int_E f_\sigma(\, \mathrm{d}\omega - \lambda \, \mathrm{d}\nu) \ge N_\sigma\Big) \\ = & \quad \mathbf{E}_{\lambda\nu}\left[\mathbf{1}_{[N_\sigma, +\infty)}\Big(\textstyle\int_E f_\sigma(\, \mathrm{d}\omega - \lambda \, \mathrm{d}\nu)\Big)\right] \end{aligned}$$

where $N_\sigma = (N_{\rm avail} - \int f \lambda \, \mathrm{d}\nu)/\sigma$. Since the indicator function $\mathbf{1}_{[N_\sigma, +\infty)}$ is not Lipschitz, we can not apply the bound given by Theorem 13. However, we can upper-bound the indicator by a continuous function whose Lipschitz norm is not greater than 1. For instance, taking

$$\phi(x) = \min(x^+, 1) \text{ and } \phi_N(x) = \phi(x - N),$$

we have

$$\mathbf{1}_{[N_\sigma + 1, +\infty)} \le \phi_{N_\sigma + 1} \le \mathbf{1}_{[N_\sigma, +\infty)} \le \phi_{N_\sigma - 1} \le \mathbf{1}_{[N_\sigma - 1, +\infty)}.$$

Hence,

$$1-Q(N_\sigma+1)-\frac{1}{2}\sqrt{\frac{2}{\pi}}\frac{m(3,\,1)}{\sqrt{\lambda}}\leq \mathbf{P}(\int_E f\ \mathrm{d}\omega\geq N_{\mathrm{avail}})\leq \\ 1-Q(N_\sigma-1)+\frac{1}{2}\sqrt{\frac{2}{\pi}}\frac{m(3,\,1)}{\sqrt{\lambda}}, \quad (3.3)$$

where Q is the cumulative distribution function of a standard Gaussian random variable.

According to Theorem 14, one can proceed with a more accurate approximation. Via polynomial interpolation, it is easy to construct a $\mathcal{C}^3$ function ψ_N^l such that

$$\|(\psi_N^l)^{(3)}\|_\infty\leq 1 \text{ and } \mathbf{1}_{[N_\sigma+3.5,+\infty)}\leq\psi_{N_\sigma}^l\leq\mathbf{1}_{[N_\sigma,+\infty)}$$

and a function ψ_N^r such that

$$\|(\psi_N^r)^{(3)}\|_\infty\leq 1 \text{ and } \mathbf{1}_{[N_\sigma,+\infty)}\leq\psi_{N_\sigma}^r\leq\mathbf{1}_{[N_\sigma-3.5,+\infty)}$$

From (10.3), it follows that

$$1-Q(N_\sigma+3.5)-\frac{m(3,\,1)}{6\sqrt{\lambda}}Q^{(3)}(N_\sigma+3.5)-E_\lambda\leq\mathbf{P}(\int_E f\ \mathrm{d}\omega\geq N_{\mathrm{avail}})\leq \\ 1-Q(N_\sigma-3.5)+\frac{m(3,\,1)}{6\sqrt{\lambda}}Q^{(3)}(N_\sigma-3.5)+E_\lambda \quad (3.4)$$

where E_λ is the right-hand-side of (8.11) with $\|F^{(3)}\|_\infty=1$.

Going again one step further, following the same lines, according to (2.27), one can show that

$$\mathbf{P}(\int_E f\ \mathrm{d}\omega\geq N_{\mathrm{avail}})\leq 1-Q(N_\sigma-6.5) \\ +\frac{m(3,\,1)}{6\sqrt{\lambda}}Q^{(3)}(N_\sigma-6.5)+\frac{m(3,1)^2}{72\lambda}Q^{(5)}(N_\sigma-6.5) \\ +\frac{m(4,1)}{24\lambda}Q^{(3)}(N_\sigma-6.5)+F_\lambda \quad (3.5)$$

where F_λ is bounded above in (2.27).

For all the approximations given above, for a fixed value of N_{avail}, an approximate value of λ can be obtained by solving numerically an equation in $\sqrt{\lambda}$.

3.3.3 Robust upper-bound

If we seek for robustness and not precision, it may be interesting to consider the so-called concentration inequality. We remark that in the present context, f is non-negative and bounded by $L=\max_k l_k$ so that we are in position to apply Theorem 12. We obtain that

$$\mathbf{P}(\int_E f\ \mathrm{d}\omega\geq\int_E f\ \mathrm{d}\nu+a)\leq\exp\left(-\frac{\int_E f^2\lambda\ \mathrm{d}\nu}{L^2}g(\frac{aL}{\int_E f^2\lambda\ \mathrm{d}\nu})\right), \quad (3.6)$$

where $g(u)=(1+u)\ln(1+u)-u$.

3.4 Applications to OFDMA and LTE

In such systems, there is a huge number of physical parameters with a wide range of variations, it is thus rather hard to explore the variety of sensible scenarios. For illustration purposes, we chose a circular cell of radius $R = 300$ meters equipped with an isotropic antenna such that the transmitted power is 1 W and the reference distance is 10 meters. The mean number of active customers per unit of surface, denoted by λ, was chosen to vary between $0,001$ and $0.000\,1$, this corresponds to an average number of active customers varying from 3 to 30, a realistic value for the systems under consideration. The minimum SINR is 0.3 dB and the random variable S defined above is a centered Gaussian with variance equal to 10. There are two classes of customers, $C_1 = 1,000$ kb/s and $C_2 = 400$ kb/s. It must be noted that our set of parameters is not universal but for the different scenarios we tested, the numerical facts we want to point out were always apparent. Since the time scale is of the order of a packet transmission time, the traffic is defined as the mean number of required subchannels at each slot provided that the time unit is the slot duration, that is to say that the load is defined as $\rho = \lambda \int_{\text{cell}} f \, \mathrm{d}\nu$.

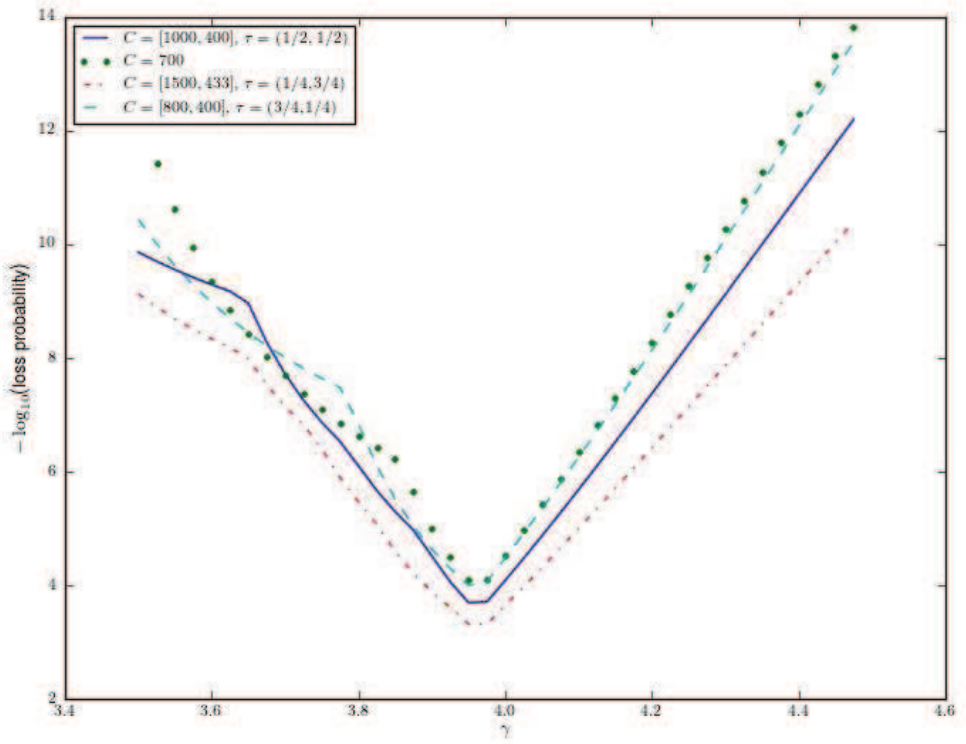


Figure 3.2: Impact of γ and τ on the loss probability ($N_{\text{avail}} = 92$, $\lambda = 0.0001$)

Figure 3.2 shows, the loss probability may vary up to two orders of magnitude when the rate and the probability of each class change even if the mean rate $\sum_k \tau_k C_k$ remains constant. Thus mean rate is not a sufficient parameter to predict the performances of such a system. The load ρ is neither a pertinent indicator as the computations show that the loads of the various scenarios differs from less than 3%.

Comparatively, Figure 3.2 shows that variations of γ have tremendous effects on the loss probability: a change of a few percents of the value of γ induces a variation of several order of magnitude for the loss probability. It is not surprising that the loss probability increases as a function of γ: as γ increases, the radio propagation conditions worsen and for a given transmission rate, the number of necessary subchannels increases, generating overloading. Beyond a certain value of γ (apparently around 3.95 on Figure 3.2), the radio conditions are so harsh that a major part of the customers are in outage since they do not satisfy the SNR criterion any longer. We remark here that the critical value of γ is almost the same for all configurations of classes. Indeed, the critical value γ_c of γ can be found by a simple reasoning: When $\gamma < \gamma_c$, a class k customer uses less than the allowed l_k subchannels because the radio conditions are good enough for $\beta_{k,\,j}^{1/\gamma} \geq R$ for some $j < l_k$ so that the load increases with γ. For $\gamma > \gamma_c$, all the $\beta_{k,\,l}^{-1/\gamma}$ are lower than R and the larger γ, the wider the gap. Hence the number of customers in outage increases as γ increases and the load decreases. Thus,

$$\gamma_c \simeq \inf\{\gamma, \beta_{s,\,l_s-1}^{-1/\gamma} \leq R\} \text{ for } s = \arg\,\max_k l_k.$$

If we proceed this way for the data of Figure 3.2, we retrieve $\gamma_c = 3.95$. This means that for a conservative dimensioning, in the absence of estimate of γ, computations may be done with this value of γ.

For a threshold given by $\epsilon = 10^{-4}$, we want to find N_{avail} such that $\mathbf{P}(N_{\text{tot}} \geq N_{\text{avail}}) \leq \epsilon$. As said earlier, the exact method gives the result at the price of a sometimes lengthy process. In view of 3.3, one could also search for α such that

$$1 - Q(\alpha) + \frac{1}{2}\sqrt{\frac{2}{\pi}} m(3, \lambda) = \epsilon \tag{3.7}$$

and then consider $\lceil 1 + \int_E f \, \mathrm{d}\nu + \alpha\sigma \rceil$ as an approximate value of N_{avail}. Unfortunately and as was expected since the Gaussian approximation is likely to be valid for *large* values of λ, the corrective term in (3.7) is far too large (between 30 and 500 depending on γ) for (3.7) to have a meaning. Hence, we must proceed as usual and find α such that $1 - Q(\alpha) = \epsilon$, i.e. $\alpha \simeq 3.71$. The approximate value of N_{avail} is thus given by $\lceil \int_E f \, \mathrm{d}\nu + 3.71\sigma \rceil$. The consequence is that we do not have any longer any guarantee on the quality of this approximation, how close it is to the true value and even more basic, whether it is greater or lower than the correct value. In fact, it is absolutely impossible to choose a dimensioning value lower than the true value since there is no longer a guarantee that the loss probability is lower than ϵ. As shows Figure 3.3, it turns out that the values returned by the Gaussian method are always under the true value. Thus this annihilates any possibility to use the Gaussian approximation for dimensioning purposes.

Going one step further, according to (3.4), one may find α such that

$$1 - Q(\alpha) - \frac{m(3,\,\lambda)}{6} Q^{(3)}(\alpha) + E_\lambda = \epsilon$$

and then use

$$\lceil 3.5 + \int_E f \, \mathrm{d}\nu + \alpha\sigma \rceil$$

as an approximate *guaranteed* value of N_{avail}. By *guaranteed*, we mean that according to (3.4), it holds for sure that the loss probability with this value of N_{avail} is smaller than ϵ even if there is an approximation process during its computation. Since the error in

the Edgeworth approximation is of the order of $1/\lambda$, instead of $1/\sqrt{\lambda}$ for the Gaussian approximation, one may hope that this method will be efficient for smaller values of λ. It turns out that for the data sets we examined, E_λ is of the order of $10^{-7}/\lambda$, thus this method can be used as long as $10^{-7}/\lambda \ll \epsilon$. Otherwise, as for the Gaussian case, we are reduced to find α such that

$$1 - Q(\alpha) - \frac{m(3,\,\lambda)}{6} Q^{(3)}(\alpha) = \epsilon$$

and consider $\lceil 3.5 + \int_E f \, \mathrm{d}\nu + \alpha\sigma \rceil$ but we no longer have any guarantee on the validity of the value. As Figure 3.3 shows, for the considered data set, Edgeworth methods leads to an optimistic value which is once again absolutely not acceptable. One can pursue the development as in (2.27) and use (3.5), thus we have to solve

$$1 \;-\; Q(\alpha) \;-\; \frac{m(3,\,\lambda)}{6} Q^{(3)}(\alpha) \;-\; \frac{m(3,1)^2}{72\lambda} Q^{(6)}(\alpha) \;+\; \frac{m(4,1)}{24\lambda} Q^{(4)}(\alpha) \;-\; F_\lambda \;=\; \epsilon.$$

For the analog of 3.4 to hold, we have to find Ψ a $\mathcal{C}_b^5$ function greater than $\mathbf{1}_{[x,\,\infty)}$ but smaller than $\mathbf{1}_{[x-\mathrm{lag},\,\infty)}$ with a fifth derivative smaller than 1. Looking for Ψ in the set of polynomial functions, we can find such a function only if lag is greater than 6.5 (for smaller value of the lag, the fifth derivative is not bounded by 1) thus the dimensioning value has to be chosen as:

$$\lceil 6.5 + \int_E f \, \mathrm{d}\nu + \alpha\sigma \rceil.$$

For the values we have, it turns out that F_λ is of the order of $10^{-9}\lambda^{-3/2}$ which is negligible compared to $\epsilon = 10^{-4}$, so that we can effectively use this method for $\lambda \geq 10^{-4}$. As it is shown in Figure 3.3, the values obtained with this development are very close to the true values but always greater as it is necessary for the guarantee. The procedure should thus be the following: compute the error bounds given by (3.3), (8.11) and (3.5) and find the one which gives a value negligible with respect to the threshold ϵ, then use the corresponding dimensioning formula. If none is suitable, use a finer Edgeworth expansion or resort to the concentration inequality approach.

Note that the Edgeworth method requires the computations of the first three (or five) moments, whose lengthiest part is to compute the $\zeta_{k,l}$ which is also a step required by the exact method. Thus Edgeworth methods are dramatically simpler than the exact method and may be as precise. However, both the exact and Edgeworth methods suffer from the same flaw: There are precise as long as the parameters, mainly λ and γ, are perfectly well estimated. The value of γ is often set empirically (to say the least) so that it seems important to have dimensioning values robust to some estimate errors. This is the goal of the last method we propose.

According to Theorem 12, if we find α such that

$$g\left(\frac{\alpha L}{\int_E f^2\lambda \, \mathrm{d}\nu}\right) = -\frac{\log(\epsilon) L^2}{\int_E f^2\lambda \, \mathrm{d}\nu}$$

and

$$N_{\mathrm{avail}} = \int_E f \, \mathrm{d}\nu + \frac{\alpha}{L^2} \int_E f^2\lambda \, \mathrm{d}\nu, \tag{3.8}$$

we are sure that the loss probability will fall under ϵ. However, we do not know a priori how larger this value of N_{avail} than the true value. It turns out that the relative oversizing

increases with γ from a few percents to 40% for the large value of γ and hence small values of N_{avail}. For instance, for $\gamma = 4.2$, the value of N_{avail} given by (3.8) is 40 whereas the exact value is 32 hence an oversizing of 25%. However, for $\gamma = 4.12$, which is 2% away from 4.2, the required number of subchannels is also 40. The oversizing is thus not as bad as it may seem since it may be viewed as a protection against traffic increase, epistemic risk (model error) and estimate error.

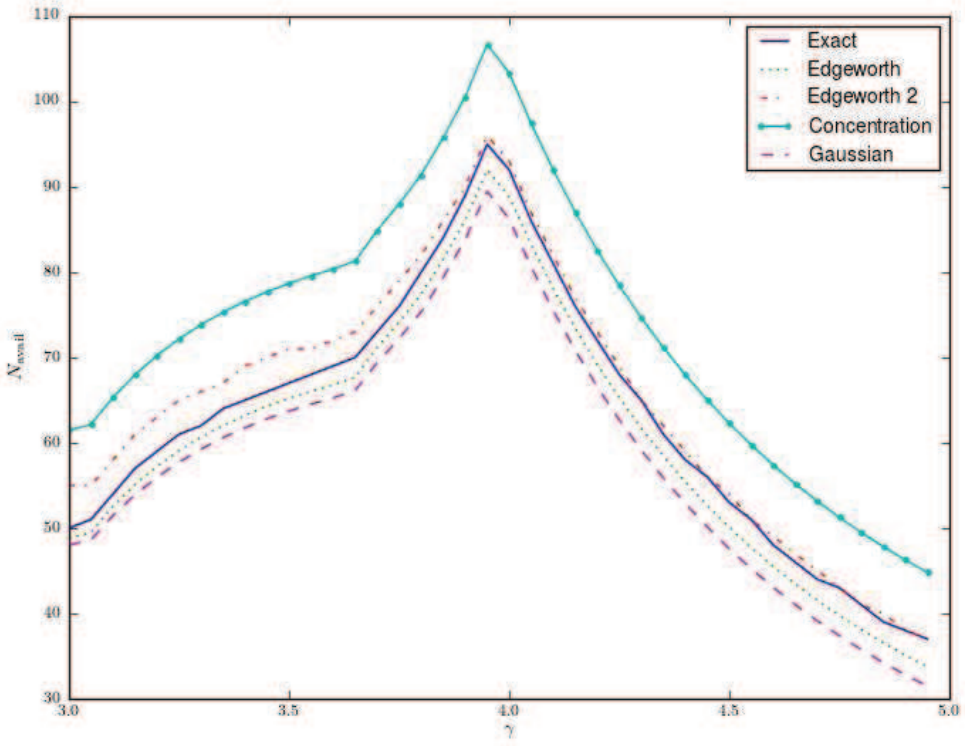


Figure 3.3: Estimates of N_{avail} as a function of γ by the different methods

Chapter 4

An analytic model for evaluating outage and handover probability of cellular wireless networks

Contents

4.1 Introduction 43
4.2 System model 44
4.3 Outage analysis 47
4.4 Handover analysis 48
4.5 Numerical results and comparison to the hexagonal model . . 50
4.6 Conclusion 51

4.1 Introduction

In a wireless network, nodes can be modeled by a fixed or a stochastic pattern of points on the plane. Fixed points models can contain a finite or an infinite number of points and usually form a lattice. This approach fails to capture the irregularity and randomness of a real network. For example, to model a wireless cellular network, the hexagonal cellular network is the most frequently used one. In reality, even if the base station (BS) nodes are fixed, it is not true that they are periodically distributed. Recently, stochastic model gained much interest. Node patterns can be represented by a stochastic process on the plane such as Poisson point process. It is worth to note that stochastic models, although more complicated at first sight, usually lead to elegant and easy calculated formulas. Actually, all the insights obtained when studying both types of models are useful for the design or the dimensioning processes of a network.

In the literature, it is very often assumed that a mobile, once active in the network, is served by its nearest BS. This holds if the effect of fading is not taken into account in the propagation model. This assumption results in a so called Poisson-Voronoi cells model (for example, [24], page 63) : the domain of the plane taken in charge by a given BS is the cell of the Voronoi tessellation it is the center of. We are interested in a system which is spatially static but with some time evolutionary elements. As its name indicates, *slow fading* varies slowly, i.e. it may be considerered as constant on a duration of the order of a

second; whereas Rayleigh fading varies much more rapidly, at the scale of a micro-second. Since we work at the time scale of a slot, i.e. of the order of micro-second, we may consider the slow fading to be constant over the period of analysis and we assume that the Rayleigh fading changes each time slot. Then, we make the very natural assumption that a mobile is served by the BS that provides it the strongest mean signal power. Mean signal power means that the effect of Rayleigh fading is averaged over a few slots. Thus, the mean signal power depends only on path loss and slow fading.

Once the mobile is attributed one BS, the signal received by this BS is the useful signal, and other signals received from other BS using the same frequency are considered as interference. It is not true if we consider for example an advanced system in which the base stations are cooperative. However our model covers almost all other existing cellular networks. To model the frequency reuse, we add a label to each BS which represents its frequency band. A BS interferes only with the other BSs that have the same label. In addition to the interference, the local noise can intervene. For a mobile to communicate with a BS, the signal-to-noise-plus-interference ratio (SINR) at this mobile location must exceed some threshold, in this case the mobile is covered, otherwise it is said to be in outage. If the mobile is in outage during several consecutive time slots, a handover decision has to be made. It is thus of paramount importance to compute the outage probability and the handover probability as explicitly as possible.

In [41], Haenggi showed that the path loss fading process is a Poisson point process on the real line in the case of path loss exponent model. In [4] Baccelli and al. found analytic expressions for outage probability of networks where each node tries to connect with a destination at fixed distance or to the nearest node in case of Rayleigh fading. In [42], Kelif et al. found an outage probability expression for cellular network by mean of the so-called fluid model. In [43], Ganti et al. developped interesting results about temporal and spatial correlation of wireless networks. In [44] and [45], outage probability of regular hexagonal cellular networks with reuse factor and adaptive beamforming were studied by simulation.

This chapter is organized as follows. In Section 4.2 we describe our model. In Section 4.3, we calculate the outage probability. In Section 4.4, we calculate the handover probability. Section 4.5 shows the numerical results and the difference between our model and the traditional hexagonal model.

Important notations and parameters used in this chapter are summarized in the table 4.1.

4.2 System model

Given a BS (base station) located at y, of transmission power P, and an MS (mobile station) located at x, the mobile's received signal has average power $L(y-x)P$ where L is the path loss function. The most used path loss function is the path loss exponent law $L(z) = K|z|^{-\gamma}$ where $|z|$ refers to the Euclid norm of z. The parameter K depends on the characteristics of the antenna and the path loss exponent γ, typically in the range $(2, 4)$ characterizes the environment under study. Actually, this path loss model gives nice closed formulas but is not correct for small distances as it implies an almost infinite power close to the BS. It is thus often preferable to consider the modified path loss exponent model $L(z) = K(\max\{R_0, |z|\})^{-\gamma}$ where R_0 is a reference distance. In addition to the deterministic large scale effect, there are two random factors that have to be considered. The first one, called *shadowing*, represents the signal attenuation caused by large obstacles

Symbols	Physical meaning
$L(y-x)$	Pathloss function from y to x
γ	Pathloss exponent
h_{yx}	Slow fading form y to x
H	Generic random variable of slow fading
σ^2	Logarithmic standard deviation of shadowing
$r_{yx}[l]$	Fast fading from y to x at time slot l
$s_x[l]$	SINR of a user at x at time slot l
k	i^2+j^2+ijFrequency reuse factor
ζ^{-1}	$h_{yx}L(y-x)P$ Average received power from y to x
$\Pi_B=\{y_n, n\geq 1\}, \lambda_B$	Poisson point process of BSs and its intensity
Ξ	$\{(h_{y,x}L(y-x)P)^{-1}, y\in\Pi_B\}$, Poisson point process of received power

Table 4.1: Notations and parameters.

such as buildings. The second, called *fast fading*, represents the impact of multi-path. The shadowing can be considered as constant during a period of communication of a mobile while the fast fading changes at each time slot. If no beamforming technique is used, the received signal power from the BS y to the MS x at the time slot l is $P_{yx}[l] = r_{y,x}[l]h_{yx}L(y-x)P$, where $\{h_{yx}\}_{x,y\in\mathbb{R}^2}$ are copies of a random variable H while $\{r_{yx}[l]\}$ are independent copies of R which is an exponential random variable of mean $1/\mu$. We suppose that for each x, the random variables $(h_{yx},\, y\in\mathbb{R}^2)$ are independent, and p_H (resp. F_H) denotes their PDF (resp. complementary CDF). The most used shadowing random model is log-normal shadowing, for which H is a log-normal random variable. In this case, we can write $H\sim 10^{G/10}$ where $G\sim\mathcal{N}(0,\sigma^2)$. We now consider the conventional beamforming technique with n_t antennas. The power radiation pattern for a conventional beam-former is the product of the array factor times the radiation pattern of a single antenna. If ϕ is the direction towards which the beam is steered, the array gain in the direction θ is given by ([45],[44]):

$$\frac{\sin^2(n_t\frac{\pi}{2}(\sin(\theta)-\sin(\phi))}{n_t^2\sin^2(\frac{\pi}{2}(\sin(\theta)-\sin(\phi))}g(\theta),$$

where $g(\theta)$ is the gain in the direction θ with one antenna. For simplicity we assume that the BS always steers to the direction of the served MS and the gain $g(\theta)$ is positive constant on $(-\pi/2,\pi/2)$ and 0 otherwise (zero front-to-back power ratio). Hence, the interference signal power from a BS to an MS attached to another BS using the same frequency, in the direction θ, will be reduced by a factor of:

$$a(\theta)=1_{\{\theta\in(-\pi/2,\pi/2)\}}\frac{\sin^2(n_t\frac{\pi}{2}(\sin(\theta)))}{n_t^2\sin^2(\frac{\pi}{2}(\sin(\theta)))}.$$

If the beamforming technique is not used $a(\theta)=1$. We assume that the bandwidth is split in k non interfering sub-bands.

Thus, for a mobile at position x, any BS is characterized by three quantities: y its position, e the sub-band in which it operates and $\xi^{-1}=h_{xy}L(y-x)P$.

Once being in the network, the mobile x is attached to (or served by) the BS that provides the best *average* signal strength in *time*: it is attached to the BS which has the

minimal ξ. We denote by y_0 the position of the chosen BS and by $(y_n,\, n \geq 1)$ the positions of the other BSs. Sub-bands and ξ's are indexed accordingly.

Assume that each BS using frequency e_0 is always serving an MS, and denote by θ_i the argument of the segment $[x, y_i]$. The SINR at time slot l is given by:

$$s_x[l] = \frac{r_{y_0x}[l]\xi_0^{-1}}{N + \sum_{i\neq 0} 1_{\{e_i=e_0\}} a(\theta_i) r_{y_ix}[l]\xi_i^{-1}} \tag{4.1}$$

where N is the noise power, assumed to be constant. The term $I_x = \sum_{i\neq b(x)} 1_{\{e_i=e_0\}} a(\theta_i) r_{y_ix}[l]\xi_i^{-1}$ is the sum of all interference. In order to communicate with the attached BS, the SINR must not fall below some threshold T.

We assume that the base stations are distributed in the plane according to a Poisson point process Π_B of intensity λ_B. The frequency e_i at which operates y_i is chosen uniformly in $\{1, \cdots, k\}$ where k is the frequency reuse factor. The BSs that have the same mark interfere to each other. Our reuse model can be considered as a worst case scenario since the sub-bands are distributed at random, in contrast with planned network patterns where frequencies are attributed to BSs in order to minimize interference. The subsequent computations rely mainly on the following theorem.

Theorem 16. *The random variables $\Xi = \{(h_{y,x}L(y-x)P)^{-1},\, y \in \Pi_B\}$ is a Poisson point process on $\mathbb{R}^+$ with intensity $d\Lambda(t) = \lambda_B B'(t)dt$ where $B(\beta) = \int_{R^2} F_H((L(z)P\beta)^{-1})\, dz$.*

Proof. Define the marked point process $\Pi^x = \{y_i, h_{y_ix}\}_{i=0}^{\infty}$. It is a Poisson point process of intensity $\lambda_B dy \otimes f_H(t)dt$ because the marks are i.i.d. Consider the probability kernel $p((z,t), A) = 1_{\{(L(z)Pt)^{-1}\in A\}}$ for all Borel $A \subset \mathbb{R}^+$ and apply the displacement theorem [24, Theorem 1.3.9], to obtain that Ξ is a Poisson point process whose intensity measure we denote by Λ. Moreover, for any β

$$\begin{aligned}\Lambda([0,\beta]) &= \lambda_B \int_{R^2\otimes R} 1_{\{t\geq(\beta P.L(z)P)^{-1}\}} p_H(t)dzdt \\ &= \lambda_B \int_{R^2} F_H((\beta L(z)P)^{-1})dz = \lambda_B B(\beta).\end{aligned}$$

This concludes the proof. □

By straightforward quadatures, we get the following proposition.

Proposition 17. *If $L(z) = K(\max\{R_0, |z|\})^{-\gamma}$ then:*

$$B(\beta) = C_1\beta^{\frac{2}{\gamma}} \int_{\frac{R_0^\gamma}{\beta PK}}^{\infty} t^{\frac{2}{\gamma}} p_H(t)dt, \tag{4.2}$$

where $C_1 = \pi(PK)^{\frac{2}{\gamma}}$. For lognormal shadowing $H \sim 10^{G/10}$ where $G \sim \mathcal{N}(0,\sigma^2)$ and we have:

$$B(\beta) = C_1\beta^{\frac{2}{\gamma}} e^{(\frac{2\sigma_1}{\gamma})^2} Q(\frac{-\ln\beta - \ln(PKR_0^{-\gamma})}{\sigma_1} - \frac{2\sigma_1}{\gamma}) \tag{4.3}$$

where $Q(u) = \frac{1}{\sqrt{2\pi}}\int_u^\infty e^{-u^2/2}du$ and $\sigma_1 = \frac{\sigma\ln 10}{10}$.

For the exponent pathloss model, it is sufficient to put $R_0 = 0$ in the above formulas. This particular result could be derived from [41]. We observe that the distribution of the point process Ξ does depend only on $E(H^{\frac{2}{\gamma}})$ but not on the distribution of H itself. This phenomenon can be explained as in [46, Page 159].

4.3 Outage analysis

The mobile at x suffers an outage at time slot l whenever its SINR falls below a threshold T at this slot. For the sake of notations,in this Section, we drop the index l as it is fixed.

Theorem 18. *The outage probability is given by*

$$p_o := P(s_x < T) = 1 - \lambda_B \int_0^\infty B'(\beta) e^{-\lambda_B B(\beta) - NT\mu\beta - \frac{\lambda_B}{2\pi k} D(\beta)} \, d\beta \tag{4.4}$$

where $D(\beta) = \int_{-\pi}^{\pi} d\theta \int_\beta^\infty B'(\xi)(1 + \xi/T\beta a(\theta))^{-1} \, d\xi$.

Proof. Since $r_{y_0 x}$ is an exponential r.v. of mean $1/\mu$ we have:

$$\begin{aligned} P(s_x \geq T | \xi_0 = \beta) &= P(r_{y_0 x} \geq T\beta(N + I_x(\beta)) \mid \xi_0 = \beta) \\ &= E(e^{-\mu T\beta(N + I_x(\beta))} \mid \xi_0 = \beta) \\ &= e^{-NT\mu\beta} \mathcal{L}_{I_x(\beta)}(T\mu\beta) \end{aligned}$$

where $I_x(\beta)$ is the distribution of the random variable I_x given $(\xi_0 = \beta))$ and $\mathcal{L}_{I_x(\beta)}$ is its Laplace transform. Given $(\xi_0 = \beta)$, according to strong Markov property, the point process $\{\xi_i\}_{i>0}$ is a Poisson point process on (β, ∞) with intensity $\lambda_B B'(\xi) d\xi$. By thinning, the point process $\{\xi_i\}_{\{i>0, e_i = e_0\}}$ is a Poisson point process on (β, ∞) with intensity $k^{-1}\lambda_B B'(\xi) d\xi$. Hence, $\mathcal{L}_{I_x(\beta)}$ can be calculated as follows (see [24]):

$$\begin{aligned} \mathcal{L}_{I_x(\beta)}(u) &= e^{-\int_\beta^\infty \frac{\lambda_B}{2\pi k} B'(\xi)(1 - E(e^{-a(\theta) u \xi^{-1} R})) d\xi} \\ &= e^{-\frac{\lambda_B}{2\pi k} \int_\beta^\infty B'(\xi) d\xi \int_0^\infty dr \int_{-\pi}^{\pi} \mu e^{-\mu r}(1 - e^{-a(\theta) u r \xi^{-1}}) d\theta} \\ &= \exp\left(-\frac{\lambda_B}{2\pi k} \int_{-\pi}^{\pi} d\theta \int_\beta^\infty B'(\xi) \frac{d\xi}{1 + \xi\mu(ua(\theta))^{-1}} \right). \end{aligned}$$

Thus, we get

$$P(s_x \geq T | \xi_0 = \beta) = e^{-NT\mu\beta - \frac{\lambda_B}{2\pi k} D(\beta)}. \tag{4.5}$$

Since the distribution density of ξ_0 is $\lambda_B B'(\beta) e^{-\lambda_B B(\beta)}$, by averaging over all ξ_0 we obtain (4.4). □

Proposition 19. *In the interference-limited regime* $(N = 0)$*, we have*

$$p_o(T) = 1 - \lambda_B \int_0^\infty B'(\beta) e^{-\lambda_B B(\beta) - \frac{\lambda_B}{2\pi k} D(\beta)} d\beta. \tag{4.6}$$

If $L(z) = K|z|^{-\gamma}$ *we have:*

$$p_o(T) = 1 - \int_0^\infty e^{-M\alpha - G\alpha^{\frac{\gamma}{2}}} d\alpha \tag{4.7}$$

where $M := M(k, T, \gamma) = 1 + \frac{1}{2\pi k} \int_{-\pi}^{\pi} d\theta \int_1^\infty \frac{du}{1 + (T.a(\theta))^{-1} u^{\frac{\gamma}{2}}}$ *and* $G = NT\mu(\lambda_B C)^{-\frac{\gamma}{2}}$. *If* $L(z) = K|z|^{-\gamma}$ *and* $N = 0$ *we have:*

$$p_o(T) = 1 - \frac{1}{M}. \tag{4.8}$$

Some interesting facts are observed from these results: Rewrite the expression of SINR as

$$s_x[l] = \frac{\overline{r}_{y_0x}[l]\xi_0^{-1}}{\mu N + \sum_{i\neq 0} 1_{\{e_i=e_0\}} a(\theta_i)\overline{r}_{y_ix}[l]\xi_i^{-1}}$$

where $\overline{r}_{y_0x}[l] = \mu r_{y_ix}[l]$. Since $r_{yx}[l]$ is an exponential random variable of mean $1/\mu$, $\overline{r}_{y_0x}[l]$ is an exponential random variable of mean 1. Hence by the above equation it is expected that the outage probability depends on the product μN but not directly on μ and N. It is an increasing function of $N\mu$ which is confirmed by (4.4). The fact that the outage probability is an increasing function of μ and N is quite natural, increasing of noise or the fast fading influence always deteriorate the system performances.

It is also expected that in the interference limited case ($N = 0$) the outage probability does not depend on μ. It is confirmed by (4.6). Physically it means that in the absence of noise, the fast fading modifies the channels (from the MS to each BS) characteristics by the same factor, thus the SINR does not change.

In the interference limited scenario with the exponent pathloss model, the outage probability does not depend neither on μ, nor on the BS density λ_B and nor on the distribution of shadowing H. It is due to the scaling properties of the pathloss function and of the Poisson point process. The outage probability is thus a decreasing function of the pathloss exponent γ.

In the presence of noise $N > 0$ and still for the exponent pathloss model case, the outage probability is an increasing function of λ_B. Hence, it can be thought that the more an operator installs BSs, the better the network is. In addition, if the density of BSs goes to infinite then outage will never occur. However it is not true. In fact, if the density of BSs is very high, the distances between a MS and BSs tend to be relatively small. Hence, the exponent pathloss model is no longer valid since it is not accurate at small distances. If the modified exponent pathloss is used, the outage probability must converge to 0. The outage probability is also an increasing function of $E(H^{\frac{2}{\gamma}})$, and if the shadowing H follows lognormal distribution then the outage probability will be an increasing function of σ. We recover an other well known fact: the increasing of uncertainty of the radio channel deteriorates the performance of the network.

4.4 Handover analysis

If the MS is in outage for n consecutive time slots, a handover decision has to be made. Keep in mind that only the Rayleigh fast fading changes each time slot. Let A_l be the event that the mobile is in outage in the time slot l, and A_l^c its complement and observe that in fact $P(\cap_{i=1}^m A_{j_i}^c) = P(\cap_{i=1}^m A_i^c)$. By definition $p_{ho} := P(\cap_{i=1}^n A_{l+i-1}) = P(\cap_{i=1}^n A_i)$. We have

$$\begin{aligned} p_{ho} &= 1 + \sum_{m=1}^{n} (-1)^m \sum_{j_1\neq\ldots\neq j_m\in\{1,..,n\}} P(\cap_{i=1}^m A_{j_i}^c) \\ &= 1 + \sum_{m=1}^{n} (-1)^m \frac{n!}{m!(n-m)!} P(\cap_{i=1}^m A_i^c)\cdot \end{aligned}$$

Theorem 20. *The handover probability is given by:*

$$p_{ho} = 1 + \sum_{m=1}^{n} (-1)^m \frac{n!}{m!(n-m)!} q_m,$$

where $q_m = P(\cap_{i=1}^{m} A_i^c)$ *is given by:*

$$q_m = \int_0^{\infty} \lambda_B B'(\beta) e^{-\lambda_B B(\beta) - NT\mu\beta - \frac{\lambda_B}{2\pi k} D_m(\beta)} d\beta,$$

and $D_m(\beta) = \int_{-\pi}^{\pi} d\theta \int_{\beta}^{\infty} B'(\xi)(1 - (\frac{1}{1+T\beta a(\theta)\xi^{-1}})^m) d\xi$.

Proof. We need to calculate the probability $P(\cap_{i=1}^{m} A_i^c)$ that is the probability that the mobile is covered in m different time slots.

$$\begin{aligned} P(\cap_{i=1}^{m} A_i^c | \xi_0 = \beta) &= P(s_x[1] \geq T, ..., s_x[m] \geq T | \xi_0 = \beta) \\ &= P(r_{y_0 x}[i] \geq \beta(TN + I_x[i]), i = 1 \dots m | \xi_0 = \beta) \\ &= E(e^{-\mu(mTN\beta + \sum_{i=1}^{m} I_x(\beta)[i])} | \xi_0 = \beta) \\ &= e^{-mNT\mu\beta} \mathcal{L}_{\sum_{i=1}^{m} I_x(\beta)[i]}(T\mu\beta) \end{aligned}$$

where $I_x(\beta)[i]$ is the distribution of the random variable $I_x[i]$ given $(\xi_0 = \beta)$. We have :

$$\sum_{i=1}^{m} I_x(\beta)[i] = \sum_{j=1}^{\infty} 1_{\{e_i = e_0\}} \xi_i^{-1} a(\theta_i) (\sum_{i=1}^{m} r_{y_i x}[i]).$$

As the random variables $r_{y_i x}[i]$ are independent copies of the exponential random variable R, the random variables $\sum_{i=1}^{m} r_{y_i x}[i]$ are also i.i.d and the common Laplace transform of the latter is :

$$\mathcal{L}_{\sum_{i=1}^{m} r_{y_i x}[i]}(u) = (\mathcal{L}_R(u))^m = (\frac{\mu}{\mu + u})^m.$$

The Laplace transform of $\sum_{i=1}^{m} I_x(\beta)[i]$ is now:

$$\mathcal{L}_{\sum_{i=1}^{m} I_x(\beta)[i]}(u) = e^{-\frac{\lambda_B}{2\pi k} \int_{-\pi}^{\pi} d\theta \int_{\beta}^{\infty} B'(\xi)(1 - (\frac{\mu}{\mu + a(\theta)\xi^{-1} u})^m) d\xi}.$$

Proceeding as for Theorem 18, we get

$$q_m = \int_0^{\infty} \lambda_B B'(\beta) e^{-\lambda_B B(\beta) - NT\mu\beta - \frac{\lambda_B}{2\pi k} D_m(\beta)} d\beta.$$

The result follows. □

We can obtain more closed expression for q_m in some special cases.

Proposition 21. *In the interference limited regime* $N = 0$*, we have:*

$$q_m = \int_0^{\infty} \lambda_B B'(\beta) e^{-\lambda_B B(\beta) - \frac{\lambda_B}{2\pi k} D_m(\beta)} d\beta.$$

If $L(z) = K|z|^{-\gamma}$ *then:*

$$q_m = \int_0^{\infty} e^{-M_m \alpha - G\alpha^{\frac{\gamma}{2}}} d\alpha$$

where

$$M_m = 1 + \frac{1}{2\pi k} \int_{-\pi}^{\pi} d\theta \int_1^{\infty} (1 - (\frac{1}{1 + Ta(\theta) u^{-\frac{\gamma}{2}}})^m) du.$$

If $N = 0$ *and* $L(z) = K|z|^{-\gamma}$ *we have:* $q_m = 1/M_m$.

From these computations, the same kind of conclusions as for outage probability can be drawn.

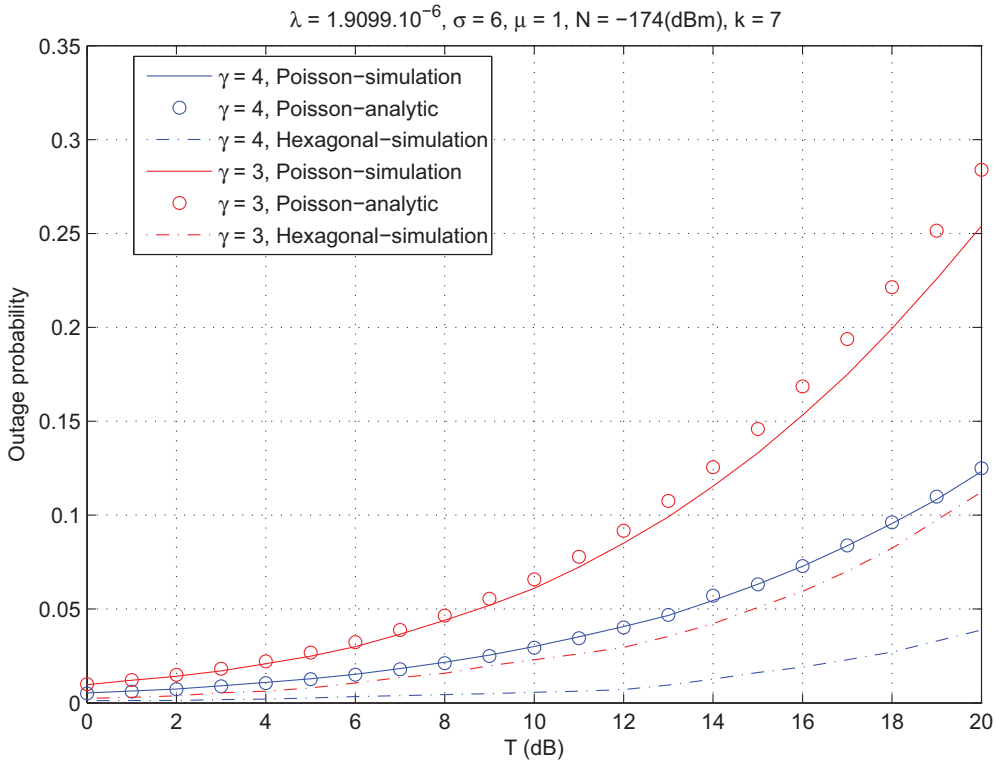


Figure 4.1: Outage probability vs SINR threshold

4.5 Numerical results and comparison to the hexagonal model

We place a MS at the origin o and consider a region $B(o, R_g)$ where $R_g = 300(m)$. The BSs are distributed according to a Poisson point process in this region. The path loss exponent model is considered. The default values of the model parameters are $K = -20$ dB, $P = 0$ dB, $n_t = 8$ and $\mu = 1$.

In the literature, the hexagonal model is widely used and studied so we would like to compare two models. For a fair comparison, the density of BSs must be chosen to be the same, i.e the area of an hexagonal cell must be $1/\lambda_B$. Unlike the Poisson model where each BS is randomly assigned a frequency, in the hexagonal model, the frequencies are well assigned so that an interfering BS is far from the transmitting BS and BSs of different frequency are grouped in reuse patterns. The reuse factor k in the hexagonal model is determined by $k = i^2 + j^2 + ij$ where integers i, j are the relative location of co-channel cell.

Figure 4.1 shows the outage probability versus the SINR threshold of the Poisson model and the hexagonal model in the case $k = 7$. As we can see, the outage probability in the case of Poisson model is always greater than that of hexagonal model as expected. The difference is about 8 (dB) in the case $\gamma = 4$ and 6(dB) in the case $\gamma = 3$.

In Figure 4.3, we can see that the outage probability is a decreasing function of γ as theoretically observed. In Figure 4.4, we see if the reuse factor k increases, the MS has to do less handover. Thus, increasing the reuse factor has a positive effect on the system performance not only in term of outage but also in term of handover.

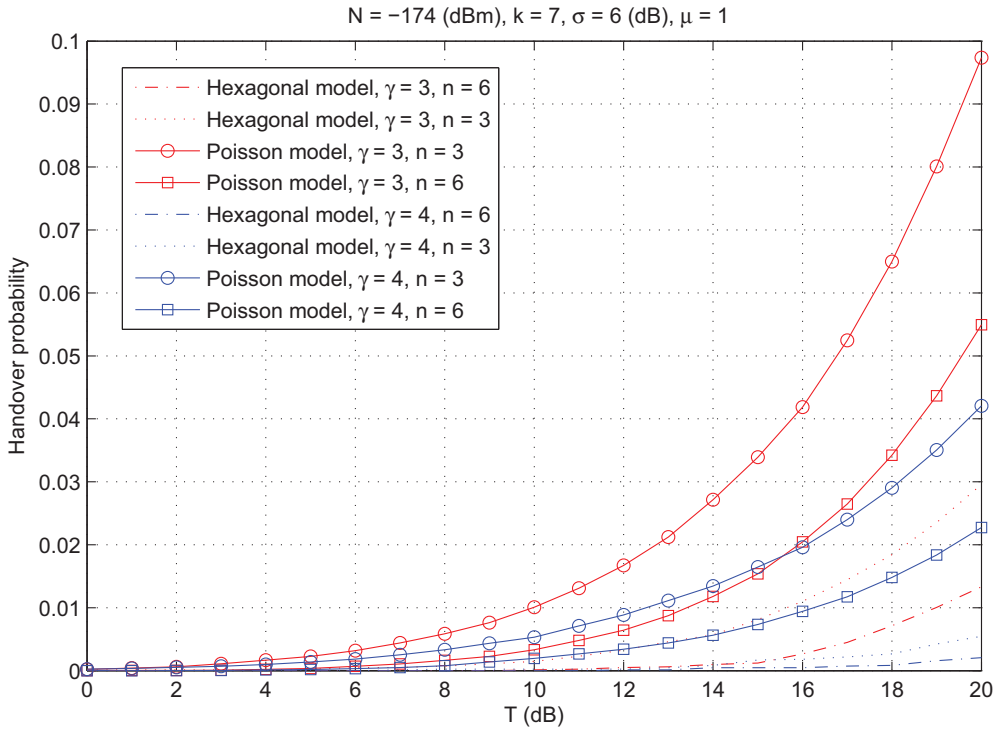


Figure 4.2: Handover probability vs SINR threshold

4.6 Conclusion

In this paper we have investigated the outage and handover probabilities of wireless cellular networks taking into account the reuse factor, the beamforming, the path loss, the slow fading and the fast fading. We valid our model by simulation and compare numerical results to that of hexagonal model. The analytic expressions derived in the this paper can be considered as an upper bound for a real system.

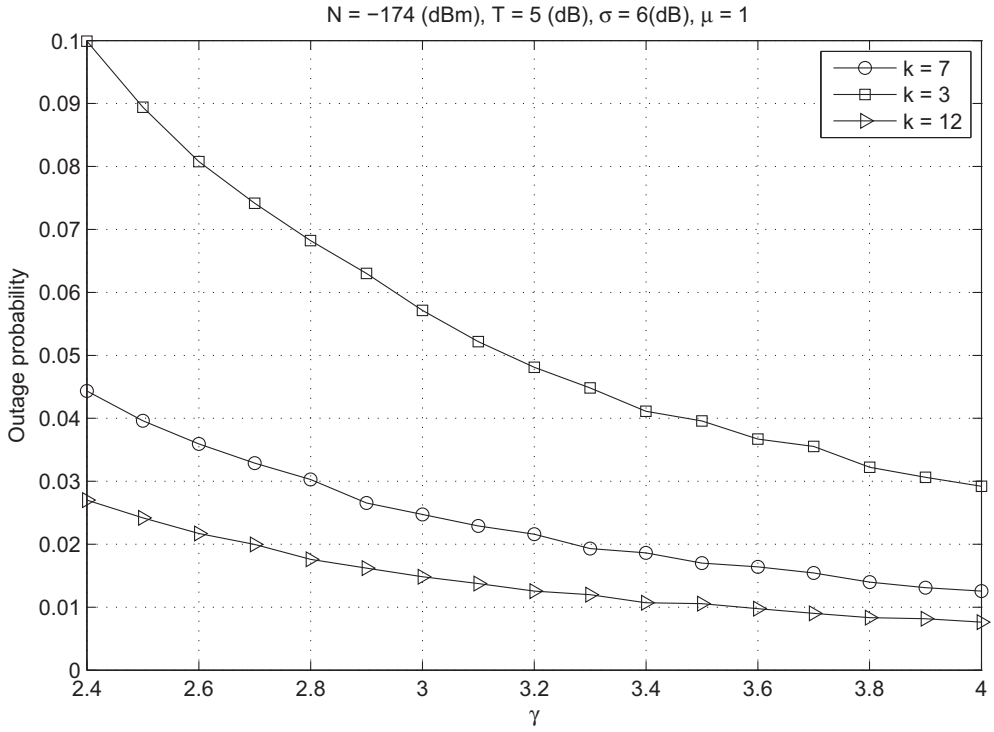


Figure 4.3: Outage probability vs path loss exponent γ, Poisson model

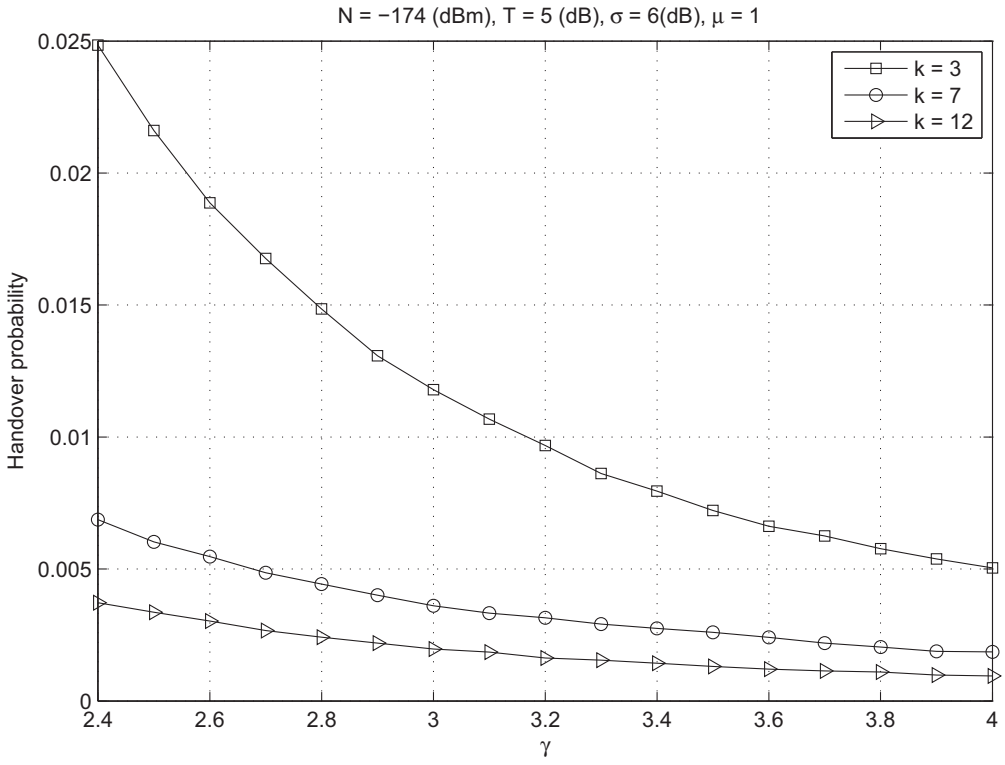


Figure 4.4: Handover probability vs path loss exponent γ, Poisson model, $n = 3$

Chapter 5

On noise-limited networks

Contents

5.1 Introduction 53
5.2 Model 54
5.3 Poisson point process of path loss fading 56
5.4 Capacity 59
5.5 Examples 64
5.5.1 Number of users in a cell 64
5.5.2 Number of users in outage in a cell 65
5.5.3 Number of covered users in a cell 65
5.5.4 Total bit rate of a cell 66
5.5.5 Discussion on the distribution of $S_o(f)$ 66
5.6 Conclusion 68

5.1 Introduction

Cellular network is a kind of radio network consisting of a number of fixed access points known as base stations and a large number of users (or mobiles). Each base station covers a geometrical region known as a cell and serve all users in this cell. Interference and noise are two factors annoying communications in cellular wireless networks. Noise is unavoidable and comes from natural sources. Interference come from users and base stations. The use of recent technologies such as SDMA (spatial division multiple access) and MIMO (multiple input multiple output) can reduce significantly interference so that we can hope that in a near future the impact of interference will be negligible and noise will become the only factor harming the network. The best case is when interference from other cells are perfectly canceled, the network is then said to be in noise limited regime. We introduce here a framework to study this kind of network.

In the existing literature, base stations (BS) locations are usually modeled as an ideal regular hexagonal lattice. In reality, base stations are irregularly located, especially in an urban area, and the cell radius is not the same for each BS. In this chapter, we model the base station locations as an homogenous Poisson point process Π_B of intensity λ_B. Such a model comes from stochastic geometry. It is sufficiently versatile by changing λ_B to cover a wide number of real situations and it is mathematically tractable. For an introduction

to the usage of stochastic geometry for wireless networks performances, we refer to [47]. Theory and number of pertinent examples can be found in [24] and [48]. For all theoretical details, we refer to the first opus.

To model cellular network cells, Voronoi tessellations are frequently used. It is based on the assumption that each user is served by the closest BS. Unfortunately, this is not always very accurate since in real life, a mobile connects to the *best* BS it can have, i.e., the BS which offers it the best Signal over Noise Ratio. The *best* BS is not always the closest because of the fading environment. In this chapter, we analyze the impact of fading by considering that users are served by the base station providing the best signal power. The location of users in the plane are modeled as another homogenous Poisson point process Π_M of intensity λ_M.

While cellular networks like GSM and GPRS provided only voice service and low data transmission rate, recent and emergent wireless cellular networks such as WIMAX or LTE offer higher data rate and other services requiring high throughput such as video calls. Each service requires a different level of signal to noise ratio (SNR). If the SNR does not reach a required threshold due to the radio condition, the service cannot be established or may be interrupted. Such calls are said to be in outage. The outage probability is one of the key measurement of the network performance. We aim to determine the outage probability of noise limited network, or equivalently the distribution of SNR, which turns out to be equivalent to determine the distribution of the smallest path loss fading. In fact, there have been some works dealing with the outage probability of noise limited wireless network, but almost all of them consider the exponent path loss model. We here derive a formula for outage probability taking into account a general model of path loss.

Once the distribution of SNR of a user is determined, the distribution of functionals related to SNR can be easily derived. In some situations, we have to study the distribution of the sum of a functional for all users in a cell. For example, in an OFDMA noise limited cellular system, the number of sub channels required for a user demanding a particular service depends on its SNR. If the total number of sub channels of all users in a cell excesses the number of available sub channels in this cell then at least one user is blocked. The probability of that to happen, sometimes called unfeasibility probability, contains extremely important information on the performance of the network. Since it is often impossible to find the explicit probability distribution of additive functionals, we calculate the expectation, and bounds on the variance of such random variables.

Important notations and parameters used in this chapter are summarized in the table 5.1.

5.2 Model

Consider a BS (base station) located at y with transmission power P and a mobile located at x. The mobile's received signal has average power $L(y-x)P$ where L is the path loss function. The most used path loss function is the so-called path loss exponent model

$$L(z) = K|z|^{-\gamma},$$

where $|z|$ refers to the Euclidean norm of z. This function gives raise to nice closed formulas but is rather unrealistic: Close to the BS, the signal is infinitely amplified. A more realistic model is the modified path loss model given by:

$$L(z) = K \min\{R_0^{-\gamma}, |z|^{-\gamma}\}$$

Symbols	Physical meaning
$L(y-x)$	Pathloss function from y to x
γ	Pathloss exponent
h_{yx}	Fading form y to x
H	Generic random variable of fading
Π_B	$\{y_0, y_1, ...\}$Poisson point process of BSs of intensity λ_B
Π_M	$\{x_0, x_1, ...\}$Poisson point process of users of intensity λ_M
Sh^x	$\{s_{yx} := h_{yx}L(y-x))^{-1}$, $y \in \Pi_B\}$, Path loss fading process at point x
Sh^x	$\{0 < \xi_0^x < \xi_1^x < \ldots\}$Path loss fading process at point x
f	Capacity function (for example $f(u) = \log_2(1+u)$)
$S_o(f)$	$\sum_{x \in C_o} f(s_{ox})$, Cell sum capacity
$m(f), v(f)$	Mean and variance of $S_o(f)$

Table 5.1: Notations.

where R_0 is a reference distance and K a constant depending on the environment. In addition to this deterministic large scale effect, we consider the fading effect, which is by essence random. The received signal power from a BS located at y to a mobile unit (MU for short) located at x is given by

$$P_{yx} = h_{y,x}L(y-x)P,$$

where $\{h_{y,x}\}_{x,y \in \mathbb{R}^2}$ are independent copies of a random variable H. Most used fading random models are log-normal shadowing and Rayleigh fading. The log-normal shadowing is such that H is a log-normal random variable and we can write $H \sim 10^{G/10}$ where $G \sim \mathcal{N}(0, \sigma^2)$. The Rayleigh fading is such that H is an exponential random variable of parameter μ. We can also consider the Rayleigh-Lognormal composite fading, in this case the fading is the product of the log-normal shadowing factor and the Rayleigh fading factor. It is worth noting that the log-normal shadowing usually improves the network performance while Rayleigh fading usually degrades performances.

We assume that once in the network, a mobile is attached to the BS that provides it the best signal strength. If the power received at this point is greater than some threshold T, we say that x is covered. If x is not covered by any BS then a MU at x cannot establish a communication and thus is said to be in outage. In the case of path loss exponent model with no fading ($H =$ constant), the best BS for given mobile is always its nearest BS.

We assume that the point process of BSs $\Pi_B = \{y_0, y_1, ...\}$ is an homogenous Poisson point process of intensity λ_B on $\mathbb{R}^2$ and that users are distributed in the plane as a Poisson point process $\Pi_M = \{x_0, x_1, ...\}$ of intensity λ_M.

To avoid any technical difficulty, from now on, we make the following assumptions:

Assumption 1. *Assume that:*

1. *All random variables h_{yx} $(x, y \in \mathbb{R}^2)$ are independent.*
2. *H admits a probability density function p_H. Its complementary cumulative distributive function is denoted by F_H, i.e.,*

$$F_H(\beta) = P(H \geq \beta) = \int_\beta^\infty p_H(t)\ dt > 0.$$

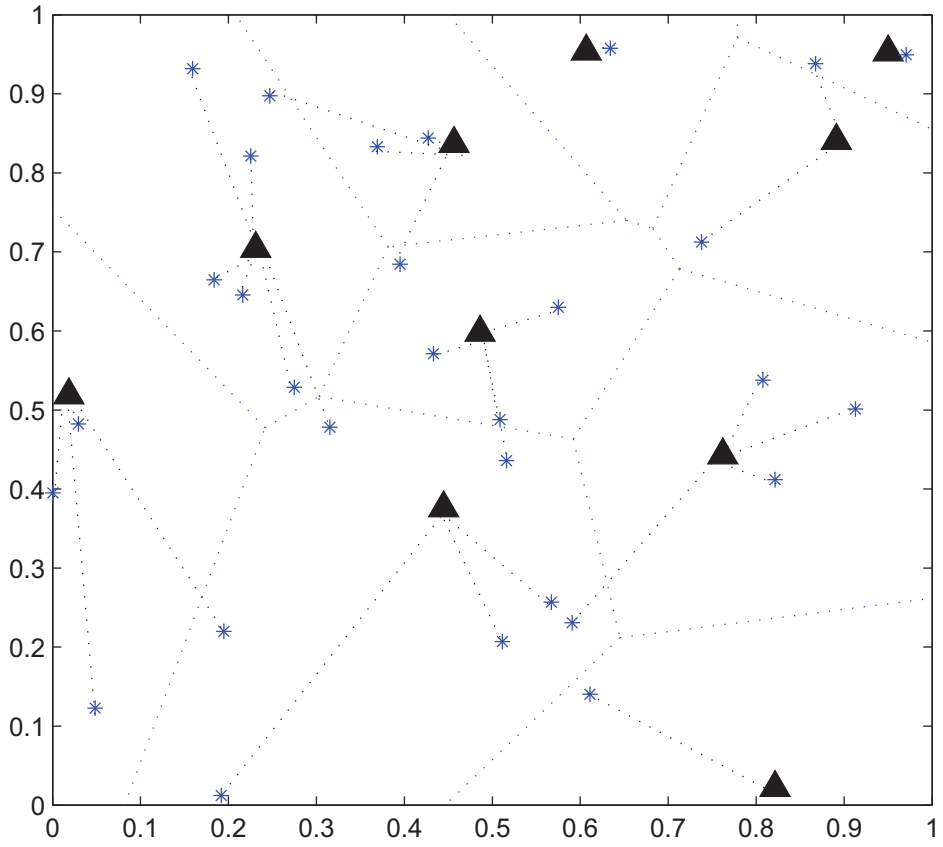


Figure 5.1: Triangles represent BS, plus represent MU. Dotted polygons are Voronoi cells induced by BS. A line between a BS and an MU means that the BS serves the MU. A mobile may be not served by the BS closest to it, due to fading.

3. Define $B(\beta) = \int_{R^2} F_H((L(z)\beta)^{-1})\ dz$. *Then, we have* $0 < B(\beta) < \infty$ *for all* $\beta > 0$.

5.3 Poisson point process of path loss fading

For each location x on $\mathbb{R}^2$, consider the path loss fading process $Sh^x = \{s_{yx} := h_{yx}L(y - x))^{-1},\ y \in \Pi_B\}$. The next proposition follows from [41].

Proposition 22. *For any* x, Sh^x *is a Poisson point process on* $\mathbb{R}^+$ *with intensity density* $d\Lambda(t) = \lambda_B B'(t)dt$. *In addition,* $B(0) = 0$ *and* $B(\infty) = \infty$.

For any point x, we can reorder the points of Sh^x. We denote ordered atoms of Sh^x by $0 < \xi_0^x < \xi_1^x < \ldots$. The CDF and PDF of ξ_m^x are easily derived according to the property of Poisson point processes:

Corollary 1. *The complementary cumulative distribution function of* ξ_m^x *is given by:*

$$P(\xi_m^x > t) = e^{-\lambda_B B(t)} \sum_{i=0}^{m} \frac{(\lambda_B B(t))^i}{i!},$$

and its probability density function is given by

$$p_{\xi_m^x}(t) = \frac{\lambda_B^{m+1} B'(t)(B(t))^m}{m!} e^{-\lambda_B B(t)}. \tag{5.1}$$

Proof. The event $(\xi_m^x > t)$ is equivalent to the event (in the interval $[0,t]$, there are at most m points) and the number of points in this interval follows a Poisson distribution of mean $\lambda_B B(t)$. Thus, we have:

$$P(\xi_m^x > t) = e^{-\lambda_B B(t)} \sum_{i=0}^{m} \frac{(\lambda_B B(t))^i}{i!}.$$

The PDF is thus given by

$$\begin{aligned} p_{\xi_m^x}(t) &= -\frac{\partial}{\partial t} P(\xi_m^x > t) \\ &= -\lambda_B B'(t) e^{-\lambda_B B(t)} \\ &\quad + \sum_{1}^{m} \lambda_B B'(t) e^{-\lambda_B B(t)} \left(\frac{(\lambda_B B(t))^{i-1}}{(i-1)!} - \frac{(\lambda_B B(t))^i}{i!} \right) \\ &= \frac{\lambda_B^{m+1} B'(t)(B(t))^m}{m!} e^{-\lambda_B B(t)}. \end{aligned}$$

The proof is thus complete. □

Corollary 2. *If $L(z) = K|z|^{-\gamma}$ then:*

$$B(\beta) = C.\beta^{\frac{2}{\gamma}},$$

where $C = \pi K^{\frac{2}{\gamma}} E(H^{\frac{2}{\gamma}})$.

Proof. The path loss function depends only on the distance from the BS to the user. By the change of variable $r = |z|$ and by integration by substitution, we have:

$$\begin{aligned} B(\beta) &= 2\pi \int_0^\infty \int_0^\infty r 1_{\{tK\beta \geq r^\gamma\}} p_H(t) \, \mathrm{d}r \, \mathrm{d}t \\ &= 2\pi \int_0^\infty p_H(t) \, \mathrm{d}t \int_0^{(tK\beta)^{1/\gamma}} r \, \mathrm{d}r \\ &= \pi (K)^{\frac{2}{\gamma}} \beta^{\frac{2}{\gamma}} \int_0^\infty p_H(t) t^{\frac{2}{\gamma}} \, \mathrm{d}t \\ &= \pi (K)^{\frac{2}{\gamma}} E(H^{\frac{2}{\gamma}}) \beta^{\frac{2}{\gamma}}. \end{aligned}$$

Hence the result. □

We observe that the distribution of the point process Sh^x does depend only on $E(H^{\frac{2}{\gamma}})$ but not on the distribution of fading H itself. This phenomenon can be explained as in [46](page 159). If the fading is log-normal shadowing, i.e $H \sim 10^{G/10}$ where $G \sim \mathcal{N}(0, \sigma^2)$ then $E(H^{\frac{2}{\gamma}}) = e^{\frac{2\sigma_1^2}{\gamma^2}}$ where $\sigma_1 = \frac{\ln(10)\sigma}{10}$. If the fading is Rayleigh fading, i.e $H \sim \exp(\mu)$ then $E(H^{\frac{2}{\gamma}}) = \Gamma(\frac{2}{\gamma} + 1, 0)\mu^{-\frac{2}{\gamma}}$ where $\Gamma(a,b) = \int_b^\infty t^{a-1} e^{-t} \, \mathrm{d}t$ is the upper incomplete gamma function.

Similarly to the distance to m-th nearest BS (which can be found in [49]), the distribution of m-th less strong path loss fading ξ_m^x can be characterized as follows:

Corollary 3. *If $L(z) = K|z|^{-\gamma}$, ξ_m^x is distributed according to the generalized Gamma distribution:*

$$p_{\xi_m^x}(t) = \frac{2}{\gamma}(\lambda_B C)^{m+1} t^{\frac{2}{\gamma}(m+1)} \frac{e^{-\lambda_B C t^{\frac{2}{\gamma}}}}{m!}\cdot$$

Proof. This is a consequence of Corollaries 1 and 2. □

We can also investigate more general and realistic path loss model.

Corollary 4. *If $L(z) = K \min\{R_0^{-\gamma}, |z|^{-\gamma}\}$ then:*

$$B(\beta) = C_1 \beta^{\frac{2}{\gamma}} \int_{\frac{R_0^\gamma}{\beta K}}^{\infty} t^{\frac{2}{\gamma}} p_H(t)\ dt, \tag{5.2}$$

where $C_1 = \pi K^{\frac{2}{\gamma}}$. In addition, we have:

$$B'(\beta) = \frac{2}{\gamma}\beta^{-1} B(\beta) + \pi R_0^2 p_H\left(\frac{R_0^\gamma}{K\beta}\right)\cdot \tag{5.3}$$

If the fading is lognormal shadowing $H \sim 10^{G/10}$ where $G \sim \mathcal{N}(0, \sigma^2)$ then we have:

$$B(\beta) = C_1 \beta^{\frac{2}{\gamma}} e^{(\frac{2\sigma_1}{\gamma})^2} Q\left(\frac{-\ln\beta - \ln(KR_0^{-\gamma})}{\sigma_1} - \frac{2\sigma_1}{\gamma}\right),$$

where $Q(a) = \frac{1}{\sqrt{2\pi}} \int_a^\infty e^{-u^2/2}\ du$ is the Q*-function and $\sigma_1 = \frac{\sigma \ln 10}{10}$. If the fading is Rayleigh $H \sim \exp(\mu)$ then*

$$B(\beta) = C_1 \left(\frac{\beta}{\mu}\right)^{\frac{2}{\gamma}} \Gamma\left(1 + \frac{2}{\gamma}, \frac{\mu R_0^\gamma}{K\beta}\right).$$

Proof. Similarly to the path loss exponent model case, we have:

$$\begin{aligned}
B(\beta) &= 2\pi \int_0^\infty r F_H((\max\{R_0, r\})^{-\gamma}(K\beta)^{-1})\ \mathrm{d}r \\
&= 2\pi \int_0^{R_0} r F_H(R_0^{-\gamma}(K\beta)^{-1})\ \mathrm{d}r + 2\pi \int_{R_0}^\infty r F_H(R_0^{-\gamma}(K\beta)^{-1})\ \mathrm{d}r \\
&= \pi R_0^2 F_H(R_0^\gamma (K\beta)^{-1}) + 2\pi \int_{\frac{R_0^\gamma}{\beta K}}^\infty p_H(t)\ \mathrm{d}t \int_{R_0}^{(tK\beta)^{1/\gamma}} r\ \mathrm{d}r \\
&= C_1 \beta^{\frac{2}{\gamma}} \int_{\frac{R_0^\gamma}{K\beta}}^\infty t^{\frac{2}{\gamma}} p_H(t)\ \mathrm{d}t\cdot
\end{aligned}$$

We then obtain Equation (5.2). Now differentiate the two sides of that equation to get:

$$\begin{aligned}
B'(\beta) &= \frac{2}{\gamma} C_1 \beta^{\frac{2}{\gamma}-1} \int_{\frac{R_0^\gamma}{\beta K}}^\infty t^{\frac{2}{\gamma}} p_H(t)\ \mathrm{d}t + \frac{C_1 R_0^2}{K^{\frac{2}{\gamma}}} p_H\left(\frac{R_0^\gamma}{K\beta}\right) \\
&= \frac{2}{\gamma}\beta^{-1} B(\beta) + \pi R_0^2 p_H\left(\frac{R_0^\gamma}{K\beta}\right).
\end{aligned}$$

That yields Equation (5.3). In the case of lognormal shadowing we have:

$$\begin{aligned} B(\beta) &= C_1\beta^{\frac{2}{\gamma}} \int_{\frac{R_0^\gamma}{K\beta}}^{\infty} \frac{1}{\sqrt{2\pi\sigma_1^2 t}} t^{\frac{2}{\gamma}} e^{-\frac{(\ln t)^2}{2\sigma_1^2}} \,\mathrm{d}t \\ &= C_1\beta^{\frac{2}{\gamma}} \int_{\ln\frac{R_0^\gamma}{K\beta}}^{\infty} \frac{1}{\sqrt{2\pi\sigma_1^2}} e^{\frac{2u}{\gamma}} e^{-\frac{u^2}{2\sigma_1^2}} \,\mathrm{d}u \\ &= C_1\beta^{\frac{2}{\gamma}} e^{(\frac{2\sigma_1}{\gamma})^2} \int_{\ln\frac{R_0^\gamma}{K\beta}}^{\infty} \frac{1}{\sqrt{2\pi\sigma_1^2}} e^{-\frac{(u-\frac{2\sigma_1^2}{\gamma})^2}{2\sigma_1^2}} \,\mathrm{d}u \\ &= C_1\beta^{\frac{2}{\gamma}} e^{(\frac{2\sigma_1}{\gamma})^2} Q\left(\frac{-\ln\beta - \ln(KR_0^{-\gamma})}{\sigma_1} - \frac{2\sigma_1}{\gamma}\right). \end{aligned}$$

In the case of Rayleigh fading we have:

$$\begin{aligned} B(\beta) &= C_1\beta^{\frac{2}{\gamma}} \int_{\frac{R_0^\gamma}{K\beta}}^{\infty} t^{\frac{2}{\gamma}} \mu e^{-\mu t} \,\mathrm{d}t \\ &= C_1 \left(\frac{\beta}{\mu}\right)^{\frac{2}{\gamma}} \Gamma\left(1+\frac{2}{\gamma}, \frac{\mu R_0^\gamma}{K\beta}\right), \end{aligned}$$

by a change of variables. Hence the result. □

Corollary 5. *Let T be the value of attenuation above which a communication is not feasible. The number of BS covering a point x is distributed according to the Poisson distribution of parameter $\lambda_B B(T)$. In particular, the outage probability is given by*

$$P(\xi_0^x > T) = e^{-\lambda_B B(T)}.$$

Proof. The path loss fading Sh^x is a Poisson point process on $\mathbb{R}^+$ with intensity $\lambda_B B'(t)\,\mathrm{d}t$, so the number of point on the interval $(0,T)$ is distributed according to Poisson distribution of parameter $\lambda_B B(T)$. □

Figure 5.2 represents the outage probability for different models of fading. This shows that the curves of modified path loss exponent model is generally higher than those of path loss exponent model but they are very close in the low outage region.

5.4 Capacity

In this section, we calculate the mean of any capacity function of a user. We call capacity function any measurable non-negative function defined on $\mathbb{R}^+$. In some cases, we can add the property that $f(0) = 0$. Examples of capacity functions are:

- $f_0(t) = 1$ is a constant function indicating that the user is in the system.
- $f_1(t) = 1(t > T)$ is the function indicating that the user is in outage or not if the path loss fading threshold is T.
- $f_2(t) = 1(t \leq T)$ is the function indicating that the user is covered or not.

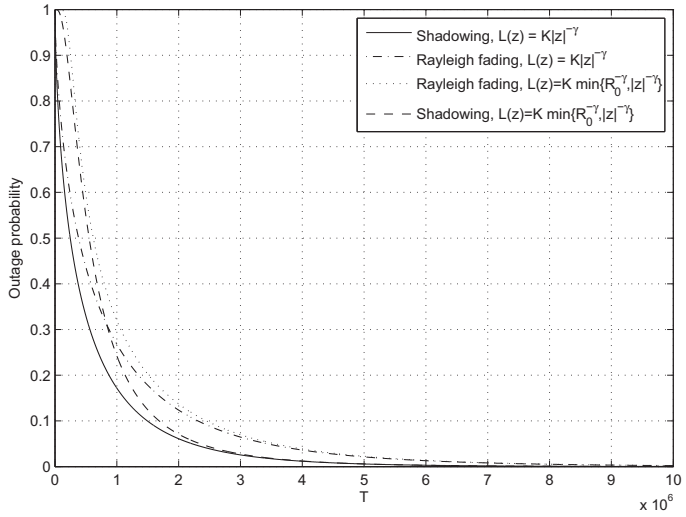


Figure 5.2: Comparison of outage probability between propagation models. For lognormal shadowing $\sigma = 4(dB)$, for Rayleigh fading $\mu = 1$; $K = 10^{-2}$, $\gamma = 2.8$.

- Shannon capacity when transmitting over a channel of bandwidth W and with noise N is $W \log_2(1+\frac{P}{tN})$ (kbs). In practice, the set of achievable rates is not continuous for all wireless systems. Indeed, the actual user bit rate can be expressed as a piecewise constant function $f_3(t) = \sum_1^n 1(T_i \leq t < T_{i+1})c_i$ with $0 < T_1 < T_2 < ... < T_n < T_{n+1} = +\infty$.

Hence, it is interesting to study the random variable $f(\sup_{y\in\Pi_B} s_{y,x})$.

Remark that since the system is spatially stationary the statistic of the path loss fading and the capacity of a user does not depend on his position. Since the PDF and the CDF of the path loss fading ξ_0^x have been already calculated in Corollary 1, the mean of a capacity function of a user follows immediately. In particular:

Theorem 23. *The average capacity per user is*

$$E(f(\xi_0^x)) = \lambda_B \int_0^\infty B'(\beta) e^{-\lambda_B B(\beta)} f(\beta)\ d\beta. \tag{5.4}$$

In the case of path loss exponent model $L(z) = K|z|^{-\gamma}$, we have:

$$E(f(\xi_0^x)) = \mathcal{L}_{\widetilde{f}}(\lambda_B C) \tag{5.5}$$

where $\mathcal{L}_g(s) = \int_0^\infty e^{-st} g(t)\ dt$ is the Laplace transform of the capacity function g and $\widetilde{f}(t) = f(t^{\frac{\gamma}{2}})$.

Proof. Equation (5.4) comes from Proposition 1. If the path loss exponent model is considered, then we have:

$$\begin{aligned} E(f(\xi_0^x)) &= \lambda_B \int_0^\infty \frac{2C}{\gamma} \beta^{\frac{2}{\gamma}-1} e^{-\lambda_B C \beta^{\frac{2}{\gamma}}} f(\beta)\ \mathrm{d}\beta \\ &= \int_0^\infty e^{-\lambda_B C \beta_1} f(\beta_1^{\frac{\gamma}{2}})\ \mathrm{d}\beta_1 \end{aligned}$$

by the change of variable $\beta_1 = \beta^{\frac{\gamma}{2}}$. □

Assume that there is a BS located at the origin o, called typical BS, and maintain the Poisson point process of other BSs Π_B. Each user is attached by the best BS according to Assumption 1. We would like to obtain defined as follows. Let C_o be the set $C_o = \{x_i \in \Pi_M \mid s_{ox_i} < \sup_{y_i \in \Pi_B} s_{y_i x}\}$ of all user attached to the BS o. We define the cell capacity as :

$$S_o(f) = \sum_{x \in C_o} f(s_{ox}).$$

The statistic of the cell capacity $S_o(f)$ is more difficult to analyze. In this section, we calculate its mean $m(f)$ and lower bound and upper bound of its variance $v(f)$. We state the following lemma, which is straightforward due to Assumption 1 but still useful:

Lemma 24. *Given a fixed configuration Π_B of BSs, the Poisson point processes of path loss fading Sh^x and Sh^y are independent for any two different points x, y.*

Lemma 25. *Let $z = y - x$. The PDF of s_{yx} is given by*

$$p_{s_{yx}}(t) = \frac{1}{l(z)t^2} p_H\left(\frac{1}{L(z)t}\right).$$

Proof. We have

$$\begin{aligned} P(s_{yx} < t) &= P(h_{yx} > \frac{1}{L(z)t}) \\ &= F_H\left(\frac{1}{L(z)t}\right). \end{aligned}$$

The density probability function is then

$$p_{s_{yx}}(t) = \frac{1}{L(z)t^2} p_H\left(\frac{1}{L(z)t}\right).$$

□

Theorem 26. *The expectation of the cell capacity of the typical BS is*

$$m(f) = \lambda_M \int_0^\infty B'(\beta) e^{-\lambda_B B(\beta)} f(\beta)\ d\beta. \tag{5.6}$$

In the case of path loss exponent model $L(z) = K|z|^{-\gamma}$, we have:

$$m(f) = \frac{\lambda_M}{\lambda_B} \mathcal{L}_{\tilde{f}}(\lambda_B C). \tag{5.7}$$

Proof. Given a fixed configuration of BSs Π_B, the random variables $1(s_{ox} < \xi_0^x) f(s_{ox})$ obtained from all $x \in \mathbb{R}^2$ are independent. Thus, the marked point process $\tilde{\Pi}_M = (x_i, 1(s_{ox_i} < \xi_0^{x_i}) f(s_{ox_i}))$ is a Poisson point process. Using the Campbell theorem we have:

$$E(S_o(f) \mid \Pi_B) = \lambda_M \int_{\mathbb{R}^2} E\left(1(s_{ox} < \xi_0^x) f(s_{ox}) \mid \Pi_B\right)\ \mathrm{d}x.$$

As a consequence,

$$\begin{aligned} E(S_o(f)) &= E\left(\lambda_M \int_{\mathbb{R}^2} E(1(s_{ox} < \xi_0^x) f(s_{ox}) \mid \Pi_B)\ \mathrm{d}x\right) \\ &= \lambda_M \int_{\mathbb{R}^2} E\left(1(s_{ox} < \xi_0^x) f(s_{ox})\right)\ \mathrm{d}x. \end{aligned}$$

In virtue of Lemma 25, Proposition 22 and Collary 1, we have:

$$\begin{aligned}
E(S_o(f)) &= \lambda_M \int_{\mathbb{R}^2} E(1(s_{ox} < \xi_0^x) f(s_{ox}))\ \mathrm{d}x \\
&= \lambda_M \int_{\mathbb{R}^2} \int_0^\infty p_{s_{ox}}(t) P(t < \xi_0^x) f(t)\ \mathrm{d}t\ \mathrm{d}x \\
&= \lambda_M \int_0^\infty f(t) e^{-\lambda_B B(t)}\ \mathrm{d}t \int_{\mathbb{R}^2} \frac{\partial F_H}{\partial t}\left(\frac{1}{L(x)t}\right)\ \mathrm{d}x \\
&= \lambda_M \int_0^\infty f(t) e^{-\lambda_B B(t)}\ \mathrm{d}t \frac{\partial}{\partial t}\left(\int_{R^2} F(\frac{1}{L(x)t})\ \mathrm{d}x\right) \\
&= \lambda_M \int_0^\infty f(t) e^{-\lambda_B B(t)} B'(t)\ \mathrm{d}t\cdot
\end{aligned}$$

For the case of path loss exponent model, Equation 5.7 follows easily. This completes the proof. □

Equation (5.6) has the following interpretation: the mean cell capacity is the product of the mean number of users per cell and the mean capacity per user.

Theorem 27. *Given two capacity functions f, g we have :*

$$\mathbf{cov}(S_o(f), S_o(g)) \geq m(f.g)\cdot \tag{5.8}$$

In particular,

$$\mathbf{var}(S_o(f)) \geq m(f^2).$$

Proof. For simplicity, let $\beta_x = s_{ox} 1(s_{ox} < \xi_0^x)$ and $f(0) = 0, g(0) = 0$, we have :

$$\begin{aligned}
\mathbf{cov}(S_o(f) S_o(g)) &= E(\mathbf{cov}(S_o(f), S_o(g) \mid \Pi_B)) \\
&\quad + E(E(S_o(f) \mid \Pi_B) E(S_o(g) \mid \Pi_B)) - E(S_o(f)) E(S_o(g)) \\
&= T_1 + T_2 - T_3\cdot
\end{aligned}$$

It is clear that

$$T_3 = m(f)m(g)\cdot$$

Consider the first term. Remind that we have assumed that all random fading $\{h_{yx}\}_{y,x\in\mathbb{R}^2}$ are independent, so given a fixed configuration Π_B of BSs, the random variables $\{\beta_x\}_{x\in\mathbb{R}^2}$ are independent. Hence by Campbell formula we have:

$$\begin{aligned}
T_1 &= \lambda_M E \int_{\mathbb{R}^2} E(f(\beta_x) g(\beta_x) \mid \Pi_B)\ \mathrm{d}x \\
&= \lambda_M \int_{\mathbb{R}^2} E(E(f(\beta_x) g(\beta_x) \mid \Pi_B))\ \mathrm{d}x \\
&= \lambda_M \int_{\mathbb{R}^2} E(f(\beta_x) g(\beta_x))\ \mathrm{d}x \\
&= m(f.g)\cdot
\end{aligned}$$

Now consider the second term

$$\begin{aligned}
T_2 &= \lambda_M^2 E\left(\int_{\mathbb{R}^2} E(f(\beta_x) \mid \Pi_B)\ \mathrm{d}x \int_{R^2} E(g(\beta_x) \mid \Pi_B)\ \mathrm{d}x\right) \\
&= \lambda_M^2 E\left(\int_{\mathbb{R}^2}\int_{\mathbb{R}^2} E(f(\beta_x) \mid \Pi_B)E(g(\beta_y) \mid \Pi_B)\ \mathrm{d}x\ \mathrm{d}y\right) \\
&= \lambda_M^2 \int_{\mathbb{R}^2}\int_{\mathbb{R}^2} E\left(E(f(\beta_x) \mid \Pi_B)E(g(\beta_y) \mid \Pi_B)\right)\ \mathrm{d}x\ \mathrm{d}y \\
&= \lambda_M^2 \int_{\mathbb{R}^2}\int_{\mathbb{R}^2} E(f(\beta_x))E(g(\beta_y))\ \mathrm{d}x\ \mathrm{d}y \\
&= \lambda_M^2 \int_{\mathbb{R}^2}\int_{\mathbb{R}^2}\int_0^\infty\int_0^\infty P(s_{ox} < \xi_0^x, s_{oy} < \xi_0^y \mid s_{ox} = t_1, s_{oy} = t_2)\times \\
&\qquad\qquad \times f(t_1)g(t_2)p_{s_{ox}}(t_1)p_{s_{oy}}(t_2)\ \mathrm{d}t_1\ \mathrm{d}t_2\ \mathrm{d}x\ \mathrm{d}y.
\end{aligned}$$

by remarking that β_x and β_y are independent if $x \neq y$ (Lemma 24). We will prove that if $x \neq y$:

$$\begin{aligned}
&P(s_{ox} < \xi_0^x, s_{oy} < \xi_0^y \mid s_{ox} = t_1, s_{oy} = t_2) \geq \\
&\qquad\qquad P(s_{ox} < \xi_0^x \mid s_{ox} = t_1)P(s_{oy} < \xi_0^y \mid s_{oy} = t_2)
\end{aligned}$$

Consider the marked point process $\Pi_B^{x,y} = \{y_i, h_{y_i x}, h_{y_i y})\}$. Since the marks are independent, it is a Poisson point process on $\mathbb{R}^4$ with intensity

$$m_a^{x,u_1,u_2}(\ \mathrm{d}y,\ \mathrm{d}u_1,\ \mathrm{d}u_2) = \lambda_M\ \mathrm{d}y \otimes p_H(u_1)\ \mathrm{d}u_1 \otimes p_H(u_2)\ \mathrm{d}u_2.$$

Consider two sets

$$A_1 = \{(y, u_1, u_2) : L(y)u_1 \geq t_1^{-1}\}$$

and

$$A_2 = \{(y, u_1, u_2) : L(y)u_2 \geq t_2^{-1}\},$$

we have:

$$\begin{aligned}
P(s_{ox} < \xi_0^x, s_{oy} < \xi_0^y \mid s_{ox} = t_1, s_{oy} = t_2) &= P(\Pi_B^{x,y}(A_1 \cup A_2) = \emptyset) \\
&= e^{-m_a^{x,y}(A_1 \cup A_2)} \\
&\geq e^{-m_a^{x,y}(A_1) - m_a^{x,y}(A_2)} \\
&= P(\Pi_B^{x,y}(A_1) = \emptyset)P(\Pi_B^{x,y}(A_2) = \emptyset) \\
&= P(s_{ox} < \xi_0^x \mid s_{ox} = t_1)P(s_{oy} < \xi_0^y \mid s_{oy} = t_2).
\end{aligned}$$

Thus,

$$\begin{aligned}
T_2 &\geq \lambda_M^2 \int_{\mathbb{R}^2}\int_{\mathbb{R}^2}\int_0^\infty\int_0^\infty P(s_{ox} < \xi_0^x \mid s_{ox} = t_1)P(s_{oy} < \xi_0^y \mid s_{oy} = t_2)\times \\
&\quad \times f(t_1)g(t_2)p_{s_{ox}}(t_1)p_{s_{oy}}(t_2)\ \mathrm{d}t_1\ \mathrm{d}t_2\ \mathrm{d}x\ \mathrm{d}y \\
&= m(f)m(g).
\end{aligned}$$

The result follows. □

Theorem 28. *For f and g two capacity functions, we have:*

$$\mathbf{cov}(S_o(f), S_o(g)) \leq m(f.g) + m(f)n(g) - m(f)m(g)$$

where

$$n(f) = \lambda_M \int_0^\infty B'(t)f(t)\ dt\cdot \tag{5.9}$$

Proof. We continue the proof of Theorem 27, we have to prove that

$$T_2 \leq m(f)n(g)\cdot$$

Indeed,

$$P(s_{ox} < \xi_0^x, s_{oy} < \xi_0^y \mid s_{ox} = t_1, s_{oy} = t_2) \leq P(s_{ox} < \xi_0^x \mid s_{ox} = t_1),$$

thus,

$$\begin{aligned} T_2 &\leq \lambda_M^2 \int_{\mathbb{R}^2}\int_{\mathbb{R}^2}\int_0^\infty\int_0^\infty P(s_{ox} < \xi_0^x \mid s_{ox} = t_1)\times \\ &\qquad \times f(t_1)g(t_2)p_{s_{ox}}(t_1)p_{s_{oy}}(t_2)\ \mathrm{d}t_1\ \mathrm{d}t_2\ \mathrm{d}x\ \mathrm{d}y \\ &\leq m(f)\int_0^\infty g(t_2)\int_{\mathbb{R}^2}\frac{\partial F_H}{\partial t}(\frac{1}{L(x)t})\ \mathrm{d}x\ \mathrm{d}t_2 \\ &= m(f)n(g)\cdot \end{aligned}$$

Hence the result. □

5.5 Examples

5.5.1 Number of users in a cell

For $f_0(t) = 1$, the random variable $n_o := S(f_0) = \sum_{i=0}^\infty 1(x_i \in C_o)$ represents the number of users who view o as the best server, and thus will be served by o.

$$\begin{aligned} E(n_o) &= \lambda_M \int_0^\infty B'(\beta)e^{-\lambda_B B(\beta)}d\beta \\ &= \frac{\lambda_M}{\lambda_B}\cdot \end{aligned}$$

The mean number of users served by a BS is $\frac{\lambda_M}{\lambda_B}$ which is easily interpreted. We rewrite the formula (5.6) by

$$E(S_o(f)) = \frac{\lambda_M}{\lambda_B}E(f(\xi_0^x)).$$

Again this is easily interpreted. The average sum rate is the product of the average user per cell and the average per user.

Now apply Theorem 27, we get that

$$\mathbf{var}(n_o) \geq m(1) = \frac{\lambda_M}{\lambda_B}\cdot$$

We cannot apply Theorem 28 because $n(f_0) = \lambda_M \int_0^\infty B'(t)\ \mathrm{d}t = \infty$.

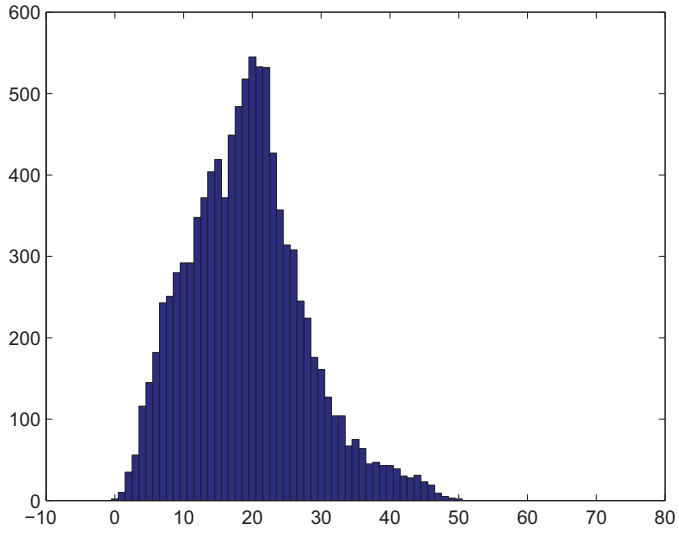


Figure 5.3: Histogram of n_o

5.5.2 Number of users in outage in a cell

Consider $f_1(t) = 1(t > T)$, then $S_o(f_1)$ is the number of users in outage in the typical cell. We have

$$\begin{aligned} m(f_1) &= \lambda_M \int_T^\infty B'(\beta) e^{-\lambda_B B(\beta)} d\beta \\ &= \frac{\lambda_M}{\lambda_B} e^{-\lambda_B B(T)}, \end{aligned}$$

and

$$v(f_1) \geq \frac{\lambda_M}{\lambda_B} e^{-\lambda_B B(T)}.$$

Note that again, we cannot apply Theorem 28 as $n(f_1) = \lambda_M \int_T^\infty B'(t)\ \mathrm{d}t$ is infinite.

5.5.3 Number of covered users in a cell

Consider $f_2(t) = 1(t \leq T)$, then $S(f_2)$ represents the number of covered users in the typical cell. We have:

$$\begin{aligned} m(f_2) &= \lambda_M \int_0^T B'(\beta) e^{-\lambda_B B(\beta)} d\beta \\ &= \frac{\lambda_M}{\lambda_B} \left(1 - e^{-\lambda_B B(T)}\right), \end{aligned}$$

$$v(f_2) \geq \frac{\lambda_M}{\lambda_B} \left(1 - e^{-\lambda_B B(T)}\right),$$

and

$$v(f_2) \leq \frac{\lambda_M}{\lambda_B} e^{-\lambda_B B(T)} + \frac{\lambda_M^2}{\lambda_B^2} e^{-\lambda_B B(T)} \left(\lambda_B B(T) - 1 + e^{-\lambda_B B(T)}\right).$$

5.5.4 Total bit rate of a cell

We now consider the piecewise constant function $f_3(t) = \sum_1^n 1(T_i \leq t < T_{i+1})c_i$ with $0 < T_1 < T_2 < ... < T_n < T_{n+1}$ and T_{n+1} can be infinite. If f_3 is the function that represents the actual bit rate then $S_o(f_3)$ represents the total bit rates of all users in the cell. We have:

$$\begin{aligned} m(f_3) &= \lambda_M \int_0^\infty B'(\beta) e^{-\lambda_B B(\beta)} \sum_1^n 1(T_i \leq \beta < T_{i+1}) c_i d\beta \\ &= \lambda_M \sum_{i=1}^n c_i \left(e^{-\lambda_B B(T_i)} - e^{-\lambda_B B(T_{i+1})} \right). \end{aligned}$$

$$v(f_3) \geq \lambda_M \sum_{i=1}^n c_i^2 \left(e^{-\lambda_B B(T_i)} - e^{-\lambda_B B(T_{i+1})} \right).$$

$$\begin{aligned} v(f_3) \leq\ & \lambda_M \sum_{i=1}^n c_i^2 \left(e^{-\lambda_B B(T_i)} - e^{-\lambda_B B(T_{i+1})} \right) + \\ & + \left(\frac{\lambda_M}{\lambda_B} \right)^2 \sum_{i=1}^n \left(e^{-\lambda_B B(T_i)} - e^{-\lambda_B B(T_{i+1})} \right) \times \\ & \times \sum_{i=1}^n \left(\lambda_B B(T_{i+1}) - \lambda_B B(T_i) - e^{-\lambda_B B(T_i)} + e^{-\lambda_B B(T_{i+1})} \right). \end{aligned}$$

5.5.5 Discussion on the distribution of $S_o(f)$

The distribution of $S_o(f)$ does not behave like a Gaussian distribution even in the limit regimes. Take, for example, the histogram of $n_o = S_o(f_0)$ and that of $S_o(f_3)$ which are shown in figures 5.3 and 5.5 respectively. For the case of no fading, $H =$ constant, in [50] the author found some approximate but not reliable bounds of the distribution of $S_o(f)$ for equivariant functions f but no approximation or bounds is found for general capacity functions. In addition, no closed expression is found for the Laplace transform of functional $S_o(f)$. In our case where the fading is considered, this is expected to be more challenging.

We can find an upper bound for the tail distribution by Chebyshev's inequality:

$$\begin{aligned} P(S_o(f) > m(f) + t) &\leq \frac{v(f)}{v(f) + t^2} \\ &\leq \frac{m(f^2) + m(f)n(f) - (m(f))^2}{m(f^2) + m(f)n(f) - (m(f))^2 + t^2} \end{aligned}$$

The above inequality provides a robust upper bound for the tail distribution and valid for all capacity function f. However the gap is large (Figure 5.4). It is well known that other types of concentration inequality based on Chernoff bound can give better bound. In this direction, [16], [28] and [15] provide concentration inequalities that apply for functional related to one PPP. These inequalities cannot be directly applied in our case because our target is a functional related to two independent PPPs. Actually we can combine the two

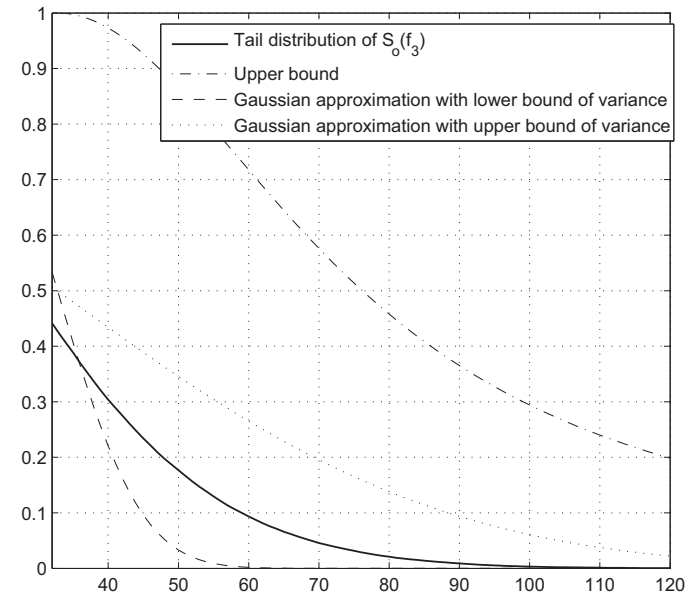


Figure 5.4: Tail distribution of $S_o(f_3)$

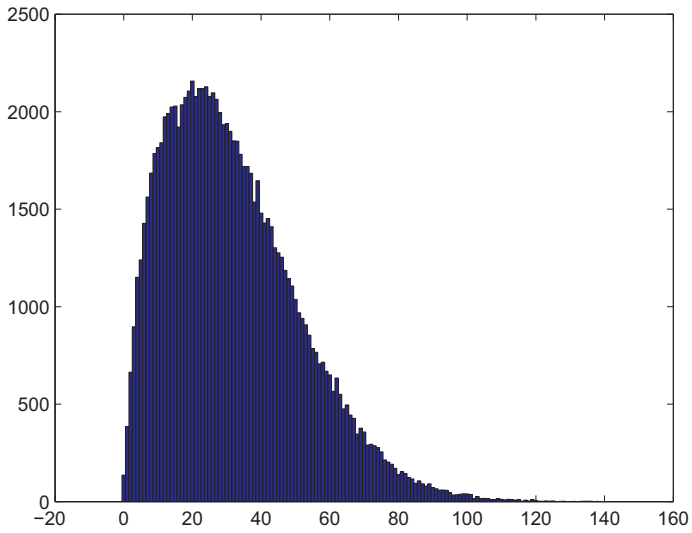


Figure 5.5: A typical histogram of $S_o(f_3)$

independent PPPs into one united PPP by the independent marking theorem. Unfortunately the functional $S_o(f)$ of the united PPP does not satisfy the required conditions for the concentration inequalities neither on [16], [15] nor on [28]. But we believe that similar techniques used in these references can be used to derive a upper bound the tail distribution of $S_o(f)$.

5.6 Conclusion

In this chapter we introduce a general model to evaluate the outage probability and the capacity of wireless noise limited network. It is in fact an extension of models introduced in series of papers [2], [3], [50]. The main difference is that we take into account the effect of fading, and that we assume that a user connects to the BS with strongest signal rather than the closest one. We first show that for a particular user, the path loss fading process from all BSs seen from this user is a Poisson point process in the positive half line. We find explicit expression for the outage probability, the expectation of capacity of a user, and the expectation of the cell capacity of the typical BS $S_o(f)$. We find the lower bound and upper bound for the variance of the cell capacity. We consider general model for path loss and fading. The results presented in this chapter actually generalizes the results on [50]. Possible further research is to find a way to compute the distribution of $S_o(f)$.

Part III

Energy consumption models

Chapter 6

Presentation of energy consumption model and mobility model

Contents

6.1 Introduction 71
6.2 Model for energy consumption 71
6.3 Model for mobility of users 74
6.4 Basic model 75
6.5 Conclusion 79

6.1 Introduction

In this chapter we introduce a general energy consumption model for cellular network. In Section 6.2, we present the power consumption model and the energy consumption model. In Section 6.3, we present the mobility model for users. In Section 6.4, we establish the relationship between the consumed energy and the parameters of the system such as intensity of users or cell radius. The energy consumption model and the mobility model are also used in the next two chapters.

Important notations and parameters used in this chapter are summarized in the table 6.1.

6.2 Model for energy consumption

We suppose that there is a cellular network with multiple base stations on $\mathbb{R}^d$ and there is a base station located at the origin o administering a geographical region C around o. We assume that there exists $0 < R_1 < R$ such that $\mathbf{B}(o, R_1) \subset C \subset \mathbf{B}(o, R)$ and C is convex and compact. We define $R_{inf} = \inf_R\{C \subset \mathbf{B}(o, R)\}$. For a given spatial configuration of active users on $\mathbb{R}^d$, denoted by η, users located inside C are served by o, users outside this region are served by another base station (or are in outage regime). The power consumed by the battery of the base station o can be divided into two parts:

- The power dedicated to transmit, receive, decode and encode the signal of any active user. The cumulated power over the whole configuration is then of the form $\sum_{x\in\eta} \phi(x)$, where ϕ is a function to be defined later.

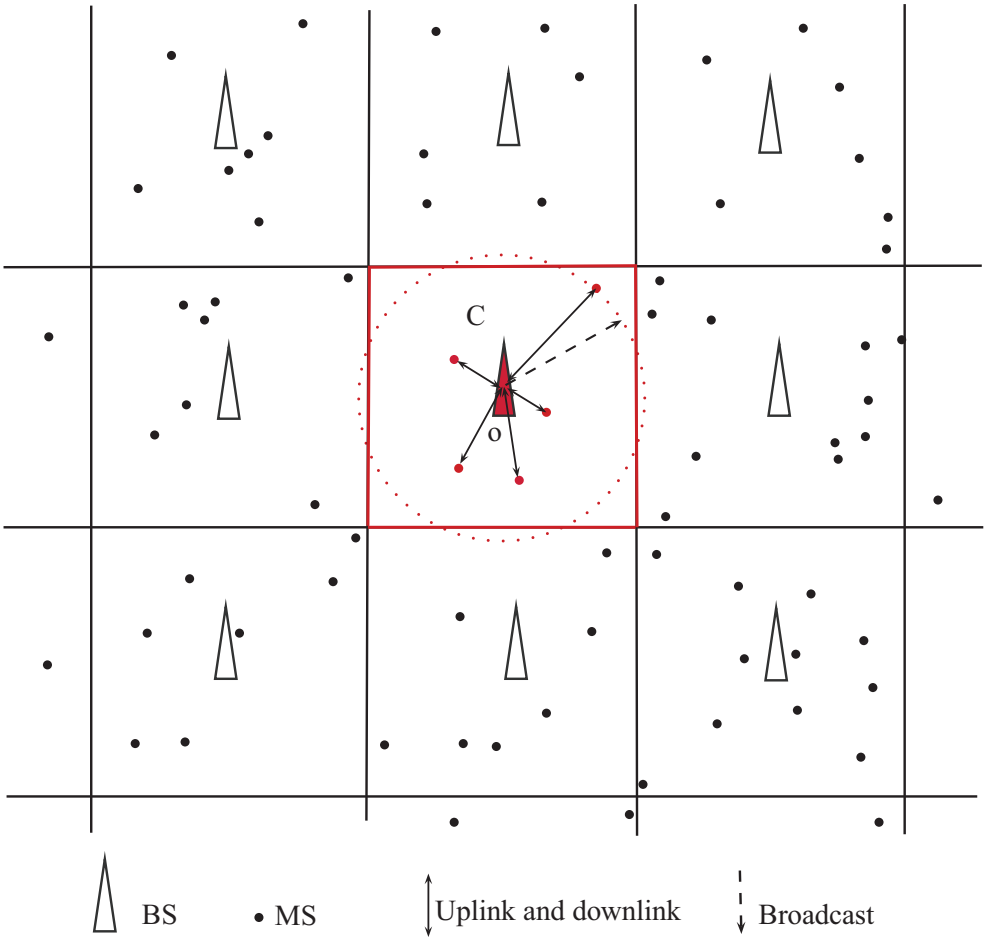


Figure 6.1: Power consumption model.

Symbols	Physical meaning
η	A configuration of active users
$\|\eta\|$	$\sup\{\|x\|, x \in C\}$
$\phi(x) = \overline{\phi}(\|x\|)$	Consumed power for a user at x
$\psi(x) = \overline{\psi}(\|x\|)$	Broadcast power for the farthest user in the cell at x
$P_A(\eta)$	$\sum_{x\in\eta} \phi(x)$, Total power served to all users
$P_B(\eta) = \overline{\psi}(\|\eta\|)$	Broadcast power
$P(\eta)$	$P_A(\eta) + P_B(\eta)$ Total consumed power
$l(x) = \overline{l}(x)$	Pathloss function
$\omega = \{om_t, t \in \mathbb{R}\}$	Time variant process of configuration of active users
$J_A = J_A(\omega, T)$	$\int_0^T P_A(\omega_s)\, \mathrm{d}s$, Additive part of consumed energy during the period $[0, T)$
$J_B = J_B(\omega, T)$	$\int_0^T P_B(\omega_s)\, \mathrm{d}s$, Broadcast part of consumed energy during the period $[0, T)$
$J_T = J_T(\omega, T)$	$= \int_0^T P(\omega_s)\, \mathrm{d}s$, Total consumed energy during the period $[0, T)$
$M = (M(t), t \leq 0)$	Random mobility model
$M/\epsilon = (M(t)/\epsilon, t \leq 0)$	High mobility model ($\epsilon \to 0$)

Table 6.1: Notations and parameters.

- The power dedicated to broadcast messages. In order to guarantee that all active users receive these messages, the power must be such that the farthest user in the cell is within the reception range (if the system performs power control) or all the cell is within reception range (if the system does not performs power control). Thus, the power is a function of $\max_{x\in\eta\cap C} |x|$ where $|x|$ is the Euclidean norm of x (the power is equal to 0 if $\eta \cap C = \emptyset$). This function is constant if power control is not performed.

It follows that the total consumed power is given by:

$$\boxed{P(\eta) = P_A(\eta) + P_B(\eta)}, \tag{6.1}$$

where $P_A(\eta) = \sum_{x\in\eta} \phi(x)$ and $P_B(\eta) = \overline{\psi}(\|\eta\|)$, $\|\eta\| = \max_{x\in\eta\cap C} |x|$ if $\eta \cap C \neq \emptyset$ and $\|\eta\| = 0$ if $\eta \cap C = \emptyset$ (the subscript A stands for "additive" and B stands for "broadcast"). For a very simple propagation model (without fading and shadowing), the Shannon's formula states that for a receiver located at x, the transmission rate is given by

$$W \log_2(1 + P_e l(x)),$$

where W is the bandwidth, P_e is the transmitted power and $l(x)$ is the pathloss function. Generally, the function $l : \mathbb{R}^d \to [0, \infty]$ takes the form $\overline{l}(|x|)$ where $\overline{l} : [0, \infty] \to [0, \infty]$ is a non decreasing function. This implies that in order to guarantee a minimum rate at position x, P_e must be proportional to $(l(x))^{-1}$. Thus, it is sensible to choose ϕ as

$$\boxed{\phi(x) = a.\overline{l}(|x|)\mathbf{1}_{\{x\in C\}}} \tag{6.2}$$

with $a > 0$. The function ψ is chosen as

$$\boxed{\psi(x) = \begin{cases} b.l(|x|)\mathbf{1}_{\{x\in C\}}, & \text{If power control is performed;} \\ b.l(R_{inf}), & \text{If power control is not performed.} \end{cases}} \tag{6.3}$$

We can divide models for path loss into two categories:

- singular path loss model $l(x) = K\,|x|^{-\gamma}$ where γ is the exponent path loss parameter and K is a positive constant.
- non-singular path loss models like $l(x) = K(r_0 \vee |x|)^{-\gamma}$ or $l(x) = K(1 + |x|^{-\gamma})^{-1}$.

More generally, we make the following assumption:

Assumption 2. *The transmitted power depends only on the distance to the base station* $\phi(x) = \overline{\phi}(|x|)\mathbf{1}_{\{x\in C\}}$. *Furthermore,* $\overline{\phi}$ *and* $\overline{\psi}$ *are continuous non decreasing function on* $\mathbb{R}^+$.

We denote $\psi(x) = \overline{\psi}(|x|)\mathbf{1}_{\{x\in C\}}$. This implies that ϕ and ψ are always bounded function. Apart from the above model for power consumption, we can define a power consumption as a general functional depending on the configuration of users $P_G : \Omega^{\mathbb{R}^d} \longrightarrow [0, \infty]$.

If $\omega = (\omega_t, t \geq 0)$ is a process of time varying configurations, the total consumed energy between time 0 and time T is given by

$$\boxed{J_T := J_T(\omega, T) = \int_0^T P(\omega_s)\mathrm{d}s\cdot} \tag{6.4}$$

As previously, we also define J_A and J_B by:

$$\boxed{J_A := J_A(\omega, T) = \int_0^T P_A(\omega_s)\mathrm{d}s \text{ and } J_B := J_B(\omega, T) = \int_0^T P_B(\omega_s)\mathrm{d}s\cdot} \tag{6.5}$$

The same definition for $J_G(\omega, T)$ if the system applies power consumption $P_G(.)$.

Also we denote $C(r) = C \cap \mathbf{B}(o, r)$ and $\overline{C}(r) = C \cap \overline{\mathbf{B}}(o, r)$. For a configuration ν, we denote x_ν the point of ν such that $|x_\nu| = \|\nu\|$ (if there are more than one point then x_{nu} is randomly chosen among these points).

6.3 Model for mobility of users

In this section, we introduce the mobility models for users.

Consider the functional space $D([0, \infty), \mathbb{R}^d)$ of Càdlàg function on $\mathbb{R}^d$ equipped with the Skorohod topology (see, for example [51], page 369). It is well known that $D([0, \infty), \mathbb{R}^d)$ is a Polish space. The subset $D_0([0, \infty), \mathbb{R}^d) = \{f \in D([0, \infty), \mathbb{R}^d), f(0) = o\}$ equipped with the Skorohod topology is also a Polish space. We consider a probability distribution $\mathbf{P}_M$ of a random variable $M = (M(t), t \in [0, \infty))$ defined on the associated Borelian $\sigma-$field of the space $D_0([0, \infty), \mathbb{R}^d)$. Each realization of M can be represented as a Càdlàg trajectory of on $\mathbb{R}^d$. Also, this probability is completely determined by the distributions of finite marginal distributions $\mathbf{P}\left(M(t_1) \in ., ..., M(t_n) \in .\right)(t_1, ..., t_n > 0)$. In some situation, for

convenience we can assume that $M(t) = o$ for $t < 0$. M is said to satisfy the property $\mathbf{T}$ if $\mathbf{P}(M(t_1) = M(t_2)) = 0$ for any $0 \leq t_1 < t_2$.

If mobility is considered, then each user is associated with a mobility process on $\mathbb{R}^d$. We make the following assumption:

Assumption 3.

- *Motion trajectories of users are i.i.d mutually independent and have the same distribution as that of M.*
- *Motion trajectories of users do not depend on the initial position of users.*

More precisely, a user i initially located at x_i is associated with an independent version of M, namely M_i and an arrival time T_i. This user will move during its sojourn along M_i, i.e the position of this user at time $t \geq T_i$ is $x + M_i(t - T_i)$. The random processes $(M_i)_{i \in \mathbf{N}}$ are mutually independent. Examples for mobility model are as follows:

- Motionless users: $M(t) = o, \forall t \in \mathbb{R}$.
- Brownian motion users: $M(t) = c(t)B_d(t)$ where $c(t) \in \mathbb{R}$ is a continuous function in $[0, \infty)$ and B_d is a standard Brownian motion on $\mathbb{R}^d$.
- Completely aimless users: $M(t) = tv$ where the speed of user v is random whose direction is chosen randomly and uniformly over the d-dimensional unit sphere and $|v|$ is a positive random variable.
- Combination of two above models: $M(t) = tv + c(t)B_d(t)$.
- High mobility regime: let $\epsilon > 0$ be a small parameter, the high mobility regime consists of considering the mobility process $(M/\epsilon)(t) = M(t)/\epsilon$ and we want to study the behavior of the system when $\epsilon \to \infty$. The high mobility regime of the completely aimless mobility model with constant speed $|v|$ is the same as considering $|v| \to \infty$, i.e when the user's speed is very high.

6.4 Basic model

In this section, we present a very basic model for energy consumption of cellular network. We assume that for each time t, ω_t follows a Poisson point process of intensity $\lambda \, \mathrm{d}x$ and the cell C is circular centered at the origin. Furthermore, $\phi(x) = \overline{\phi}(|x|) = a\,|x|^{\gamma}\,\mathbf{1}_{\{x \in \mathbf{B}(o,R)\}}$ and $\overline{\psi}(r) = br^{\gamma}\mathbf{1}_{\{x \in \mathbf{B}(o,R)\}}$. We are interested in the average energy $\mathbf{E}\left[J_T(\omega, T)\right]$ that the BS consumes during the period $[0, T)$.

As the configuration at any time follows the same distribution, we have $\mathbf{E}\left[J_T(\omega, T)\right] = T\mathbf{E}\left[P(\omega_0)\right] = T\mathbf{E}\left[P_A(\omega_0)\right] + T\mathbf{E}\left[P_B(\omega_0)\right]$. Therefore, it is sufficient to find $\mathbf{E}\left[P_A(\omega_0)\right]$ and $\mathbf{E}\left[P_B(\omega_0)\right]$.

Since P_A is linear functional of ω_0, thanks to the Campbell's theorem and the lemma 29 we can calculate the expectation of P_A as follows:

$$\mathbf{E}\left[P_A(\omega_0)\right] = aV_d^{'}\frac{R^{\gamma+d}}{\gamma+d}.$$

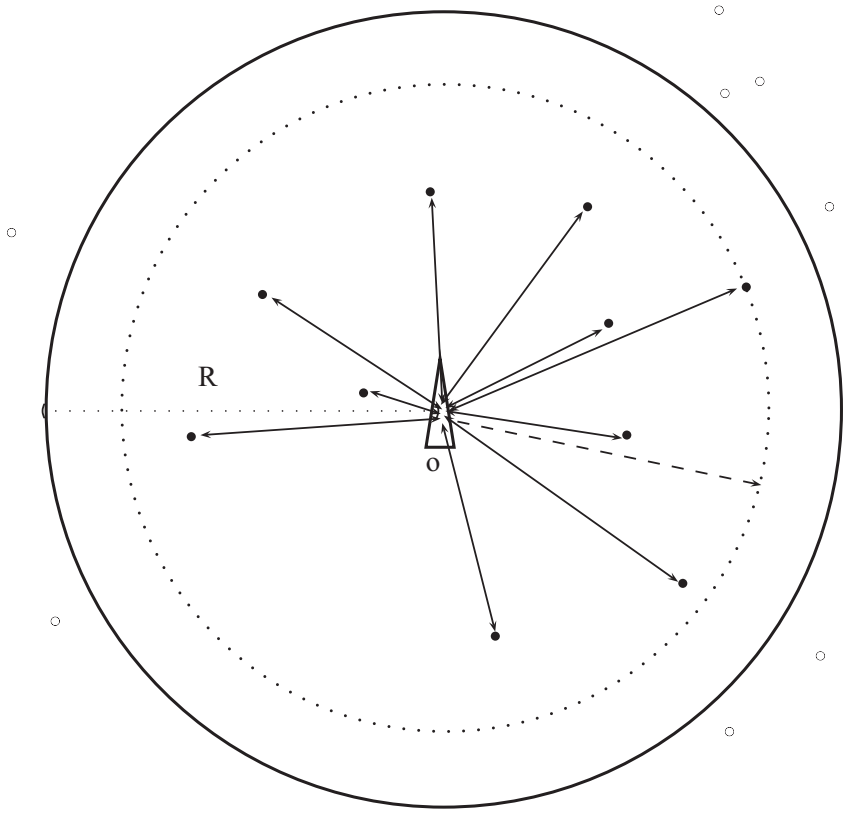


Figure 6.2: Basic model.

Lemma 29. *Denote* $V_d = \frac{\pi^{d/2}}{\Gamma(\frac{d}{2}+1)}$ *the volume of a ball of radius* 1 *in* $\mathbb{R}^d$*, and* $V_d^{'} = dV_d$ *then*

$$\int_{\mathbf{B}(o,R)} |x|^k \ dx \ = \ V_d^{'} \frac{R^{k+d}}{k+d}$$

for all real $k > -d$*.*

Proof. We have:

$$\begin{aligned} \int_{\mathbf{B}(o,R)} |x|^k \ \mathrm{d}x &= \int_0^R r^k \ \mathrm{d}\left(V_d r^k\right) \\ &= \int_0^R V_d^{'} r^{k+d-1} \ \mathrm{d}r \\ &= V_d^{'} \frac{R^{k+d}}{k+d}. \end{aligned}$$

□

We are now interested in P_B.

Lemma 30. *Let* ν *be a Radon measure on* $\mathbb{R}^d$ *absolutely continuous with respect to the Lebesgue measure, let* Π *be a Poisson point process of intensity* ν *on* $\mathbb{R}^d$ *then the CDF of* $\|\Pi\|$ *is given as:*

$$F_{\|\Pi\|}(r) = e^{-\nu(\overline{C}(r))},$$

and its PDF is given by

$$p_{\|\Pi\|}(r) = \frac{d\nu(C \cap \overline{\mathbf{B}}(o,r))}{dr} e^{-\nu(\overline{C}(r))}.$$

In particular, if $d\nu(x) = \lambda \ dx$ *and* $C = \mathbf{B}(o,R)$ *then:*

$$F_{\|\Pi\|}(r) = \begin{cases} e^{-\lambda V_d (R^d - r^d)}, & 0 \leq r < R; \\ 1, & R \leq r. \end{cases}$$

and

$$p_{\|\Pi\|}(r) = \begin{cases} \lambda V_d^{'} r^{d-1} e^{-\lambda V_d (R^d - r^d)}, & 0 \leq r < R; \\ 0, & R \leq r. \end{cases}$$

Proof. We have, as Π is a Poisson point process:

$$\begin{aligned} F_{\|\Pi\|}(r) &= \mathbf{P}\left(\overline{C}(r) \cap \Pi = \emptyset\right) \\ &= e^{-\nu(\overline{C}(r))}. \end{aligned}$$

for $r \leq R$. The PDF of $\|\Pi\|$ then follows. Now if $\mathrm{d}\nu(x) = \lambda \, \mathrm{d}x$ and $C = \mathbf{B}(o,R)$ then $\nu(C \cap \overline{\mathbf{B}}(o,r)) = V_d(R^d - r^d)$, then the expressions for CDF and PDF of $\|\Pi\|$ follows. □

Remark 1. *If the cell C has the regular $n-$polygon ($n = 3, 4$ or 6 in a regular network) on $\mathbb{R}^2$ ($d = 2$) with circumradius R, and $d\nu(x) = \lambda\, dx$ then the CDF of $\|\Pi\|$ in the previous lemma can be expressed as follows:*

$$F_{\|\Pi\|}(r) = \begin{cases} \exp\left\{-\lambda\pi(R^2 - r^2)\right\}, \text{if } 0 \le r < R\cos\frac{\pi}{n}; \\ \exp\left\{-\lambda\left(R^2 - \left(\pi - n\arccos\frac{R\cos\frac{\pi}{n}}{r} + \frac{n}{2}\sin\left(2\arccos\frac{R\cos\frac{\pi}{n}}{r}\right)\right)r^2\right)\right\}, \\ \quad \text{if } R\cos\frac{\pi}{n} \le r < R; \\ 1, \text{ if } R < r. \end{cases}$$

Following the above lemma, the moments of P_B are given as

$$\mathbf{m}_n\left[P_B(\omega_0)\right] = b^n \int_0^R r^{n\gamma} \lambda V_d' r^{d-1} e^{-\lambda V_d(R^d - r^d)}\, \mathrm{d}r.$$

For simplicity, let

$$H_d(u, v, \alpha) = dv \int_0^u r^\alpha r^{d-1} e^{-v(u^d - r^d)}\, \mathrm{d}r \tag{6.6}$$

where $\alpha \ge 0$ then, $\mathbf{m}_n\left[P_B(\omega_0)\right] = b^n H_d(R, \lambda V_d, n\gamma)$. In particular,

$$\mathbf{E}\left[P_B(\omega_0)\right] = bH_d(R, \lambda V_d, \gamma).$$

Consequently, we obtain

$$\boxed{\mathbf{E}\left[J_T(\omega, T)\right] = TaV_d' \frac{R^{\gamma+d}}{\gamma + d} + TbH_d(R, \lambda V_d, \gamma).} \tag{6.7}$$

We note that $0 \le H_d(u, v, \alpha) \le R^\alpha$ so $TaV_d' \frac{R^{\gamma+d}}{\gamma+d} \le \mathbf{E}\left[J_T\right] \le TaV_d' \frac{R^{\gamma+d}}{\gamma+d} + TbR^\alpha$. If $\lambda \to \infty$ then $\mathbf{E}\left[J_B\right] \to TbR^d$, which is intuitive: as the intensity goes larger, the farthest user is located closer to the border of the cell. Nevertheless, bTR^γ is the consumed energy if the operator wants to broadcast message to all points of the cell, not just all active users in the cell. Thus, it is fair to assume that $\mathbf{E}\left[J_B(\omega, T)\right] \sim Tb'R^\gamma$ with $b' \ge 0$.

Consider an operator aiming to design the optimal cell radius R to cover a region of total area (volume) $S \in \mathbb{R}^d$. The average total cost of the network is assumed to be the sum of the operation cost during the life time of the network (says T) and the cost of facilities (base stations). The number of base station is then proportional to $\frac{S}{R^d}$, say $\frac{C}{R^d}$, so the installation cost of base stations is $\frac{c_1}{R^d}$ with $c_1 > 0$. The operation cost is assumed to be proportional to the consumed energy.

We assume that $l(x) = K.|x|^\gamma$, $\phi(x) = a.l(x)\mathbf{1}_{\{x \in C\}}$, $\psi(x) = b.l(x)\mathbf{1}_{\{x \in C\}}$ with $K > 0$ and furthermore $\gamma \ge d$. The expectations of the two parties of energy consumed by a singe base station are then $\mathbf{E}\left[J_A(\omega, T)\right] = \lambda Ta'R^{\gamma+d}$ and $\mathbf{E}\left[J_B(\omega, T)\right] = Tb'R^\gamma$ with $a', b' \ge 0$. The energy consumed by the network during its operating time is:

$$\frac{C}{R^d}\left(a'\lambda TR^{d+\gamma} + b'TR^\gamma\right) = a_1\lambda TR^\gamma + b_1 TR^{\gamma-d}.$$

This is a increasing function of R, which means that small cell systems will consume less energy than larger cell system. The average total cost for the network is then

$$\boxed{Cost(R) = a_1\lambda TR^\gamma + b_1 TR^{\gamma-d} + \frac{c_1}{R^d}} \tag{6.8}$$

It is interesting for operator to find the optimal R in order to minimize the cost function. As $Cost(R) > 0$ for all $R > 0$ and $\lim_{R\to 0} Cost(R) = \lim_{R\to\infty} Cost(R) = \infty$ there exists a minimum for $Cost$. By differentiation, the optimal cell radius is the unique positive solution of the following equation:

$$a_1\lambda\gamma T R_{opt}^{\gamma+d} + b_1 T(\gamma - d)R_{opt}^{\gamma} = dc_1$$

As the RHS is increasing in T, the optimal cell radius R_{opt} must be a decreasing function of T. This reveals a characteristic of the optimal choice of cell radius. In the economical point of view, to operate a network with longer life time it is preferable to exploit smaller cells system.

If $b_1 = 0$, i.e the broadcast part of transmitted power is small comparing to the additive part, then the problem reduces to minimizing $a_1\lambda T R^{\gamma} + \frac{c_1}{R^d}$. Simple manipulations yields:

$$\boxed{R_{opt} = \left(\frac{dc_1}{\gamma\lambda a_1 T}\right)^{\frac{1}{\gamma+d}}.} \tag{6.9}$$

That is to say theoretically the optimal cell radius is proportional to $(\lambda T)^{-\frac{1}{\gamma+d}}$.

Similarly the network operates only in broadcast, the optimal cell radius will be

$$R_{opt} = \left(\frac{dc_1}{(\gamma - d)b_1 T}\right)^{-\frac{1}{\gamma}}.$$

6.5 Conclusion

In this chapter we have proposed a general energy consumption on cellular networks and a model for mobility for users. We have also considered a basic model for energy consumption and in order to minimize the cost of the network we derive some theoretical results on the optimal choice of cell radius.

Chapter 7

ON-OFF model

Contents

7.1 Introduction 81
7.2 Model 82
7.3 Motionless case 84
7.4 Impact of mobility 89
7.5 Special cases 94
7.5.1 Completely aimless mobility model 94
7.5.2 Always on users 96
7.6 Summary and Conclusion 98

7.1 Introduction

The previous chapter introduced a new energy consumption model for cellular network. In this chapter, we apply it in a specific scenario. At time $t = 0$, users are dispatched in the plane according to a Poisson point process. With each of them, is associated a random process with two states ON-OFF (active or inactive) which represents their activity. Moreover, users randomly move. Only "on" users are served by the network. This is the very first approach we can think of to model the activity of entities in a network. As usual, this assumption reflects the fact that a user can disconnect from a wireless network to switch to a new wire network or the channel from the BS to the user can become so bad so that the connection is no longer possible,... . Although this approach seems to be simple at the first sight, it is still a complex object to study and need a lot of calculation.

The ON-OFF model is well studied in the queueing literature. It is used to explain phenomenons called heavy tails, self-similarity and long range dependence of traffic observed by measurement in many types of networks, see for example [52] and references therein. We do not address this problem here in this thesis.

This chapter is organized in the following way. The section 7.2 describes the model. Section 7.3 presents analysis in the case where users are motionless. Section 7.4 investigates the impact of mobility. Section 7.5 considers some special cases of mobility model, including the completely aimless mobility model. Important notations and parameters used in this chapter are summarized in the table 7.1.

Symbols	Definition, Physical meaning
$I = (I(t), t \in \mathbb{R})$	ON-OFF model of user's activity
$A(T) = \int_0^T I(t)\ \mathrm{d}t$	Total fraction of ON time
$I_i = (I_i(t), t \in \mathbb{R})$	ON-OFF activity of user i
N	$\sum_{i\geq 1} \delta_{X_i}$, Poisson point process of initial position of users of intensity measure $\mathrm{d}\Lambda(x)$
ω_t	$\sum_{i\geq 1} \mathbf{1}_{\{I_i(t)=0\}}\delta_{X_i}$Poisson point process of active users at t if users are motionless
ω_t^M	$\sum_{i\geq 1} \mathbf{1}_{\{I_i(t)=0\}}\delta_{X_i+M_i(t)}$, Poisson point process of active users at t if users move
$\Phi_n^M(f, t_1, ..., t_n)$	$\mathbf{E}\left[\int_{\mathbb{R}^d} f(x + M(t_1))...f(x + M(t_n))\ \mathrm{d}x\right]$
$F_n^M(f, T)$	$\int_{\mathbb{R}^d} \mathbf{E}\left[\left(\int_0^T f(x + M(t))I(t)\ \mathrm{d}t\right)^n\right]\ \mathrm{d}x$
$H_n^M(f, u)$	$\int_{\mathbb{R}^d} \mathbf{E}\left[\left(\int_0^u f(x + M(t))\ \mathrm{d}t\right)^n\right]\ \mathrm{d}x$

Table 7.1: Notations and parameters in this chapter.

7.2 Model

An ON-OFF process on the real line alternates between values 1 (for on state) and 0 (for OFF state). ON-periods (and OFF-periods) are i.i.d positive random variables. Furthermore, the sequences of ON-periods and OFF-periods are independent. Each realization of an ON-OFF source is a Càdlàg function. An ON-OFF process is called exponential if ON-periods and OFF-periods are exponential distributed.

More precisely, consider an ON-OFF sources $(I(t), t \in \mathbb{R})$ such that the ON-periods are continuous positive random variable of mean μ_1^{-1} and the OFF-periods are continuous positive random variable of mean μ_0^{-1} and denote by U and V the generic ON-period and OFF-period. We can write:

$$I(t) = \sum_{i=-\infty}^{\infty} \mathbf{1}_{\{T_{2i}\leq t<T_{2i+1}\}}.$$

where $... < T_{-3} < T_{-2} < T_{-1} < T_0 < T_1 < T_2 < T_3 < ...$ such that $(T_{2i} - T_{2i-1})_{i=-\infty}^{\infty}$ are i.i.d and have the same distribution as V, and $(T_{2i+1} - T_{2i})_{i=-\infty}^{\infty}$ are i.i.d and have the same distribution as U. We can assume that $T_0 \vee T_1 \geq 0$. I can be seen as a random variable on $D(\mathbb{R}, \mathbb{R})$ with probability measure $\mathrm{d}\mathbf{P}_I$. We assume that I is stationary. From [53] for example, we have $\mathbf{P}(I(t) = 1) = \frac{\mu_0}{\mu_0+\mu_1} \triangleq \pi_1$ and $\mathbf{P}(I(t) = 0) = \frac{\mu_1}{\mu_0+\mu_1} \triangleq \pi_0$ for all t. Furthermore, we have

$$\mathbf{P}\left(I(t) = 1 \forall t \in [0, u)\right) = \frac{\pi_1}{\mathbf{E}\left[U\right]} \int_u^{\infty} \mathbf{P}\left(U > s\right)\ \mathrm{d}s.$$

for all $u > 0$.

With a little abuse of notation, we write $\pi_{j_1,...,j_n}(t_1, ..., t_n) = \mathbf{P}\left(I(t_i) = j_i \forall i = 1..n\right)$ where $j_1, ..., j_n \in \{0, 1\}$ and $t_1, ..., t_n \in \mathbb{R}$. Let $A(T) = \int_0^T I(t)\ \mathrm{d}t$. Since the process I is stationary, we have $\mathbf{E}\left[A(T)\right] = \pi_1 T$. In the case of exponential ON-OFF process, the expressions for $\pi_{j_1,...,j_n}(t_1, ..., t_n)$ and the moments of $A(T)$ are given in the appendix.

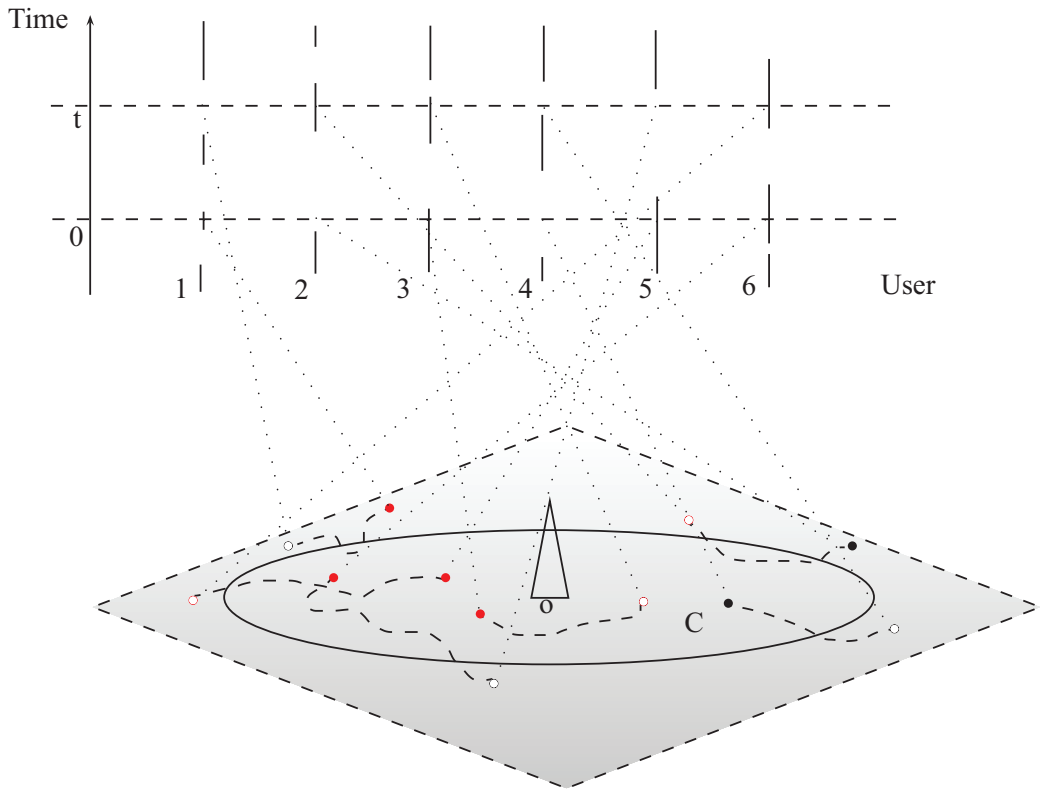


Figure 7.1: Illustration of the model, each user is associated with a ON-OFF process and a mobility process.

Lemma 31. *We have, for all* T

$$\pi_1^n T^n \leq \mathbf{m}_n\left[A(T)\right] \leq T^n.$$

Proof. Since $A(T) \leq T$ a.s. we have $\mathbf{m}_n\left[A(T)\right] \leq T^n$. Now $\mathbf{m}_n\left[A(T)\right] \geq \left(\mathbf{E}\left[A(T)\right]\right)^n = \pi_1^n T^n$ by Cauchy−Schwarz inequality. □

Let $\mathrm{d}\Lambda(x)$ be a $\sigma-$finite Radon measure on $\mathbb{R}^d$, absolutely continuous with respect to the Lebesgue measure. We make the following assumptions:

Assumption 4. *The positions of users at* $t = 0$ *follow a Poisson point process* $N = \{X_i\}_{i\geq 1}$ *of intensity measure* $\mathrm{d}\Lambda(x)$. *User* i *is associated with an ON-OFF process of activity* $(I_i(t), t \in \mathbb{R})$,*i.e users are active during their ON-periods and are inactive during their OFF-periods. The activity processes of users are assumed to be i.i.d and have the same distribution as that of* $(I(t), t \geq 0)$.

Following the above assumptions, the configuration of active users at time t is

$$\omega_t^M = \sum_{i\geq 1} \mathbf{1}_{\{I_i(t)=1\}} \delta_{X_i + M_i(t)}.$$

The system can be described by a Poisson point process on $\mathbb{R}^d \times D(\mathbb{R}, \mathbb{R}) \times D([0, +\infty), \mathbb{R}^d)$

$$\Phi^{I,M} = \{(X_i, I_i, M_i)\}_{i\geq 1}.$$

of intensity $\mathrm{d}\Lambda(x) \times \mathrm{d}\mathbf{P}_I \times \mathrm{d}\mathbf{P}_M$. The consumed energy is defined in the same way as in the previous chapter for the time varying configuration process $\omega^M = (\omega^M(t), t \geq 0)$. In particular, the additive part of consumed energy can be rewritten as:

$$J_A(\omega^M, T) = \sum_{i \geq 1} \int_0^T I_i(t) \phi(X_i + M_i(t)) \, \mathrm{d}t$$

and the broadcast part is:

$$J_B(\omega^M, T) = \int_0^T \overline{\psi}(\|\omega_t^M\|) \, \mathrm{d}t.$$

The total consumed energy is $J_T(\omega^M, T) = J_A(\omega^M, T) + J_B(\omega^M, T)$.

When users are motionless, i.e $M_i(t) = o$, the system is described as a Poisson point process

$$\Phi^I = \{(X_i, I_i)\}_{i \geq 1}.$$

of intensity measure $\mathrm{d}\Lambda(x) \times \mathrm{d}\mathbf{P}_I$. In this case, we drop the superscript. Thus, the configuration of users at time t is:

$$\omega_t = \sum_{i=1}^{n} \mathbf{1}_{\{I_i(t)=0\}} \delta_{X_i}.$$

The additive part of consumed energy is

$$J_A(\omega, T) = \sum_{i \geq 1} \phi(X_i) \int_0^T I_i(t) \, \mathrm{d}t$$

and the broadcast part is:

$$J_B(\omega, T) = \int_0^T \overline{\psi}(\|\omega_t\|) \, \mathrm{d}t.$$

The total consumed energy in this case is $J_T(\omega, T) = J_A(\omega, T) + J_B(\omega, T)$. In the next two sections we present analytical results on the motionless case and the general case.

7.3 Motionless case

In this section, we assume that users are motionless. We derive analytical expressions for the moments of $J_A(\omega, T), J_B(\omega, T), J_T(\omega, T)$ in this case.

Theorem 32. *The moments of $J_A(\omega, T)$ are given by:*

$$\mathbf{m}_n\left[J_A(\omega, T)\right] = B_n\left(\mathbf{m}_1\left[A(T)\right] \int_{\mathbb{R}^d} \phi(x) \; d\Lambda(x), ..., \mathbf{m}_n\left[A(T)\right] \int_{\mathbb{R}^d} \phi^n(x) \; d\Lambda(x)\right),$$

and the central moments of $J_A(\omega, T)$ are given by:

$$\mathbf{c}_n\left[J_A(\omega, T)\right] = B_n\left(0, \mathbf{m}_2\left[A(T)\right] \int_{\mathbb{R}^d} \phi^2(x) \; d\Lambda(x), ..., \mathbf{m}_n\left[A(T)\right] \int_{\mathbb{R}^d} \phi^n(x) \; d\Lambda(x)\right).$$

In particular, the expectation of $J_A(\omega, T)$ is given as:

$$\mathbf{E}\left[J_A(\omega, T)\right] = \pi_1 \int_{\mathbb{R}^d} \phi(x) \; d\Lambda(x). \tag{7.1}$$

Proof. As $J_A(\omega,T)$ is a linear functional of Φ^I which is a Poisson point process, we then apply Theorem 7.4 and note that:

$$\int_{\mathbb{R}^d\times D(\mathbb{R},\mathbb{R}))} f(x)\left(\int_0^T I(t)\ \mathrm{d}t\right)^n\ \mathrm{d}\Lambda(x)\ \mathrm{d}\mathbf{P}_I = \int_{\mathbb{R}^d} f^n(x)\ \mathrm{d}\Lambda(x)\mathbf{E}\left[\left(\int_0^T I(t)\ \mathrm{d}t\right)^n\right]$$
$$= \mathbf{m}_n\left[A(T)\right]\int_{\mathbb{R}^d} f^n(x)\ \mathrm{d}x\cdot$$

□

We see that, from the above theorem, the expectation of $J_A(\omega,T)$ depends on the distribution of ON-periods and OFF-periods only by the activity rate μ_0/μ_1.

Corollary 4. *If* $C=\mathbf{B}(o,R)$, $\phi(x)=a\left|x\right|^\gamma\mathbf{1}_{\{x\in\mathbf{B}(o,R)\}}$ *and* $d\Lambda(x)=\lambda\ dx$ *then:*

$$\mathbf{m}_n\left[J_A(\omega,T)\right]=B_n\left(\frac{\lambda aV_d^{'}\mathbf{m}_1\left[A(T)\right]R^{\gamma+d}}{\gamma+d},\frac{\lambda V_d^{'}a^2\mathbf{m}_2\left[A(T)\right]R^{2\gamma+d}}{2\gamma+d},...,\frac{\lambda V_d^{'}a^n\mathbf{m}_n\left[A(T)\right]R^{n\gamma+d}}{n\gamma+d}\right),$$

$$\mathbf{c}_n\left[J_A(\omega,T)\right]=B_n\left(0,\frac{\lambda V_d^{'}a^2\mathbf{m}_n\left[A(T)\right]R^{2\gamma+d}}{2\gamma+d},...,\frac{\lambda V_d^{'}a^n\mathbf{m}_n\left[A(T)\right]R^{n\gamma+d}}{n\gamma+d}\right)\cdot$$

In particular,

$$\mathbf{E}\left[J_A(\omega,T)\right]=\frac{\pi_1 d\lambda aR^{\gamma+d}}{(\gamma+d)\Gamma(\frac{d}{2}+1)}.$$

Proof. We have that $\int_{\mathbf{B}(o,R)}\left|x\right|^k\ \mathrm{d}x=V_d^{'}\frac{R^{k+n}}{k+n}$ with $k>-n$. The proof is, thus, completed. □

Applying Theorem 11, an error bound for Gaussian approximation of $J_A(\omega,T)$ is found as follows:

Theorem 33. *Let* $\overline{J_A}(\omega,T)=\frac{J_A(\omega,T)-\mathbf{E}[J_A(\omega,T)]}{\mathbf{V}[J_A(\omega,T)]}$ *then for any* u *we have:*

$$\left|\mathbf{P}\left(\overline{J_A}(\omega,T)>u\right)-\overline{Q}(u)\right|\leq\frac{\mathbf{m}_3\left[A(T)\right]\int_{\mathbb{R}^d}\phi^3(x)\ d\Lambda(x)}{\left(\mathbf{m}_2\left[A(T)\right]\int_{\mathbb{R}^d}\phi^2(x)\ d\Lambda(x)\right)^{\frac{3}{2}}}.$$

As shown in Lemma 31, $T^2\geq\mathbf{m}_2\left[A(T)\right]\geq\pi_1^2T^2$ and $mm3A(T)\leq T^3$, so the bound decays as $\Theta(1)$ as $T\to\infty$. We obtain a less sharp bound but depending only on the activity rate π_1 but not on the distribution of ON-periods and OFF-periods and on T:

$$\left|\mathbf{P}\left(\overline{J_A}(\omega,T)>u\right)-\overline{Q}(u)\right|\leq\frac{\int_{\mathbb{R}^d}\phi^3(x)\ \mathrm{d}\Lambda(x)}{\pi_1^3\left(\int_{\mathbb{R}^d}\phi^2(x)\ \mathrm{d}\Lambda(x)\right)^{\frac{3}{2}}}.$$

As already noted in the case of exponential ON-OFF source, when T goes to infinity, $\mathbf{m}_2\left[A(T)\right]\sim\pi_1^2T^2$ and $\mathbf{m}_3\left[A(T)\right]\sim\pi_1^3T^3$. Consequently, in this case the bound has the following limit when $T\to\infty$:

$$\frac{\int_{\mathbb{R}^d}\phi^3(x)\ \mathrm{d}\Lambda(x)}{\sqrt{\pi_1}\left(\int_{\mathbb{R}^d}\phi^2(x)\ \mathrm{d}\Lambda(x)\right)^{\frac{3}{2}}}.$$

Now let $\Lambda(x) = \lambda \, \mathrm{d}x$, the bound becomes:

$$\frac{\mathbf{m}_3 \left[A(T)\right] \int_{\mathbb{R}^d} \phi^3(x) \, \mathrm{d}x}{\sqrt{\lambda} \left(\mathbf{m}_2 \left[A(T)\right] \int_{\mathbb{R}^d} \phi^2(x) \, \mathrm{d}x\right)^{\frac{3}{2}}}$$

which decays as $\Theta(\frac{1}{\sqrt{\lambda}})$ as $\lambda \to \infty$.

Theorem 34. *The joint distribution of* $(\|\omega_{t_1}\|, ..., \|\omega_{t_n}\|)$ *is given by:*

$$F_{(\|\omega_{t_1}\|,...,\|\omega_{t_n}\|)}(u_1, ..., u_n) = \sum_{i=1}^{n} (-1)^{i-1} \sum_{1 \le k_1 < ... < k_i \le n} e^{-\pi_{1,1,...,1}(t_{k_1},...,t_{k_i})\Lambda(\overline{C}(\max\{u_{k_1},...,u_{k_i}\}))}.$$

In particular,

$$F_{\|\omega_t\|}(u) = e^{-\pi_1 \Lambda(\overline{C}(u))}. \tag{7.2}$$

The n^{th} *order moment of* $J_B(\omega, T)$ *are given by:*

$$\mathbf{m}_n \left[J_B(\omega, T)\right] = \int_{[0,T)^n} dt_1 ... \, dt_n \int_{(\mathbb{R}^+)^n} \overline{\psi}(u_1) ... \overline{\psi}(u_n) \; dF_{(\|\omega_{t_1}\|,...,\|\omega_{t_n}\|)}(u_1, ..., u_n) \cdot$$

Proof. Let A_i be the event $\{|\omega_{t_i}|_\infty \le u_i\}$. Simple joint probability rule gives us

$$\mathbf{P}\left(\bigcap_{i=1}^{n} A_i\right) = \sum_{i=1}^{n} (-1)^{i-1} \sum_{1 \le k_1 < ... < k_i \le n} \mathbf{P}\left(\cup_{j=1}^{i} A_{k_i}\right) \cdot$$

Thus, we must evaluate $\mathbf{P}\left(\cup_{j=1}^{i} A_{k_i}\right)$. The event $\cup_{j=1}^{i} A_{k_i}$ is equivalent to the event: there is no user on C being active at all instances $t_{k_1}, ..., t_{k_i}$ having distance to the origin larger than $\max\{u_{k_1}, ..., u_{k_i}\}$. We recall that the ON-OFF processes of users are i.i.d, so the users being active at all these instances $t_{k_1}, ..., t_{k_i}$ form a Poisson point process of intensity $\pi_{1,...,1}(t_{k_1}, ..., t_{k_i}) \, \mathrm{d}\Lambda(x)$ and thus

$$\mathbf{P}\left(\cup_{j=1}^{i} A_{k_i}\right) = e^{-\pi_{1,1,...,1}(t_{k_1},...,t_{k_i})\Lambda(\overline{C}(\max\{u_{k_1},...,u_{k_i}\}))}.$$

The expression for the joint distribution of $(\|\omega_{t_1}\|, ..., \|\omega_{t_n}\|)$ follows. Now we can write:

$$\begin{aligned}
\mathbf{m}_n \left[J_B(\omega, T)\right] &= \mathbf{E}\left[\left(\int_0^T \overline{\psi}(\|\omega_t\|) \, \mathrm{d}t\right)^n\right] \\
&= \int_0^T ... \int_0^T \mathbf{E}\left[\overline{\psi}(|\omega_{t_1}|) ... \overline{\psi}(|\omega_{t_n}|)\right] \, \mathrm{d}t_1 ... \, \mathrm{d}t_n \\
&= \int_{[0,T)^n} \mathrm{d}t_1 ... \, \mathrm{d}t_n \int_{(\mathbb{R}^+)^n} \overline{\psi}(u_1) ... \overline{\psi}(u_n) \, \mathrm{d}F_{(\|\omega_{t_1}\|,...,\|\omega_{t_n}\|)}(u_1, ..., u_n).
\end{aligned}$$

This completes the proof. □

Theorem 35. *The second order moment of* $J_T(\omega, T)$ *is given by:*

$$\begin{aligned}
\mathbf{m}_2 \left[J_T(\omega, T)\right] &= \left(\mathbf{m}_1 \left[A(T)\right] \int_{\mathbb{R}^d} \phi(x) \; d\Lambda(x)\right)^2 + \mathbf{m}_2 \left[A(T)\right] \int_{\mathbb{R}^d} \phi^2(x) \; d\Lambda(x) \\
&\quad + \int_{[0,T)^2} dt_1 \; dt_2 \int_{(\mathbb{R}^+)^2} \overline{\psi}(u_1) \overline{\psi}(u_2) \; dF_{(\|\omega_{t_1}\|,\|\omega_{t_2}\|)}(u_1, u_2) \\
&\quad + 2 * \textit{RHS of (7.4)}.
\end{aligned} \tag{7.3}$$

Proof. We have:

$$\begin{aligned}\mathbf{E}\left[(J_T(\omega,T))^2\right] &= \mathbf{E}\left[(J_A(\omega,T)+J_B(\omega,T))^2\right] \\ &= \mathbf{E}\left[(J_A(\omega,T))^2\right]+\mathbf{E}\left[(J_B(\omega,T))^2\right]+2\mathbf{E}\left[J_A(\omega,T)J_B(\omega,T)\right].\end{aligned}$$

We have already expressions for $\mathbf{E}\left[(J_A(\omega,T))^2\right]$ and $\mathbf{E}\left[(J_B(\omega,T))^2\right]$, thus it remains to evaluate $\mathbf{E}\left[J_A(\omega,T)J_B(\omega,T)\right]$.

$$\begin{aligned}\mathbf{E}\left[J_A(\omega,T)J_B(\omega,T)\right] &= \mathbf{E}\left[\int_0^T P_A(\omega_t)\ \mathrm{d}t\int_0^T P_B(\omega_t)\ \mathrm{d}t\right] \\ &= \int_0^T\int_0^T \mathbf{E}\left[P_A(\omega_t)\overline{\psi}(\|\omega_s\|)\right]\ \mathrm{d}t\ \mathrm{d}s.\end{aligned}$$

We have to evaluate $\mathbf{E}\left[P_A(\omega_t)\psi\left|\omega_s\right|\right]$. We can do it by determining the conditional expectation $\mathbf{E}\left[P_A(\omega_t)\right|\left\|\omega_s\right\|=r]$ then deconditioning on the distribution of $|\omega_s|$. Now consider the event "$|\omega_s|=r$". Given this event, the configuration of users being active at t is a Poisson point process of intensity measure $\pi_{10}(t,s)\mathbf{1}_{\{x\in\overline{C}(r)\}}\ \mathrm{d}\Lambda(x)+\pi_1\mathbf{1}_{\{x\in C(r)\}}\ \mathrm{d}\Lambda(x)$ plus the user at distance r if it is active. Consequently, using Campbell's formula we have:

$$\begin{aligned}\mathbf{E}\left[P_A(\omega_t)P_B(\omega_s)\right|\left\|\omega_s\right\|=r] &= \pi_{10}(t,s)\overline{\psi}(r)\int_{\overline{C}(r)}\phi(x)\ \mathrm{d}\Lambda(x) \\ &\quad +\pi_1\psi(r)\int_{C(r)}\phi(x)\ \mathrm{d}\Lambda(x)+p_{11}(t,s)\overline{\phi}(r)\overline{\psi}(r).\end{aligned}$$

Note that the distribution of $\|\omega_s\|$ is the same as that of $\|\omega_0\|$, we finally obtain an expression for $\mathbf{E}\left[J_A(\omega,T)J_B(\omega,T)\right]$:

$$\begin{aligned}\mathbf{E}\left[J_A(\omega,T)J_B(\omega,T)\right] &= \int_0^T\int_0^T\pi_{10}(t,s)\int_0^\infty\overline{\psi}(r)\int_{\overline{C}(r)}\phi(x)\ \mathrm{d}\Lambda(x)\ \mathrm{d}F_{\|\omega_0\|}(r)\ \mathrm{d}s\ \mathrm{d}t \\ &\quad +\pi_1\int_0^T\int_0^T\int_0^\infty\overline{\psi}(r)\int_{C(r)}\phi(x)\ \mathrm{d}\Lambda(x)\ \mathrm{d}F_{\|\omega_0\|}(r)\ \mathrm{d}s\ \mathrm{d}t \\ &\quad +\int_0^T\int_0^T\int_0^\infty\pi_{11}(t,s)\overline{\phi}(r)\overline{\psi}(r)\ \mathrm{d}F_{\|\omega_0\|}(r)\ \mathrm{d}s\ \mathrm{d}t \qquad (7.4)\end{aligned}$$

□

We have obtained closed form formulas for $\mathbf{V}\left[J_B(\omega,T)\right]$ and $\mathbf{V}\left[J_T(\omega,T)\right]$, however it requires to solve triple integrals. We now present bounds for $\mathbf{V}\left[J_B(\omega,T)\right]$ and $\mathbf{V}\left[J_T(\omega,T)\right]$, which requires only one easily computed integral.

Theorem 36. *We have:*

$$\mathbf{V}\left[J_B(\omega,T)\right]\leq\mathbf{m}_2\left[A(T)\right]\int_{\mathbb{R}^d}\psi^2(x)\ d\Lambda(x), \qquad (7.5)$$

and

$$\mathbf{m}_2\left[A(T)\right]\int_{\mathbb{R}^d}\phi^2(x)\ d\Lambda(x)\leq\mathbf{V}\left[J_T(\omega,T)\right]\leq\mathbf{m}_2\left[A(T)\right]\int_{\mathbb{R}^d}\left(\phi(x)+\psi(x)\right)^2\ d\Lambda(x). \qquad (7.6)$$

Proof. As (7.5) is covered by (7.6) by setting $\phi(x) = 0$, it is sufficient to prove (7.6). Since $J_T(\omega, T)$ is a linear functional of the Poisson point process Φ^I we can apply the corollary 1. By definition, adding a point (X, I) to Φ will increase the consumed power for at most $\phi(X) + \psi(X)$ at each instance where the new user X is active. Consequently, $0 \leq D_{(X,I)} J_A(\omega, T) \leq (\phi(x) + \psi(x)) \int_0^T I(t)\ \mathrm{d}t$. It follows that:

$$\mathbf{V}\left[J_T(\omega, T)\right] \leq \int_{\mathbb{R}^d} (\psi(x) + \phi(x))^2\ \mathrm{d}\Lambda(x) \mathbf{E}\left[\left(\int_0^T I(t)\right)^2\right],$$

where the last expectation is taken with respect to the distribution of I.

Now we apply Theorem 6. We consider two functionals $J_A(\omega, T)$ and $J_B(\omega, T)$. Adding a point (X, I) will not decrease both the functionals, so:

$$\mathbf{m}_2\left[A(T)\right] \int_{\mathbb{R}^d} \phi^2(x)\ \mathrm{d}\Lambda(x) = \mathbf{V}\left[J_A(\omega, T)\right] \leq \mathbf{V}\left[J_A(\omega, T) + J_B(\omega, T)\right] = \mathbf{V}\left[J_T(\omega, T)\right].$$

□

From theorem 6, we also note that

$$\mathbf{V}\left[J_T(\omega, T)\right] \geq \mathbf{V}\left[J_A(\omega, T)\right] + \mathbf{V}\left[J_B(\omega, T)\right].$$

Corollary 5. *If* $C = \mathbf{B}(o, R)$, $\phi(x) = a\,|x|^\gamma\, \mathbf{1}_{\{x \in \mathbf{B}(o,R)\}}, \psi(x) = b\,|x|^\gamma\, \mathbf{1}_{\{x \in \mathbf{B}(o,R)\}}$ $(a, b > 0)$ *and* $d\Lambda(x) = \lambda\ dx$ *then:*

$$\begin{aligned} \mathbf{V}\left[J_B(\omega, T)\right] &\leq \frac{\lambda a^2 \mathbf{m}_2\left[A(T)\right] V_d' R^{d+2\gamma}}{d + 2\gamma} \\ \mathbf{V}\left[J_T(\omega, T)\right] &\leq \frac{\lambda (a+b)^2 \mathbf{m}_2\left[A(T)\right] V_d' R^{d+2\gamma}}{d + 2\gamma}. \end{aligned}$$

The following theorem gives an upper bound on the distribution of $J_T(\omega, T)$:

Theorem 37. *Assume that* $\phi(x) + \psi(x) \leq K$ *for all* $x \in \mathbb{R}^d$, *let*

$$\alpha^2 = \mathbf{m}_2\left[A(T)\right] \int_{\mathbb{R}^d} (\psi(x) + \phi(x))^2\ \ d\Lambda(x)$$

then

$$\mathbf{P}\left(J_T(\omega, T) > \mathbf{E}\left[J_T(\omega, T)\right] + u\right) \leq \exp\left\{-\frac{T^2 K^2}{\alpha^2} g\left(\frac{uTK}{\alpha^2}\right)\right\}$$

for all $u > 0$.

Proof. As proved above, $0 \leq D_{X,I} J_T(\omega, T) \leq (\phi(x) + \psi(x)) \int_0^T I(t)\ \mathrm{d}t \leq TK$. Thus, applying Theorem 8 (or its corollary 1) we obtain the desired result. □

By setting $\phi(x) = 0$ or $\psi(x) = 0$ in the above theorem, we can derive upper bound on the distribution of $J_A(\omega, T)$ and $J_B(\omega, T)$:

Corollary 6. *Let*

$$\begin{aligned} \alpha_A^2 &= \mathbf{m}_2\left[A(T)\right] \int_{\mathbb{R}^d} (\phi(x))^2\ \ d\Lambda(x) \\ \alpha_B^2 &= \mathbf{m}_2\left[A(T)\right] \int_{\mathbb{R}^d} (\psi(x))^2\ \ d\Lambda(x). \end{aligned}$$

Assume that $\phi(x) \leq K$ for all $x \in \mathbb{R}^d$ then for any $u > 0$,

$$\mathbf{P}\left(J_A(\omega,T) > \mathbf{E}\left[J_A(\omega,T)\right] + u\right) \leq \exp\left\{-\frac{T^2K^2}{\alpha_A^2} g\left(\frac{uTK}{\alpha_A^2}\right)\right\}.$$

Similarly, assume that $\phi(x) \leq K$ for all $x \in \mathbb{R}^d$ then for any $u > 0$,

$$\mathbf{P}\left(J_B(\omega,T) > \mathbf{E}\left[J_B(\omega,T)\right] + u\right) \leq \exp\left\{-\frac{T^2K^2}{\alpha_B^2} g\left(\frac{uTK}{\alpha_B^2}\right)\right\}.$$

7.4 Impact of mobility

To consider the effect of mobility, we always assume that $\mathrm{d}\Lambda(x) = \lambda\ \mathrm{d}x$.

Lemma 38. *ω_t^M is a Poisson point process of intensity measure $\pi_1\lambda\ dx$ for all t.*

Proof. Consider the point process $\sum_{i\geq 1}\delta_{X_i+M_i(t)}$. By the displacement theorem, it is a Poisson point process of intensity measure $\mathrm{d}\Lambda_t(x)$ characterized by:

$$\begin{aligned}
\Lambda_t(A) &= \lambda \int_{\mathbb{R}^d} \mathbf{P}(x + M(t) \in A)\ \mathrm{d}x \\
&= \lambda \int_{\mathbb{R}^d} \mathrm{d}x \int_{\mathbb{R}^d} p_{M(t)}(y)\mathbf{1}_{\{x+y\in A\}}\ \mathrm{d}y \\
&= \lambda \int_{\mathbb{R}^d} p_{M(t)}(y)\ \mathrm{d}y \int_{\mathbb{R}^d} \mathbf{1}_{\{x+y\in A\}}\ \mathrm{d}x \\
&= \lambda l_d(A).
\end{aligned}$$

Thus, it is a Poisson point process of intensity $\lambda\ \mathrm{d}x$. Now by thinning property, $\omega_t^M = \sum_{i\geq 1}\mathbf{1}_{\{I_i(t)=1\}}\delta_{X_i+M_i(t)}$ is a Poisson point process of intensity $\pi_1\lambda\ \mathrm{d}x$. □

Theorem 39. *For any power allocation policy P_G, and for any mobility model M, the expectation of energy consumed is the same as in motionless case, i.e:*

$$\mathbf{E}\left[J_G(\omega^M,T)\right] = \mathbf{E}\left[J_G(\omega,T)\right].$$

In particular $\mathbf{E}\left[J_A(\omega^M,T)\right] = \mathbf{E}\left[J_A(\omega,T)\right]$, $\mathbf{E}\left[J_B(\omega^M,T)\right] = \mathbf{E}\left[J_B(\omega,T)\right]$ and $\mathbf{E}\left[J_T(\omega^M,T)\right] = \mathbf{E}\left[J_T(\omega,T)\right]$.

Proof. As for each t, ω_t^M and ω_t follow the same distribution (Poisson point processof intensity $\pi_1\lambda\ \mathrm{d}x$). Consequently, $\mathbf{E}\left[J_G(\omega^M,T)\right] = \int_0^T \mathbf{E}\left[P_G(\omega_t^M)\right]\ \mathrm{d}t$ and $\mathbf{E}\left[J_G(\omega,T)\right] = \int_0^T \mathbf{E}\left[P_G(\omega_t)\right]\ \mathrm{d}t$ must be equal. □

For a non negative function $f \in L^n(\mathbb{R}^d)$ and $t_1, ..., t_n \in \mathbb{R}$ and furthermore we assume that $f(x) = 0$ if $x \in \mathbb{R}^d/C$. Define

$$\Phi_n^M(f, t_1, ..., t_n) = \int_{\mathbb{R}^d} \mathbf{E}\left[f(x + M(t_1))...f(x + M(t_n))\right]\ \mathrm{d}x.$$

Lemma 40. *We have* $\Phi_n^M(f,t) = \int_{\mathbb{R}^d} f(x)\ dx$ *and:*

$$\Phi_n^M(f,t_1,...,t_n) \leq \int_{\mathbb{R}^d} f^n(x)\ dx.$$

Moreover, if M *has the property* $\mathbf{T}$ *and* $n \geq 2$ *then* $\Phi_n^{M/\epsilon}(f,t_1,...,t_n) \to 0$ *as* $\epsilon \to 0$ *with* $n \geq 2$. *If* $f(x) = a\mathbf{1}_{\{x\in C\}}$ *with* $a > 0$ *and* $n \geq 2$ *then* $\Phi_n^{M/\epsilon}(f,t_1,...,t_n)$ *is decreasing function of* ϵ.

Proof. Note that for all $y \in \mathbb{R}^d$, $\int_{\mathbb{R}^d} f(x+y)\ \mathrm{d}x = \int_{\mathbb{R}^d} f(x)\ \mathrm{d}x$. We have, by Fubini's theorem and Cauchy−Schwarz inequality:

$$\begin{aligned}
\Phi_n^M(f,t_1,...,t_n) &= \mathbf{E}\left[\int_{\mathbb{R}^d} f(x+M(t_1))...f(x+M(t_n))\ \mathrm{d}x\right] \\
&\leq \mathbf{E}\left[\int_{\mathbb{R}^d} ((f(x+M(t_1)))^n\ \mathrm{d}x)^{\frac{1}{n}} ... ((f(x+M(t_n))\ \mathrm{d}x)^n)^{\frac{1}{n}}\ \mathrm{d}x\right] \\
&= \int_{\mathbb{R}^d} f^n(x)\ \mathrm{d}x,
\end{aligned}$$

and it is easy seen that inequality occurs if $n = 1$.

Since for each realization of M one has $\frac{|M(t_1)-M(t_2)|}{\epsilon} \to \infty$ as $M(t_1) \neq M(t_2)$ (a.s), thus for ϵ small enough, one of 2 points $x+\frac{M(t_1)}{\epsilon}$ and $x+\frac{M(t_2)}{\epsilon}$ must be located outside C, then $f(x+\frac{M(t_1)}{\epsilon})...f(x+\frac{M(t_n)}{\epsilon}) = 0$. It means that $f(x+\frac{M(t_1)}{\epsilon})...f(x+\frac{M(t_n)}{\epsilon}) \to 0$ (a.s) and it is bounded by $(\sup f)^n$, so its expectation tends to 0. By dominated convergence theorem, we obtain that

$$\mathbf{E}\left[\int_{\mathbb{R}^d} f\left(x+\frac{M(t_1)}{\epsilon}\right)...f\left(x+\frac{M(t_n)}{\epsilon}\right)\ \mathrm{d}x\right] \to 0.$$

Now assume $f(x) = a\mathbf{1}_{\{x\in C\}}$ and $n \geq 2$, we have:

$$\begin{aligned}
\Phi_n^{M/\epsilon}(f,t_1,...,t_n) &= \mathbf{E}\left[\int_{\mathbb{R}^d} \mathbf{1}_{\{x+\frac{M(t_1)}{\epsilon},...,x+\frac{M(t_n)}{\epsilon}\in C\}}\ \mathrm{d}x\right] \\
&= \mathbf{E}\left[\int_C \mathbf{1}_{\{x+\frac{M(t_2)-M(t_1)}{\epsilon},...,x+\frac{M(t_n)-M(t_1)}{\epsilon}\in C\}}\ \mathrm{d}x\right].
\end{aligned}$$

Consider $0 < \epsilon_1 < \epsilon_2$, due to the convexity of C, for each $1 < i \leq n$ if $x+\frac{M(t_i)-M(t_1)}{\epsilon_1} \in C$ then $x+\frac{M(t_i)-M(t_1)}{\epsilon_2} \in C$. Since C is bounded, it implies that $\mathbf{1}_{\{x+\frac{M(t_2)-M(t_1)}{\epsilon},...,x+\frac{M(t_2)-M(t_1)}{\epsilon}\in C\}}$ is decreasing function of ϵ. It means that $\Phi_n^{M/\epsilon}(f,t_1,...,t_n)$ is also decreasing function of ϵ. □

Now let $F_n^M(f,T) = \int_{\mathbb{R}^d} \mathbf{E}\left[\left(\int_0^T f(x+M(t))I(t)\ \mathrm{d}t\right)^n\right]\ \mathrm{d}x$.

Lemma 41. *We have:*

$$F_n^M(f,T) \leq \mathbf{m}_n\left[A(T)\right]\int_{\mathbb{R}^d} f^n(x)\ dx.$$

If M *has the property* $\mathbf{T}$ *then* $F_f^{M/\epsilon}(T,n) \to 0$ *as* $\epsilon \to 0$ *for* $n \geq 2$. *If* $f(x) = a\mathbf{1}_{\{x\in C\}}$ *with* $a > 0$ *then* $F_f^{M/\epsilon}(T,n)$ *is decreasing function of* ϵ *for* $n \geq 2$.

Proof. We can write, by the same way as previously done and using Lemma 40:

$$\begin{aligned}
\digamma_n^M(f,T) &= \int_{\mathbb{R}^d}\int_0^T ... \int_0^T \mathbf{E}\left[\prod_{i=1}^n (f(x+M(t_i))I(t_i))\right] \mathrm{d}t_1 ... \mathrm{d}t_n \ \mathrm{d}x \\
&= \int_{\mathbb{R}^d}\int_0^T ... \int_0^T \mathbf{E}\left[\prod_{i=1}^n f(x+M(t_i))\right]\mathbf{E}\left[\prod_{i=1}^n I(t_i)\right] \mathrm{d}t_1 ... \mathrm{d}t_n \ \mathrm{d}x \\
&= \int_0^T ... \int_0^T \mathbf{E}\left[\prod_{i=1}^n I(t_i)\right]\int_{\mathbb{R}^d}\mathbf{E}\left[\prod_{i=1}^n f(x+M(t_i))\right] \mathrm{d}x \ \mathrm{d}t_1 ... \mathrm{d}t_n \\
&= \int_0^T ... \int_0^T \mathbf{E}\left[\prod_{i=1}^n I(t_i)\right]\Phi_n^M(f,t_1,...,t_n) \ \mathrm{d}t_1 ... \mathrm{d}t_n \\
&\leq \int_0^T ... \int_0^T \mathbf{E}\left[\prod_{i=1}^n I(t_i)\right]\int_{\mathbb{R}^d} f^n(x) \ \mathrm{d}x \ \mathrm{d}t_1 ... \mathrm{d}t_n \\
&= \int_{\mathbb{R}^d} f^n(x) \ \mathrm{d}x \int_0^T ... \int_0^T \mathbf{E}\left[\prod_{i=1}^n I(t_i)\right] \mathrm{d}t_1 ... \mathrm{d}t_n \\
&= \int_{\mathbb{R}^d} f^n(x) \ \mathrm{d}x \mathbf{E}\left[\left(\int_0^T I(t) \ \mathrm{d}t\right)^n\right] \\
&= \mathbf{m}_n\left[A(T)\right]\int_{\mathbb{R}^d} f^n(x) \ \mathrm{d}x\cdot
\end{aligned}$$

The first part of lemma is, thus, proved. Now the second part follows the fact that $\Phi_n^{M/\epsilon}(f,t_1,...,t_n) \to 0$ as $\epsilon \to 0$; $\Phi_n^{M/\epsilon}(f,t_1,...,t_n)$ is bounded by $\int_{\mathbb{R}^d} f^n(x) \ \mathrm{d}x$ and the dominated convergence theorem. If $f(x) = a\mathbf{1}_{\{x\in C\}}$ and $n \geq 2$ then $\digamma_f^{M/\epsilon}(T,n)$ is a decreasing function of ϵ because $\Phi_n^{M/\epsilon}(f,t_1,...,t_n)$ is. □

Theorem 42. *The moments of $J_A(\omega^M,T)$ are given by*

$$\begin{aligned}
\mathbf{m}_n\left[J_A(\omega^M,T)\right] &= B_n(\lambda\digamma_\phi^M(T,1),\lambda\digamma_\phi^M(T,2),...,\lambda\digamma_\phi^M(T,n)) \\
\mathbf{c}_n\left[J_A(\omega^M,T)\right] &= B_n(0,\lambda\digamma_\phi^M(T,2),...,\lambda\digamma_\phi^M(T,n))
\end{aligned}$$

Mobility reduces moments of J_A; i.e

$$\mathbf{m}_n\left[J_A(\omega^M,T)\right] \leq \mathbf{m}_n\left[J_A(\omega,T)\right], \ \textit{and} \ \mathbf{c}_n\left[J_A(\omega^M,T)\right] \leq \mathbf{c}_n\left[J_A(\omega,T)\right]$$

Furthermore, we have:

$$\mathbf{E}\left[\exp\left\{\alpha J_A(\omega^M,T)\right\}\right] \leq \mathbf{E}\left[\exp\left\{\alpha J_A(\omega,T)\right\}\right] \tag{7.7}$$

for all $\alpha \in \mathbb{R}$. If M has the property $\mathbf{T}$ then the central moments of J_A goes to 0 in high mobility regime; i.e

$$\mathbf{c}_n\left[J_A(\omega^{M/\epsilon},T)\right] \to 0, \ \textit{and} \ \mathbf{m}_n\left[J_A(\omega^{M/\epsilon},T)\right] \to \left(\pi_1\lambda\int_{\mathbb{R}^d}\phi(x) \ dx\right)^n \ \textit{as} \ \epsilon \to 0\cdot$$

If $\phi(x) = a\mathbf{1}_{\{x\in C\}}$ with $a > 0$, M has the property $\mathbf{T}$ and $n \geq 2$ then $\mathbf{m}_n\left[J_A(\omega^{M/\epsilon},T)\right], \mathbf{c}_n\left[J_A(\omega^{M/\epsilon},T)\right]$ are decreasing functions of ϵ.

Proof. The proof is similar to that of Theorem **??**. As $J_A(\omega^M, T)$ is a linear functional of $\Phi^{I,M}$ we can apply Theorem . We derive that

$$\begin{aligned}
&\int_{\mathbb{R}^d \times D(\mathbb{R},\mathbb{R}) \times D([0,+\infty),\mathbb{R}^d)} \left(\int_0^T f(x + M(t)) I(t) \, \mathrm{d}t \right)^n \lambda \, \mathrm{d}x \, \mathrm{d}\mathbf{P}_I \, \mathrm{d}\mathbf{P}_M \\
&= \quad \lambda \int_{\mathbb{R}^d} \mathbf{E} \left[\left(\int_0^T f(x + M(t)) I(t) \, \mathrm{d}t \right)^n \right] \mathrm{d}x \\
&= \quad \lambda \digamma_\phi^M(T, n).
\end{aligned}$$

Hence the expressions of $\mathbf{m}_n \left[J_A(\omega^M, T) \right]$ follow and $\mathbf{c}_n \left[J_A(\omega^M, T) \right]$. Now using results of Lemma 41 and the fact that a Bell polynomial has non negative coefficients, we have $\mathbf{m}_n \left[J_A(\omega^M, T) \right] \leq \mathbf{m}_n \left[J_A(\omega, T) \right]$, and $\mathbf{c}_n \left[J_A(\omega^M, T) \right] \leq \mathbf{c}_n \left[J_A(\omega, T) \right]$. Now assume M has the property $\mathbf{T}$ and following lemma 41, we have, as $\epsilon \to 0$ and $n \geq 2$:

$$\begin{aligned}
\mathbf{c}_n \left[J_A(\omega^{M/\epsilon}, T) \right] &\to B_n(0, 0, ..., 0) = 0 \\
\mathbf{m}_n \left[J_A(\omega^{M/\epsilon}, T) \right] &\to B_n(\pi_1 \lambda \int_{\mathbb{R}^d} \phi(x) \, \mathrm{d}x, 0, ..., 0) = \left(\pi_1 \lambda \int_{\mathbb{R}^d} \phi(x) \, \mathrm{d}x \right)^n.
\end{aligned}$$

Now, following the Laplace functional of Poisson point process and the Jensen's inequality, we have:

$$\begin{aligned}
\mathbf{E} \left[\exp \left\{ \alpha J_A(\omega^M, T) \right\} \right] &= \exp \left\{ \lambda \int_{\mathbb{R}^d} \left(\mathbf{E} \left[e^{\alpha \int_0^T \phi(x + M(t)) I(t) \, \mathrm{d}t} \right] - 1 \right) \, \mathrm{d}x \right\} \\
&= \exp \left\{ \lambda \int_{\mathbb{R}^d} \left(\mathbf{E}_I \left[\mathbf{E}_M \left[e^{\alpha \int_0^T \phi(x + M(t)) I(t) \, \mathrm{d}t} \right] - 1 \right] \right) \, \mathrm{d}x \right\} \\
&\leq \exp \left\{ \lambda \int_{\mathbb{R}^d} \left(\mathbf{E}_I \left[\mathbf{E}_M \left[\int_0^T \frac{I(t)}{A(T)} e^{\alpha \phi(x + M(t)) A(T)} \right] \, \mathrm{d}t - 1 \right] \right) \, \mathrm{d}x \right\} \\
&= \exp \left\{ \lambda \mathbf{E}_I \left[\mathbf{E}_M \left[\int_0^T \frac{I(t)}{A(T)} \int_{\mathbb{R}^d} \left(e^{\alpha \phi(x + M(t)) A(T)} - 1 \right) \, \mathrm{d}x \, \mathrm{d}x \right] \right] \right\} \\
&= \exp \left\{ \lambda \mathbf{E}_I \left[\mathbf{E}_M \left[\int_0^T \frac{I(t)}{A(T)} \int_{\mathbb{R}^d} \left(e^{\alpha \phi(x) A(T)} - 1 \right) \, \mathrm{d}x \, \mathrm{d}t \right] \right] \right\} \\
&= \exp \left\{ \lambda \mathbf{E}_I \left[\int_{\mathbb{R}^d} \left(e^{\alpha \phi(x) A(T)} - 1 \right) \, \mathrm{d}x \right] \right\} \\
&= \mathbf{E} \left[\exp \left\{ \alpha J_A(\omega, T) \right\} \right]
\end{aligned}$$

If $\phi(x) = a \mathbf{1}_{\{x \in C\}}$ with $a > 0$ and $n \geq 2$ then $\mathbf{m}_n \left[J_A(\omega^{M/\epsilon}, T) \right], \mathbf{c}_n \left[J_A(\omega^{M/\epsilon}, T) \right]$ are decreasing functions of ϵ because $\digamma_f^{M/\epsilon}(T, n)$ is. □

Theorem 43. *The variance of $J_B(\omega^M, T)$ and $J_T(\omega^M, T)$ are bounded as follows:*

$$\begin{aligned}
\mathbf{V} \left[J_B(\omega^M, T) \right] &\leq \lambda \digamma_\psi^M(T, 2) \\
\lambda \digamma_\phi^M(T, 2) \leq \mathbf{V} \left[J_T(\omega^M, T) \right] &\leq \lambda \digamma_{\phi+\psi}^M(T, 2).
\end{aligned}$$

Moreover, if M has the property $\boldsymbol{T}$ then in high mobility regime, the variance of J_B and J_T tends to 0, i.e

$$\mathbf{V} \left[J_B(\omega^{M/\epsilon}, T) \right], \mathbf{V} \left[J_T(\omega^{M/\epsilon}, T) \right] \to 0 \text{ as } \epsilon \to 0.$$

Proof. The proof is similar to that of Theorem 36. We need only to prove results for $J_T(\omega^M, T)$, the results for $J_B(\omega^M, T)$ follows by setting $\phi(x) = 0$. We apply Corollary 1. By definition,

$$0 \leq D_{(X,I,M)} J_A(\omega^M, T) \leq \int_0^T (\phi(X + M(t)) + \psi(X + M(t))) \, I(t) \, \mathrm{d}t.$$

Thus,

$$\mathbf{V}\left[J_T(\omega^M, T)\right] \quad \leq \quad \lambda F^M_{\phi+\psi}(T, 2).$$

We also note that adding a point (X, I, M) to ω^M will not decrease $J_A(\omega^M, T)$ and $J_B(\omega^M, T)$, so:

$$\mathbf{V}\left[J_T(\omega^M, T)\right] \quad \geq \quad \mathbf{V}\left[J_A(\omega^M, T)\right] = \lambda F^M_{\phi}(T, 2).$$

Finally, the convergence to 0 of $\mathbf{V}\left[J_T(\omega^{M/\epsilon}, T)\right]$ follows the fact that $F^{M/\epsilon}_{\phi+\psi}(T, 2)$ tends to 0 as ϵ tends to 0. □

The above results say that, when users move the total consumed energy by a base station does not change *in average*, and the moments and central moments of the additive part are reduced. Moreover, when users move very fast, the consumed energy during a time period is almost constant. We can see this fact as a consequence of weak central limit theorem. When users move faster, the configuration of users takes more "value" on $\Omega^{\mathbb{R}^d}$ during a same period of time, thus converge faster to the mean.

We find an error bound for Gaussian approximation of $J_A(\omega^M, T)$ as follows:

Theorem 44. *Let* $\overline{J_A}(\omega^M, T) = \frac{J_A(\omega^M,T) - \mathbf{E}[J_A(\omega^M,T)]}{\mathbf{V}[J_A(\omega^M,T)]}$ *then:*

$$\left|\mathbf{P}\left(\overline{J_A}(\omega^M, T) > u\right) - \overline{Q}(u)\right| \leq \frac{F^M_{\phi}(T, 2)}{\sqrt{\lambda}\left(F^M_{\phi}(T, 3)\right)^{3/2}}$$

Proof. This result is consequence of Theorem 2.19. □

Theorem 45. *Assume that* $\phi(x) + \psi(x) \leq K$ *for all* $x \in \mathbb{R}^d$, *then*

$$\mathbf{P}\left(J_T(\omega^M, T) > \mathbf{E}\left[J_T(\omega^M, T)\right] + u\right) \leq \exp\left\{-\frac{T^2K^2}{\lambda F^M_{\phi+\psi}(T, 2)} g\left(\frac{uTK}{F^M_{\phi+\psi}(T, 2)}\right)\right\}$$

for all $u > 0$.

Proof. The proof is similar to the proof of Theorem 37, and it is the consequence of Corollary 2. □

By setting $\phi(x) = 0$ or $\psi(x) = 0$ in the above theorem, we can derive upper bounds on the distribution of $J_A(\omega^M, T)$ and $J_B(\omega^M, T)$:

Corollary 7. *Assume that* $\phi(x) \leq K$ *for all* $x \in \mathbb{R}^d$, *then for any* $u > 0$,

$$\mathbf{P}\left(J_A(\omega^M, T) > \mathbf{E}\left[J_A(\omega^M, T)\right] + u\right) \leq \exp\left\{-\frac{T^2K^2}{\lambda F^M_{\phi}(T, 2)} g\left(\frac{uTK}{\lambda F^M_{\phi}(T, 2)}\right)\right\}.$$

Assume that $\psi(x) \leq K$ *for all* $x \in \mathbb{R}^d$, *then for any* $u > 0$,

$$\mathbf{P}\left(J_B(\omega^M, T) > \mathbf{E}\left[J_B(\omega^M, T)\right] + u\right) \leq \exp\left\{-\frac{T^2K^2}{\lambda F^M_{\psi}(T, 2)} g\left(\frac{uTK}{\lambda F^M_{\psi}(T, 2)}\right)\right\}.$$

7.5 Special cases

In this section we consider some special mobility model M.

7.5.1 Completely aimless mobility model

Consider the completely aimless mobility model M with constant speed, i.e $M(t) = tv$ where $|v| = constant$ and the direction of v is uniformly distributed.

Lemma 46. *Let $f(x)$ be a positive measurable function on $\mathbb{R}^d$ such that $f(x) = 0$ for $x \in R^d/C$, $f(x) \leq c_1$ for all $x \in C$ and $f(x) \geq c_2$ for all $x \in C/B(o, \frac{R_1}{4})$ where $c_1, c_2 > 0$ are constant then*

$$F_n^M(f,T) = \Theta\left(\frac{1}{|v|^{n-1}}\right), |v| \to \infty$$

and $F_n^M(f,T) = \Theta(T), T \to \infty$ for $n \geq 2$.

Proof. (see Figure 7.2) Assume that $T \geq \frac{2R}{|v|}$. Let $C' = B(0, \frac{3R_1}{4})/B(0, \frac{R_1}{2})$ and we note that if $t \leq \frac{R_1}{4|v|}$ and $x \in C'$ then $x + tv \in C/B(o, \frac{R_1}{4})$. As a consequence,:

$$\begin{aligned}
F_n^M(f,T) &\geq c_2^n \mathbf{E}\left[\int_{C'} \mathrm{d}x \int_0^{T-\frac{R_1}{4|v|}} \mathrm{d}t_1 \int_{t_1}^{t_1+\frac{R_1}{4|v|}} \mathrm{d}t_2 \cdots \int_{t_1}^{t_1+\frac{R_1}{4|v|}} I(t_1)\cdots I(t_n)\ \mathrm{d}t_n\right] \\
&= c_2^n l_d(C') \int_0^{T-\frac{R_1}{4|v|}} \mathrm{d}t_1 \int_{t_1}^{t_1+\frac{R_1}{4|v|}} \mathrm{d}t_2 ... \int_{t_1}^{t_1+\frac{R_1}{4|v|}} \mathbf{P}\left(I(t_1) = \cdots = I(t_n) = 1\right)\ \mathrm{d}t_n \\
&\geq c_2^n l_d(C') \left(T - \frac{R_1}{4\,|v|}\right) \int_0^{\frac{R_1}{4|v|}} \mathrm{d}t_2 ... \int_0^{\frac{R_1}{4|v|}} \mathbf{P}\left(I(t) = 1 \forall t \in [0, \frac{R_1}{4\,|v|})\right)\ \mathrm{d}t_n \\
&= c_2^n l_d(C') \left(T - \frac{R_1}{4\,|v|}\right) \left(\frac{R_1}{4\,|v|}\right)^{n-1} \frac{\pi_1}{\mathbf{E}\,[U]} \int_{\frac{R_1}{4|v|}}^{\infty} \mathbf{P}\left(U > t\right)\ \mathrm{d}t.
\end{aligned}$$

Similarly, note that for $|t| \geq \frac{2R}{|v|}$ then for all x, at least one of two points x or $x + vt$ must be outside the cell, thus

$$\begin{aligned}
F_n^M(f,T) &\leq c_1^n \mathbf{E}\left[\int_C \mathrm{d}x \int_0^T \mathrm{d}t_1 \int_{\left(t_1-\frac{2R}{|v|}\right)^+}^{\left(t_1+\frac{2R}{|v|}\right)\wedge T} \mathrm{d}t_2 \cdots \int_{\left(t_1-\frac{2R}{|v|}\right)^+}^{\left(t_1+\frac{2R}{|v|}\right)\wedge T} I(t_1)...I(t_n)\ \mathrm{d}t_n\right] \\
&\leq c_1^n l_d(C) \left(T - \frac{2R}{|v|}\right) \left(\frac{4R}{|v|}\right)^{n-1}.
\end{aligned}$$

Remarking that $\frac{1}{\mathbf{E}[V]} \int_{\frac{R_1}{4|v|}}^{\infty} \mathbf{P}\left(V > t\right)\ \mathrm{d}t \to 1$ as $|v| \to \infty$, we obtain the desired result. □

Theorem 47. *Consider the completely aimless mobility model M with constant speed $|v|$ then*

1. *$\mathbf{V}\left[J_A(\omega^M, T)\right]$ and $\mathbf{V}\left[J_T(\omega^M, T)\right]$ decay as $\Theta(\frac{1}{|v|})$ as $|v| \to \infty$ and decay as $O(T)$ as $T \to \infty$. The ratios $\frac{\sqrt{\mathbf{V}[J_A(\omega^M,T)]}}{\mathbf{E}[J_A(\omega^M,T)]}$ and $\frac{\sqrt{\mathbf{V}[J_T(\omega^M,T)]}}{\mathbf{E}[J_T(\omega^M,T)]}$ decay as $\Theta(\frac{1}{\sqrt{|v|}})$ as $|v| \to \infty$ and $\Theta(\frac{1}{\sqrt{T}})$ as $T \to \infty$.*

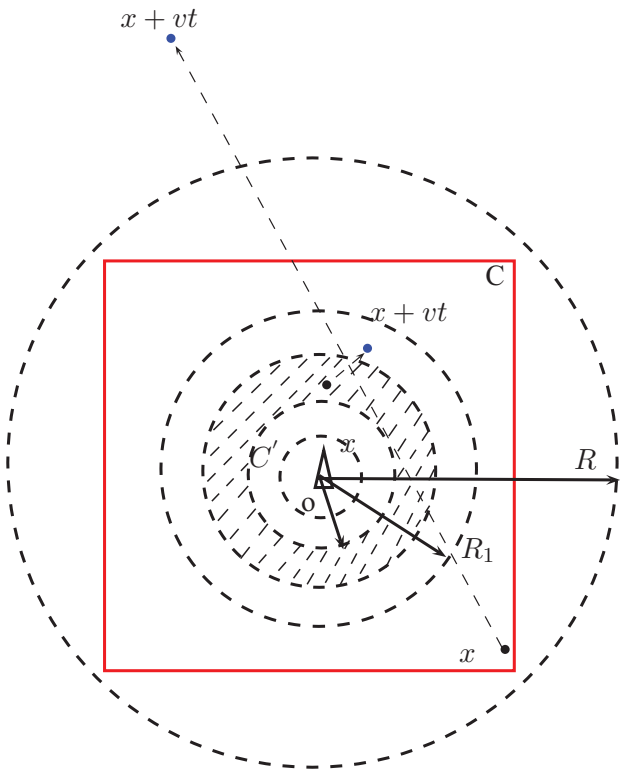


Figure 7.2: Illustration of the proof of Theorem 47.

2. *The error bound of Gaussian approximation in Theorem 44 decays as* $\Theta(|v|^2)$ *as* $|v| \to \infty$ *and decays as* $\Theta(\frac{1}{\sqrt{T}})$ *as* $T \to \infty$.

Proof. From the assumption 2 we have $\phi(x) \leq c_1$ for all $x \in C$, $\phi(x) \geq c_2$ for all $x \in C/B(o, \frac{R_1}{4})$ and $0 \leq \psi(x) \leq c_3$ for all $x \in C$ for some finite positive constants c_1, c_2, c_3. Now, according to Theorem 43:

$$\lambda F_{\phi}^{M}(T,n) = \mathbf{V}\left[J_A(\omega^M,T)\right] \leq \mathbf{V}\left[J_T(\omega^M,T)\right] \leq \lambda F_{\phi+\psi}^{M}(T,n).$$

The results then follow from Lemma 46. □

We also see that, if $|v|$ is small, the variance of $J_T(\omega^M, T)$ is proportional to $\frac{T}{|v|}$ while in the motionless case, it is $\Theta(T^2)$. We also notice that mobility makes the Gaussian approximation of J_A more accurate when T is large as the bound decays as $\Theta(\frac{1}{\sqrt{T}})$ instead of $\Theta(1)$ in the motionless case. In the motionless case the position of users are always fixed over time, only their state change, thus the configuration of active users can take only some possible values on $\Omega^{\mathbb{R}^d}$. So it is intuitive that one cannot guarantee that the Gaussian approximation is good if T is large. On the contrary, in the mobility case, the configuration of active users can take all possible values on $\Omega^{\mathbb{R}^d}$. When T grows larger, it take more values. Thus, Gaussian approximation is better when T grows larger. Quite surprisingly, when $|v|$ is large, the variance of J_A tends to 0 but the bound on Gaussian approximation does not decrease.

Remark 2. *From the above proof and using the properties of Bell polynomial, we can prove that* $\mathbf{c}_3\left[J_A(\omega^M,T)\right] = \Theta(\frac{1}{|v|^2})$, $\mathbf{c}_4\left[J_A(\omega^M,T)\right] = \Theta(\frac{1}{|v|^2})$, $\mathbf{c}_5\left[J_A(\omega^M,T)\right] = \Theta(\frac{1}{|v|^3})$,...

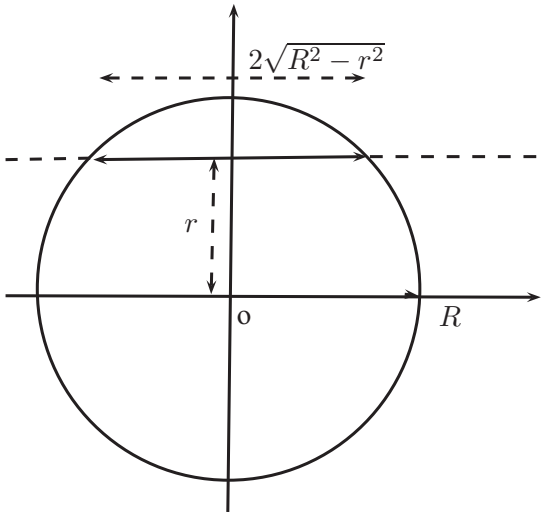


Figure 7.3: Illustration of the proof of Lemma 48.

7.5.2 Always on users

We now consider the following special case: users are always ON, i.e $I(t) = 1$ for all t. We always assume the mobility of users. The configuration of users at time t is

$$\omega_t^M = \delta_{X_i + M_i(t)}.$$

In this case, the analysis is simpler than in the ON-OFF case and the results obtained in the previous section can be inherited.

Let

$$H_n^M(f,u) = \int_{\mathbb{R}^d} \mathbf{E}\left[\left(\int_0^u f(x+M(t))\,\mathrm{d}t\right)^n\right]\,\mathrm{d}x \tag{7.8}$$

We see that $H_n^M(f,u)$ is a version of $\digamma_n^M(f,T)$ for $I(t) = 1, t \in \mathbb{R}$. In particular, the moments of $J_A(\omega^M, T)$ is given as

$$\begin{aligned}
\mathbf{m}_n\left[J_A(\omega^M,T)\right] &= B_n(\lambda H_1^M(\phi,T), \lambda H_2^M(\phi,T), ..., \lambda H_n^M(\phi,T)) \leq \mathbf{m}_n\left[J_A(\omega,T)\right] \\
\mathbf{c}_n\left[J_A(\omega^M,T)\right] &= B_n(0, \lambda H_2^M(\phi,T), ..., \lambda H_n^M(\phi,T)) \leq \mathbf{c}_n\left[J_A(\omega,T)\right].
\end{aligned}$$

In the following lemma, we provide explicit expression for $H_n^M(f,T)$ in the case where $d = 1$ or 2, $f(x) = a\mathbf{1}_{\{|x|\leq R\}}$:

Lemma 48. *1. If $d = 1$, $C = [-R, R]$ and $f(x) = a\mathbf{1}_{\{|x|\leq R\}}$ with $a > 0$ then:*

$$H_n^M(f,u) = \begin{cases} 2Ru^n a^n - \frac{n-1}{n+1} u^{n+1} |v|\, a^n, & u \leq \frac{2R}{|v|}; \\ \frac{u(2R)^n}{|v|^{n-1}} a^n - \frac{n-1}{n+1} \frac{(2R)^{n+1}}{|v|^n} a^n, & u \geq \frac{2R}{|v|}. \end{cases} \tag{7.9}$$

2. If $d = 2$, $C = \mathbf{B}(o, R)$ and $f(x) = a\mathbf{1}_{\{|x|\le R\}}$ with $a > 0$ then:

$$\begin{aligned} H_n^M(f,u) &= \frac{2u(2R)^n U_n(r_0)}{|v|^{n-1}}a^n - \frac{2(n-1)}{n+1}\frac{(2R)^{n+1}U_{n+1}(r_0)}{|v|^n}a^n \\ &\quad +4u^n R^2(U_1(1) - U_1(r_0))a^n - \frac{2(n-1)}{n+1}u^{n+1}R(1-r_0)\,|v|\,a^n \end{aligned}$$

if $u \le \frac{2R}{|v|}$ and

$$H_n^M(f,u) = \frac{2u(2R)^n U_n(1)}{|v|^{n-1}}a^n - \frac{2(n-1)}{n+1}\frac{(2R)^{n+1}U_{n+1}(1)}{|v|^n}a^n$$

if $u \ge \frac{2R}{|v|}$ where $U_n = \int_0^1 \left(1-r^2\right)^{\frac{n}{2}}\ dr$ and $r_0 = \sqrt{1 - \frac{u^2|v|^2}{(2R)^2}}$.

Proof. 1) We can assume that $a = 1$. We have,

$$\begin{aligned} H^M(f,u) &= \int_{-\infty}^{\infty} \mathbf{E}\left[\left(\int_0^u \mathbf{1}_{\{|x+vt|\le R\}}\,\mathrm{d}t\right)^n\right]\,\mathrm{d}x \\ &= \int_{-\infty}^{\infty}\left(\int_0^u \mathbf{1}_{\{|x+|v|t|\le R\}}\,\mathrm{d}t\right)^n\,\mathrm{d}x \\ &= \int_{-\infty}^{\infty}\mathrm{d}x\int_{[0,u)^n}\mathbf{1}_{\{|x+|v|t_1|,\ldots,|x+|v|t_n|\le R\}}\,\mathrm{d}t_1\ldots\,\mathrm{d}t_n \\ &= \int_{[0,u)^n}\mathrm{d}t_1\ldots\,\mathrm{d}t_n\int_{-\infty}^{\infty}\mathbf{1}_{\{|x+|v|t_1|,\ldots,|x+|v|t_n|\le R\}}\,\mathrm{d}x \\ &= \int_{[0,u)^n}(2R - |v|\,(\max\{t_1,t_2,\ldots,t_n\} - \min\{t_1,t_2,\ldots,t_n\}))^+\,\mathrm{d}t_1\ldots\,\mathrm{d}t_n \\ &= n!\int_0^u \mathrm{d}t_1\int_{t_1}^u \mathrm{d}t_2\ldots\int_{t_{n-1}}^u (2R - |v|\,(t_n - t_1))^+\,\mathrm{d}t_n \\ &= n(n-1)\int_0^u \mathrm{d}t_1\int_{t_1}^u (2R - |v|\,(t_n - t_1))^+\,(t_n - t_1)^{n-2}\,\mathrm{d}t_n. \end{aligned}$$

By some elementary manipulations, the last integral can be easily computed and it is equal to the LHS of equation (7.9).

2) We will use 1) to prove 2) (see figure 7.3). We also assume that $a = 1$. Firstly we note that the direction of v does not make any impact, so without loss of generality we assume that v follows the direction of the vector $(1, 0)$. We then have:

$$\begin{aligned} H^M(f,u) &= \int_C \mathbf{1}_{\{x+vt_2,\ldots,x+vt_n\in C\}}\,\mathrm{d}x \\ &= 2\int_0^R \mathrm{d}r\int_{-\sqrt{R^2-r^2}}^{\sqrt{R^2-r^2}}\mathbf{1}_{\{|r_1+|v|t_2|,\ldots,|r_1+|v|t_n|\le\sqrt{R^2-r^2}\}}\,\mathrm{d}r_1 \\ &= 2\int_0^R g_n(r)\,\mathrm{d}r. \end{aligned}$$

Here $g_n(r)$ can be calculated by applying 1). If $u \ge \frac{2R}{|v|}$ then we have

$$g_n(r) = 2\sqrt{R^2 - r^2}u^n - \frac{n-1}{n+1}u^{n+1}\,|v|\,.$$

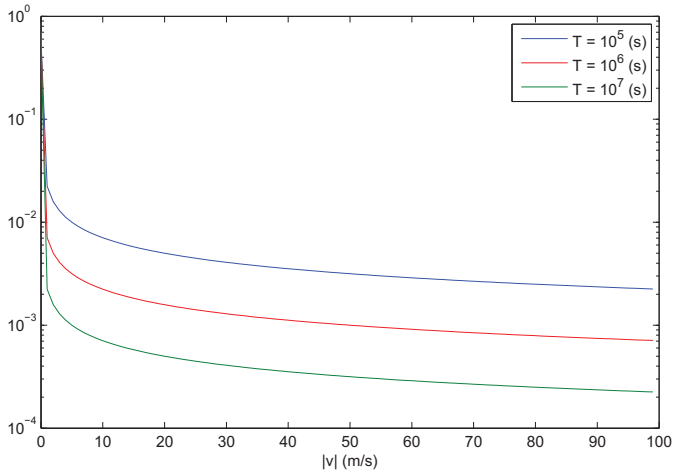


Figure 7.4: Influence of user's speed on the ratio $\frac{\sqrt{\mathbf{V}[J_A(\omega^M,T)]}}{\mathbf{E}[J_A(\omega^M,T)]}$

If $u \leq \frac{2R}{|v|}$ then

$$g_n(r) = \begin{cases} \frac{u(2\sqrt{R^2-r^2})^n}{|v|^{n-1}} - \frac{n-1}{n+1}\frac{(2\sqrt{R^2-r^2})^{n+1}}{|v|^n}, & 0 \leq r \leq r_0; \\ 2\sqrt{R^2-r^2}u^n - \frac{n-1}{n+1}u^{n+1}|v|, & R \geq r \geq r_0. \end{cases}$$

This concludes the proof. □

From the above lemma, we see that in the case where $\phi(x) = constant$, the low (and high) mobility regime can be characterized as $T \leq \frac{2R}{|v|}$ (and $T \geq \frac{2R}{|v|}$).

For a numerical example we choose the simplest case where we have exact expressions: $d = 1$, $\lambda = 0.02$ (users/m) $2R = 100(m)$, $\phi(x) = 1$ and $M(t) = vt$ with $v = |v|$ or $v = -|v|$ with equal probability and we consider only J_A. In the figure 7.4 we plot the ratio $\frac{\sqrt{\mathbf{V}[J_A(\omega^M,T)]}}{\mathbf{E}[J_A(\omega^M,T)]}$ in function of $|v|$ in the case $T = 10^6(x) \sim 11(\text{days})$ and $T = 10^7(s) \sim 115(\text{days})$. As expected it is a decreasing function of $|v|$. We see that in the low mobility regime, the ratio decreases very fast. For the motionless case, $|v| = 0(m/s)$, the ratio in all three cases is the same and equal to $\frac{1}{\sqrt{\lambda R}} = 0.7071$ while for $|v| = 1(m/s)$, the ratio is 0.0022 for $T = 10^7(s)$ and 0.0071 for $T = 10^6(s)$.

7.6 Summary and Conclusion

Throughout this chapter, we have assumed that each user is associated with an ON-OFF process of activity. We have derived analytical expressions for the distribution of energy consumed by a base station. We have found that, with or without mobility, the base station is expected to consume the same amount of energy in average. We have proved that mobility reduced moments of the additive part of energy. We have also proved that high mobility leads the variance of energy to 0. These results are strong since they hold true for any mobility model. In the case of completely aimless mobility model, we have characterized the convergence rate to 0 of the variance, which is $\frac{1}{|v|}$.

Chapter 8

Generalized Glauber model

Contents

8.1 Introduction 99
8.2 Model description and main results 100
8.2.1 Generalized Glauber dynamic 100
8.2.2 Generalized Glauber dynamic with mobility 103
8.3 Analysis in no mobility case 105
8.3.1 Proof of Theorem 49 110
8.3.2 Proof of theorem 50 110
8.3.3 Proof of theorem 51 111
8.4 Impact of mobility 111
8.4.1 Lemmas 111
8.4.2 Proof of Theorem 54 113
8.4.3 Special case: Completely aimless mobility model 114
8.5 Conclusion 116

8.1 Introduction

The previous chapter considers users presented by a random configuration on d dimension, each user is associated with an ON-OFF process of activity to study the distribution of consumed energy. We consider in this chapter another model called generalized Glauber dynamic.

Glauber dynamic can be described as following. It starts at $t = 0$ with a configuration on a bounded domain D. Each point of this configuration has an exponential life time, after the life time the point disappears. In parallel, there is new arriving points. The arriving time follows a Poisson point process on $\mathbb{R}^+$ and points are randomly placed on D according to some distribution. Glauber dynamic has been already successfully applied to study the blocking rate of cellular network. For this it requires that the sojourn time is exponentially distributed so that the system can be modeled as a Markov process that takes value in the space of finite point measures. The author of [54] call it spatial Markov queueing process. In queueing theory, under many situations it can be argued that the blocking rate does not depend on the distribution of sojourn time but only on its mean. This property is well known as insensibility property. On the contrary, the distribution of

Symbols	Definition, Physical meaning
$\mathrm{d}\Lambda(x)$	A $\sigma-$finite Radon measure on $\mathbb{R}^d$
S	Generic sojourn time
$L^{\Lambda,S}$	Space-Time Poisson point process of calls (no mobility)
N_t	$\sum_{i\geq 1}\mathbf{1}_{\{T_i\leq t<T_i+S_i\}}\delta_{X_i}$, Poisson point process of active users at time t (no mobility)
$L^{\lambda\ \mathrm{d}x,S,M}$	Space-Time-Movement Poisson point process of calls (with mobility)
N_t^M	$\sum_{i\geq 1}\mathbf{1}_{\{T_i\leq t<T_i+S_i\}}\delta_{X_i+M(t-T_i)}$, Poisson point process of active users at time t (with mobility)
$\Gamma_n^M(f,T)$	$\int_{-\infty}^{T}\ \mathrm{d}t\int_0^\infty p_S(s)H_n^M(f,(t+s)^+\wedge T-t^+)\ \mathrm{d}s$

Table 8.1: Notations and parameters.

energy consumed during certain duration depends heavily on the distribution of sojourn time, as showed latter in this chapter.

We consider in this chapter a more general scenario and so we call it generalized Glauber dynamic because of the following arguments. Firstly the domain we consider is no longer bounded but it can be, for instance, $\mathbb{R}^d$. Secondly the system starts at $-\infty$. Thirdly we no longer assume that the sojourn time is exponential distributed but we only assume that the sojourn time is positive and has the finite mean. Furthermore we use the Poisson point process approach instead of Markov process approach.

This chapter is organized as follows. Section 8.2 describes the model and presents main results. Section 8.3 presents proofs in the no mobility case. In the section 8.4 the impact of mobility is treated.

Important notations and parameters used in this chapter are summarized in the table 8.1.

8.2 Model description and main results

8.2.1 Generalized Glauber dynamic

Let Λ be a $\sigma-$finite Radon measure on $\mathbb{R}^d$, absolutely continuous with respect to the Lebesgue measure with density p_Λ. Let $L^{\Lambda,S}$ be the Poisson point process of intensity measure given by

$$\mathrm{d}\nu(t,s,x) = \ \mathrm{d}t\times p_S(s)\ \mathrm{d}s\times\ \mathrm{d}\Lambda(x)\cdot$$

where $p_S(s)$ is a probability density function of a positive random variable S with finite mean.

A realization of this process, if $\Lambda(\mathbb{R}^d)<\infty$, can be obtained as follows. Let $N_A=(T_i, i\geq 0)$ be a Poisson point process of intensity $\Lambda(\mathbb{R}^d)$ on $\mathbb{R}$ and $((X_i,S_i), i\geq 0)$ be a sequence of i.i.d random variable, independent of N_A, such that

$$\mathrm{d}\mathbf{P}_{X_i}(x)=\frac{\mathrm{d}\Lambda(x)}{\Lambda(\mathbb{R}^d)}\ \text{and}\ \ \mathrm{d}F_{S_i}(s)=p_S(s)\ \mathrm{d}s\cdot$$

Then $L^{\Lambda,S}=\sum_{i\geq 0}\delta_{(T_i,X_i,S_i)}\cdot$

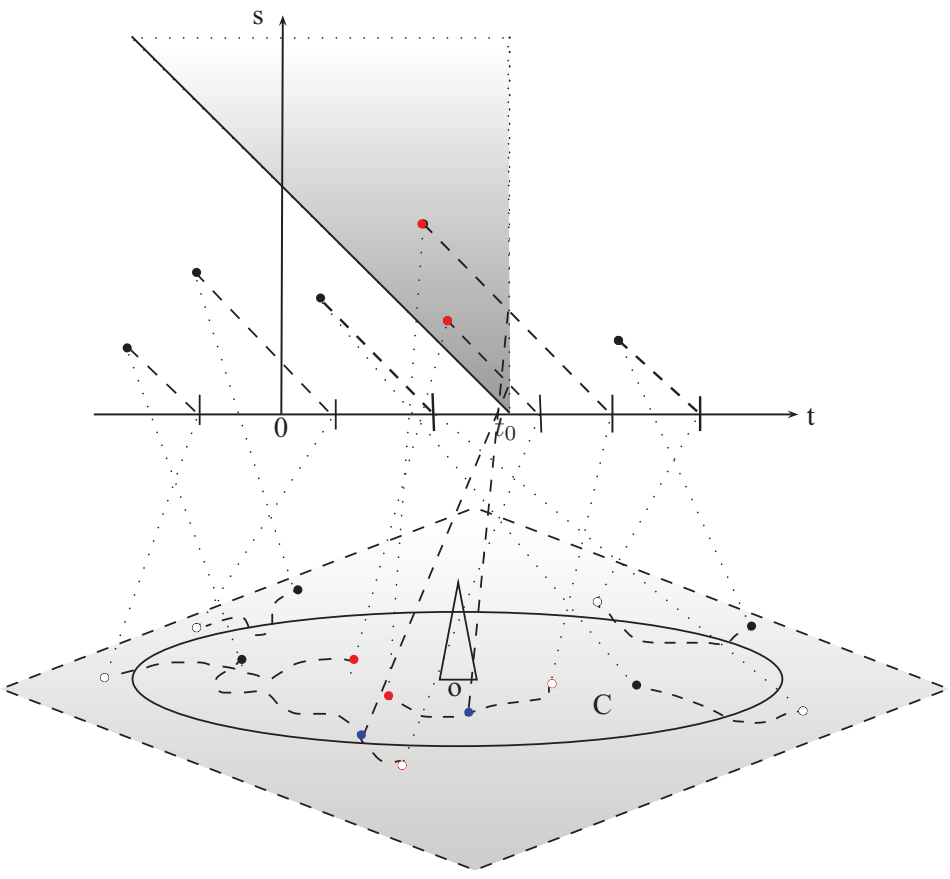


Figure 8.1: Generalized Glauber spatial dynamic, similar to a $M/G/\infty$ queue a user is characterized by an arrival time, a sojourn duration, however in our model he is also characterized by his position and his mobility process. Consequently there may be infinite users at a time t but the number of users in cell C is always finite.

In particular, for a bounded domain C, one can choose Λ as the Lebesgue measure restricted on C. If $\Lambda(\mathbb{R}^d) = \infty$, since Λ is $\sigma-$finite, there exists a sequence of compact sets $(K_k, k \geq 1)$ such that $\Lambda(K_k) \leq \infty$ and $\cup_k K_k = \mathbb{R}^d$, then $L^{\Lambda,S}$ is the weak limit of the sequence $(L^{\Lambda_k,S}, k \geq 1)$ where Λ_k is the restricted of Λ to K_k.

The configuration of active users at time t is

$$N_t = \sum_{i\geq 1} \mathbf{1}_{\{T_i \leq t < T_i + S_i\}} \delta_{X_i}.$$

Roughly speaking, in this model a user i arrives at time T_i at location X_i and stays in the system during S_i units of time.

From definitions in the chapter 6, for this configuration model, it follows that the total energy consumed between 0 and T is given by:

$$\begin{aligned} J_T(N,T) &= \sum_{i\geq 0} \mathbf{1}_{\{T_i \leq T\}} (((T_i + S_i)^+ \wedge T) - T_i^+)\phi(X_i) + \int_0^T \overline{\psi}(\|N_t\|)\ \mathrm{d}t \\ &= J_A(N,T) + J_B(N,T). \end{aligned}$$

Theorem 49. *Assume that $\Lambda(\mathbb{R}^d) < \infty$, the expectation of $J_T(N,T)$ is given by:*

$$\mathbf{E}\left[J_T(N,T)\right] = T\mathbf{E}\left[S\right] \int_{\mathbb{R}^d} \phi(x)\ d\Lambda(x) + T \int_0^\infty p_{\|N_0\|}(r)\overline{\psi}(r)\ dr, \tag{8.1}$$

where $p_{\|N_0\|}$ is the probability density function of $\|N_0\|$ and is given by:

$$p_{\|N_0\|}(r) = \frac{\mathbf{E}\left[S\right]\ d\Lambda(\overline{C}(r))}{dr} e^{-\mathbf{E}[S]\Lambda(\overline{C}(r))}. \tag{8.2}$$

The second order moment of $J_T(N,T)$ is given by:

$$\begin{aligned} \mathbf{m}_2\left[J_T(N,T)\right] &= \left(T \int_{\mathbb{R}^d} \phi(x)\ d\Lambda(x)\right)^2 + K_2(T) \int_{\mathbb{R}^d} \phi^2(x)\ d\Lambda(x) \\ &\quad + LHS\ of\ (8.13) + 2 * LHS\ of\ (8.11) + 2 * LHS\ of\ (8.14) \end{aligned}$$

where

$$\begin{aligned} K_n(T) &= \int_{-\infty}^T dt \int_0^\infty \left(\left((t+s)^+ \wedge T\right) - t^+\right)^n p_S(s)\ ds \\ &= \int_{-\infty}^T \mathbf{E}\left[\left(\left((t+S)^+ \wedge T\right) - t^+\right)^n\right]\ dt. \end{aligned}$$

In order to gain some insights on the behavior of $J_T(N,T)$, we use the concentration inequality for Poisson point process to obtain the following result:

Theorem 50. *Assume that $S \leq \beta_S$ (a.s) and $\phi(x) + \psi(x) \leq \beta_B$ for any $x \in \mathbb{R}^d$ with $\beta_S, \beta_B > 0$. Let*

$$\beta(T) = (\beta_S \wedge T)\beta_B$$

and

$$\alpha^2(T) = K_2(T) \int_{\mathbb{R}^d} (\phi(x) + \psi(x))^2\ d\Lambda(x)$$

then

$$\mathbf{P}(J_T(N,T) \geq \alpha) \leq \exp\left\{ -\left(\frac{\alpha(T)}{\beta(T)}\right)^2 g\left(\frac{L - \mathbf{E}\left[J_T(N,T)\right])\beta(T)}{\alpha^2(T)}\right)\right\}. \tag{8.3}$$

where $g(u) = (1+u)\ln(1+u) - u$.

If we count only the number of users in the cell C, the system can be seen as a $M/G/\infty$ queue. The returning time to empty state of this queue always has finite mean. Consequently, the time varying configuration process N is a regenerative process since it can be split into i.i.d cycles. It is well known that under appropriate conditions, for a general model of power consumption P_G, the consumed energy $J_G(N,T) = \int_0^T P_G(N_t)\ \mathrm{d}t$ can be well approximated by a Gaussian random variable as $T \to \infty$. Unfortunately, we can only find an error bound on Gaussian approximation of $J_A(N,T)$, as follows:

Theorem 51. *We have:*

$$\left|\mathbf{P}\left(J_A(N,T) \geq u\right) - \overline{Q}\left(\frac{u - \mathbf{E}\left[J_A(N,T)\right]}{\sqrt{\mathbf{V}\left[J_A(N,T)\right]}}\right)\right| \leq \frac{K_3(T)\int_{\mathbb{R}^d}\phi^3(x)\ d\Lambda(x)}{(K_2(T)\int_{\mathbb{R}^d}\phi^2(x)\ d\Lambda(x))^{3/2}}$$

for any $u > 0$.

As showed later in Lemma 60, $K_n(T) \sim T\mathbf{m}_n[S]$, thus the bound becomes

$$\frac{\mathbf{m}_3[S]\int_{\mathbb{R}^d}\phi^3(x)\ \mathrm{d}\Lambda(x)}{\sqrt{T}\left(\mathbf{m}_2[S]\int_{\mathbb{R}^d}\phi^2(x)\ \mathrm{d}\Lambda(x)\right)^{3/2}}$$

when T is large. In contrary to the ON-OFF model without mobility where the bound decays as $O(1)$, in this model the bound decays as $\Theta\left(\frac{1}{\sqrt{T}}\right)$ as $T \to \infty$.

Now, if $\mathrm{d}\Lambda(x) = \lambda\ \mathrm{d}x$ then the bound becomes:

$$\frac{K_3(T)\int_{\mathbb{R}^d}\phi^3(x)\ \mathrm{d}x}{\sqrt{\lambda}(K_2(T)\int_{\mathbb{R}^d}\phi^2(x)\ \mathrm{d}x)^{3/2}}$$

which decays as $\Theta(\frac{1}{\sqrt{\lambda}})$.

8.2.2 Generalized Glauber dynamic with mobility

From now on, when considering mobility, we will make the assumption that $\mathrm{d}\Lambda(x) = \lambda\ \mathrm{d}x$.

The model is the same as the above Generalized Glauber dynamicmodel, except that each user moves during its sojourn. The mobility model is already described in the chapter 6. Let $M_1(t), M_2(t), ...$ be independent versions of $M(t)$ and be the movement of users $1, 2, ...$ respectively. In other words, the position of user i during at time $t \in [T_i, T_i + S_i)$ is $X_i + M(t - T_i)$. The marked point process $L^{\lambda\ \mathrm{d}x,S,M} = ((T_i, S_i, X_i, (M_i(t), t \in \mathbb{R})))_{i=1}^{\infty}$ is Poisson point process on $\mathbb{R} \times \mathbb{R} \times \mathbb{R}^d \times D([0,\infty), \mathbb{R}^d)$ due to the independent marking property. Its measure intensity is:

$$\mathrm{d}\underline{\nu}(t, s, x, (m(t), t \in \mathbb{R})) = \ \mathrm{d}t \times p_S(s)\ \mathrm{d}s \times\ \mathrm{d}\Lambda(x)\ \mathrm{d} \times \mathbf{P}_M(m)\cdot$$

At time t, the configuration of active users is

$$N^M = \sum_{i \geq 1} \mathbf{1}_{\{T_i \leq t < T_i + S_i\}} \delta_{X_i + M_i(t - T_i)}\cdot$$

Lemma 52. *N^M is a Poisson point process of intensity measure $\lambda \mathbf{E}[S]\ dx$ for all t.*

The proof of the above lemma is given in the subsection 8.4.1.
Let

$$\Gamma_n^M(f,T) = \int_{-\infty}^{T} \mathrm{d}t \int_0^{\infty} p_S(s) H_n^M(f,(t+s)^+ \wedge T - t^+)\ \mathrm{d}s \tag{8.4}$$

with $u \in \mathbb{R}^+$ and $f : \mathbb{R}^d \to \mathbb{R}^+$ such that $f(x) = 0$ in $\mathbb{R}^d/C$ and $H_n^M(f,u)$ is defined in equation (7.8).

From the above lemma, we immediately deduce that:

Theorem 53. *For any power consumption model P_G and mobility model M, we have $\mathbf{E}\left[J_G(N^M,T)\right] = \mathbf{E}\left[J_G(N,T)\right]$. In particular $\mathbf{E}\left[J_A(N^M,T)\right] = \mathbf{E}\left[J_A(N,T)\right]$, $\mathbf{E}\left[J_B(N^M,T)\right] = \mathbf{E}\left[J_B(N,T)\right]$ and $\mathbf{E}\left[J_T(N^M,T)\right] = \mathbf{E}\left[J_T(N,T)\right]$.*

We obtain the same result as in the previous chapter. In fact, mobility makes the same impact on the consumed energy in both model, as we will investigate now.

Theorem 54. *We have,*

$$\mathbf{E}\left[\exp\left\{\alpha J_A\left(N^M,T\right)\right\}\right] \quad \leq \quad \mathbf{E}\left[\exp\left\{\alpha J_A\left(N,T\right)\right\}\right]$$

for any $\alpha \in \mathbb{R}$ and

$$\begin{aligned} \mathbf{c}_n\left[J_A\left(N^M,T\right)\right] &\leq \mathbf{c}_n\left[J_A\left(N,T\right)\right] \\ \mathbf{m}_n\left[J_A\left(N^M,T\right)\right] &\leq \mathbf{m}_n\left[J_A\left(N,T\right)\right]. \end{aligned}$$

for all $n \geq 2$. If M satisfies the property T then

$$\mathbf{c}_n\left[J_A\left(N^{M/\epsilon},T\right)\right] \to 0 \text{ and } \mathbf{m}_n\left[J_A\left(N^{M/\epsilon},T\right)\right] \to \left(\lambda \mathbf{E}[S] \int_{\mathbb{R}^d} \phi(x)\ dx\right)^n$$

and

$$\mathbf{V}\left[J_B(N^{M/\epsilon},T)\right], \mathbf{V}\left[J_T\left(N^{M/\epsilon},T\right)\right] \to 0 \text{ as } \epsilon \to 0.$$

Furthermore, if $\phi(x) = a\mathbf{1}_{\{x \in C\}}$ $(a > 0)$ and M satisfies the property T then $\mathbf{c}_n\left[J_A\left(N^{M/\epsilon},T\right)\right]$ and $\mathbf{m}_n\left[J_A\left(N^{M/\epsilon},T\right)\right]$ are decreasing functions of ϵ.

A bound for Gaussian approximation of $J_A(N^M,T)$ is found as follows

Theorem 55. *We have*

$$\left|\mathbf{P}\left(J_A(N^M,T) \geq u\right) - Q\left(\frac{u - \mathbf{E}\left[J_A(N^M,T)\right]}{\mathbf{V}\left[J_A(N^M,T)\right]}\right)\right| \leq \frac{\Gamma_2^M(\phi,T)}{\sqrt{\lambda}(\Gamma_3^M(\phi,T))^{3/2}}$$

for any $u > 0$. Here $\Gamma_n^M(\phi,T)$ is defined in equation (8.4).

When T is large, the bound becomes:

$$\frac{\mathbf{E}\left[H_2^M(\phi,S)\right]}{\sqrt{\lambda T}\mathbf{E}\left[H_3^M(\phi,S))^{3/2}\right]}.$$

Using the concentration inequality (corollary 2) we obtain the following bound for the distribution of $J_T(N^M,T)$. The proof is similar to that of theorem 50 so we omit it here.

Theorem 56. *Assume that $S \leq \beta_S$ (a.s) and $\phi(x) + \psi(x) \leq \beta_B$ for any $x \in \mathbb{R}^d$ with $\beta_S, \beta_B > 0$. Let*

$$\beta(T) = (\beta_S \wedge T)\beta_B$$

then

$$\mathbf{P}(J_T(N^M, T) \geq u + \mathbf{E}\left[J_T(N^M, T)\right]) \leq \exp\left\{-\left(\frac{\lambda\Gamma_2^M(\phi+\psi, T)}{\beta(T)}\right)^2 g\left(\frac{u\beta(T)}{\lambda\Gamma_2^M(\phi+\psi, T)}\right)\right\}. \tag{8.5}$$

where $g(u) = (1+u)\ln(1+u) - u$.

8.3 Analysis in no mobility case

In this section we present calculations and proof in the case where users do not move during their sojourn. Let S_e be the random variable with the associated stationary-excess (or equilibrium-residual-lifetime) CDF ([55], [56])

$$\overline{F}_{S_e}(s) = \frac{\int_s^\infty \overline{F}_S(s_1)\ \mathrm{d}s_1}{\mathbf{E}\left[S\right]}.$$

Its PDF,MGF and n^{th} moments are given by

$$p_{S_e}(s) = \frac{\overline{F}_S(s)}{\mathbf{E}\left[S\right]},$$

$$\mathbf{E}\left[e^{-tS_e}\right] = \frac{1 - \mathbf{E}\left[e^{-tS}\right]}{t\mathbf{E}\left[S\right]},$$

$$\mathbf{m}_n\left[S_e\right] = \frac{\mathbf{m}_{n+1}\left[S\right]}{(n+1)\mathbf{E}\left[S\right]}.$$

It is easily seen that if $S \sim Exponential(\mu)$ then S_e follows the same distribution. We also note that if $S \leq u$ a.s. then $S_e \leq u$ a.s. .

Lemma 57. *For any $t_0 \in \mathbb{R}$, N_t is a Poisson point process on $\mathbb{R}^d$ with intensity measure $\mathbf{E}\left[S\right]\ d\Lambda(x)$. Given a realization of N_t, the residual sojourn time of users are independent and follow the same distribution as that of S_e.*

Moreover, the probability distribution function of $\|N_t\|$ is given by:

$$\mathbf{P}(\|N_t\| > r) = e^{-\mathbf{E}[S]\Lambda(\overline{C}(r)))} \tag{8.6}$$

and its probability density function is given by:

$$p_{\|N_t\|}(r) = \frac{\mathbf{E}\left[S\right]\ d\Lambda(\overline{C}(r))}{dr} e^{-\mathbf{E}[S]\Lambda(\overline{C}(r)))}. \tag{8.7}$$

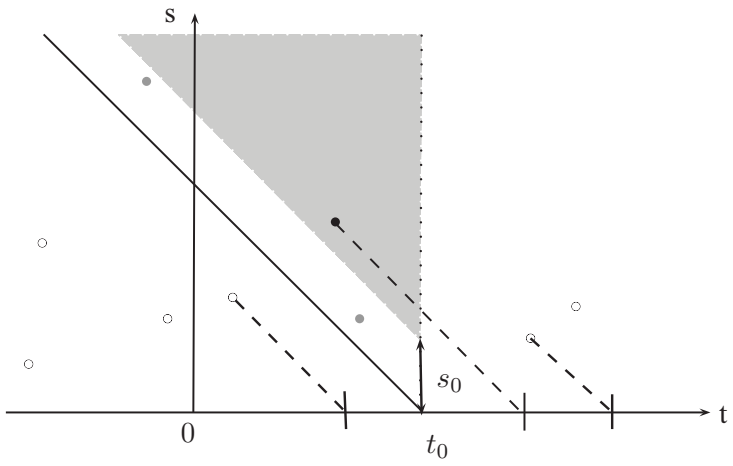


Figure 8.2: Illustration of the proof of lemma 57.

Proof. As above defined, the configuration of active users at t, associated with their residual service time is

$$\sum_{i\geq 1} \mathbf{1}_{\{T_i\leq t_0<T_i+S_i\}}\delta_{(X_i,S_i-(t_0-T_i))}.$$

By displacement theorem, this is a Poisson point processwith intensity measure characterized by

$$\begin{aligned} intensity(D\times(s_0,\infty)) &= \int_0^\infty \mathrm{d}t \int_0^\infty p_S(s)\mathbf{1}_{\{t\leq t_0, s>s_0+t-t_0\}}\,\mathrm{d}s \int_D \mathrm{d}\Lambda(x) \\ &= \int_{t_0}^\infty \overline{F}_S(s_0+t-t_0)\,\mathrm{d}t\Lambda(D) \\ &= \int_0^\infty \overline{F}_S(s_0+t)\,\mathrm{d}t\Lambda(D) \\ &= \mathbf{E}\left[S\right]\Lambda(D)\overline{F}_{S_e}(s_0) \end{aligned}$$

for all measurable set $D\in\mathbb{R}^d$ and $s_0\geq 0$. This is exactly the same intensity of a independently marked Poisson point process with underlying intensity measure $\mathbf{E}\left[S\right]\ \mathrm{d}\Lambda(x)$ and the distribution of marks are the same as that of S_e. Thus, the lemma is proved.

□

Remark 3. *For a domain D such that $\Lambda(D)<\infty$, the dynamic of the number of users on D follows exactly the same as the dynamic of the $M/G/\infty$ queue with arrival rate $\Lambda(D)$ and service time distribution dF_S. Thus, the model can be called spatial $M/G/\infty$ queue.*

Lemma 58. *$N_{t_1}-N_{t_2}, N_{t_1}\cup N_{t_2}, N_{t_2}-N_{t_1}$ are 3 independent Poisson point processes of intensity measure $F_{S_e}(|t_2-t_1|)\mathbf{E}\left[S\right]\ d\Lambda(x)$, $\overline{F}_{S_e}(|t_2-t_1|)\mathbf{E}\left[S\right]\ d\Lambda(x)$ and $F_{S_e}(|t_2-t_1|)\mathbf{E}\left[S\right]\ d\Lambda(x)$ on $\mathbb{R}^d$, respectively.*

Proof. We note that, a user i is in $N_{t_1}-N_{t_2}, N_{t_1}\cup N_{t_2}, N_{t_2}-N_{t_1}$ if and only if the point (T_i,S_i) is in the domain I,II,III respectively. Thus, by thinning property, $N_{t_1}-N_{t_2}$ is

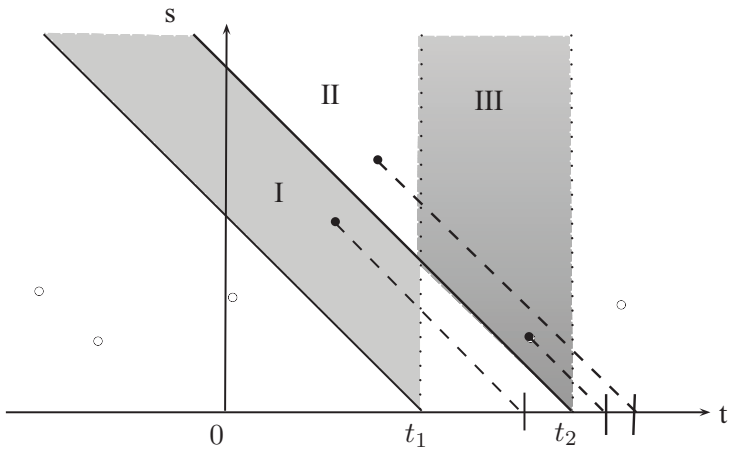


Figure 8.3: Illustration of the proof of lemma 58.

Poisson point process of intensity characterized by:

$$\begin{aligned} intensity(D) &= \Lambda(D)\int_{-\infty}^{t_1} \mathrm{d}t \int_{t_1-t}^{t_2-t} p_S(s)\ \mathrm{d}s \\ &= \Lambda(D)\int_0^{\infty} (\overline{F}_S(t) - \overline{F}_S(t+t_2-t_1))\ \mathrm{d}t \\ &= \mathbf{E}\left[S\right]\Lambda(D)\left(1 - \int_0^{\infty} \frac{\overline{F}_S(t+t_2-t_1)}{\mathbf{E}\left[S\right]}\ \mathrm{d}t\right) \\ &= \mathbf{E}\left[S\right]\Lambda(D)F_{S_e}(t_2-t_1) \end{aligned}$$

for all measurable set $D \in \mathbb{R}^d$. Therefore $N_{t_1} - N_{t_2}$ is a Poisson point process with intensity $\mathbf{E}\left[S\right]\overline{F}_{S_e}(t_2-t_1)\ \mathrm{d}\Lambda(x)$. Similarly $N_{t_1} \cup N_{t_2}, N_{t_2} - N_{t_1}$ are 2 Poisson point processes of intensity measure $F_{S_e}(t_2-t_1)\mathbf{E}\left[S\right]\ \mathrm{d}\Lambda(x)$ and $\overline{F}_{S_e}(t_2-t_1)\mathbf{E}\left[S\right]\ \mathrm{d}\Lambda(x)$ on $\mathbb{R}^d$, respectively. The independence between the three Poisson point process follows that fact that I,II and III are pairwise disjoint.

□

From the above lemma, we can see that the time varying process N is time reversible. It can be deduced from the time reversibility of a $M/G/\infty$ queue. Moreover, if $S \leq u$ a.s. then $S_e \leq u$ a.s. and N_{t_1} and N_{t_2} are independent for $|t_2 - t_1| > u$.

Theorem 59. *For $n \geq 1$ we have:*

$$\mathbf{m}_n\left[J_A(N,T)\right] = B_n\left(K_1(T)\int_{\mathbb{R}^d}\phi(x)\ d\Lambda(x), ..., K_n(T)\int_{\mathbb{R}^d}\phi^n(x)\ d\Lambda(x)\right)$$

and

$$\mathbf{c}_n\left[J_A(N,T)\right] = B_n\left(0, K_2(T)\int_{\mathbb{R}^d}\phi^2(x)\ d\Lambda(x), ..., K_n(T)\int_{\mathbb{R}^d}\phi^n(x)\ d\Lambda(x)\right)$$

In particular,

$$\mathbf{E}\left[J_A(N,T)\right] = T\mathbf{E}\left[S\right]\int_{\mathbb{R}^d}\phi(x)\ d\Lambda(x). \tag{8.8}$$

Proof. As $J_A(N,T)$ is a linear functional of $L^{\Lambda,S}$, we can apply the theorem 7.4. It is sufficient to note that:

$$\int_{\mathbb{R}\times\mathbb{R}\times\mathbb{R}^d} \left(\left(\left((t+s)^+ \wedge T\right) - t^+\right)\phi(x)\right)^n p_S(s)\,\mathrm{d}t\,\mathrm{d}s\,\mathrm{d}\Lambda(x) = K_n(T)\int_{\mathbb{R}^d}\phi^n(x)\,\mathrm{d}\Lambda(x).$$

□

Lemma 60. *We have the following properties:*

1. $K_n(T) = \mathbf{E}\left[(S\wedge T)^n(S\vee T) - \frac{n-1}{n+1}(S\wedge T)^{n+1}\right]$.
2. *Assume that* $\mathbf{m}_n[S] < \infty$ *then* $K_n(T) \sim T\mathbf{m}_n[S]$ *as* $T\to\infty$.

Proof. 1) We have:

$$\begin{aligned} K_n(T) &= \int_0^\infty p_S(s)\,\mathrm{d}s \int_{-\infty}^T \left(\left((t+s)^+\wedge T\right) - t^+\right)^n\,\mathrm{d}t \\ &= \int_0^\infty p_S(s)\,\mathrm{d}s \left(\int_{-\infty}^0 + \int_0^T\right)\left(\left((t+s)^+\wedge T\right)\right) - t^+)^n\,\mathrm{d}t \\ &= \int_0^\infty p_S(s)\,\mathrm{d}s \left(\int_{-s}^0 ((t+s)^+\wedge T)^n\,\mathrm{d}t + \int_0^T (((t+s)\wedge T) - t)^n\,\mathrm{d}t\right) \end{aligned}$$

By some simple manipulations we get:

$$\left(\int_{-s}^0 ((t+s)^+\wedge T)^n\,\mathrm{d}t + \int_0^T (((t+s)\wedge T) - t)^n\,\mathrm{d}t\right) = \begin{cases} s^nT - \frac{n-1}{n+1}s^{n+1}, & s\le T; \\ T^ns - \frac{n-1}{n+1}T^{n+1}, & T\le s. \end{cases}$$

Thus, 1) is proved.

2) We have

$$\begin{aligned} \frac{K_n(T)}{T} &= \mathbf{E}\left[\frac{(S\wedge T)^n(S\vee T)}{T} - \frac{\frac{n-1}{n+1}(S\wedge T)^{n+1}}{T}\right] \\ &\le \mathbf{E}[S^n] \end{aligned}$$

and $\lim_{T\to\infty}\frac{(S\wedge T)^n(S\vee T)}{T} - \frac{\frac{n-1}{n+1}(S\wedge T)^{n+1}}{T} = S^n$. Thus, by dominated convergence theorem we have $\lim_{T\to\infty}\frac{K_n(T)}{T} = \mathbf{m}_n[S]$. □

We see that, from the above lemma, when T goes larger, the "border effect" is negligible. Furthermore, we have

$$K_n(T) \sim T\mathbf{m}_n[S]\int_{\mathbb{R}^d}\phi^n(x)\,\mathrm{d}\Lambda(x) \ge T\left(\mathbf{E}[S]\right)^n\int_{\mathbb{R}^d}\phi^n(x)\,\mathrm{d}\Lambda(x). \tag{8.9}$$

That is to say, when T is large, among all positive random variable S having the same expectation, the constant one minimizes the moments of $J_A(N,T)$.

Lemma 61. *The joint distribution of* $(\|N_{t_1}\|, \|N_{t_2}\|)$ *is given as:*

$$F_{(\|N_{t_1}\|,\|N_{t_2}\|)}(u_1,u_2) = \left(1-e^{-\mathbf{E}[S]F_{S_e}(|t_2-t_1|)\Lambda(\overline{C}(u_1))}\right)\left(1-e^{-\mathbf{E}[S]F_{S_e}(|t_2-t_1|)\Lambda(\overline{C}(u_2))}\right)\times \\ \times\left(1-e^{-\mathbf{E}[S]\overline{F}_{S_e}(|t_2-t_1|)\Lambda(\overline{C}(u_1\vee u_2))}\right) \tag{8.10}$$

for all $t_1, t_2 \in \mathbb{R}$ *and* $u_1, u_2 > 0$.

The expectation of $J_B(N,T)$ *is given by:*

$$\mathbf{E}\left[J_B(N,T)\right] = T\int_0^\infty \overline{\psi}(r)\ dF_{\|N_0\|}(r)$$

and its second order moment is given as:

$$\mathbf{m}_2\left[J_B(N,T)\right] = \int_0^T\int_0^T\ dt_1\ dt_2\int_0^\infty\int_0^\infty \overline{\psi}(u_1)\overline{\psi}(u_2)\ dF_{(\|N_{t_1}\|,\|N_{t_2}\|)}(u_1,u_2). \tag{8.11}$$

Proof. We have

$$\begin{aligned}
F_{(\|N_{t_1}\|,\|N_{t_2}\|)}(u_1,u_2) &= \mathbf{P}(\|N_{t_1}\|\le u_1, \|N_{t_2}\|\le u_2)\\
&= \mathbf{P}\left(\|N_{t_1}-N_{t_2}\|\le u_1, \|N_{t_2}-N_{t_1}\|\le u_2, \|N_{t_1}\cap N_{t_2}\|\le u_1\wedge u_2\right)\\
&= \mathbf{P}(\|N_{t_1}-N_{t_2}\|\le u_1)\mathbf{P}(\|N_{t_2}-N_{t_1}\|\le u_2)\mathbf{P}(\|N_{t_1}\cap N_{t_2}\|\le u_1\wedge u_2)\\
&= \left(1-e^{-\mathbf{E}[S]F_{S_e}(|t_2-t_1|)\Lambda(\overline{C}(u_1))}\right)\left(1-e^{-\mathbf{E}[S]F_{S_e}(|t_2-t_1|)\Lambda(\overline{C}(u_2))}\right)\times\\
&\quad\times\left(1-e^{-\mathbf{E}[S]\overline{F}_{S_e}(|t_2-t_1|)\Lambda(\overline{C}(u_1\wedge u_2))}\right)
\end{aligned}$$

as $N_{t_1}-N_{t_2}, N_{t_2}-N_{t_1}, N_{t_1}\cap N_{t_2}$ are three independent Poisson point processes (lemma 58).

Using Fubini's theorem the expectation of $J_B(N,T)$ is expressed as:

$$\begin{aligned}
\mathbf{E}\left[J_B(N,T)\right] &= \int_0^T \mathbf{E}\overline{\psi}(\|N_t\|)\ \mathrm{d}t\\
&= T\int_0^\infty \overline{\psi}(r)\ \mathrm{d}F_{\|N_0\|}(r)
\end{aligned}$$

as $\|N_t\|$ has the same distribution for all t.

Similarly, the second order moment of $J_B(N,T)$ is:

$$\begin{aligned}
\mathbf{m}_2\left[J_B(N,T)\right] &= \mathbf{E}\left[\left(\int_0^T \overline{\psi}(\|N_t\|)\ \mathrm{d}t\right)^2\right]\\
&= \int_0^T\int_0^T \mathbf{E}\left[\overline{\psi}(\|N_{t_1}\|)\overline{\psi}(\|N_{t_2}\|)\right]\ \mathrm{d}t_1\ \mathrm{d}t_2\\
&= \int_0^T\int_0^T\ \mathrm{d}t_1\ \mathrm{d}t_2\int_0^\infty\int_0^\infty \overline{\psi}(u_1)\overline{\psi}(u_2)\ \mathrm{d}F_{(\|N_{t_1}\|,\|N_{t_2}\|)}(u_1,u_2).
\end{aligned}$$

□

It is worth noting that we can generalize result of lemma 58 to calculate n^{th} order moment of $J_B(N,T)$. For example, for $n=3$ and $t_1<t_2<t_3$ one can prove that $N_{t_3}-N_{t_2}, N_{t_3}\cap N_{t_2}-N_{t_2}, N_{t_2}-N_{t_1}-N_{t_3}, N_{t_3}\cap N_{t_1}, N_{t_2}\cap N_{t_1}-N_{t_3}, N_{t_1}-N_{t_2}$ are six independent Poisson point processes on $\mathbb{R}^d$.

8.3.1 Proof of Theorem 49

In this subsection we prove the results presented in theorem 49.

As $J_T(N,T) = J_A(N,T) + J_B(N,T)$ we apply lemmas 59 and 61 we obtain the analytical expression of $\mathbf{E}[J_T(N,T)]$. We are now interested in $\mathbf{m}_2[J_T(N,T)]$. We have

$$\mathbf{m}_2[J_T(N,T)] = \mathbf{m}_2[J_A(N,T)] + 2\mathbf{E}[J_A(N,T)J_B(N,T)] + \mathbf{m}_2[J_B(N,T)]. \tag{8.12}$$

Expressions for $\mathbf{m}_2[J_A(N,T)]$ and $\mathbf{m}_2[J_B(N,T)]$ have been found in the lemmas 59 and 61 so it remains to calculate $\mathbf{E}[J_A(N,T)J_B(N,T)]$. Using Fubini's theorem the later can be written as:

$$\begin{aligned}
\mathbf{E}[J_A(N,T)J_B(N,T)] &= \mathbf{E}\left[\int_0^T P_A(N_{t_1})\ \mathrm{d}t_1 \int_0^T \overline{\psi}(\|N_{t_2}\|)\ \mathrm{d}t_2\right] \\
&= \int_0^T \int_0^T \mathbf{E}\left[P_A(N_{t_1})\overline{\psi}(\|N_{t_2}\|)\right]\ \mathrm{d}t_1\ \mathrm{d}t_2 \\
&= \int_0^T \int_0^T \mathbf{E}\left[P_A(N_{t_1} - N_{t_2})\overline{\psi}(\|N_{t_2}\|)\right]\ \mathrm{d}t_1\ \mathrm{d}t_2 \\
&\quad + \int_0^T \int_0^T \mathbf{E}\left[P_A(N_{t_1}\cap N_{t_2})\overline{\psi}\left(\|N_{t_2} - N_{t_1}\| \vee (\|N_{t_2}\cap N_{t_1}\|)\right]\ \mathrm{d}t_1\ \mathrm{d}t_2\right. \\
&= term_1 + term_2
\end{aligned}$$

Recall from lemma 58 that $N_{t_1} - N_{t_2}$ is independent of N_{t_2} so

$$\begin{aligned}
term_1 &= \mathbf{E}[S]\int_{\mathbb{R}^d}\phi(x)\ \mathrm{d}\Lambda(x)\int_0^\infty \overline{\psi}(r)\ \mathrm{d}F_{\|N_0\|}(r)\int_0^T\int_0^T F_{S_e}(|t_2-t_1|)\ \mathrm{d}t_1\ \mathrm{d}t_2 \\
&= 2\mathbf{E}[S]\int_{\mathbb{R}^d}\phi(x)\ \mathrm{d}\Lambda(x)\int_0^\infty \overline{\psi}(r)\ \mathrm{d}F_{\|N_0\|}(r)\int_0^T (T-t)F_{S_e}(t)\ \mathrm{d}t
\end{aligned} \tag{8.13}$$

Now, also from 58, the joint distribution of $(\|N_{t_1}\cap N_{t_2}\|, \|N_{t_2} - N_{t_1}\|)$ is given as:

$$\begin{aligned}
&F_{(\|N_{t_1}\cap N_{t_2}\|,\|N_{t_2}-N_{t_1}\|)}(u_1,u_2) = \\
&\quad\left(1 - e^{-\mathbf{E}[S]F_{S_e}(|t_2-t_1|)\Lambda(\overline{C}(u_1))}\right)\left(1 - e^{-\mathbf{E}[S]\overline{F}_{S_e}(|t_2-t_1|)\Lambda(\overline{C}(u_2\vee u_2))}\right).
\end{aligned}$$

Note that conditioning on the event "$\|N_{t_1}\cap N_{t_2}\| = u_1$", $N_{t_1}\cap N_{t_2}$ is a Poisson point process of intensity $\mathbf{E}[S]\,\overline{F}_{S_e}(|t_2-t_1|)$ on $C(u_1)$. Thus, by Campbell's theorem, we have:

$$\begin{aligned}
term_2 &= \mathbf{E}[S]\int_0^T\int_0^T \overline{F}_{S_e}(|t_2-t_1|)\ \mathrm{d}t_1\ \mathrm{d}t_2\times \\
&\times\int_0^\infty\int_0^\infty\int_{C(u_1)}\phi(x)\ \mathrm{d}x\overline{\psi}(u_1\vee u_2)\ \mathrm{d}F_{(\|N_{t_1}\cap N_{t_2}\|,\|N_{t_2}-N_{t_1}\|)}(u_1,u_2).
\end{aligned} \tag{8.14}$$

8.3.2 Proof of theorem 50

We now have give a proof for theorem 50. Note that $J_T(N,T)$ is a functional of $L^{\Lambda,S}$ and:

$$\begin{aligned}
D_{(t,s,x)}J_T(N,T) &\le (((t+s)^+\wedge T) - t^+)(\phi(x) + \overline{\psi}(|x|)) \\
&\le (\beta_S\wedge T)\beta_B
\end{aligned}$$

Then we apply the theorem 1 we obtain the desired result.

8.3.3 Proof of theorem 51

The result is consequence of 11 as $J_A(N,T)$ is a linear functional of $L^{\Lambda,S}$.

8.4 Impact of mobility

In this section we consider the impact of mobility. In this case, the consumed energy can be written as

$$\begin{aligned} J_T(N^M,T) &= \sum_{i\geq 0}\int_0^{((T_i+S_i)^+\wedge T)-(T_i^+\wedge T)} \phi(X_i+M_i(u))\ \mathrm{d}u + \int_0^T \overline{\psi}(\left\|N_t^M\right\|)\ \mathrm{d}t \\ &= J_A(N^M,T)+J_B(N^M,T)\cdot \end{aligned}$$

Consequently, $J_A(N^M,T)$ is a linear functional of $L^{\lambda\ \mathrm{d}x,M,S}$.

8.4.1 Lemmas

Proof. (of lemma 52)

It is sufficient to prove that for all t, $((T_i,X_i+M(t-T_i)))_{i=1}^{\infty}$ is a Poisson point process with the same intensity measure as that of $((T_i,X_i))_{i=1}^{\infty}$, i.e $\lambda\ \mathrm{d}t\ \mathrm{d}x$. To prove that, we apply the displacement theorem. Let l_1, l_d be the Lebesgue measures on $\mathbb{R}$ and $\mathbb{R}^d$. For any subsets $A\subset\mathbb{R}$ and $B\subset\mathbb{R}^d$, applying the displacement theorem we have that $((T_i,X_i+M(t-T_i)))_{i=1}^{\infty}$ is a Poisson point process on $\mathbb{R}\times\mathbb{R}^d$ with intensity measure given by:

$$\begin{aligned} \overline{\Lambda}(A\times B) &= \lambda\int_A \mathrm{d}u\int_{\mathbb{R}^d}\mathbf{P}(M(t-u)+x\in B)\ \mathrm{d}x \\ &= \lambda\int_A \mathrm{d}u\int_{\mathbb{R}^d}\int_{\mathbb{R}^d} p_{M(t-u)}(y)\ \mathrm{d}y\mathbf{1}_{\{y+x\in B\}}\ \mathrm{d}x \\ &= \lambda\int_A \mathrm{d}u\int_{\mathbb{R}^d} p_{M(t-u)}(y)\ \mathrm{d}y\int_{\mathbb{R}^d}\mathbf{1}_{\{y+x\in B\}}\ \mathrm{d}x \\ &= \lambda l_d(B)\int_A \mathrm{d}u\int_{\mathbb{R}^d} p_{M(t-u)}(y)\ \mathrm{d}y \\ &= \lambda l_1(A)l_d(B) \end{aligned}$$

We conclude the proof. □

We have

$$\Gamma_n^M(f,T) = \int_{-\infty}^T \mathrm{d}t\int_0^{\infty} p_S(s)\ \mathrm{d}s\int_0^{(t+s)^+\wedge T-t^+}\ldots\int_0^{(t+s)^+\wedge T-t^+}\Phi_n^M(f,u_1,...,u_n)\ \mathrm{d}u_1\ \mathrm{d}u_2...\ \mathrm{d}u_n.$$

If $S=$ *constant* then:

$$\Gamma_n^M(f,T) = \begin{cases} 2\int_0^T H_n^M(f,u)\ \mathrm{d}u + (S-T)H_n^M(f,T), & S\leq T; \\ 2\int_0^S H_n^M(f,u)\ \mathrm{d}u + (T-S)H_n^M(f,S), & S\geq T. \end{cases} \tag{8.15}$$

We see that in this case when $T\to\infty$ then $\Gamma_n^M(f,T)\sim TH_n^M(f,S)$. In the lemma 63 we generalize this in the case where S is random.

Lemma 62. *We have* $H_n^M(f,u) \le u^n \int_{\mathbb{R}^d} f^n(x)\ dx$, *and* $\Gamma_n^M(f,T) \le K_n(T)\int_{\mathbb{R}^d} f^n(x)\ dx$ *for all* $n \ge 1$, $u \in [0,\infty)$. *Equality occurs if* $n = 1$. *Moreover, if* M *has the property* T *then:*

$$\lim_{\epsilon\to 0} H_n^{M/\epsilon}(f,u) = \lim_{\epsilon\to 0}\Gamma_n^{M/\epsilon}(f,T) = 0.$$

If $f(x) = a\mathbf{1}_{\{x\in C\}}$ *then* $\Gamma_n^M(f,u)$ *and* $H_n^{M/\epsilon}(f,u)$ *are decreasing function of* ϵ *with* $n \ge 2$ *and* $a > 0$.

Proof. We have $\int_{\mathbb{R}^d} f^n(x+y)\ \mathrm{d}x = \int_{\mathbb{R}^d} f^n(x)\ \mathrm{d}x$ for any $y \in \mathbb{R}^d$. Now for $n \ge 2$, for any $y_1, ..., y_n \in \mathbb{R}^d$, apply the Cauchy−Schwarz inequality we have:

$$\begin{aligned}\int_{\mathbb{R}^d}\prod_{i=1}^n f(x+y_i)\ \mathrm{d}x &\le \prod_{i=1}^n\left(\int_{\mathbb{R}^d} f^n(x+y_i)\ \mathrm{d}x\right)^{\frac{1}{n}}\\ &= \int_{\mathbb{R}^d} f^n(x)\ \mathrm{d}x.\end{aligned}$$

Therefore,

$$\begin{aligned}\Phi_n^M(f,u_1,u_2,...,u_n) &= \mathbf{E}\left[\int_{\mathbb{R}^d}\prod_{i=1}^n f(x+M(u_i))\ \mathrm{d}x\right]\\ &\le \int_{\mathbb{R}^d} f^n(x)\ \mathrm{d}x.\end{aligned}$$

and

$$\begin{aligned}H_n^M(f,u) &= \int_0^u ... \int_0^u \Phi_n^M(f,u_1,...,u_n)\ \mathrm{d}u_1\ \mathrm{d}u_2 ...\ \mathrm{d}u_n\\ &\le u^n\int_{\mathbb{R}^d} f^n(x)\ \mathrm{d}x.\end{aligned}$$

$$\begin{aligned}\Gamma_n^M(f,u) &\le \int_{-\infty}^T \mathrm{d}t\int_0^\infty ((t+s)^+ \wedge T - t^+)^n p_S(s)\ \mathrm{d}s\int_{\mathbb{R}^d} f^n(x)\ \mathrm{d}x\\ &= K_n(T)\int_{\mathbb{R}^d} f^n(x)\ \mathrm{d}x.\end{aligned}$$

Now as $\frac{M(u_1)-M(u_2)}{\epsilon} \to \infty$ as $\epsilon \to 0$ then for ϵ sufficiently small one of two point $x+\frac{M(u_1}{\epsilon}$ and $x + \frac{M(u_2)}{\epsilon}$ must be outside the support of f. Consequently $\prod_{i=1}^n f(x + \frac{M(u_i)}{\epsilon}) \to 0$ as $\epsilon \to 0$. By dominated convergence theorem we obtain $\lim_{\epsilon\to 0}\Phi^{M/\epsilon}(f,u_1,u_2,...,u_n) = 0$ and we have

$$\lim_{\epsilon\to 0} H_n^{M/\epsilon}(f,u) = 0.$$

Using (8.4) and applying the dominated convergence theorem we have:

$$\lim_{\epsilon\to 0}\Gamma_n^{M/\epsilon}(f,u) = 0.$$

Finally, if $n \ge 2$ and $f(x) = a\mathbf{1}_{\{x\in C\}}$ with $a > 0$ then $H_n^{M/\epsilon}(f,u)$ and $\Gamma_n^{M/\epsilon}(f,u)$ are decreasing functions because $\Phi^{M/\epsilon}(f,u_1,...,u_n)$ is. □

Lemma 63. *We have* $\Gamma_n^M(f,T) \sim T\mathbf{E}\left[H_n^M(\phi,S)\right]$ *as* $T \to \infty$.

Proof. We have:

$$\begin{aligned}\frac{\Gamma_n^M(f,T)}{T} &= \frac{1}{T}\int_{-\infty}^{0} \mathrm{d}t \int_0^{\infty} H_n^M(f,(t+s)^+ \wedge T - t^+)p_S(s)\ \mathrm{d}s \\ &\quad + \frac{1}{T}\int_0^{T} \mathrm{d}t \int_0^{\infty} H_n^M(f,(t+s)\wedge T - t)p_S(s)\ \mathrm{d}s \\ &= term_1 + term_2.\end{aligned}$$

It is easy seen that $term_1 \to 0$ as $T \to \infty$. We then consider $term_2$. We can write

$$term_2 = \int_0^1 \mathbf{E}\left[H_n^M(f,(tT+S)\wedge T - tT)\right]\ \mathrm{d}t$$

Since $(Tt+s)\wedge T - tT \le s$, $\lim_{T\to\infty}((Tt+S)\wedge T - tT) = s$ and $H_n^M(f,s)$ is an increasing function of s, by monotone convergence theorem we have:

$$\lim_{T\to\infty} term_2 = \mathbf{E}\left[H_n^M(f,S)\right].$$

□

Theorem 64. *The moments and central moments of* $J_A(N^M,T)$ *are given as:*

$$\begin{aligned}\mathbf{c}_n\left[J_A(N^M,T)\right] &= B_n(0,\lambda\Gamma_2^M(\phi,T),...,\lambda\Gamma_n^M(\phi,T)) \\ \mathbf{m}_n\left[J_A(N^M,T)\right] &= B_n(\lambda\Gamma_1^M(\phi,T),\lambda\Gamma_2^M(\phi,T),...,\lambda\Gamma_n^M(\phi,T))\end{aligned}$$

for all positive integer n.

Proof. The result follows the linearity property of $J_A(N^M,T)$ and the theorem 7.4 and we note that:

$$\begin{aligned}&\int_{\mathbb{R}\times\mathbb{R}\times\mathbb{R}^d\times D(\mathbb{R},\mathbb{R}^d)} \left(\int_0^{((t+s)^+\wedge T)-(t^+\wedge T)} \phi(x+M(u))\ \mathrm{d}u\right)^n \mathrm{d}tp_S(s)\ \mathrm{d}s\lambda\ \mathrm{d}x\ \mathrm{d}\mathbf{P}_M \\ &\quad = \lambda\Gamma_n^M(\phi,T).\end{aligned}$$

□

When T is large, use lemma 63 we can write: $\mathbf{V}\left[J_A(N^M,T)\right] \sim T\lambda\mathbf{E}\left[H_2^M(\phi,S)\right]$.

8.4.2 Proof of Theorem 54

With the assumption $\mathrm{d}\Lambda(x) = \lambda\ \mathrm{d}x$, applying theorem 64 and lemma 62 we have:

$$\begin{aligned}\mathbf{m}_n\left[J_A(N,T)\right] &= B_n\left(\lambda K_1(T)\int_{\mathbb{R}^d}\phi(x)\ \mathrm{d}x,...,\lambda K_n(T)\int_{\mathbb{R}^d}\phi^n(x)\ \mathrm{d}x\right) \\ &\ge B_n\left(\lambda\Gamma_1^M(\phi,T),...,\lambda\Gamma_n^M(\phi,T)\right) \\ &= \mathbf{m}_n\left[J_A(N^M,T)\right]\end{aligned}$$

and

$$\begin{aligned}\mathbf{c}_n\left[J_A(N,T)\right] &= B_n\left(0, \lambda K_2(T)\int_{\mathbb{R}^d}\phi^2(x)\ \mathrm{d}\Lambda(x), ..., \lambda K_n(T)\int_{\mathbb{R}^d}\phi^n(x)\ \mathrm{d}x\right)\\ &\geq B_n\left(0, \lambda\Gamma_2^M(\phi,T), ..., \lambda\Gamma_n^M(\phi,T)\right)\\ &= \mathbf{c}_n\left[J_A(N^M,T)\right].\end{aligned}$$

Now we have, as $\epsilon \to 0$:

$$\mathbf{m}_n\left[J_A(N^{M/\epsilon},T)\right] \to B_n(\lambda T\int_{\mathbb{R}^d}\phi(x)\ \mathrm{d}x, 0..., 0) = \left(\lambda T\int_{\mathbb{R}^d}\phi(x)\ \mathrm{d}x\right)^n$$

and

$$\mathbf{c}_n\left[J_A(N^{M/\epsilon},T)\right] \to B_n(0, ..., 0) = 0.$$

Now, using the property of linear functional of Poisson point process and Jensen's inequality, we have

$$\begin{aligned}&\mathbf{E}\left[\exp\left\{\alpha J_A(N^M,T)\right\}\right] = \exp\left\{\lambda\int_{-\infty}^T \mathrm{d}t\int_0^\infty p_S(s)\ \mathrm{d}s\int_{\mathbb{R}^d}\left(e^{\alpha\int_{t^+}^{(t+s)^+\wedge T}\phi(x+M(u))\ \mathrm{d}u} - 1\right)\ \mathrm{d}x\right\}\\ &\leq \exp\left\{\lambda\int_{-\infty}^T \mathrm{d}t\int_0^\infty p_S(s)\ \mathrm{d}s\int_{\mathbb{R}^d}\mathrm{d}x\left(\frac{1}{((t+s)^+\wedge T)-t^+}\int_{t^+}^{(t+s)^+\wedge T} e^{\alpha\phi(x+M(u))(((t+s)^+\wedge T)-t^+)} - 1\right)\ \mathrm{d}u\right\}\\ &= \exp\left\{\lambda\int_{-\infty}^T \mathrm{d}t\int_0^\infty p_S(s)\ \mathrm{d}s\frac{1}{((t+s)^+\wedge T)-t^+}\int_{t^+}^{(t+s)^+\wedge T}\mathrm{d}u\int_{\mathbb{R}^d}\left(e^{\alpha\phi(x)(((t+s)^+\wedge T)-t^+)} - 1\right)\right\}\\ &\exp\left\{\lambda\int_{-\infty}^T \mathrm{d}t\int_0^\infty p_S(s)\ \mathrm{d}s\int_{\mathbb{R}^d}\left(e^{\alpha\phi(x)((t+s)^+\wedge T)-t^+} - 1\right)\right\}\\ &= \mathbf{E}\left[\exp\left\{\alpha J_A(N,T)\right\}\right].\end{aligned}$$

Here we use convention $\frac{1}{0}\int_t^t e^{\alpha\cdots}\ \mathrm{d}u = 1$.

Now we have:

$$\begin{aligned}0 \leq \mathbf{V}\left[J_T(N^M,T)\right] &\leq \lambda\Gamma_1^{M/\epsilon}(\phi+\psi,T)\\ 0 \leq \mathbf{V}\left[J_B(N^M,T)\right] &\leq \lambda\Gamma_1^{M/\epsilon}(\psi,T).\end{aligned}$$

Apply lemma 62 we have

$$\lim_{\epsilon\to 0}\mathbf{V}\left[J_T(N^{M/\epsilon},T)\right] = \lim_{\epsilon\to 0}\mathbf{V}\left[J_B(N^{M/\epsilon},T)\right] = 0.$$

8.4.3 Special case: Completely aimless mobility model

We consider now the complete aimless mobility model with constant speed, i.e $M(t) = tv$ where $|v| = constant$ and the direction of v is uniformly distributed.

Lemma 65. *Consider the completely aimless mobility model then:*

1. *If* $f(x) = a\mathbf{1}_{\{x\in C\}}$ *then*

$$H_n^M(f,u) = O\left(\frac{1}{|v|^{n-1}}\right), |v| \to \infty$$

and $H_n^M(f,u) = O(u), u \to \infty$ *for* $n \geq 2$.

2. *If* $d = 1$ *and* $C = [-R, R]$ *and* $f(x) = a\mathbf{1}_{\{|x| \le R\}}$ *with* $a > 0$ *then: we have*

$$\Gamma_n^M(f,T) = \mathbf{E}\left[h(S \wedge T, T \vee S)\right] \tag{8.16}$$

where:

$$h(s,t) = \begin{cases} t\left(2Rs^n - \frac{n-1}{n+1}s^{n+1}|v|\right)a^n - \frac{n-1}{n+1}2Rs^{n+1} + \frac{n(n-1)}{(n+1)(n+2)}|v|\, s^{n+2}a^n, & s \le \frac{2R}{|v|}; \\ t\left(\frac{(2R)^n s}{|v|^{n-1}} - \frac{n-1}{n+1}\frac{(2R)^{n+1}}{|v|^n}\right)a^n - \frac{n-1}{n+1}\frac{(2R)^{n+1}s}{|v|^n}a^n, & s \ge \frac{2R}{|v|}. \end{cases}$$

Proof. 1) can be proved following the same lines as the proof of lemma 46 in the previous chapter, thus we omit here.

Now we prove 2) . Using equations (8.4) (8.15) we need only prove (8.16) in the case where $S = constant < T$. In this case if $S \le \frac{2R}{|v|}$ then:

$$\begin{aligned} \Gamma_n^M(f,T) &= 2\int_0^S \left(2Ru^n - \frac{n-1}{n+1}u^{n+1}|v|\right)\,\mathrm{d}u + (T-S)\left(2RS^n - \frac{n-1}{n+1}S^{n+1}|v|\right) \\ &= T\left(2RS^n - \frac{n-1}{n+1}S^{n+1}|v|\right) - \frac{n-1}{n+1}2RS^{n+1} + \frac{n(n-1)}{(n+1)(n+2)}|v|\, S^{n+2} \end{aligned}$$

and if $S \ge \frac{2R}{|v|}$:

$$\begin{aligned} \Gamma_n^M(f,T) &= 2\int_0^{\frac{2R}{|v|}} \left(2Ru^n - \frac{n-1}{n+1}u^{n+1}|v|\right)\,\mathrm{d}u \\ &\quad +2\int_{\frac{2R}{|v|}}^S \left(\frac{(2R)^n u}{|v|^{n-1}} - \frac{n-1}{n+1}\frac{(2R)^{n+1}}{|v|^n}\right)\,\mathrm{d}u + (T-S)\left(\frac{(2R)^n S}{|v|^{n-1}} - \frac{n-1}{n+1}\frac{(2R)^{n+1}}{|v|^n}\right) \\ &= T\left(\frac{(2R)^n S}{|v|^{n-1}} - \frac{n-1}{n+1}\frac{(2R)^{n+1}}{|v|^n}\right) - \frac{n-1}{n+1}\frac{(2R)^{n+1}S}{|v|^n} + \frac{n(n-1)}{(n+1)(n+2)}\frac{(2R)^{n+2}}{|v|^{n+1}}. \end{aligned}$$

This completes the proof. □

Applying the above results, we have expressions in the special case: $d = 1, C = [-R, R]$, $\phi(x) = \mathbf{1}_{\{|x| \le R\}}$, $\psi(x) = b\mathbf{1}_{\{|x| \le R\}}$ and $M(t) = tv$ with $v = |v|$ or $-|v|$ with equal probability $\frac{1}{2}$. In particular, if $S = constant < T$ we have:

$$\begin{aligned} \mathbf{E}\left[J_T(N^M,T)\right] &= \mathbf{E}\left[J_A(N^M,T)\right] + \mathbf{E}\left[J_B(N^M,T)\right] \\ &= 2\lambda TRS + Tb(1 - e^{-2\lambda SR}), \end{aligned}$$

$$\mathbf{V}\left[J_A(N^M,T)\right] = \lambda T\left(2RS^2 - \frac{|v|\,S^3}{3}\right) - \frac{2\lambda RS^3}{3} + \frac{\lambda|v|\,S^4}{6}$$

if $S \le \frac{2R}{|v|}$ and

$$\mathbf{V}\left[J_A(N^M,T)\right] = \lambda T\left(\frac{(2R)^2 S}{|v|} - \frac{(2R)^3}{3|v|^2}\right) - \frac{\lambda(2R)^3 S}{3|v|^2} + \frac{\lambda(2R)^4}{6|v|^3}$$

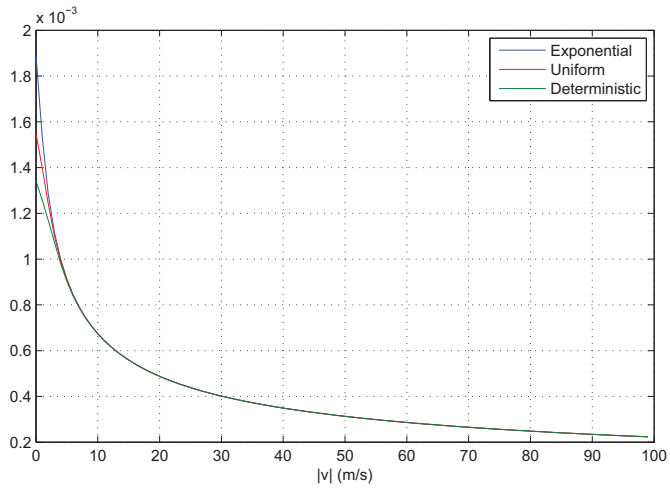


Figure 8.4: Impact of distribution of sojourn time and user's speed on the $\frac{\sqrt{\mathbf{V}[J_A(N^M,T)]}}{J_A(N,T)}$ in the motionless case.

if $S \geq \frac{2R}{|v|}$. We can think that, in this case, the low mobility regime corresponds to $S \leq \frac{2R}{|v|}$ and the high mobility regime corresponds to $S \leq \frac{2R}{|v|}$. If S is random and $|v| \to \infty$, then $\Gamma_n^M(\phi,T) \sim \frac{T\mathbf{E}[S](2R)^n}{|v|^{n-1}}$. In particular,

$$\mathbf{V}\left[J_A(N^M,T)\right] \sim \frac{\lambda T \mathbf{E}\left[S\right](2R)^2}{|v|}$$

For a numerical application, we take $d = 1$, $2R = 1000(m)$, $T = 10^7(s) \sim 115(days)$, $\lambda = 5.55555556.10^{-5}(users/(m.s))$. We also choose $\phi(x) = \mathbf{1}_{\{|x|\leq R\}}$ so that we have exact expressions for J_A. For the distribution of sojourn time, we consider the three cases: $S = 360(s)$ (deterministic), $S \sim exponential(360)$ (exponential distributed) and $S \sim uniform(0,720)$ (uniformly distributed). In all three cases, the average sojourn time is the same as $360(s) = 6(mins)$. Figure 8.4 plots the ratio $\frac{\sqrt{\mathbf{V}[J_A(N^M,T)]}}{J_A(N,T)}$ in function of $|v|$. Since $\phi(x) = \mathbf{1}_{\{|x|\leq R\}}$, the ratio is decreasing function of $|v|$, as expected. The variance is smallest in the case of deterministic sojourn time, which seems intuitive. We observe that for $|v| \geq 3(m/s)$ the ratios are almost the same in three distributions of sojourn time while they differ enormously in small values of user's speed. Figure 8.5 plots the PDF of $\mathbf{V}\left[J_A(N,T)\right]$ (motionless users). We see that even in this simple case, there is difference between the distribution of $J_A(N,T)$. The variance of $J_A(N,T)$ in the case of deterministic is smallest as predicted in equation 8.9 because T is large.

8.5 Conclusion

In this chapter we have presented a model called generalized Glauber dynamic to evaluate the consumed energy in a base station of cellular networks between 0 and T where user arrives according to a Poisson point process in time-space and they are associated with a random sojourn time and a mobility process. For the additive part of consumed energy J_A, the moments can be expressed in term of Bell's polynomial for both cases: motionless

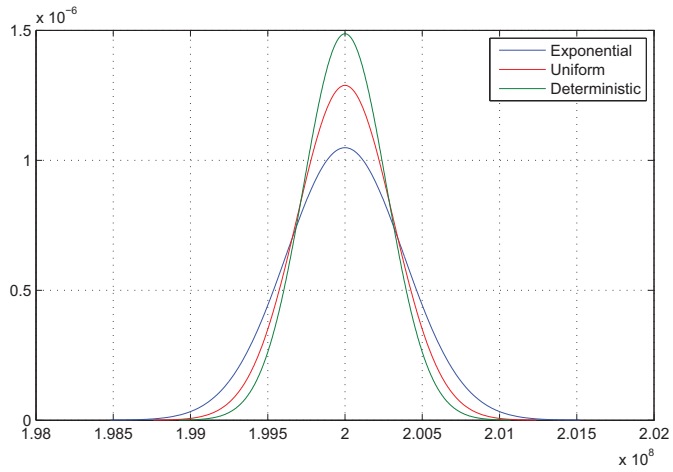


Figure 8.5: Impact of distribution of sojourn time on the distribution of $J_A(N,T)$ in the motionless case.

and mobile users. We have also determined an upper bound for the distribution of J_A and that of the Gaussian one with the same mean and variance. In the case of no mobility, we have found an ideal to calculate the moments of J_T but it is too complex for $n \geq 3$ so we have done it for the 2^{th} moment. We have found asymptotic approximations of the moments of J_A when T is large. We have determined the effect of mobility of users. In particular we have showed that it reduces the moments of J_A and in high mobility regime, it reduced the variance of J_T, J_A to 0.

Part IV

Conclusion

Chapter 9

Conclusion and future works

Contents

9.1 Summary 121
9.2 Future works 122

9.1 Summary

In this thesis we explored tools of stochastic analysis and Poisson point process applied to cellular networks. We first introduced some basics on Poisson point process and Malliavin calculus. In the first application, we found a relationship between the probability of overloading the system, the density of active users and the number of available subcarriers, thus providing a large number of possibilities to design OFDMA systems. We calculated the probability of loosing a user in a OFDMA system because all subcarriers of the base station are already in use by several methods including Gaussian approximation, Edgeworth's expansion and upper bound derived from the concentration inequality. We apply to dimension the number of subcarriers so that the loss probability is small. We also compared the numerical results with simulations and note that the upper bound of overloading probability leads to an overestimate of the number of subcarriers by about 15% of the simulated one. We also compared it to Gaussian approximation and Edgeworth's expansion and found that it is more robust against uncertainty on system's parameters. The margin provided by the bounds may be viewed as a protection against errors in the modeling or in the estimations of parameters.

In the second application, we developed energy consumption models for cellular networks. We first defined the power consumption model for base station as a function of the collection of positions of users. The consumed power consists of the power dedicated to broadcast the same information to all active users in the cell and the power dedicated to transmit, receive, decode and encode the signal of any active user. The total consumed energy during a period is the sum of all consumed power, which in turn is divided into the broadcast part and the additive part. We consider the first model where at each instance, the configuration of active users follows a homogenous Poisson point process. In this model, we proved that the consumed energy is a increasing function of cell radius. Taking into account the cost of base stations, we proved that there exists an optimal cell radius in the economical point of view. We also present the mobility model for users where each user moves independently from others but statistically identical .

We then define two models for user's activity. In the first model, each user is associated with an on-off process and the system serves only on users. In the second model, called generalized Glauber model, calls arrive following a Poisson point process being in the system for some time period and then disappear. The key idea is that the system can be described by a Poisson point process, so we can apply theoretical results. In both models, we were able to find analytical expressions for the statistics of the consumed energy as well as bounds on its distribution. We showed that the additive part can be approximated by Gaussian random variable and we found an error bound. We then considered the impact of mobility and again we can provide some analytical expressions. Mobility is known to improve the performance of networks in various aspects and we showed that somewhat it has a positive impact on the energy consumption. It turns out that, in both models, with or without mobility the network consumes the same amount of energy *in average*. However mobility decreases the moments of the additive part and high mobility decreases the variance of consumed energy to zero. In the first model, we found the decay rate of variance in function of user's speed which is $O(\frac{1}{|v|})$. Nevertheless , there are tons of questions that we have not been able to answer yet.

We finally remark that, the mathematical frameworks developed to analyze the energy consumption in cellular networks in this thesis can be applied in other studies of wireless system or in queueing theory.

9.2 Future works

In this thesis we employed abstract models to analyze the energy consumption on cellular networks which simplifies hypotheses on traffic, mobility,... Our energy consumption model is only at the initial state and we need a lot of improvement to model more accurately. Still, we have derived from these abstract models a large number of interesting results that deserve to be further pursued. There are some directions for future research as below:

1. **Inhomogeneous Poisson process or Non-Poisson process of arrivals, non-Poisson process of positions:** In this thesis we assumed a homogeneous Poisson arrival of users (or calls) in the Generalized Glauber model. This means that we assumed that the arrival is always at peak rate. The models can be generalized to inhomogeneous Poisson arrival or periodic inhomogeneous Poisson arrival to reflect the fact that in a real network, the arrival of calls is non homogenous or periodic. For example there is always less of calls during the night time than in day time. Moreover, we assumed a Poisson process of positions of users at each instance to take advantage of its randomness and independence aspects. For this reason, we can also expect non-Poisson arrival of calls, or non-Poisson process of positions in the future works to make the model more complete. We can imagine a renewal process as calls arrival process. We can also assume non-Poisson point process such as determinantal point process or cluster process point process to model user's position. In this case the system still can be modeled as a point process, but no longer a Poisson point process and therefore need a lot of reflection.

2. **Loss model:** In this thesis, we assumed that the system is not limited on transmitted power or resources so there is no loss of call. In a real system like OFDMA one, the resource is always limited so there is always a small fraction of call to be lost, delayed, or interrupted. If the system is designed so that the probability of losing

a communication is very small, out no-loss model can be a good approximation. However, we would like to build a model to capture this fact and we want to know, for instance, if the tendency made by mobility is the same as in non-loss model. We note that spatial loss network is already considered in the literature [54],[57],[58],.... It can be used in the subsequent analysis.

3. **Considering shadowing, fading, interference:** For the sake of tractability, we assumed that channels between users and base stations are not affected by shadowing or fading. It is possible to take into account these elements in a future research as the system can also described as a Poisson point process. Moreover, cellular network is particularly interference limited. Thus, it would be interesting to measure the impact of interference on the energy consumption of cellular networks.

4. **Comparing with simulation/test/real data:** Our energy consumption models are purely theoretical. Due to the limit of time, we have not build a simulator. As a matter of fact, in the future we would like to compare the results obtained in this thesis to a numerical simulation, or a real data. One of our conclusion is that the mobility make no impact on the mean of consumed energy but high mobility decreases its variance to zero. It would be interesting to see if this conclusion is accurate enough in a real situation.

Chapter 10

Appendix

10.1 ON-OFF exponential process: Basic properties

In this section, assume that $I(t)$ is a stationary ON-OFF exponential process where on-periods and off-periods have mean μ_1^{-1} and μ_0^{-1} respectively. Let

$$\pi_1 = \frac{\mu_0}{\mu_0 + \mu_1} \text{ and } \pi_0 = \frac{\mu_1}{\mu_0 + \mu_1}.$$

By stationarity we have:

$$\mathbf{P}(I(t) = 1) = \pi_1 \text{ and } \mathbf{P}(I(t) = 0) = \pi_0$$

Lemma 66. *[59] We have*

$$p_{ij}(t,s) = \pi_j(1 - e^{-(\mu_0+\mu_1)(t-s)}) + \delta_{ij}e^{-(\mu_0+\mu_1)|t-s|}.$$

for all $i, j \in \{0, 1\}$. *Moreover, let* $t_1 < t_2 < ... < t_n$ *and* $i_1, i_2, ..., i_n \in \{0, 1\}$ *then*

$$\pi_{i_1,i_2,...,i_n}(t_1, ..., t_n) = \mathbf{P}(\cap_{j=1}^{n}\{I(t_j) = i_j\}) = \pi_{i_1} \prod_{j=1}^{n-1} p_{i_{j+1}i_j}(t_{j+1}, t_j).$$

Let $A(T) = \int_0^T I(t)\ \mathrm{d}t$ is the total active time of the user. We can obtain its moment generating function, its expectation, its moments, which is important for the analysis in the next sections. Let

$$V \triangleq \begin{pmatrix} -\mu_0 & \mu_0 \\ \mu_1 & -\mu_1 \end{pmatrix},\ R \triangleq \begin{pmatrix} 0 & 0 \\ 0 & 1 \end{pmatrix},\ B(\theta, t) = \exp\left((V + \theta R)t\right)$$

$$v_{\pm}(\theta) \triangleq \frac{1}{2}\left(-\mu_1 - \mu_0 + \theta \pm \sqrt{(\mu_1 + \mu_0 - \theta)^2 + 4\mu_0\theta}\right)$$

and

$$\kappa_{00}(\theta) = \frac{-\mu_0 - v_-(\theta)}{v_+(\theta) - v_-(\theta)},\ \kappa_{01}(\theta) = \frac{-\mu_0}{v_+(\theta) - v_-(\theta)},$$

$$\kappa_{10}(\theta) = \frac{\mu_1}{v_+(\theta) - v_-(\theta)},\ \kappa_{01}(\theta) = \frac{-\theta - \mu_1 - v_-(\theta)}{v_+(\theta) - v_-(\theta)}$$

Lemma 67. *[59] For $i, j = 0, 1$, we have:*

$$B_{ii}(\theta, t) = \kappa_{ii}(\theta)e^{v_+(\theta)t} + (1 - \kappa_{ii}(\theta))e^{v_-(\theta)t}$$
$$B_{ij}(\theta, t) = \kappa_{ij}(\theta)e^{v_+(\theta)t} - \kappa_{ij}(\theta)e^{v_-(\theta)t},$$

and

$$\mathbf{E}\left[e^{\theta A(t)}\right] = \sum_{i=0}^{1}\sum_{j=0}^{1}\pi_i B_{ij}(\theta, t)\cdot$$

To find the moments of $A(t)$, however it is cumbersome to use the above expression of $\mathbf{E}\left[e^{\theta A(t)}\right]$. We have another way to compute the moments of $A(t)$.

Lemma 68. *[60] We have:*

$$\mathbf{m}_n\left[A(T)\right] = n!\pi_1 \int_0^T dt_n \int_0^{t_{n-1}} p_{11}(t_n, t_{n-1})\ dt_{n-1} ... \int_0^{t_2} p_{11}(t_2, t_1)\ dt_1\cdot \tag{10.1}$$

In particular,

$$\mathbf{E}\left[A(T)\right] = \frac{\mu_0 T}{\mu_0 + \mu_1}$$

and

$$\mathbf{m}_2\left[A(T)\right] = \frac{T^2\mu_0^2}{(\mu_0+\mu_1)^2} + \frac{2T\mu_0\mu_1}{(\mu_0+\mu_1)^3} + \frac{2\mu_0\mu_1}{(\mu_0+\mu_1)^4}\left(e^{-(\mu_0+\mu_1)T} - 1\right)\cdot$$

and

$$\begin{aligned}\mathbf{m}_3\left[A(T)\right] &= \frac{T^3\mu_0^3}{(\mu_0+\mu_1)^3} + \frac{6T^2\mu_0^2\mu_1}{(\mu_0+\mu_1)^4} - \frac{6T(\mu_1-2\mu_0)\mu_0\mu_1}{(\mu_0+\mu_1)^5}\left(1 - e^{-T(\mu_0+\mu_1)}\right)\\ &+ \frac{12\mu_0\mu_1(\mu_1-\mu_0)}{(\mu_0+\mu_1)^6} + \frac{6T\mu_0\mu_1^2}{(\mu_0+\mu_1)^5}e^{-T(\mu_0+\mu_1)}.\end{aligned}$$

Proof. We have:

$$\begin{aligned}\mathbf{m}_n\left[A(T)\right] &= \mathbf{E}\left[\left(\int_0^T I(t)\ \mathrm{d}t\right)^n\right]\\ &= \mathbf{E}\left[\int_0^T ... \int_0^T I(t_1)...I(t_n)\ \mathrm{d}t_n ...\ \mathrm{d}t_1\right]\\ &= \int_0^T ... \int_0^T \mathbf{E}\left[I(t_1)...I(t_n)\right]\ \mathrm{d}t_n ...\ \mathrm{d}t_1\\ &= \int_0^T ... \int_0^T \mathbf{P}(I(t_1) = 1, ..., I(t_n) = 1)\ \mathrm{d}t_n ...\ \mathrm{d}t_1\\ &= n!\int_0^T \int_0^{t_n} ... \int_0^{t_2} \mathbf{P}(I(t_1) = 1, ..., I(t_n) = 1)\ \mathrm{d}t_n ...\ \mathrm{d}t_1\\ &= n!\int_0^T \int_0^{t_n} ... \int_0^{t_2} p_{11}(t_n, t_{n-1})...p_{11}(t_2, t_1)\pi_1\ \mathrm{d}t_n ...\ \mathrm{d}t_1,\end{aligned}$$

where we use the Fubini's theorem and exploit the fact that $I(t) = 0$ or 1 and $I(t)$ is a Markov chain. Thus, (10.1) is proved. To find expressions of $\mathbf{m}_n\left[A(T)\right]$ for $n = 1, 2, 3$ it suffices to apply (10.1) with some simple manipulations. □

Note that for large T,

$$\mathbf{V}\left[A(T)\right] \sim \frac{2T\mu_0\mu_1}{(\mu_0+\mu_1)^3}, \mathbf{m}_2\left[A(T)\right] \sim \frac{\mu_0^2T^2}{(\mu_0+\mu_1)^2}, \mathbf{m}_3\left[A(T)\right] \sim \frac{\mu_0^3T^3}{(\mu_0+\mu_1)^3}(T\to\infty)\cdot$$

In general, we can prove that $\mathbf{m}_n\left[A(T)\right] \sim \frac{\mu_0^nT^n}{(\mu_0+\mu_1)^n}$ as $T\to\infty$.

We also note that for small T, $\mathbf{m}_n\left[A(T)\right] \sim \frac{\mu_0T^n}{(\mu_0+\mu_1)}$ as $T\to 0$.

10.2 Hermite polynomials

Let Φ be the Gaussian probability density function: $\Phi(x) = \exp(-x^2/2)/\sqrt{2\pi}$ and μ the Gaussian measure on $\mathbb{R}$. Hermite polynomials $(H_k,\, k\geq 0)$ are defined by the recursion formula:

$$H_k(x)\Phi(x) = (-1)^k\frac{d^k}{dx^k}\Phi(x).$$

For the sake of completness, we recall that

$$H_0(x)=1,\, H_1(x)=x,\, H_2(x)=x^2-1,\, H_3(x)=x^3-3x$$
$$H_4(x)=x^4-6x^2+3,\; H_5(x)=x^5-10x^3+15x.$$

Thus, for $F\in\mathcal{C}_b^k$, using integration by parts, we have

$$\int_{\mathbb{R}} F^{(k)}(x)\ \mathrm{d}\mu(x) = \int_{\mathbb{R}} F(x)H_k(x)\ \mathrm{d}\mu(x). \tag{10.2}$$

Let $Q(x)=\int_{-\infty}^x \Phi(u)\ \mathrm{d}u = \int_{\mathbb{R}} \mathbf{1}_{(-\infty;\,x]}(u)\Phi(u)\ \mathrm{d}u$. Then, $Q'=\Phi$ and

$$\int_{\mathbb{R}} \mathbf{1}_{(-\infty;\,x]}(u)H_k(u)\ \mathrm{d}\mu(u)$$
$$= (-1)^k\int_{-\infty}^x \Phi^{(k)}(u)\ \mathrm{d}u = (-1)^kQ^{(k)}(x) = -H_{k-1}(x)\Phi(x). \tag{10.3}$$

10.3 Ornstein-Uhlenbeck semi-group

To prove the Edgeworth expansion and its error bound, we introduce some notions of Gaussian calculus. For $F\in\mathcal{C}_b^2(\mathbb{R};\,\mathbb{R})$, we consider

$$AF(x) = xF'(x) - F''(x),\ \text{for any } x\in\mathbb{R}.$$

The Ornstein-Uhlenbeck semi-group is defined by

$$P_tF(x) = \int_{\mathbb{R}} F(e^{-t}x + \sqrt{1-e^{-2t}}y)\ \mathrm{d}\mu(y) \text{ for any } t\geq 0.$$

The infinitesimal generator A and P_t are linked by the following identity

$$F(x) - \int_{\mathbb{R}} F(y)\ \mathrm{d}\mu(y) = -\int_0^\infty AP_tF(x)\ \mathrm{d}t. \tag{10.4}$$

It is well known that for $F \in \mathcal{C}^k$, $(x \mapsto P_t F(x))$ is $k+1$-times differentiable and that we have two expressions of the derivatives (see [61]):

$$(P_t F)^{(k+1)}(x) = \frac{e^{-(k+1)t}}{\sqrt{1-e^{-2t}}} \int_{\mathbb{R}} F^{(k)}(e^{-t}x + \sqrt{1-e^{-2t}}y) y \, \mathrm{d}\mu(y).$$

and $(P_t F)^{(k+1)}(x) = e^{-(k+1)t} P_t F^{(k)}(x)$. The former equation induces that

$$\|(P_t F)^{(k+1)}\|_\infty \leq \frac{e^{-(k+1)t}}{\sqrt{1-e^{-2t}}} \|F^{(k)}\|_\infty \int_{\mathbb{R}} |y| \, \mathrm{d}\mu(y) = \frac{e^{-(k+1)t}}{\sqrt{1-e^{-2t}}} \sqrt{\frac{2}{\pi}} \, \|F^{(k)}\|_\infty.$$

List of Figures

1 Une architecture typique des réseaux cellulaires (Source: Internet). vii
2 La consommation énergétique dans un réseau cellulaire. viii
3 Les axes de recherche actuelles en Green Networking([1]). ix
4 Trade-off between tractability et modélisation réaliste. ix
5 Impact de γ et τ en probabilité de surcharge (chapitre 3) xv
6 Estimation de N_{avail} en fonction de γ par des différents méthodes (chapitre 3) xvi
7 Probabilité d'outage vs le seuil de SINR(chapitre 4) xvii
8 Probabilité de handover vs seuil de SINR (chapitre 4) xviii
9 Probabilité d'outage vs path loss exponent γ, modèle de Poisson (chapitre 4) xix
10 Probabilité de handover vs path loss exponent γ, modèle de Poisson, $n = 3$(chapitre 4) xx
11 Modèle de consommation de puissance (chapitre 6). xxi
12 Modèle ON-OFF (chapitre 7). xxii
13 Modèle Glauber généralisé (chapitre 8) xxiii

2.1 Trade-off between tractability and realistic modeling. 14
2.2 A realization of homogenous Poisson point process of intensity $\lambda = 2.10^{-3}$ and its thinning with $p(z) = 0.2$. 16

3.1 OFDMA principle : subcarriers are allocated according to the required transmission rate 32
3.2 Impact of γ and τ on the loss probability ($N_{\text{avail}} = 92$, $\lambda = 0.0001$) 39
3.3 Estimates of N_{avail} as a function of γ by the different methods 42

4.1 Outage probability vs SINR threshold 50
4.2 Handover probability vs SINR threshold 51
4.3 Outage probability vs path loss exponent γ, Poisson model 52
4.4 Handover probability vs path loss exponent γ, Poisson model, $n = 3$ 52

5.1 Triangles represent BS, plus represent MU. Dotted polygons are Voronoi cells induced by BS. A line between a BS and an MU means that the BS serves the MU. A mobile may be not served by the BS closest to it, due to fading. 56
5.2 Comparison of outage probability between propagation models. For lognormal shadowing $\sigma = 4(dB)$, for Rayleigh fading $\mu = 1$; $K = 10^{-2}$, $\gamma = 2.8$. . 60
5.3 Histogram of n_o 65
5.4 Tail distribution of $S_o(f_3)$ 67
5.5 A typical histogram of $S_o(f_3)$ 67

6.1 Power consumption model. 72
6.2 Basic model. 76

7.1 Illustration of the model, each user is associated with a ON-OFF process and a mobility process. 83
7.2 Illustration of the proof of Theorem 47. 95
7.3 Illustration of the proof of Lemma 48. 96
7.4 Influence of user's speed on the ratio $\frac{\sqrt{\mathbf{V}[J_A(\omega^M,T)]}}{\mathbf{E}[J_A(\omega^M,T)]}$ 98

8.1 Generalized Glauber spatial dynamic, similar to a $M/G/\infty$ queue a user is characterized by an arrival time, a sojourn duration, however in our model he is also characterized by his position and his mobility process. Consequently there may be infinite users at a time t but the number of users in cell C is always finite. 101
8.2 Illustration of the proof of lemma 57. 106
8.3 Illustration of the proof of lemma 58. 107
8.4 Impact of distribution of sojourn time and user's speed on the $\frac{\sqrt{\mathbf{V}[J_A(N^M,T)]}}{J_A(N,T)}$ in the motionless case. 116
8.5 Impact of distribution of sojourn time on the distribution of $J_A(N,T)$ in the motionless case. 117

List of Tables

1.1 Abbreviations 9
1.2 Mathematical notations. 9

3.1 Notations and parameters in this chapter. 33

4.1 Notations and parameters. 45

5.1 Notations. 55

6.1 Notations and parameters. 73

7.1 Notations and parameters in this chapter. 82

8.1 Notations and parameters. 100

Bibliography

[1] Z. Hasan, H. Boostanimehr, and V. K. Bhargava, "Green cellular networks: A survey, some research issues and challenges," *CoRR*, vol. abs/1108.5493, 2011.

[2] F. Baccelli, M. Klein, M. Lebourges, and S. Zuyev, "Stochastic geometry and architecture of communication networks," *Telecommunication Systems*, vol. 7, pp. 209–227, 1997.

[3] F. Baccelli, M. Klein, M. Lebourges, and S. Zuyev, "Géométrie aléatoire et architecture de réseaux," *Annals of Telecommunications*, vol. 51, pp. 158–179, 1996.

[4] F. Baccelli, B. Błaszczyszyn, and P. Mühlethaler, "An Aloha protocol for multihop mobile wireless networks," *IEEE Trans. Inf. Theory*, vol. 52, pp. 421–436, 2006.

[5] F. Baccelli, B. Błaszczyszyn, and P. Mühlethaler, "Stochastic analysis of spatial and opportunistic Aloha," *IEEE JSAC, special issue on Stochastic Geometry and Random Graphs for Wireless Networks*, vol. 27, pp. 1105–1119, 2009.

[6] F. Baccelli and B. Błaszczyszyn, "A new phase transition for local delays in MANETs," in *Proc. of IEEE INFOCOM*, (San Diego CA), 2010.

[7] B. Błaszczyszyn and P. Mühlethaler, "Stochastic analysis of non-slotted Aloha in wireless ad-hoc networks," in *Proc. of IEEE INFOCOM*, (San Diego, CA), 2010.

[8] A. Hunter, J. Andrews, and S. Weber, "Transmission capacity of ad hoc networks with spatial diversity," *Wireless Communications, IEEE Transactions on*, vol. 7, pp. 5058 –5071, december 2008.

[9] A. Busson, "An overview of results on ad hoc network performances using spatial model," in *Computers and Communications, 2009. ISCC 2009. IEEE Symposium on*, pp. 36 –41, july 2009.

[10] M. Haenggi, "Outage, local throughput, and capacity of random wireless networks," *Trans. Wireless. Comm.*, vol. 8, pp. 4350–4359, Aug. 2009.

[11] B. Liu, P. Brass, O. Dousse, P. Nain, and D. Towsley, "Mobility improves coverage of sensor networks," in *Proceedings of the 6th ACM international symposium on Mobile ad hoc networking and computing*, MobiHoc '05, (New York, NY, USA), pp. 300–308, ACM, 2005.

[12] P.-J. Wan and C.-W. Yi, "Coverage by randomly deployed wireless sensor networks," *IEEE/ACM Trans. Netw.*, vol. 14, pp. 2658–2669, June 2006.

[13] R. Ganti, F. Baccelli, and J. Andrews, "A new way of computing rate in cellular networks," in *Communications (ICC), 2011 IEEE International Conference on*, pp. 1 –5, june 2011.

[14] H. Dhillon, R. Ganti, F. Baccelli, and J. Andrews, "Coverage and ergodic rate in k-tier downlink heterogeneous cellular networks," in *Communication, Control, and Computing (Allerton), 2011 49th Annual Allerton Conference on*, pp. 1627 –1632, sept. 2011.

[15] L. Wu, "A new modified logarithmic Sobolev inequality for Poisson point processes and several applications," *Probability Theory and Related Fields*, vol. 118, no. 3, pp. 427–438, 2000.

[16] C. Houdré and N. Privault, "Concentration and deviation inequalities in infinite dimensions via covariance representations," *Bernoulli*, vol. 8, no. 6, pp. 697–720, 2002.

[17] N. Privault, *Stochastic Analysis in Discrete and Continuous Settings With Normal Martingales*, vol. 1982 of *Lecture Notes in Mathematics*. Springer, 2009.

[18] G. Peccati, J. L. Solé, M. S. Taqqu, and F. Utzet, "Stein's method and normal approximation of poisson functionals," *Annals of Probability*, vol. 38, no. 2, p. 32, 2008.

[19] E. Ferraz, *Algebraic Topology of Random Simplicial Complexes and Applications to Sensor Networks*. PhD thesis, Telecom Paristech, 2012.

[20] L. Decreusefond, E. Ferraz, P. Martins, and T.-T. Vu, "Robust methods for LTE and WiMAX dimensioning," in *Valuetools*, (Cargese, France), 2012.

[21] T. Vu, L. Decreusefond, and P. Martins, "An analytical model for evaluating outage and handover probability of cellular wireless networks," in *The 15th International Symposium on Wireless Personal Multimedia Communications (WPMC'12)*, (Taipei, Taiwan), Sept. 2012.

[22] L. Decreusefond, P. Martins, and T.-T. Vu, "Energy consumption in cellular network: ON-OFF model," in *submitted to IEEE Infocom*, (Turin, Italy), 2013.

[23] L. Decreusefond, P. Martins, and T.-T. Vu, "Energy consumption in cellular network: generalized Glauber model," in *submitted to IEEE Infocom*, (Turin, Italy), 2013.

[24] F. Baccelli and B. Blaszczyszyn, "Stochastic geometry and wireless networks, volume 1: Theory," *Foundations and Trends in Networking*, vol. 3, no. 3-4, pp. 249–449, 2009.

[25] D. J. Daley and D. Vere-Jones, *An introduction to the theory of point processes. Vol. I: Elementary theory and methods*. Probability and its Applications (New York), New York: Springer, second ed., 2003.

[26] D. J. Daley and D. Vere-Jones, *An introduction to the theory of point processes. Vol. II: General theory and structure*. Probability and its Applications (New York), New York: Springer, second ed., 2008.

[27] D. Stoyan, W. Kendall, and J. Mecke, *Stochastic geometry and its applications*. Wiley series in probability and statistics, 1995.

[28] L. Decreusefond, A. Joulin, and N. Savy, "Upper bounds on Rubinstein distances on configuration spaces and applications," *Communications on stochastic analysis*, vol. 4:3, pp. 377–399, 2010.

[29] S. Janson, "Bounds on the distributions of extremal values of a scanning process," *Stochastic Processes and their Applications*, vol. 18, no. 2, pp. 313–328, 1984.

[30] L. Decreusefond and P. Moyal, *Stochastic Modeling and Analysis of Telecoms Networks*. John Wiley & Sons, 2012.

[31] R. Agarwal, V. R. Majjigi, Z. Han, R. Vannithamby, and J. M. Cioffi, "Low complexity resource allocation with opportunistic feedback over downlink ofdma networks," *IEEE Journal on Selected Areas in Communications*, vol. 26, no. 8, pp. 1462–1472, 2008.

[32] J. Huang, V. Subramanian, R. Agrawal, and R. Berry, "Downlink scheduling and resource allocation for ofdm systems," *Wireless Communications, IEEE Transactions on*, vol. 8, no. 1, pp. 288 –296, 2009.

[33] K. Seong, M. Mohseni, and J. Cioffi, "Optimal resource allocation for ofdma downlink systems," in *Information Theory, 2006 IEEE International Symposium on*, pp. 1394 –1398, 2006.

[34] Z. Shen, J. G. Andrews, and B. L. Evans, "Adaptive resource allocation in multiuser OFDM systems with proportional rate constraints," *Wireless Communications, IEEE Transactions on*, vol. 4, no. 6, pp. 2726–2737, 2005.

[35] R. Giuliano and F. Mazzenga, "Dimensioning of ofdm/ofdma-based cellular networks using exponential effective sinr," *IEEE Trans. Wireless Commun.*, vol. 58, pp. 4204 – 4213, Oct. 2009.

[36] M. Maqbool, M. Coupechoux, S. Doirieux, and B. Baynat, "Dimensioning methodology for ofdma networks," in *Proc. of the Wireless World Research Forum (WWRF22)*, 2009.

[37] B. Błaszczyszyn and M. Karray, "Dimensioning of the downlink in OFDMA cellular networks via an erlang's loss model," in *Proc. of European Wireless Conference*, (Aalborg), 2009.

[38] M. K. Karray, "Analytical evaluation of qos in the downlink of ofdma wireless cellular networks serving streaming and elastic traffic," *IEEE Trans. Wireless Commun.*, vol. 9, pp. 1799–1807, 2010.

[39] B. Błaszczyszyn and M. Karray, "Fading effect on the dynamic performance evaluation of OFDMA cellular networks," in *Proc. of the 1st International Conference on Communications and Networking (ComNet)*, 2009.

[40] A. Dembo and O. Zeitouni, *Large Deviations Techniques and Applications*. Stochastic Modelling and Applied Probability, Springer, 2009.

[41] M. Haenggi, "A Geometric Interpretation of Fading in Wireless Networks: Theory and Applications," *IEEE Transaction on Information Theory*, vol. 54, pp. 5500–5510, Dec. 2008.

[42] J. M. Kelif, M. Coupechoux, and P. Godlewski, "Spatial outage probability for cellular networks," in *GLOBECOM*, pp. 4445–4450, 2007.

[43] R. K. Ganti and M. Haenggi, "Spatial and temporal correlation of the interference in aloha ad hoc networks," *IEEE Communications Letters*, vol. 13, pp. 631–633, September 2009.

[44] X. Lagrange, "Cir cumulative distribution in a regular network," tech. rep., ENST Paris, 2000.

[45] *Comparison of Various Frequency Reuse Patterns for WiMAX Networks with Adaptive Beamforming*, 2008.

[46] M. Haenggi and R. Ganti, "Interference in Large Wireless Networks," *Foundations and Trends in Networking*, vol. 3, no. 2, pp. 127–248, 2008.

[47] M. Haenggi, J. G. Andrews, F. Baccelli, O. Dousse, and M. Franceschetti, "Stochastic geometry and random graphs for the analysis and design of wireless networks," *IEEE Journal of Selected Areas in Communications*, vol. 27, pp. 1029–1046, September 2009.

[48] F. Baccelli and B. Blaszczyszyn, "Stochastic geometry and wireless networks, volume 2: Applications," *Foundations and Trends in Networking*, vol. 4, no. 1-2, pp. 1–312, 2009.

[49] S. Srinivasa and M. Haenggi, "Distance Distributions in Finite Uniformly Random Networks: Theory and Applications," *IEEE Transactions on Vehicular Technology*, vol. 59, pp. 940–949, Feb. 2010.

[50] S. Foss and S. Zuyev, "On a voronoi aggregative process related to a bivariate poisson process," *Advance in Applied Probability*, pp. 965–981, 1996.

[51] P. Robert, *Stochastic Networks and Queues*, vol. 52 of *Applications of Mathematics*. Berlin: Springer-Verlag, first ed., 2003.

[52] K. Park and W. Willinger, *Self-Similar Network Traffic and Performance Evaluation*. New York, NY, USA: John Wiley and Sons, Inc., 1st ed., 2000.

[53] P. Kuusela, I. Norros, J. Lapuyade-Lahorgue, and M. Naldi, "On reliability modeling with stationary on/off processes," *Submitted for publication*.

[54] M. K. Karray, *Analytic evaluation of wireless cellular networks performance by a spatial Markov process accounting for their geometry, dynamics and control schemes*. PhD thesis, Ecole Nationale Supérieure des Télécommunications, 2007.

[55] S. G. Eick, W. A. Massey, and W. Whitt, "The physics of the $m_t/g/\infty$ symbol queue," *Oper. Res.*, vol. 41, pp. 731–742, July 1993.

[56] S. G. Eick, W. A. Massey, and W. Whitt, "$m_t/g/\infty$ queues with sinusoidal arrival rates," *Management Science*, vol. 39, no. 2, pp. 241–252, 1993.

[57] W. A. Massey and W. Whitt, "Networks of infinite-server queues with nonstationary poisson input," *Queueing Syst.*, vol. 13, no. 1-3, pp. 183–250, 1993.

[58] B. Błaszczyszyn and M. Karray, "Impact of mean user speed on blocking and cuts of streaming traffic in cellular networks," in *Proc. of European Wireless Conference*, (Prague), 2008.

[59] M. Mandjes and P. Mannersalo, "Queueing systems fed by many exponential on-off sources: an infinite-intersection approach," *Queueing Syst. Theory Appl.*, vol. 54, pp. 5–20, September 2006.

[60] A. Brandt and M. Brandt, "On the distribution of the number of packets in the fluid flow approximation of packet arrival streams," *Queueing Syst.*, vol. 17, no. 1-2, pp. 275–315, 1994.

[61] H. Kuo, *Gaussian Measures in Banach Spaces*. Lecture Notes in Mathematics, Springer-Verlag, 1975.